Foot-and-mouth disease virus capsid assembly

Kristensen, Thea

Publication date:
2018

Document Version
Publisher's PDF, also known as Version of record

Foot-and-mouth disease virus capsid assembly

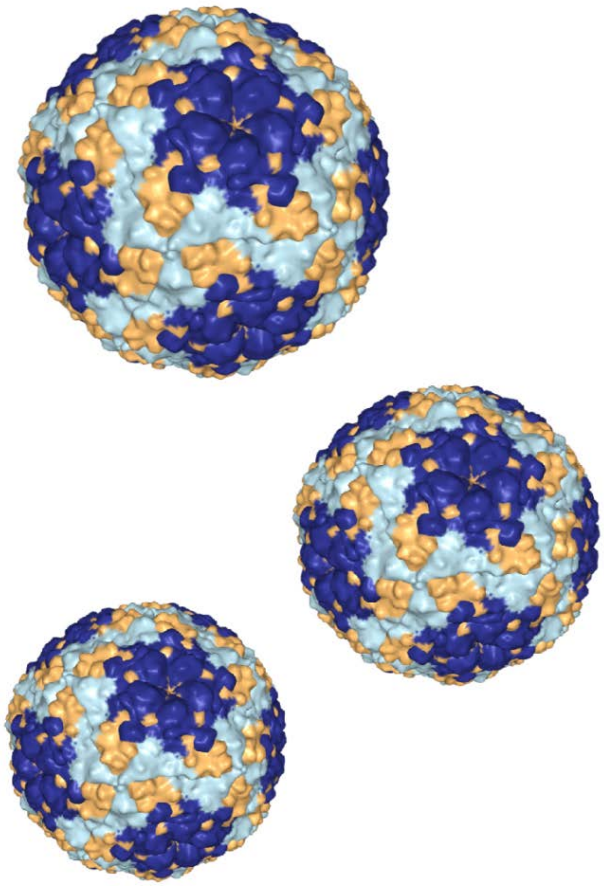

Ph.D. Thesis September 2018

Thea Kristensen

Lindholm, National Veterinary Institute

Technical University of Denmark

Supervisors

Professor Graham J. Belsham

National Veterinary Institute, Technical University of Denmark, Kalvehave, Denmark

Senior Researcher Thomas Bruun Rasmussen

National Veterinary Institute, Technical University of Denmark, Kalvehave Denmark

Cover artwork: The structure of FMDV A22 Iraq (PDB 4GH4) (Curry et al., 1996).

Foot-and-mouth disease virus capsid assembly

Table of contents

Preface

This Ph.D. thesis is the result of various experiments conducted through three good years on the island of Lindholm. The laboratory is a part of the National Veterinary Institute within the Technical University of Denmark (DTU Vet). The studies were conducted under the supervision of my main-supervisor Professor Graham J. Belsham and co-supervisor Senior Researcher Thomas Bruun Rasmussen. The studies were supported by core funds from within DTU Vet. Furthermore, a short research stay at the Pirbright Institute (United Kingdom) was supported by a Short Term Mission from Epizone.

This Ph.D. thesis is divided into four main chapters. **Chapter 1** describes the current knowledge about foot-and-mouth disease virus (FMDV), including the status of foot-and-mouth disease (FMD) and the FMDV life-cycle at a molecular level. It focuses on the processing of the capsid precursor and the assembly pathway to generate virus particles.

Chapter 2 briefly describes the aim of the three different manuscripts. Furthermore, it also provides the reader with a short summary of the manuscripts. **Chapter 3** is presented as three manuscripts listed below. In this chapter, the results are described and discussed.

1. **Kristensen T**., Normann P., Gullberg M., Fahnøe U., Polacek C., Rasmussen T. B. and Belsham G. J. (2016). Determinants of the VP1/2A junction cleavage by the 3C protease in foot-and-mouth disease virus-infected cells. Journal of General Virology, 98 (385-395).

2. **Kristensen T**., Newman J., Guan S. H., Tuthill T. J. and Belsham G. J. (2018). Cleavages at the three junctions within the foot-and-mouth disease virus capsid precursor (P1-2A) by the 3C protease are mutually independent. Virology, 522 (260-270).

3. **Kristensen T**. and Belsham G. J. Identification of a short, highly conserved, motif required for picornavirus capsid precursor processing at distal sites. Manuscript submitted.

Chapter 4 provides the overall conclusions of the results obtained and discussed in the three manuscripts. It also provides future perspectives for research resulting from the three manuscripts.

Acknowledgements

My time as a Ph.D. student at Lindholm is something that I will always remember and look back at with extreme joy. The time has been both interesting and good, and I feel that I have learned a lot during the last three years. No doubt, there has also been times of frustrations, when things (especially experiments) did not go as planned. The work leading up to this thesis would not have been possible without the support from many people two whom I am very grateful.

First, I would like to thank my two supervisors, Professor Graham J. Belsham and Senior Researcher Thomas Bruun Rasmussen for giving me the opportunity to carry out this Ph.D. project. It has been three wonderful years and I have learned so much from both of you. I would like to express my gratitude to my main supervisor Professor Graham J. Belsham. We have had so many good talks and scientific discussions. Thank you for always answering your emails within seconds and for always providing good and constructive feedback on manuscripts and presentations. You have always supported and guided me when I came with new ideas for new experiments. Numerous times, I have entered your office to discuss some new results or new ideas, left five minutes later, and then an hour has passed. So thank you for always taking your time and always keeping your door open. I also wish to acknowledge my co-supervisor, Senior Researcher Thomas Bruun Rasmussen. You have always kept your door open, and been available when I needed to discuss something with you, from the project economy to troubleshooting about a mutagenic PCR, so thank you.

Special thanks also go to Laboratory technician Preben Normann who has assisted me in the lab when time was limited. You have been an incredible help, especially in the creation and sequencing of new constructs and you have impressed me every time you managed to create 15 new constructs at your first go. I also wish to thank Laboratory technician Jani Christiansen, Jane Borch and Hanne Petersen for their assistance in reading plates, performing ELISAs and virus titrations. Special thanks also go to the laboratory technicians in the cell-lab, Lone Koch Nielsen, Dorota Wolkanowska, Hanne Egelund Hansen and Hanne Petersen. You have provided me with so many cells, and every cell has always been of first class quality!

I also wish to thank all of the Ph.D. students who are, and have been, employed during my time at Lindholm. I wish to thank Ph.D. Jonas Kjær, who was also in the FMDV group at the time of my employment. We have had so many good talks about FMDV, but certainly also about everything else. I also wish to thank my good friend and colleague Ph.D. student Ann Sofie Olesen. You have been by my side since we conduced our master thesis at University of Copenhagen and I am so glad that we had the opportunity to follow each other through our Ph.D. studies as well.

I also wish to acknowledge all of the incredible people working at Lindholm. I have been so pleased to work there during the last three years. There is an amazing work environment and a nice and relaxed atmosphere. In relation to this, I especially want to thank the Head of the Virology group, Professor Anette Bøtner. You have contributed very much for maintaining this good environment, even though the future for Lindholm has been uncertain. I have always felt comfortable coming to you, no matter the reason. The list is too long to mention all of your names, but you should know, that you have all contributed to making this a fantastic place to work! Huge thanks also goes out to the card-playing club on the ferry. I have so many good memories from the mornings and afternoons with many good games, wonderful talks and incredibly many laughs. I still find it very incredible that I have managed not to lose a single time in this game during the last three years (even though some of you might think that I did)!

I also wish to thank Dr Tobias J. Tuthill for letting me work in his lab at the Pirbright Institute (United Kingdom). It was a very pleasant stay, and everyone in the group was so friendly and welcoming. Special thanks also goes out to Ph.D. student Chris Neil, for helping to arrange the practical stuff associated with my stay. Furthermore, I also wish to thank Postdoc. Joseph Newman for assisting me in the laboratory and for helping me successfully accomplish the objective of my stay. Furthermore, I would like to thank Epizone for the funding of this stay.

Finally, I would like to thank my family and friends who have supported me in fulfilling this journey. I wish to thank my dad, who has always been very interested and asked questions about my research but far from always understood the answers. My deepest thanks goes to my boyfriend Jonas Pedersen, for always believing in me and supporting me through the last ten years, and in particular the last three.

List of abbreviations

17-AAG	17-allyl-17-demethoxygeldanamycin
17-DMAG	17-desmethoxy-17-N,N-dimethylaminoethylaminogeldanamycin
$3C^{pro}$	3C protease
$3D^{pol}$	3D polymerase
aa	Amino acids
BEV	Bovine enterovirus
cDNA	Complementary DNA
CHIP	Carboxyl terminus of Hsp70-interacting protein
CPE	Cytopathic effect
cre	*cis*-acting replication element
DI	Defective interfering
DNA	Deoxyribonucleic acid
dsRNA	Double stranded RNA
eIF	Eukaryotic translation initiation factor
ELISA	Enzyme linked immunosorbent assay
ER	Endoplasmic reticulum
EMCV	Encephalomyocarditis virus
FMD	Foot-and-mouth disease
FMDV	Foot-and-mouth disease virus
GAO	United States Government Accountability Office
GA	Geldanamycin
HAV	Hepatitis A virus
HRV	Human rhinovirus
Hsp	Heat-shock protein
Ig	Immunoglobin
IFN	interferon
IRES	Internal ribosome entry site

ISG	interferon-stimulated genes
L^{pro}	Leader protease
MKS	Mund- og klovsyge (Danish FMD)
MKSV	Mund- og klovsyge virus (Danish FMDV)
mRNA	Messenger ribonucleic acid
nm	Nano meters
nt	Nucleotides
O1K	O1 Kaufbeuren
O1M	O1 Manisa
OIE	Office International des Épizooties (World Organisation for Animal Health)
ORF	Open reading frame
p.i.	Post infection
PCBP2	Poly-r(C)-binding Protein 2
PCR	Polymerase chain reaction
PV	Poliovirus
RNA	Ribonucleic acid
RT-PCR	Reverse transcription-polymerase chain reaction
SVD	Swine vesicular virus
UK	United Kingdome
UTR	Untranslated region
US	United States
VNT	Virus neutralization test
wt	wild type

Objectives and summary

Foot-and-mouth disease (FMD) is caused by a highly contagious virus (FMDV) that infects cloven-hoofed animals, including both domesticated and wildlife. FMD is one of the most important threats to the agricultural industry. Europe is usually free of FMD, however sometimes outbreaks occur and can result in large productivity losses and severe trade restrictions. One example of such an outbreak of FMD occurred in the United Kingdom (UK) in 2001, where the total costs were estimated to around 8 billion pounds. An outbreak of FMD has not occurred in Denmark since 1983. However, introduction of the disease back into Denmark would have huge consequences for the Danish industrialized pig production, and remains a continuing threat.

FMDV belongs to the picornavirus family. The virus particles consist of a capsid surrounding a single-stranded, positive sense genomic RNA of approximately 8,400 nucleotides. The capsids consist of 60 copies of four different structural proteins, termed VP1, VP2, VP3 and VP4. These capsid proteins are generated by cleavage of the capsid precursor P1-2A into VP0, VP3, VP1 and a short 2A peptide by the viral encoded 3C protease ($3C^{pro}$). The 2A peptide is not included in the virus particle. During assembly of the capsid proteins, VP0 is cleaved to generate VP4 and VP2 by a process that is currently unknown. The processing of the capsid precursor into the capsid proteins is necessary for virus capsid assembly, and thus essential in the virus life cycle. Blocking the processing of the junctions between the capsid proteins, might be fatal for the virus, and thus might be a possible antiviral target.

The focus of this Ph.D. thesis has been to determine the importance of the amino acid sequences flanking the junctions within the FMDV P1-2A precursor in relation to correct processing by the $3C^{pro}$. Furthermore, studies have also been performed on analyzing a specific motif within VP1, which is important for correct capsid precursor processing.

Manuscript 1: In an earlier study it was found that the VP1 K210E (the P2 position in the VP1/2A junction) in FMDV O1 Manisa, blocked cleavage of this junction. The mutant virus acquired a second site mutation, VP1 E83K. Introduction of this VP1 E83K alone caused the virus to generate a new second-site mutation near the VP1/2A junction, at the 2A L2P (the P2´ position). Interestingly, this

substitution also severely inhibited cleavage of this junction. In this manuscript virus adaptions within these two mutant viruses (e.g. FMDV VP1 K210E and FMDV VP1 E83K) were analyzed by next generation sequencing. This identified variants within the FMDV VP1 E83K, where the VP1 K210N was observed. To identify which amino acids could be tolerated at this site for processing of the VP1/2A junction, various alternative amino acids (aa) were introduced at VP1 K210 in the FMDV A22 Iraq. Interestingly, only the presence of a positively charged aa (e.g. lysine or arginine) at this position permitted efficiently cleavage of the VP1/2A junction by the $3C^{pro}$, whereas the presence of either an aa with neutral or negative charge severely blocked cleavage of this junction.

Manuscript 2: In this manuscript, the impact of different substitutions near the junctions separating the capsid proteins within the capsid precursor, was investigated. The VP0/VP3- and the VP3/VP1 junctions were modified with different aa substitutions within a construct encoding the P1-2A area. These constructs were expressed in a transient expression assay in either the presence or absence of $3C^{pro}$. The VP2 K217R and the VP3 I2P (2 aa upstream and downstream the VP0/VP3 junction respectively), strongly reduced cleavage of this junction. The VP2 K217E substitution completely prevented cleavage of this junction by the $3C^{pro}$. Both the VP3 Q221P and the VP1 T1P (1 aa upstream and downstream the junction) each severely inhibited cleavage of the VP3/VP1 junction. Interestingly, blocking either of these junctions, did not prevent processing of any other junction within the capsid precursor. Thus, it seems that there is no strict order of $3C^{pro}$ processing of the capsid precursor. The modifications were also introduced into full-length FMDV RNA. However, only the wt and the mutant having the VP2 K217R substitution could be rescued as infectious virus. Higher levels of the VP0-VP3 intermediate were observed within cells infected with the mutant virus. The VP0-VP3 intermediate was not incorporated in either empty capsids or virus particles. Thus, processing of this junction seems necessary for capsid assembly.

Manuscript 3: This manuscript identified a short motif required for correct FMDV capsid precursor processing. Various modifications were introduced into the VP1-coding region of FMDV P1-2A cDNA. Truncations removing the 2A peptide and 27 aa of the C-terminus of VP1, resulted in severe blocking of the processing of both the VP0/VP3- and VP3/VP1 junctions within the capsid precursor. Introducing small deletions identified the region VP1 185-190, as being necessary for correct

processing by the $3C^{pro}$. Five of these aa (YCPRP) are highly conserved among all seven serotypes of FMDV. Furthermore, these residues are also conserved in many other picornaviruses, including poliovirus. Single aa substitutions in the motif revealed that VP1 Y185A and VP1 R188A individually impeded cleavage of both the VP0/VP3- and the VP3/VP1 junctions, which are more than 400 aa and around 200 aa away from the site of modification. Interestingly, this conserved motif can also explain earlier observations on the poliovirus capsid precursor, which is highly resistant to cleavage following truncation (which removed this motif). The results suggest that the identified motif, is important for correct folding of picornavirus capsid precursors and their subsequent processing.

Formål og resumé (objective and summary in Danish)

Mund- og klovsyge (MKS) forårsages af en meget smitsom virus (MKSV), som inficerer klovbærende dyr, heriblandt både vilde dyr og produktionsdyr. MKS er en af de værste infektiøse sygdomme i forhold til landbrugets produktionsdyr. Europa har været fri for MKS i mange år, dog kommer der indimellem udbrud, hvilket forårsager store økonomiske tab for erhvervet i forbindelse med aflivning og restriktioner for handlen med produktionsdyr. I 2001 havde England et alvorligt udbrud af MKS, hvilket blev estimeret til at have kostet i omegnen af 67 milliarder DKK. Siden 1984 har der ikke været nogen udbrud af MKS i Danmark, dog udgør et potentielt udbrud stadig en kæmpe trussel, da det ville have store konsekvenser for det danske landbrug.

MKSV tilhører familien *Picornaviridae*. Viruspartiklen består af en proteinskal, også kaldet et kapsid, som indeholder et positivt enkelstrenget RNA-genom på ca. 8.400 nukleotider. Kapsidet består af 60 kopier af 4 forskellige strukturelle proteiner: VP1, VP2, VP3 og VP4. Disse 4 kapsidproteiner samt et kort 2A-peptid, som ikke inkorporeres i viruspartiklen, bliver dannet ved kløvning af kapsidprecursoren. Denne kløvning foretages af et af virussens egne enzymer, 3C proteasen ($3C^{pro}$). Under dannelsen af viruspartiklen bliver VP0 kløvet til VP4 og VP2, ved en, indtil videre, ukendt proces. Kløvningen af kapsidprecursoren er nødvendig i dannelsen af nye viruspartikler, og derfor også afgørende for virussens livscyklus. Blokering af et af disse kløvningssteder mellem kapsidproteinerne er højst sandsynligt fatalt for virussen, og de kunne derfor være oplagte mål for antivirale midler.

Formålet med denne ph.d. afhandling har været at undersøge aminosyresekvensen nær forskellige kløvningssteder i MKSV kapsidprecursoren i forhold til korrekt kløvning. Derudover har der også været fokus på at identificere en region i VP1, som er vigtig for korrekt kløvning af kapsidprecursoren.

Manuskript 1: Et tidligere studie har vist, at en aminosyreændring, VP1 K210E, (P2 positionen i VP1/2A kløvningsstedet) i MKSV O1 Manisa forhindrede kløvning af VP1/2A. Denne mutantvirus

viste sig at have genereret yderligere en mutation i VP1 E83K. VP1 E83K mutationen blev introduceret alene i MKSV, og denne virus genererede en mutation nær VP1/2A kløvningsstedet, i 2A L2P (på P2´positionen). Også denne mutation viste sig at blokere kløvningen af VP1/2A kløvningsstedet. I dette manuskript, har vi brugt next generation sequencing til at identificere adaptioner i disse to virusmutanter (MKSV VP1 K210E og MKSV VP1 E83K). MKSV VP1 E83K mutanten viste sig at have genereret en mutation i VP1 K210N. Forskellige aminosyrer blev introduceret i MKSV A22 Iraq på VP1 K210 positionen for at identificere, hvilke der kunne tolereres i forhold til korrekt kløvning af VP1/2A kløvningsstedet. Kun positivt ladede aminosyrer på denne position resulterede i at $3C^{pro}$ kunne kløve dette kløvningssted. Både negativt og neutralt ladede aminosyrer blokerede kløvningen af kløvningsstedet.

Manuskript 2: I dette manuskript har vi undersøgt effekten af forskellige substitutioner nær de to kløvningssteder som adskiller kapsidproteinerne. Forskellige aminosyresubstitutioner blev introduceret enkeltvis nær VP0/VP3- og VP3/VP1 kløvningsstederne i et konstrukt som kodede for P1-2A kapsidprecursoren. Disse konstrukter blev udtrykt i celler både alene og sammen med $3C^{pro}$. Substitutionerne VP2 K217R og VP3 I2P (2 aminosyrer før og efter VP0/VP3 kløvningsstedet), reducerede individuelt kløvningen af dette site. Substitutionen VP2 K217E blokerede kløvningen af VP0/VP3 kløvningsstedet. Substitutionerne VP3 Q221P og VP1 T1P (1 aminosyre før og efter kløvningsstedet) blokerede individuelt kløvningen af VP3/VP1 kløvningsstedet. Blokering af ét af disse kløvningssteder forhindrede ikke kløvning af andre kløvningssteder i kapsidprecursoren. De forskellige modificeringer blev også genereret i fuld-længde MKSV RNA. Dog var det kun vildtypen (wt) og mutanten MKSV VP2 K217R der genererede infektiøs virus. Der blev observeret et højere niveau af et mellemprodukt bestående af VP0-VP3 i celler inficeret med denne mutantvirus sammenlignet med celler inficeret med wt virus. Dette VP0-VP3 mellemprodukt blev ikke inkorporeret i hverken tomme kapsider eller i viruspartikler, og det virker derfor sandsynligt, at kløvning af dette VP0/VP3 kløvningssted er nødvendig for dannelsen af kapsidet i viruspartiklen.

Manuskript 3: I dette manuskript har vi identificeret en kort region, som er nødvendig for korrekt kløvning af MKSV kapsidprecursoren. Forskellige modificeringer blev genereret i VP1 regionen i et

konstrukt som indeholdt MKSV P1-2A cDNA. Fjernelsen af 2A peptidet og 27 aminosyre af VP1 C-terminalen resulterede i, at kapsidprecursoren ikke kunne kløves af $3C^{pro}$. Ved at introducere små deletioner i dette område blev det tydeligt, at regionen VP1 185-190 var nødvendig for korrekt kløvning af kapsidprecursoren. Fem af disse aminosyrer (YCPRP) viste sig at være meget konserverede i alle syv serotyper af MKSV. Derudover viste det sig, at dette motiv også var meget konserveret i mange andre picornavirus som fx poliovirus. Enkeltvise aminosyresubstitutioner i dette område afslørede, at VP1 Y185A og VP1 R188A hver især kunne forhindre kløvning af både VP0/VP3- og VP3/VP1 kløvningsstedet. Disse to kløvningssteder ligger hver især henholdsvis mere end 400 aminosyrer og omkring 200 aminosyrer væk fra den modificerede region. Identificeringen af dette konserverede motiv kan forklare tidligere observationer, hvor trunkation af poliovirus kapsidprecursoren (inklusiv fjernelse af det konserverede motiv) resulterede i, at denne ikke kunne kløves. Det virker sandsynligt, at dette nyligt identificerede motiv er vigtigt for korrekt foldning af kapsidprecursoren og for kløvningen af denne.

1. Introduction

1.1. Introduction to and status of foot-and-mouth disease

Foot-and-mouth disease virus (FMDV) infects cloven-hoofed animals including both domesticated animals and wildlife (Alexandersen & Mowat, 2005; Jamal & Belsham, 2013). FMDV infections result in high productivity losses and, as the disease is extremely contagious, it is considered a very important animal health concern worldwide (Grubman & Baxt, 2004). Foot-and-mouth disease (FMD) is one of the most important threats to the agricultural industry as outbreaks are difficult to control, result in trade restrictions and hence have huge economic impact.

The mortality resulting from FMDV infection is low in adult animals but due to the rapid spread, high morbidity and huge devastating economic impact, the disease is one of the listed infectious diseases of the World Organisation for Animal Health (Office International des Épizooties (OIE)) (Grubman & Baxt, 2004). Countries that are a member of the OIE are classified with a particular FMD status, and the FMD control strategy depends on the status of the country. FMDV is able to spread via transport of milk or other animal products and thus disease-free countries have strict controls on imports of such products to prevent entry of the disease to the country (Grubman & Baxt, 2004).

FMD has been eradicated from Europe but it is still endemic in many parts of Africa and Asia (Alexandersen et al., 2003), see Fig. 1. Sometimes outbreaks of FMD occur in previously disease-free areas. The United Kingdom (UK) experienced a huge outbreak of FMD in 2001. More than 10 million cattle, sheep and pigs were slaughtered and burned. The direct cost in compensation to farmers that had lost their animals were estimated to around 1.1 billion pounds, whereas the total costs were estimated to around 8 billion pounds, since the associated effects on trade in the agriculture industry and tourism were also very costly and long lasting (Rowlands, 2017). This outbreak brought FMD back into focus, for at least Europe, which had been free of the disease for many years. Other massive outbreaks of FMD include Taiwan in 1997 where around 40% of the pig population was lost, and Argentina which also had a huge outbreak in 2000-2001 (Rowlands, 2017). The trauma associated with these FMD outbreaks has caused a higher focus on FMDV research, surveillance and control. Indeed, new high containment facilities for working with FMDV have been built in several places around the world, e.g. at The Pirbright Institute in the UK, at DTU National Veterinary

Institute, Lindholm, in Denmark and at Plum Island in the United States (US) (Rowlands, 2017). However, both Denmark and the US are now planning on moving their facilities to the mainland i.e. Copenhagen (Vilhelmsen, 2017) and Kansas respectively (Kingsbury, 2008). However, in 2008 the US Government Accountability Office (GAO) stated that evidence was lacking to conclude that FMD research could be carried out safely on the US mainland. The GAO pointed out that data from earlier releases of FMD from laboratory facilities had not been proper examined. This raised numerous concerns about the danger related to having such facilities on the mainland close to susceptible animals (Kingsbury, 2008). Later on, the National Academy of Sciences suggested that the possibility of FMD release from the laboratories in Kansas was estimated to be around 70% over the next 50 years, most likely due to human error (Walsh & Yeibio, 2010). However, the plan is still for the new FMD facilities in Kansas to open in 2022.

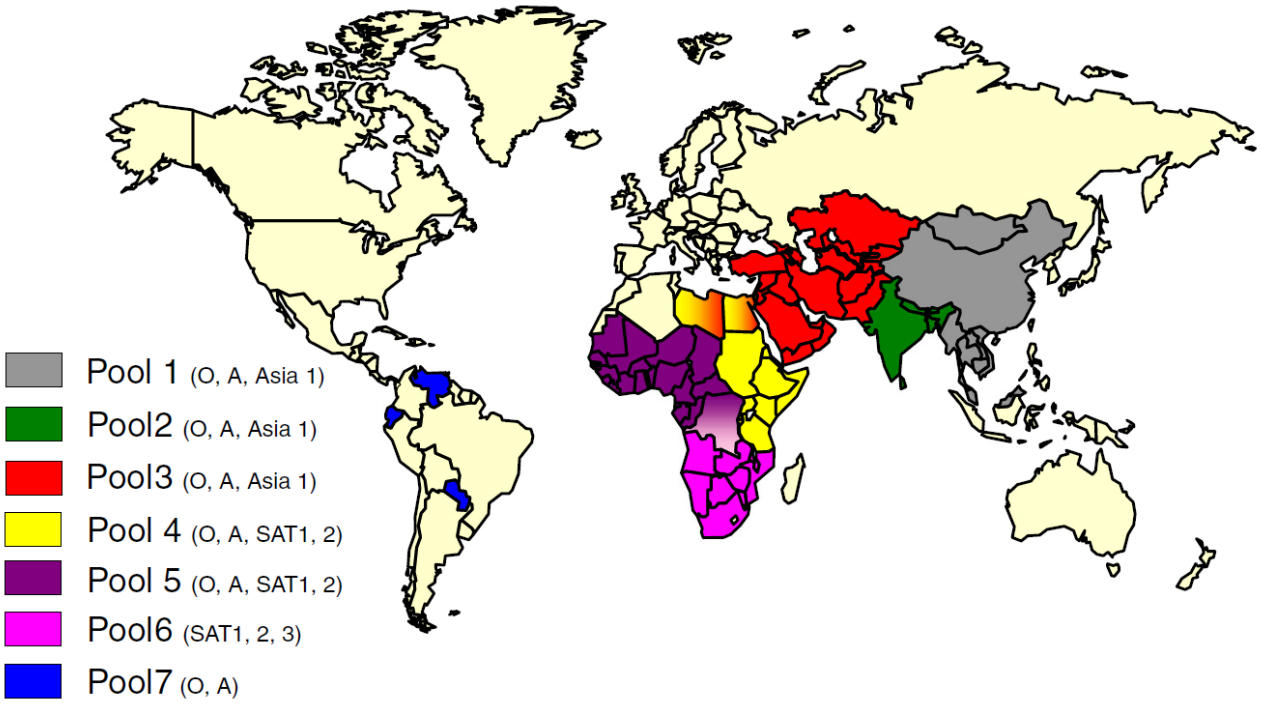

Figure 1 shows the geographical distribution of foot-and-mouth disease virus (FMDV) divided into seven pools. Countries, which are normally free of disease, are marked in beige (Jamal & Belsham, 2013).

FMDV is a small, non-enveloped, single-stranded positive-sense RNA virus belonging to the genus *Aphthovirus* within the large family of picornaviruses. The FMDV RNA genome is about 8,400

nucleotides (nt) in length and is surrounded by a protein shell (capsid), which is roughly spherical and around 25-30 nm in diameter. The capsids consist of 60 copies of four different structural proteins, termed VP1, VP2, VP3 and VP4. Seven different serologically distant serotypes of FMDV exist, namely O, A, C, SAT1, SAT2, SAT3 and Asia-1 (Jamal & Belsham, 2013). There is no cross-protection between these serotypes due to huge sequence diversity and thus significant antigenic variation especially within the capsid coding regions.

Since FMDV is extremely contagious and has huge economic impact, effective surveillance is very important. The first step in good surveillance is based on the observation of clinical symptoms, which include high temperature, excessive salivation, vesicles in and around the mouth and on the feet, resulting in loss of appetite and lameness (Jamal & Belsham, 2013; Nfon et al., 2017). In cattle these symptoms are normally very easy to recognize, whereas it can be rather difficult to detect the disease in sheep due to mild or unapparent signs of infection (Grubman & Baxt, 2004). Furthermore, other diseases such as swine vesicular disease (SVD) and vesicular stomatitis can cause similar symptoms in certain species (Jamal & Belsham, 2013). Upon observation of clinical signs, samples from the suspected cases must be tested by various laboratory techniques to diagnose the disease and if positive, to determine the serotype of the virus. Some of the most widely used techniques for diagnosis include the virus neutralization tests (VNT), enzyme linked immunosorbent assay (ELISA) (for antigen or antibody), reverse transcription-polymerase chain reaction (RT-PCR) and virus passage on cells. The antigen ELISA can be used with an integrin as the capture reagent, since this is able to capture all FMDV serotypes (Rowlands, 2017). Moreover, the primers used in the RT-PCR have to be complementary to the genome of all serotypes. To ensure that the virus concentration is high enough to detect, it sometimes has to be propagated in susceptible cell cultures (Jamal & Belsham, 2013).

FMDV can cause persistent infection in cattle, sheep and goats (i.e. so called carrier animals). Pigs on the other hand, do not become carriers since they clear the infection within 3-4 weeks (persistence is defined as animals being positive for virus for at least 28 days after infection) (Alexandersen et al., 2002). Cattle frequently continue to shed virus after clinical symptoms have

disappeared. In wildlife animals, the African buffalo has been reported to “carry” the virus for up to 5 years (Alexandersen et al., 2002). There has been some controversy over whether FMD is transmissible from long-term carriers. The virus shed from persistently infected animals is often present as virus-antibody complexes. However, infectious virus can be isolated from such samples by removing antibodies with organic solvent (Rowlands, 2017). Over time, there have been a few observations in southern Africa indicating the possibility of transmission from persistently infected buffalo into herds of cattle. However, several controlled experiments were unable to show that the virus could spread to another animal from a persistently infected animal (Sutmoller & Olascoaga, 2002). However, a recent study has shown that exposure of susceptible cattle to oropharyngeal fluid (collected from the throat and then deposited in the pharynx, not injection) from persistently infected cattle caused clinical FMD (Arzt et al., 2018). However, neither this fluid nor tissues harvested from the cattle were able to transmit the infection to pigs.

Another issue is that some vaccinated animals do not show clinical signs following exposure to FMDV but their immune status might not prevent them from becoming carriers. The carrier-issue, with vaccinated animals, has intensely influenced the decisions about not using vaccines unless an outbreak occurs (Alexandersen et al., 2002; Rowlands, 2017). However, in countries where the disease is endemic and control is by vaccination, it is important to be able to discriminate between vaccinated animals and potential carriers. One strategy is to remove epitopes from the vaccine virus without interrupting its protective ability (Fowler et al., 2010, Fowler et al., 2014). Antibodies against the deleted epitope would thereby indicate that the animal had been infected with the wildtype (wt) virus.

1.2. Foot-and-mouth disease virus – a member of the picornavirus family

Picornaviruses are a large family of non-enveloped RNA viruses that includes significant human and animal pathogens. Clinically important picornaviruses in humans include poliovirus, rhinovirus (causing the common cold), echovirus 71 (causing hand, foot and mouth disease and severe neurological disease in children), hepatitis A virus, Coxsackievirus A (also causing hand, foot and mouth disease) and Coxsackievirus B (causing pain and inflammation in the chest), the last two infections can also lead to meningitis or myocarditis. Picornaviruses affecting animals include swine

vesicular virus and foot-and-mouth disease virus (FMDV). The picornavirus family is still growing, and in 2014 consisted of 46 species grouped into 26 genera, the best known being *Enterovirus* (e.g. poliovirus (PV), rhinovirus and coxsackievirus), *Aphthovirus* (e.g. FMDV), *Cardiovirus* (e.g. encephalomyocarditis virus (EMCV) and Theiler's murine encephalitis virus) and *Hepatovirus* (e.g. hepatitis A virus (HAV)) (Jiang et al., 2014). See Fig. 2 for an overview of the picornavirus family, illustrated by a phylogenetic tree.

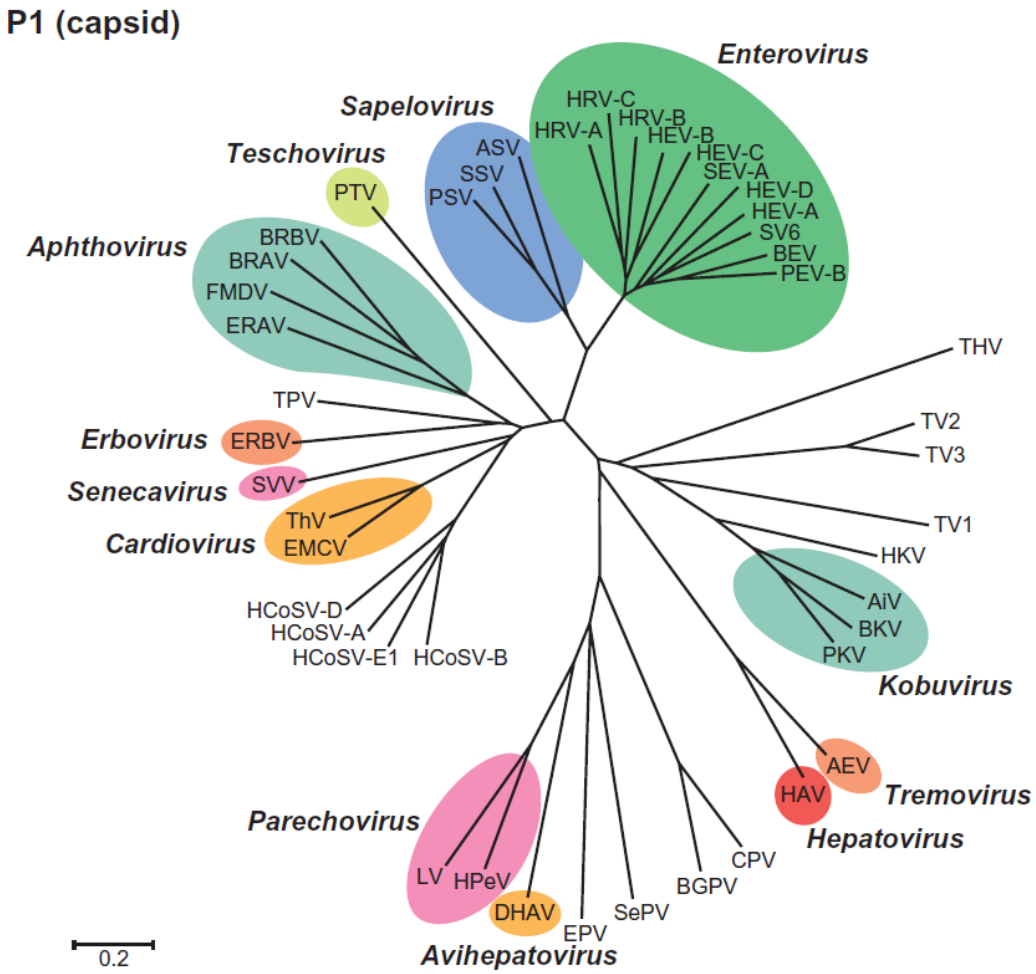

Figure 2 shows a phylogenetic tree of the major genera within the picornavirus family. The tree is based on the amino acid sequence relationships for the capsid precursor. The branch length corresponds to the amino acid substitutions per position (King et al., 2011).

Picornaviruses are approximately 25-30 nm in diameter, and have a capsid with an icosahedral symmetry surrounding a single-stranded, positive sense genomic RNA of approximately 7,100-8,900 nt. Both the 5´ and 3´ terminus of the RNA contain an untranslated region (UTR). A virus-encoded

protein, VPg (3B) is covalently linked to the 5´ terminus. The capsid is comprised of 60 copies of each of the four capsid proteins VP4 (also designated 1A), VP2 (1B), VP3 (1C) and VP1 (1D) with the exception of parechoviruses and kobuviruses in which the VP0 (the precursor of VP2 and VP4) remains uncleaved (Jiang et al., 2014). The capsid proteins VP1, VP2 and VP3 are exposed on the outside surface of the particle while VP4 is located internally (Hogle et al., 1985; Rossmann et al., 1985; Acharya et al., 1989; Jiang et al., 2014).

The receptors used for entering host cells by different picornaviruses are very diverse. PV, Coxsackie B virus and certain rhinoviruses use the immunoglobin (Ig)-like domains as receptors. Other picornaviruses are known to use heparan sulfate, low-density lipoproteins and integrins (Tuthill et al., 2010; MacLachlan & Dubovi, 2017). In addition, the pathway for releasing the RNA into the cytoplasm of the host cell also varies among different picornavirus genera. For instance, when PV interacts with its receptor it causes structural changes in the virus particle, which results in the release of the internal VP4 and the N-termini of the VP1s are re-localized to the surface of the particle. The N-terminus of VP1 is hydrophobic and is (perhaps together with VP4) involved in forming a pore in the cell membrane through which the viral genome can enter the cytoplasm (Tuthill et al., 2010). The FMDV VP1 protein lacks the equivalent N-terminal region present in PV, and thus the entry mechanism for FMDV is different (Tuthill et al., 2010). FMDV enters the host cell through an endosomal pathway by a docking mechanism. The mildly acidic pH within the endosomes causes the capsid to disassemble into pentameric subunits and releases the viral genome (Tuthill et al., 2010) (described in further detail in section 1.5.1.). The specific pathways used by different genera within the picornavirus family might reflect their differences in pH stability, i.e. PV is stable at low pH while FMDV is not (MacLachlan & Dubovi, 2017).

Only the virus genome needs to enter the cell cytoplasm as the RNA is infectious, and can initiate the infection alone. After reaching the cytoplasm, the RNA genome is translated in a cap-independent mechanism in which the ribosome binds via the translation initiation factors, to the internal ribosomal entry site (IRES) within the 5’ UTR of the viral RNA (Martinez-Salas & Belsham, 2017). The RNA contains a single, large, open reading frame that is translated and processing of the encoded polyprotein occurs both during and after translation (Jiang et al., 2014). Three or four

proteins are formed rapidly after the translation, the Leader (not in all picornaviruses), the capsid precursor P1 or P1-2A (depending on the genus), also referred to as the structural protein precursor, and P2 and P3 (the non-structural protein precursors). Many picornaviruses, e.g. members of the *Cardiovirus*, *Hepatovirus* and *Aphthovirus* genera, have a Leader protein at the N-terminus of the polyprotein. In the *Aphthovirus* genus, the Leader protein is a protease (L^{pro}), which is responsible for cleavage at its own C-terminus, thereby separating itself from the P1-2A capsid precursor. Separation of the structural and non-structural proteins in the cardio- and aphthoviruses is mediated at the 2A/2B junction in a protease independent manner during translation, by a process termed "ribosomal skipping" (Donnelly et al., 2001) or "StopGo" (Atkins et al., 2007). In contrast, the 2A protein in enteroviruses is a chymotrypsin-like protease, and is responsible for cleavage at its own N-terminus (at the VP1/2A junction) to separate the capsid precursor from the non-structural proteins (Toyoda et al., 1986; Sommergruber et al., 1989).

The P2-P3 junction and most other protein junctions within these three precursors (P1/P1-2A, P2 and P3) are cleaved by $3C^{pro}$ to produce the mature proteins. However, the P1 capsid precursor of enteroviruses is processed by the 3CD protease ($3CD^{pro}$) (Jore et al., 1988; Ypma-Wong et al., 1988) whereas the $3C^{pro}$ is responsible for cleavage of the P1-2A precursor of cardio- and aphthoviruses into three structural proteins (VP0, VP3 and VP1) plus 2A (Belsham, 2005; Gullberg et al., 2013a). During capsid assembly and usually encapsidation of the viral RNA, VP0 is cleaved (in most picornaviruses) to generate VP2 and VP4 by a process that is currently unknown.

The non-structural proteins, especially the 2C and the 2BC precursor, are involved in relocation of cellular membranes into structures that are essential for the formation of RNA replication complexes (Jiang et al., 2014). The positive sense RNA is used as the template for the synthesis of a negative sense RNA, which in turn is used as template to synthesize more positive sense RNA. The RNA is synthesized by the 3D polymerase ($3D^{pol}$) and requires the uridylylation of a free VPg protein, to function as a primer for both the synthesis of positive- and negative-sense RNA (Belsham, 2005). The newly made positive sense RNA can either be used for translation, as the template for RNA synthesis or as the viral genome in new virus particles (Jiang et al., 2014).

Many picornaviruses are relatively heat stable and may survive for several weeks if protected by saliva or feces and shielded from strong sunlight. The stability of the capsids among different genera are affected differently by pH, and thus certain disinfectants are suitable for some genera but not for other, i.e. sodium carbonate is an effective disinfectant for FMDV but not for SVD virus (MacLachlan & Dubovi, 2017).

1.3. FMDV genome organization

The FMDV particle has a protein shell (capsid) that consists of 60 copies of the four different capsid proteins, VP1, VP2, VP3 and VP4. The VP1, VP2 and VP3 are exposed on the outside of the virus shell, whereas VP4 is internal (reviewed by Jiang et al., (2014)). The capsid serves to protect the viral genome and to deliver it to the cytoplasm of a cell. Each particle contains a single stranded positive-sense RNA genome, which has structures that resemble cellular mRNAs, i.e. with one long open reading frame (ORF) and a poly(A) tail at its 3´-terminus. However, unlike cellular mRNAs, the FMDV RNA has no cap structure at its 5´-terminus. The large ORF encodes a large polyprotein that is rapidly processed, mostly by virus-encoded protease to generate four primary protein precursors, namely the leader (L^{pro}), the capsid precursor (P1-2A) and the two non-structural protein precursors (P2 and P3). These precursors are processed to generate some 15 mature proteins (Belsham, 2005). For an overview of the genome organization, see Fig. 3.

1.3.1. The 5´-untranslated region (5´-UTR)

The 5´-UTR of FMDV is extraordinarily long compared to other picornaviruses, comprising ca. 1,300 nucleotides, whereas PV 5´-UTR only comprises approximately 740 nt and EMCV 5´-UTR around 830 nt (Belsham, 2005). The 5´-UTR can be divided into five different regions, namely the S-fragment, the poly(C) tract, several pseudoknots, the *cis*-acting replication element (*cre*) and the internal ribosome entry site (IRES). An overview of the different regions can be seen in Fig. 4.

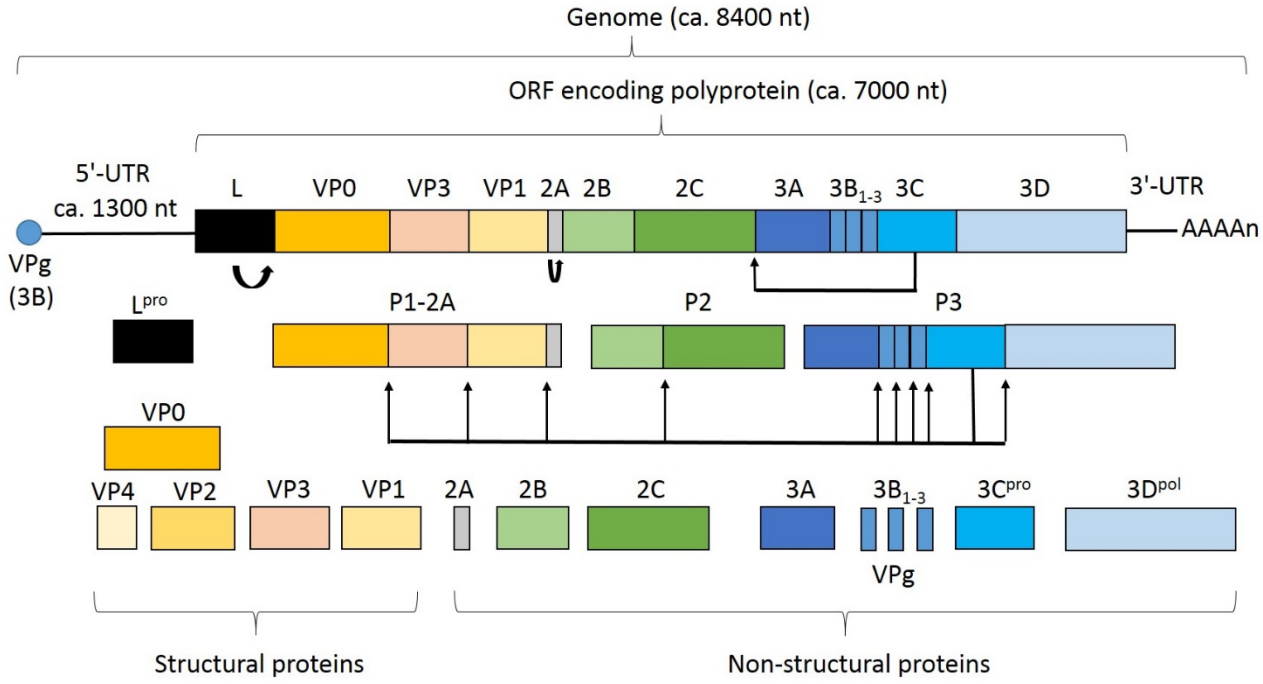

Figure 3 shows the genome organization of FMDV. The RNA genome encodes a large polyprotein. The Leader protease (L^{pro}) cleaves at its own C-terminus. The capsid precursor P1-2A is separated from the non-structural proteins by a mechanism referred to as ribosomal skipping at the 2A/2B junction. The 3C protease ($3C^{pro}$) is responsible for cleavage of all other junctions with the exception of the maturation cleavage of VP0 into VP4 and VP2 (adapted from Jamal & Belsham (2018)).

The first region is the S-fragment, which is around 360 nt and is predicted to fold into a large hairpin structure (Clarke et al., 1987; Escarmís et al., 1992). It is assumed that the S-fragment is required for the viral RNA replication, since the initiation of the positive strand RNA replication will initiate at the S-region complement on the negative strand. It has also been reported that the S-fragment interacts with the cellular RNA helicase A (involved in alterations of RNA secondary structures) and that reducing the level of this protein inhibited FMDV replication (Lawrence & Rieder, 2009). It has earlier been suggested that the S-fragment was involved in host-species specificity. A recent study provided evidence that the S-fragment was involved in the host innate immune response. Interestingly they found that a FMDV$_{-S4}$ A24 mutant, having a 164 nt deletion in the S-fragment was highly attenuated in mice. The mice were given a dose 1,000-fold higher than the one causing lethality by the FMDV A24 wt, and all of these animals survived. Additionally, mice given the high dose of FMDV$_{-S4}$ A24 were protected when challenged with FMDV A24 wt (Kloc et al., 2017). Furthermore, this study found a correlation between the size of the deletion within the S-fragment in different FMDV

mutants and the mutant's ability to cause an increase in the level of interferon-β (IFN-β) mRNA and several interferon-stimulated genes (ISG) mRNAs within infected cells. Moreover, infection of cells with the FMDV$_{-S4}$ A24 mutant caused a higher upregulation of cytokines in comparison with infection with the wt virus (Kloc et al., 2017). Together these results suggest that the innate immune response and the virus pathogenesis in animals is highly affected by the S-fragment.

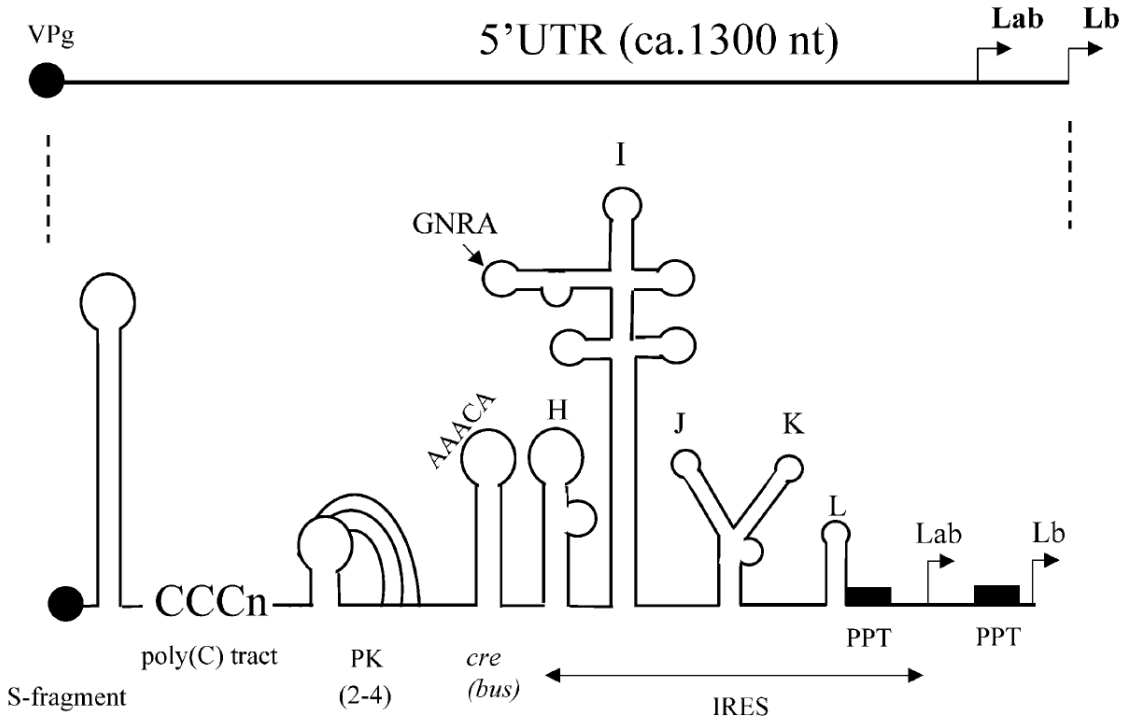

Figure 4 shows the structural elements within the FMDV 5´UTR. From the 5´-terminus, these are: poly(C) tract, pseudoknots (PKs), *cis*-acting replication element (*cre*)/ 3B-uridylylation site (*bus*), internal ribosome entry site (IRES), the polypyrimidine tracts (PPTs) and the two different initiation codons that give rise to Lab and Lb (Belsham, 2005).

The next region is the poly(C) tract. This is a contiguous stretch of cytidines that varies in length among different FMDVs ranging from around 80 nt to 420 nt (reviewed by Martinez-Salas & Belsham (2017)). In general, the shorter regions are found in laboratory strains, whereas field strains typically have a longer poly(C) tract. The exact function for this region is not known, however there is a strong selection pressure for the poly(C) tract in cell cultures (Rieder et al., 1993). A study has introduced infectious RNA transcripts only containing between 6 and 35 C residues into cells, and interestingly upon rescue the poly(C) tract in the replicated RNA had increased to contain around 75 to 140 C

residues. In contrast, RNA transcripts only containing two C residues, did not increase the number of C residues upon RNA rescue; however this virus grew much slower in cell culture compared to the wt. Interestingly, all of the mutant viruses, with various lengths of Poly(C) tract, were equally virulent in mice (Rieder et al., 1993).

The third region of the 5´-UTR is around 250 nt in length, and is believed to contain a variable number of pseudoknots in different FMDVs. One pseudoknot is predicted to be 43 nt in length and interestingly different isolates have been reported to have deletions of either 43 nt or 86 nt within this region, thus it seems that deletions or additions in this specific area always include a full-length 43 nt pseudoknot (Escarmís et al., 1995).

The fourth region is called the *cis*-acting replication element (*cre*), which is a specific stem-loop structure and is required for RNA replication. The stem-loop structure, includes a conserved AAACA motif within the loop, and functions as a template for the uridylylation (attachment of U) to the VPg (3B) (Paul et al., 2000; Gerber et al., 2001; Nayak et al., 2005). The uridylylation generates the primers (VPgpU and/or VPgpUpU) for viral RNA synteses. Interestingly, the *cre* structures are located within different regions of the genome among different picornaviruses, i.e. in the coding regions for VP1, 2A, VP2 and 2C in HRV-14, HRV-2, cardioviruses and PV respectively (Mcknight & Lemon, 1998; Lovert et al., 1999; Goodfellow et al., 2000; Gerber et al., 2001). An earlier study showed that PV bearing lethal mutations in the native structure of the *cre* in the 2C coding region could be restored to replication competency by the introduction of the *cre* at another site within the genome (Goodfellow et al., 2000). The FMDV *cre* is, in contrast to other picornaviruses, located within the 5´-UTR just upstream of the IRES (Mason et al., 2002). Similarly, to PV, the position of the *cre* within the FMDV genome was not found to be important (Mason et al., 2002). Moreover, it was later shown that the *cre* did not have to function in *cis*, since a mutant FMDV with a critical mutation in the *cre* structure could be complemented in *trans* by co-infection with other FMDVs having defects elsewhere in the genome (Tiley et al., 2003).

The fifth region is the IRES, which is responsible for the initiation of translation on the FMDV genome. The IRES is approximately 450 nt in length and is predicted to contain several complex stem-loop structures. The initiation of translation on the FMDV genome occurs by a cap-independent mechanism in contrast to cellular mRNAs that use a cap-dependent mechanism. The cellular mRNAs have a cap structure (m^7GpppN), which is recognized by the initiation factor complex eIF4F and this is necessary for translation initiation. The eIF4F complex comprises other translation initiation factors, i.e. eIF4E (that binds to the cap), eIF4A (an RNA helicase) and eIF4G (involved in binding the small ribosomal subunit to the mRNA). It has been suggested that the small ribosomal subunit interacts with the eIF4F complex and then scans the mRNA until an AUG codon (in a suitable context) is reached. At this point, the large ribosomal subunit joins and translation starts. The scanning can be affected by complex RNA structures and by the presence of other AUG codons. This mechanism is in contrast to the initiation of translation mediated by the FMDV IRES, where the translation machinery is directly recruited to an internal position in the RNA. Due to the properties of the cap-independent translation initiation, FMDV can continue polypeptide translation when cap-dependent translation is inhibited following cleavage of the eIF4G by the L^{pro} (reviewed by (Martinez-Salas & Belsham, 2017)). The IRES-dependent initiation of translation of the FMDV genome does not require the N-terminus of the eIF4G and its associated eIF4E (cap binding protein). The translation is described in further detail in section 1.5.2.

1.3.2. The Leader protease

The Leader protease (L^{pro}) is responsible for cleavage between its own C-terminus and the N-terminus of VP4, i.e. at the L/P1-2A junction. This viral protease is required not only to process the viral polyprotein but also to cleave certain host proteins such as the eIF4G to impair protein synthesis from capped mRNA in the infected cell (Devaney et al., 1988; Gradi et al., 2004). Many other picornaviruses also induce cleavage of the eIF4G during infection, but the cleavage is here mediated by the 2A protease i.e. for entero- and rhinoviruses (reviewed by Belsham (2005)). Two forms of the L^{pro} (Lab and Lb) exist, having different initiation sites (84 nt apart) and thus differing by 28 amino acids in length, see Fig. 4. The exact reason for this is still unclear, however many ribosomes fail to initiate translation at the first AUG codon and are then believed to scan along the FMDV genome to the second AUG codon (Belsham, 1992). Both the Lab and Lb forms of protease

are able to cleave the L/P1-2A junction within the polyprotein and also the eIF4G (Medina et al., 1993). The L^{pro} also stimulates the activity of the IRES, however it has yet not been determined whether this is a direct effect of cleavage of the eIF4G or if the L^{pro} also cleaves other proteins that modify the IRES activity (reviewed by Martinez-Salas & Belsham (2017)).

Another advantage of shutting down host cell protein synthesis, besides taking over the translation machinery, may be the reduction of antiviral response. During an FMDV infection, the α/β interferon mRNAs are induced, likely due to the presence of dsRNA. The blocking of host cell protein synthesis will inhibit synthesis of the α/β interferons and thereby reduce the antiviral response (Chinsangaram et al., 1999).

The Lb^{pro} is not needed for virus viability. A study has shown that it is possible to delete the Lb coding sequence and the mutant FMDV could still replicate in cattle, but displayed reduced pathogenicity (Brown et al., 1996). In contrast to this, FMDV was not viable when the whole Lab encoding sequence was removed. However, removing the 84 nt (between the two initiation sites of Lab and Lb) still produced viable virus, and thus the whole leader encoding sequence can be removed, but not at the same time (Belsham, 2013).

1.3.3. The capsid proteins

The P1-2A is the precursor of the structural (capsid) proteins. The precursor is separated from the rest of the polypeptide at the N-terminus of P1-2A by the L^{pro} (see above). The processing of the P1-2A/P2 junction is mediated by a mechanism that occurs in a co-translational manner, known as "ribosomal skipping" (Donnelly et al., 2001) or "StopGo" (Atkins et al., 2007) (for further details see next section). The $3C^{pro}$ is responsible for cleavage of the P1-2A precursor to generate three mature structural proteins (VP0, VP3 and VP1) and a short 2A peptide. The capsid proteins VP0, VP3 and VP1 remain associated with each other (in a protomer) and assemble into pentamers. Twelve of these pentamers can then assemble around a single RNA molecule to form a virus particle. During this process, the VP0 is cleaved to generate VP2 and VP4 by a mechanism that is currently not

understood. The VP1, VP2 and VP3 proteins are exposed on the capsid surface, contributing to the antigenic properties of the virus and are responsible for interacting with cell surface receptors to promote virus entry into cells (Jackson et al., 2000). The VP4 protein is entirely internal within the virus particle. The pentamers are also able to assemble into empty capsid particles (a particle not containing any RNA) (Abrams et al., 1995; Gullberg et al., 2013b). In empty capsid particles, cleavage of VP0 into VP2 and VP4 can also occur, however unprocessed VP0 is also present in the empty particles (Curry et al., 1997; Gullberg et al., 2013b). The properties of the capsid precursor, the processing of this and the capsid assembly process are described in more detail in section 1.6.

1.3.4. The 2A peptide

Cleavage of the junction between the structural and non-structural proteins, at either the VP1/2A or the 2A/2B junction, is usually mediated by the 2A protein, but the function of the 2A protein varies between the picornavirus genera (Luke et al., 2008). In entero- and rhinoviruses, the 2A protein is a protease, referred to as the $2A^{pro}$, which cleaves at its own N-terminus, i.e. at the P1/2A junction (Toyoda et al., 1986; Sommergruber et al., 1989). In the cardio- and aphthoviruses "cleavage" occurs at the C-terminus of 2A i.e. at the 2A/2B junction. This process is protease independent and happens during translation by a process termed "ribosomal skipping" (Donnelly et al., 2001) or "StopGo" (Atkins et al., 2007). In this case, the 2A protein remains attached to the capsid precursor, as P1-2A, until it is removed by the $3C^{pro}$. The 2A peptide in FMDV is only 18 residues long, in contrast to the 2A protein of cardioviruses, which is ca. 150 residues long. The C-terminus of the 2A proteins from cardio- and aphthoviruses are highly conserved and contain the motif D(V/I)E(T/S)NPG/P (Palmenberg et al., 1992). When the elongating ribosome reaches the end of 2A it skips the synthesis of the peptide bond between the glycine and proline. The eukaryotic translation release factor 1 and 3 are believed to release the protein from the ribosome thereby creating the cleavage between 2A and 2B (Doronina et al., 2008a, Doronina et al., 2008b). A recent study showed that substitutions could be tolerated by the FMDV at the E14, S15 and N16 residue within the 2A sequence, even though cleavage activity for these mutant was only around 30-50% compared to the wt. No FMDV mutants containing substitutions at the P17, G18 and P19 (first amino acid in the 2B protein) could be rescued (Kjær & Belsham, 2018a). In addition to this study it was investigated which amino acids and nucleotides that could be tolerated at these highly conserved

codons for the residues P17, G18 and P19. Each codon was changed to NNN (encoding all different nucleotides thus providing the possibility of different amino acids) in separate constructs. Interestingly, only the wt amino acids were tolerated by the virus at these specific sites, and furthermore there was a clear selection towards the wt codons through several passages (Kjær & Belsham, 2018b). Interestingly, earlier studies has shown that cleavage of the FMDV VP1/2A junction, i.e. at the N-terminus of 2A, is not necessary for capsid assembly and for virus viability (Gullberg et al., 2013a, Gullberg et al., 2014; Kristensen et al., 2016).

1.3.5. The 2B, 2C and the 2BC precursor

Different genera of the picornavirus family have very different 2B proteins, thus it is unlikely that they share similar functions (Martinez-Salas & Belsham, 2017). The 2B protein from PV has been described as a hydrophobic transmembrane protein, which can increase cell membrane permeability and thereby induces the release of virus particles from the host cell (Doedens & Kirkegaard, 1995; Agirre et al., 2002). It has been suggested that 2C is involved in viral RNA replication, as mutations that overcome the RNA replication inhibitory action of guanidine are located in this protein (Saunders & King, 1982). However, exactly how 2C is related to the replication complex is not understood.

The 2B and 3A proteins of PV have individually been reported to block trafficking of proteins to the cell surface (Doedens & Kirkegaard, 1995). Immunofluorescence microscopy showed that the PV 3A protein caused the secreted proteins to be associated with the endoplasmic reticulum (ER), whereas the PV 2B protein caused the secreted proteins to be associated with the Golgi apparatus. Thus, it seems that these two PV proteins inhibit the protein secretory pathway by different mechanisms (Doedens & Kirkegaard, 1995). In contrast to PV 3A, the FMDV 3A protein does not prevent trafficking to the cell surface, but inhibition was observed when the FMDV 2BC precursor was expressed in cells (Moffat et al., 2005). This effect could also be achieved by the co-expression of 2B and 2C. Interestingly, the 2B and the 2C proteins were not individually able to block the trafficking, indicating the importance of the intermediate precursors within a FMDV infection. It is likely that the FMDV 2BC precursor plays a similar role as the PV 2B and 3A protein, which is able to block the

secretory pathway. This will prevent trafficking of interferons and other cytokines and also prevent the presentation of viral peptides on the cell surface, thereby inhibiting immune defenses and contributing to persistent infections (Doedens & Kirkegaard, 1995; Moffat et al., 2005).

1.3.6. The 3A protein

The 3A protein has hydrophobic sequences that enables binding to membranes, which might explain why RNA replication complexes are associated with membrane vesicles. Moreover, the 3A protein has also been suggested to be involved in transporting the 3B peptides to the RNA replication complex (reviewed by Martinez-Salas & Belsham (2017)). The FMDV 3A protein also seems to be involved in virulence and host specificity, since the FMDV strain that caused the outbreak in Taiwan in 1997, which interestingly only infected swine and also had an exceptionally high mortality rate, was found to have a 10 amino acid deletion and several substitutions within the 3A coding region (Knowles et al., 2001). Subsequently, it has been shown that the strain with this deletion grows preferentially in porcine cells and has restricted growth in bovine cells (Pacheco et al., 2003).

1.3.7. The three 3B proteins

The FMDV 3B coding region is unique in that it encodes three non-identical copies of the 3B (termed $3B_1$, $3B_2$ and $3B_3$), whereas other picornaviruses only have one copy. The 3B (VPg) peptide, following uridylyation, serves as a primer for viral RNA synthesis and is attached to the 5´-terminus of both positive and negative sense FMDV RNA. Interestingly all three copies are used equally in the initiation of viral RNA replication (Nayak et al., 2005), but it is not certain whether they have different roles besides initiation of RNA replication. It has been suggested that the VPg3 may be involved in encapsidation (Arias et al., 2010). However, FMDVs that have had one or even two copies of VPg deleted are still able to replicate in cells, but with a lower efficiency than wt virus (Pacheco et al., 2003). Furthermore, the mutant FMDVs, with just a single VPg, produced only a mild disease in pigs, indicating that the copy number of 3B is important in relation to virulence (Pacheco et al., 2003). Furthermore, it was recently shown, using a replicon system that $3B_1$ and $3B_2$ could be deleted, whereas deletion of $3B_3$ alone was detrimental to replication (Herod et al., 2017). However, mutating the uridylated tyrosine residue of $3B_3$ Y2F had no significant effect on replication. This

suggested that the $3B_3$ might have an important role in FMDV replication besides its role as a primer for RNA synthesis. The study demonstrated that $3B_3$ were able to direct the processing of the P3 precursor and thereby control the release of the $3D^{pol}$ (Herod et al., 2017).

1.3.8. The 3C protease

The function of the $3C^{pro}$ is well described. It is responsible for cleavage of most of the junctions within the polyprotein, thereby generating the precursors, processing intermediates and mature proteins. The structure of FMDV $3C^{pro}$ closely resembles the conformation of chymotrypsin (Allaire et al., 1994), and indeed, it belongs to the family of chymotrypsin-like serine proteases, although the serine in the active site is replaced by a cysteine, and thus has Cys-His-Asp/Glu at the active site (Gosert et al., 1997; Birtley et al., 2005; Sweeney et al., 2007). The active site is responsible for the substrate binding and is located between two six-stranded β-barrels (Matthews et al., 1999). The amino acid residues near the cleavage sites are designated as P4 P3 P2 P1 / P1´ P2´ P3´ P4´. In many picornaviruses (e.g. the enteroviruses), the cleavage sites always contain a glutamine residue (Q) at the P1 residue, however FMDV $3C^{pro}$ is able to process junctions containing either a glutamate (E) or a glutamine at the P1 position. The active site is responsible for recognition of the different side chains of the amino acids near the cleavage site. The correct binding and orientation of the polyprotein in the active site are determined by the side chains of the amino acids. During this binding, hydrogen bonds are formed between the substrate and the protease. The S1 pocket of the FMDV $3C^{pro}$ is responsible for binding to the side chain of the P1 residue of the polyprotein (Birtley et al., 2005). The side chains of both E and Q bind in almost the same manner, thus making the FMDV $3C^{pro}$ able to process junctions containing either of these amino acids at this position.

Besides acting as a protease, the FMDV 3C protein also displays an RNA binding function, which is important in relation to the uridylylation of VPg. It was earlier shown that the VPg uridylylation required the $3D^{pol}$, the 3CD protein and the RNA template containing the *cre* (Nayak et al., 2005). Later on, it was found that the FMDV 3C protein was able to replace the 3CD protein for the VPg uridylylation, although the efficiency of the 3C protein was lower than with the 3CD protein (Nayak et al., 2006).

1.3.9. The 3D RNA polymerase

The FMDV 3D protein is an RNA-dependent RNA polymerase. The FMDV has a positive-sense RNA genome, and thus this RNA acts as a template for the initial synthesis of a negative-sense RNA, which is then used for the synthesis of new positive-sense RNA genomes. The 3D polymerase has a preference for the negative-sense RNA template, which might explain the excess of positive-sense RNA over negative-sense RNA within infected cells (Belsham, 2005). The 3´-terminus of the positive-sense RNA is the poly(A) tail, whereas the 3´-terminus of the negative-sense is the S-fragment. The 3D RNA polymerase requires uridylylated 3B (VPg) as a primer to initiate replication (reviewed by Martinez-Salas & Belsham (2017)). The replication mechanism is described in further detail in section 1.5.3.

1.3.10. The 3´-untranslated region (3´-UTR)

The FMDV 3´-UTR contains two components, a heteropolymeric region of around 100 nt and a poly(A) tail. Within the heteropolymeric region, there exist two stem loops that are involved in FMDV replication. Furthermore, deletion of this sequence blocks infectivity of FMDV RNA (Sáiz et al., 2001). Interaction between the two stem loops and sequences within the 5´-UTR has been suggested, the hypothesis is that they contribute to genome circularization during replication (Serrano et al., 2006).

1.4. Quasispecies

The rapid evolution of RNA viruses, including FMDV, is mainly because these viruses replicate with extremely high mutation rate due to the properties of their RNA-dependent RNA polymerases. The RNA polymerase lacks proofreading capabilities in contrast to the mammalian DNA-dependent RNA polymerase that has several different features for proofreading. Continuous error-prone replication leads to extensive genetic heterogeneity of the virus within a single host cell. These mutant-populations are similar but not identical, and are called a quasispecies (Lauring & Andino, 2010). The significant mutation rate allows the virus to adapt more easily to the environment, escape the immune response and evolve resistance towards vaccines and antiviral drugs, a process known as

positive selection. This, in turn, complicates the management and control of the diseases caused by these RNA viruses. In contrast, there is also a risk for the virus, that important biological information gets lost due to these mutations, this process is referred to as negative selection (Domingo et al., 2012).

Viral RNA polymerases have a mutation rate of approximately 10^{-4} (Lauring & Andino, 2010), which means that on average, for every 10,000 nucleotides that are synthesized, one mutation will be introduced. Since the FMDV genome is around 8,400 nucleotides, there will be introduced approximately two new mutations every time the genome is replicated, since synthesis of negative-sense RNA needs to occur, before the synthesis of a new positive-sense RNA. Due to the large virus population in both cell cultures and natural infections, it is estimated that at every site within the genome every possible mutation is generated upon just one passage of the virus in cell culture, and thus will be present within the virus population (Lauring & Andino, 2010).

Thus, RNA viruses exist as a cloud of similar variants that is constantly changing due to new mutations. This also means that the introduction of a defined RNA transcript derived from a unique clone into cells, will quickly evolve into a collection of related viruses. These viruses are the quasispecies, and is based around the consensus sequence. Several rounds of replication can result in a more complex mutant distribution with mutants giving rise to higher levels of variation (Lauring & Andino, 2010), see Fig. 5.

The high mutation rate and the resulting heterogeneity has huge consequences in relation to the virus generating resistance against vaccines or antiviral drugs (Gerrish & García-Lerma, 2003). However, some useful information can also be obtained from this high mutation rate. For instance, in PV a mutation encoding a substitution that causes the capsid to become more unstable has been introduced into a PV clone and introduced into cells. After harvest of the new virus population, several secondary mutations within the capsid-coding region were identified. These new secondary mutations were found to increase capsid stability and were used to increase capsid stability of

empty capsids in relation to a potential vaccine production (Fox et al., 2017). Another study has taken advantage of the high mutation rate to identify a genetic link between two distant sites. In this study, a lysine residue (K) was substituted by a glutamate (E) at residue 210 in VP1 (the P2 residue in the VP1/2A junction) which blocked processing of this junction, and a secondary mutation was observed at VP1 E83K in the rescued virus. Interestingly, introducing this latter substitution alone, caused a new secondary mutation at the P2´ residue in the VP1/2A junction (2A L2P), which also blocked the processing of the VP1/2A junction (Gullberg et al., 2014). The basis for this linkage is still unknown.

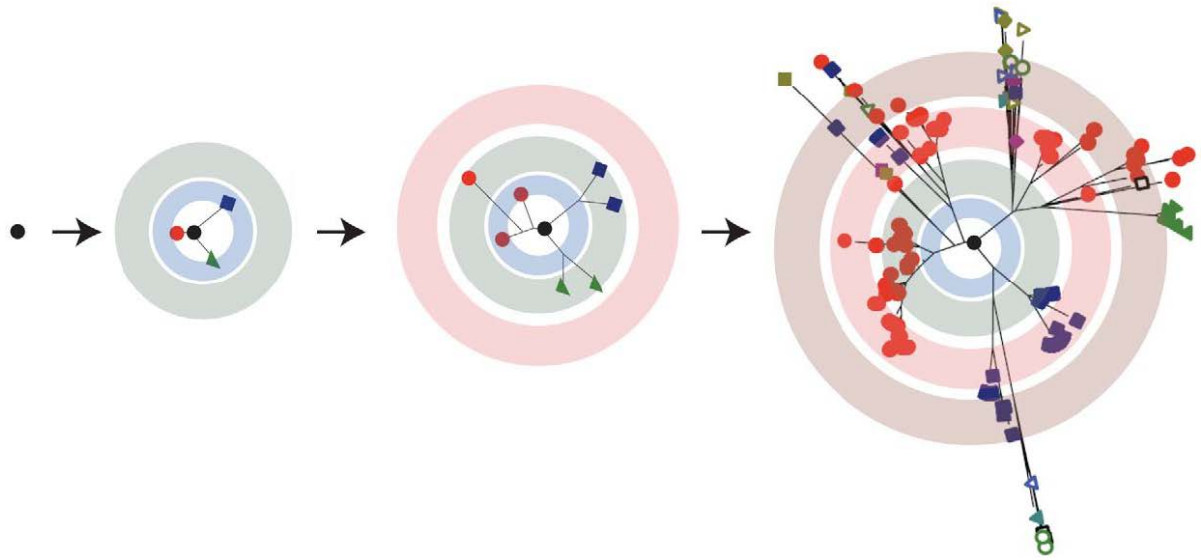

Figure 5 shows an illustration of quasispecies. FMDV replicates with a high mutation rate, which generates a cloud of diverse mutants. Within a few generations there will be a high number of different variants that originate from the first original virus (Lauring & Andino, 2010).

1.5. The FMDV life cycle

FMDV has a relatively short life cycle of around 4-6 hours within cultured cells. The virus causes morphological changes, which include cell rounding and redistribution of internal cellular membranes together referred to as cytopathic effect (CPE) (Grubman & Baxt, 2004). An important feature of the FMDV RNA is that it is infectious (e.g. see Belsham & Bostock, 1988), hence, no viral protein is necessary for the viral RNA to initiate the infection. Thus, the first step after entering into the cytoplasm is to take over the cellular translation machinery to start producing the viral proteins that are required for virus replication. The RNA genome encodes a large polyprotein that is co- and

post- translationally processed into some 15 mature proteins and a variety of precursors. Besides acting like an mRNA for synthesis of the polyprotein, the RNA genome also has to act as template for RNA replication. Initially, negative-sense RNA strands are synthesized, using the positive-sense genome as template. Afterwards, new positive-sense RNA genomes are produced, using the negative-sense RNA molecules as template. The processed capsid proteins assemble around a single infectious RNA genome to produce a new virus particle. Roughly, the infectious cycle can be considered in four steps:

- Attachment and entry
- Translation of the FMDV genome
- Replication of the FMDV RNA
- Encapsidation, maturation and release

An overview of the FMDV life cycle can be seen in Fig. 6

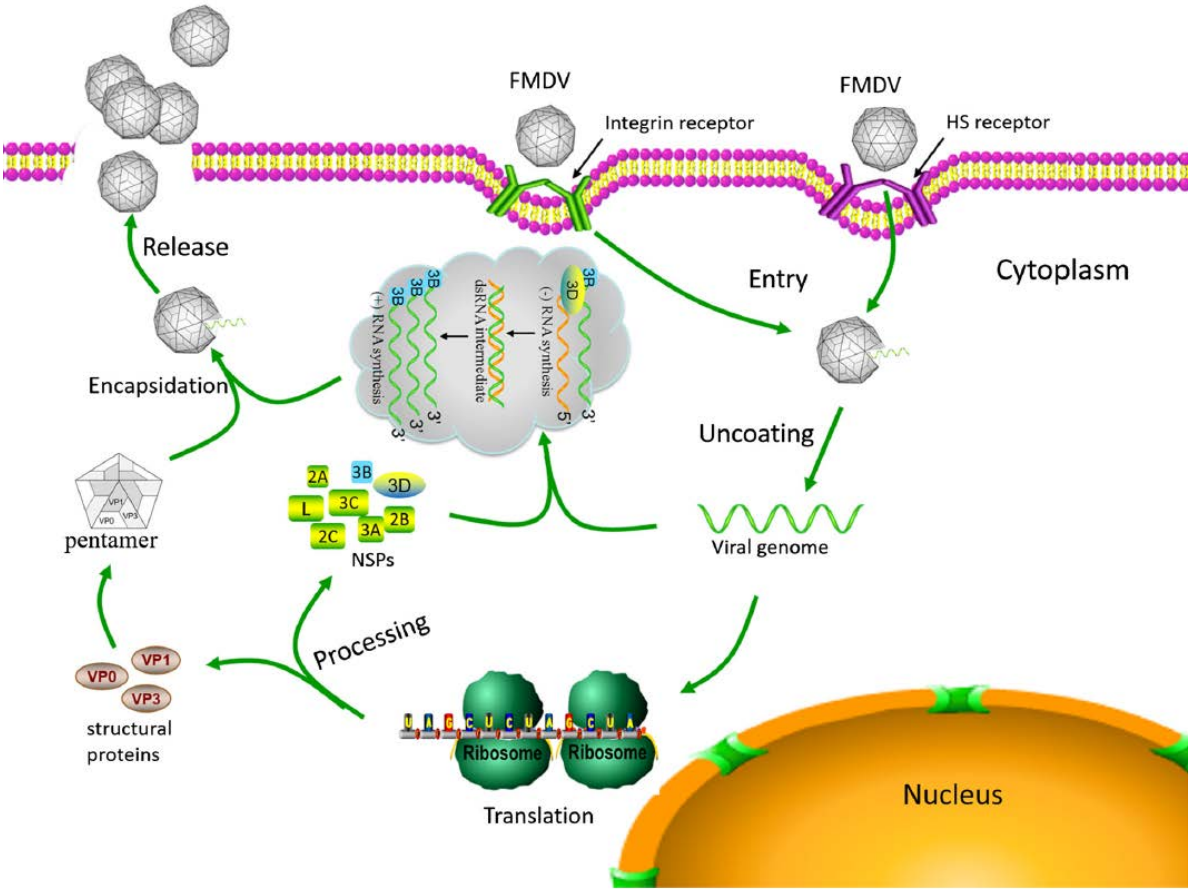

Figure 6 shows the lifecycle of FMDV. The virus can attach to an integrin receptor or the heparan sulfate (HS) receptor. It enters the cell via endocytosis. Within the endosomes there is a mildly acidic

environment, which causes the capsid to disassemble and releases the RNA genome and it enters the cytoplasm. The viral genome is translated and the encoded polyprotein is processed to generate the structural (capsid) proteins and the non-structural proteins (NSPs). The RNA is replicated, and the capsid proteins can assemble around a single stranded positive sense viral RNA genome to form new virus particles. These virus particles are released upon cell lysis (Gao et al., 2016).

1.5.1 Virus attachment and entry into cells

The choice of receptors play a role in tissue and cell tropism and thereby in disease pathogenesis for all viruses. The FMDV can use several receptors from within the large family of transmembrane glycoproteins called integrins (Grubman & Baxt, 2004). These receptors consist of two subunits (α and β) bound to the cell surface and are involved in cell adhesion and lymphocyte interactions. The region of the FMDV capsid involved in attachment to the integrins is present on the VP1 capsid protein. This region is called the G-H loop because it exists as a surface exposed loop connecting the G and H stands of the protein. Within this loop, the sequence is highly variable except for a highly conserved tripeptide sequence, Arg-Gly-Asp (RGD), involved in the interaction with the integrin receptors (Pierschbacher & Ruoslahti, 1984). The first indication that this sequence might be involved in the attachment to the integrins came from a study showing that small peptides, having the RGD motif inhibited virus adsorption in a dose-dependent manner (Fox et al., 1989). Moreover, substitutions within these peptides of any of the three amino acids (RGD) lowered the inhibitory effect (Baxt & Becker, 1990). Later on, it was shown that amino acid substitutions within the RGD motif of FMDV O1 Kaufbeuren (O1K) resulted in FMDV particles that were noninfectious in susceptible cells (Leippert et al., 1997). Another study showed that transfection of an RNA transcript, derived from a full-length cDNA of FMDV A12 with a deletion of the sequence encoding the RGD motif did not result in CPE upon passage on BHK cells. However, some virus particles could be isolated directly from the transfected cells. These virus particles were used to vaccinate steers intramuscularly. Neither of the animals developed any clinical signs of FMD but were protected from FMD upon subsequent virus challenge (McKenna et al., 1995).

Within the family of 24 known integrin receptors, only 8 recognize the RGD motif. However, so far only 4 integrins ($\alpha_v\beta_1$, $\alpha_v\beta_3$, $\alpha_v\beta_6$ and $\alpha_v\beta_8$) have been confirmed to bind to FMDV (Grubman & Baxt, 2004). FMDV can use a co-receptor, depending on the passage history of the individual virus strain;

specifically, field strains of foot-and-mouth disease virus bind to integrins, whereas cell-culture-passaged virus can also use heparan sulfate as a receptor (Jackson et al., 1996).

A study showed that a variant of the serotype O virus having a positively charged Arginine as residue 56 of VP3 could grow in CHO cells that lack the integrin receptors for FMDV. Interestingly this virus was highly attenuated in cattle. However, viruses recovered from animals inoculated with high doses of this virus had lost their ability to grow in CHO cells. Sequencing revealed that the VP3 R53 had been changed to an un-charged amino acid or that a closely positioned residue VP2 134 had been changed from the positively charged lysine to the negatively charged glutamate (Sa-carvalho et al., 1997). Comparison of these animal-derived viruses to other viruses showed that positively charged amino acids were required at both VP2 134 and VP3 53 in order for the virus to bind to the heparan sulfate receptors (Sa-carvalho et al., 1997). Later on, it was shown that another cell-culture-adapted B64 strain of the O1 Kaufbeuren virus (O1K B64), which has had 64 passages in cell-culture was highly attenuated in cattle. However, replacing the surface exposed capsid proteins with those from field strains either the O/UKG/34/2001 (O-UKG), from the outbreak in the UK in 2001, or the A/Turkey 2/2006 (A-TUR), resulted in FMD in the inoculated cattle (Bøtner et al., 2011).

FMDV can also enter cells via Fc receptors if the virus exists as virus-antibody complexes with non-neutralizing IgG molecules. This pathway is of unknown significance, but may be important in the long-term carrier state, where the virus sometimes is shed as virus-antibody complexes (Alexandersen et al., 2002; MacLachlan & Dubovi, 2017).

Upon interaction with one of the integrin receptors, the FMDV can enter the cell through clathrin-mediated endocytosis. The FMDV particle is delivered to the early endosome where they are exposed to a mildly acidic environment. This drop in pH is crucial for the FMDV particle to disassemble into pentamers and thereby release the RNA genome into the cytoplasm (Carrillo et al., 1984). The pentamer interfaces of the FMDV particle are stabilized by β-sheet interactions, which bind the subunits together. The acidic environment within the early endosome changes the

ionization state of the histidine residues at the pentamer interfaces and this, most likely, disturbs the β-sheet interactions causing the FMDV particle to disassemble (Curry et al., 1995). The FMDV particle disassembles into pentameric subunits comprising five copies of VP2, VP3 and VP1. This releases the RNA and the internally located VP4. Pentamers formed during disassembly therefore differ from those formed during the assembly pathway as they lack the VP4 protein (present within VP0 in the assembled pentamers) (Fry et al., 2005).

1.5.2. Translation of the FMDV genome

The FMDV RNA genome is, by itself, infectious and does not bring with it any viral proteins used for either translation or replication. Thus, after the uncoating and release into the cytosol, the first step is for the RNA-genome to associate with the cellular translation system. As mentioned above, the FMDV genome lacks the typical cap-structure at its 5´-terminus, but uses instead the IRES for initiation of proteins synthesis. The IRES is an RNA sequence that consists of complex three-dimensional structures that can function in both *cis* and *trans* (Drew & Belsham, 1994) and recruits the cellular translation machinery. Normally, the cellular capped mRNA is recognized by a trimeric complex of initiation factors called eIF4F that consists of eIF4A (an RNA helicase), eIF4E (a cap-binding protein) and eIF4G (a scaffold protein). Nearly all cellular translation initiation factors are required for the translation initiation of the FMDV genome, with the exception of eIF4E. The L^{pro} and the $3C^{pro}$ induce the cleavage of eIF4G and remove the N-terminus of this protein, which is the binding site for eIF4E (Devaney et al., 1988; Belsham et al., 2000). Thus, translation of the FMDV genome eventually leads to shut down of the cap-dependent translation, and thus the FMDV is able to take over the translation machinery without competing with the cellular mRNA. The C-terminus of eIF4G is not affected by the cleavage and thus retains the binding sites for eIF4A and the 40S ribosomal subunit via eIF3, that is required for IRES-dependent translation initiation, see Fig. 7. During translation initiation on cellular mRNAs, the translation initiation complex scans along the mRNA until it reaches an initiation (usually AUG) codon at which the 60S ribosomal subunit is recruited and protein synthesis starts. In the FMDV genome, translation can start at two separate in-frame start codons, resulting in two different size forms of the L^{pro} (for more details, see section 1.3.2). The full-length polyprotein is never observed within infected cells, as the protein is rapidly processed both co- and post-translationally by the viral encoded proteases, L^{pro} and $3C^{pro}$, and by

the ribosomal skipping process at the 2A/2B junction (this mechanism is described in further detail in the section 1.3.4). The L^{pro} is responsible for the cleavage at its own C-terminus, i.e. at the L/P1-2A junction, while the 2A peptide is required for the "cleavage" at the 2A/2B junction and the $3C^{pro}$ is responsible for the cleavage of the P2/P3 junction. The cleavage of the polyprotein results in four primary products: the L^{pro}, P1-2A precursor, the P2 precursor and the P3 precursor. After this initial processing, all other cleavages are mediated by the $3C^{pro}$, except for cleavage of VP0 into VP2 and VP4. The processing of the P1-2A precursor by the $3C^{pro}$ is explained in detail in section 1.6.2.

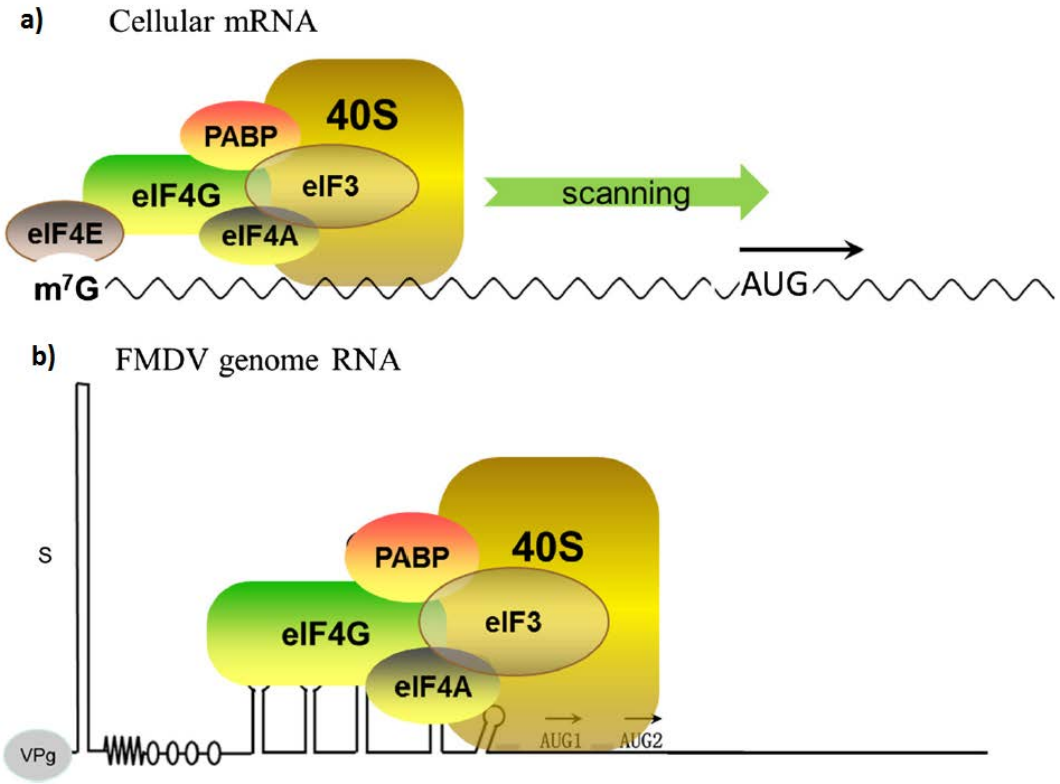

Figure 7: a) intact eIF4G is required for its interaction with the eIF4E cap-binding protein. The cap-binding protein is required for the initiation of cap-dependent protein translation of cellular mRNA. b) IRES dependent translation does not require the cap-binding protein, eIF4E, and can thus initiate translation when eIF4G is cleaved (Gao et al., 2016).

1.5.3. Genome replication

Picornavirus infection causes huge rearrangements of cellular membranes to form replication complexes and the $2BC^{ATPase}$ and $2C^{ATPase}$ are very active in this rearrangement. The replication of viral RNA takes place within these replication complexes that are assembled from several of the viral

encoded non-structural proteins and cellular membranes i.e. the ER and Golgi apparatus. These FMDV replication complexes form in the cytoplasm adjacent to the nucleus and appear to be present in lower numbers compared to other picornaviruses, such as PV (Monaghan et al., 2004).

The FMDV particle has a positive-sense RNA genome and thus the first step in RNA replication is the synthesis of a minus-strand RNA molecule. The switch from translation of the RNA genome to RNA replication, has not been extensively studied in FMDV. However, translation needs to occur prior to synthesis of the negative strand RNA, due to the need for the viral proteins required for the RNA replication. Translation take place from the 5´-end towards the 3´-end and replication vice versa, and it has been shown that the passage of the ribosome along the RNA prevents RNA replication (reviewed by Belsham, (2005)). Thus, it is believed that the translation of the input RNA must be stopped in order for replication to occur. However, the exact mechanism is not known. It is likely, that this switch from translation to replication is mediated by blocking the IRES function of the initial RNA. Once new RNA molecules are generated, these can again function as template for translation. Thus, only a one-way switch is required. It is likely that the translation and replication are separated in the cell in different compartments to limit the amount of competition between the two processes (Belsham, 2005).

In PV the Poly-r(C)-binding Protein 2 (PCBP2) is involved in both replication and translation. The PCBP2 acts as a sequence specific RNA-binding protein to regulate the translation and stability of the target sequence. To make the switch from translation to replication, it has been suggested that the polymerase precursor (3CD) cleaves the PCBP2, which inhibits interaction with the IRES, but does not affect viral RNA replication (Grubman & Baxt, 2004; Chase et al., 2014). However, the FMDV IRES does not seem to require the PCBP2 protein for translation (Grubman & Baxt, 2004), and thus it is likely that other factors contributes to the inhibition of the FMDV IRES.

FMDV RNA replication is initiated at the 3´-terminus of the template RNA strand in a primer-dependent manner. The VPg (3B) protein is uridylylated by the $3D^{pol}$ using the *cre* as a template and

functions then as a primer for the $3D^{pol}$ to initiate replication. Both the FMDV genome and cellular mRNAs have a poly(A) tail at their 3´ termini, and thus the $3D^{pol}$ must be able to distinguish between them. The discovery of the *cre* (cis-acting replication element) provided a possible explanation for the ability of the viral polymerase to distinguish between cellular and viral RNA. The conserved motif AAACA within the stem loop of the *cre* is required for entero- and rhinovirus minus-strand synthesis, where the two first A's serves as a template for the uridylylation of VPg (Mcknight & Lemon, 1998; Goodfellow et al., 2000).

1.5.4. Capsid assembly and RNA packaging

The final step in the FMDV life cycle is the encapsidation of a positive-sense RNA molecule by the viral capsid proteins and the maturation of VP0 into VP2 and VP4. It has been suggested that there exists a *cis*-acting packaging signal within the positive-sense RNA molecule that is involved in the encapsidation (Grubman & Baxt, 2004). This will be described in further detail in section 1.6.5.

The P1-2A precursor is cleaved by the $3C^{pro}$ into the structural proteins VP0, VP3, VP1 and a short 2A peptide. The VP0, VP3 and VP1 remain associated with each other in a protomer containing one copy of each of the capsid proteins. Five protomers then combine to form a pentamer and 12 pentamers can them assemble into the mature capsid. The 12 pentamers either assemble around a single RNA molecule to form a virus particle or they assemble into empty capsid particles without any RNA (Abrams et al., 1995; Gullberg et al., 2013b). One of the final steps that happens during the assembly of the pentamers into a virus particle, is the cleavage of VP0 to generate VP2 and VP4. The VP4 is entirely internal within the virus particle, whereas VP1, VP2 and VP3 are exposed partly on the capsid surface. In FMDV empty capsid particles, cleavage of VP0 into VP2 and VP4 can also occur, however unprocessed VP0 is also present (Curry et al., 1997; Gullberg et al., 2013b; Kristensen et al., 2018). The maturation of VP0 to VP2 and VP4 is important for FMDV particle stability and is required for generation of infectious virus (Knipe et al., 1997). After assembly and maturation of VP0, the host cells are lysed and the newly produced viruses are released. Polyprotein processing and capsid assembly is described in further detail in section 1.6. An overview of the FMDV capsid assembly is shown in Fig. 8.

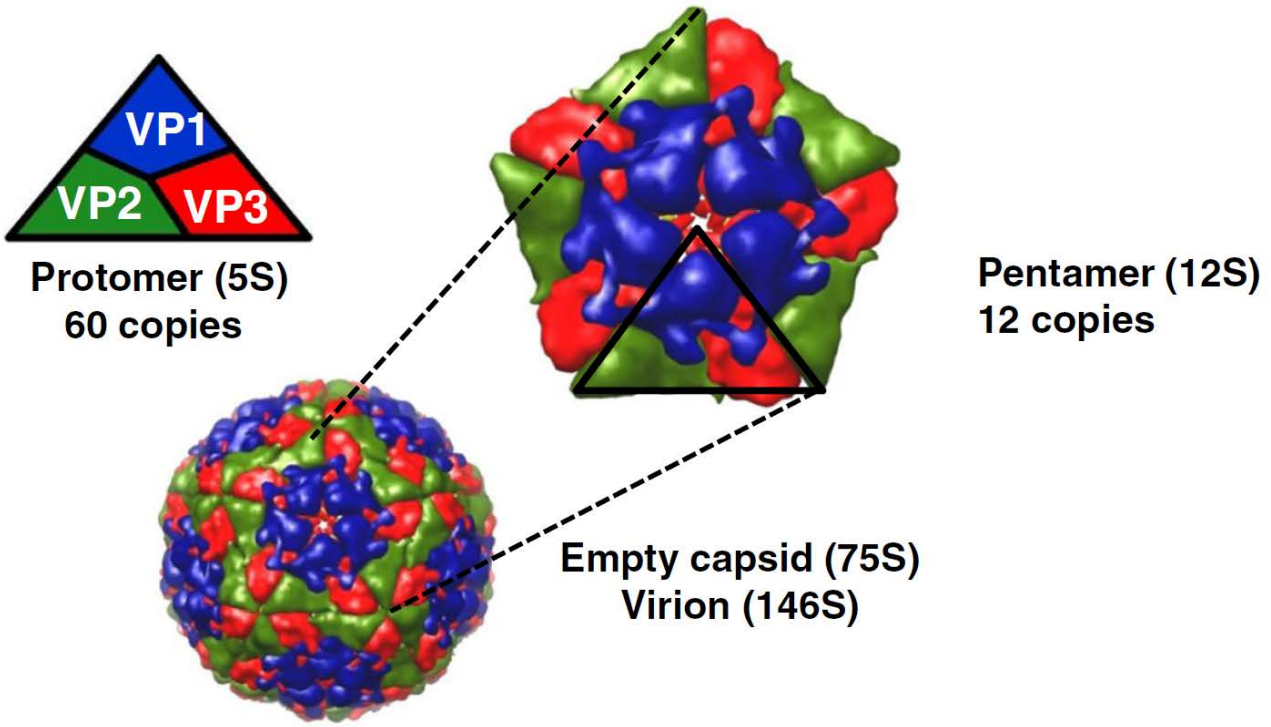

Figure 8 shows an overview of the FMDV capsid assembly process. The P1-2A capsid precursor is processed by the $3C^{pro}$ to generate VP0 comprising VP2 and VP4 (internal), VP3 and VP1, which stay together as a protomer. Five protomers assembles to one pentamer, and 12 of these pentamers can assemble around a viral RNA genome or they can form empty capsids (Jamal & Belsham, 2013).

1.6. FMDV – from polyprotein to virus particle

The FMDV genome encodes a single protein produced from one large open reading frame (ORF). Nevertheless, the full-length polyprotein is not observed within infected cells due to rapid co- and post-translational processing. The separation of the FMDV capsid precursor (P1-2A) from the non-structural proteins occur co-translationally by ribosomal skipping at the 2A/2B junction (Donnelly et al., 2001). The 2A peptide is removed from the P1-2A precursor by the $3C^{pro}$, however removal of the 2A peptide is not necessary for capsid assembly (Gullberg et al., 2013a). The L^{pro} cleaves itself from the N-terminus of the P1-2A precursor. The free N-terminus of the P1-2A precursor contains a myristoylation signal sequence (G X X X S/T) and is myristoylated by a cellular enzyme (Towler & Gordon, 1988).

The cleavage of the capsid precursor into the structural proteins (VP0, VP3 and VP1) is necessary for virus assembly and maturation, however the products never separate but stay together as a protomer. Five of these protomers make up the pentamer subunits, and twelve of these can assemble into either a proviron (contains RNA but still uncleaved VP0) or empty capsids (no RNA). The final event of virus maturation is the processing of VP0 into VP2 and VP4. All of these steps will be described in detail in the next sections.

1.6.1. Myristoylation

The N-myristoylation of the P1-2A occurs co-translationally after the auto proteolytic cleavage by the L^{pro}. The L^{pro} cleaves at either K/G or R/G and thus exposes a glycine at the N-terminus of VP4. In picornaviruses that do not produce a leader protein, i.e. entero- and rhinoviruses, a cellular aminopeptidase removes the initiator methionine residue, which exposes a glycine at the N-terminus of VP1. A 14-carbon saturated fatty acid myristate is covalently attached to the glycine by the host N-myristoyl-transferase.

The myristoylation of proteins is important to determine subcellular targeting, protein-protein and protein-membrane interactions. Blocking of the FMDV myristoylation site does not prevent cleavage of the capsid precursor, but interestingly prevents assembly of empty capsid particles (Belsham et al., 1991; Abrams et al., 1995). The myristoylated N-terminus of VP4 in PV has been shown to participate in stabilizing interactions between the five protomers in the pentamer (Hogle et al., 1985). The lack of myristoylation also reduces the efficiency of receptor binding in FMDV (Goodwin et al., 2009). Furthermore, blocking myristoylation of PV P1 alters the late steps of PV capsid assembly but does not totally prevent it. These resulting PV particles are not infectious, which most likely reflects the inability of un-myristoylated VP4 to penetrate the membrane (Marc et al., 1990). These findings suggest that myristoylation of the capsid precursor and the VP4 N-terminus have an influence on the overall structure of both the precursor, the intermediates and the virus particle. Moreover, since myristoylation is important for protein-membrane interaction, the myristoylation of the capsid precursor might also be involved in directing the capsid precursors to

the membranes where newly synthesized RNA could then associate with the capsid proteins after synthesis (Paul et al., 1987).

1.6.2. FMDV capsid precursor processing by the 3C protease

The FMDV life cycle is critically dependent on correct processing of the polyprotein by the $3C^{pro}$ of specific junctions, which contain non-identical sequences. Within the capsid precursor (P1-2A), the $3C^{pro}$ is responsible for cleavage at the VP0/VP3-, VP3/VP1- and VP1/2A junctions. The cleavages at these junctions occur at different rates, most likely determined by the amino acids flanking the junctions (Zunszain et al., 2010), these amino acids are designated P5 P4 P3 P2 P1/ P1´ P2´ P3´ P4´ P5´.

The FMDV $3C^{pro}$ shows greater diversity in sequence recognition in comparison to many other picornavirus 3C proteins. The FMDV $3C^{pro}$ is able to cleave junctions containing either a glutamine (Q) or a glutamate (E) at the P1 position in contrast to the $3C^{pro}$ from other picornaviruses (like PV and human rhinovirus (HRV)), which only cleave junctions with a Q at the P1 position. The two types of junctions that can be cleaved by the FMDV $3C^{pro}$ are designated as the Q/x and the E/x group, where x is any amino acid. The Q side chain of the P1 residue binds in almost the same manner as the alternative E side chain to the FMDV $3C^{pro}$, thus making the protease able to process both types of junctions (Birtley et al., 2005). The P1 and the P1´ residues are considered the most important for correct processing, however several residues are required for recognition by the $3C^{pro}$, since several P1-P1´ sites that are not cleaved are present within the polyprotein. The specificity of junction recognition is important since slower processing of some sequences, such as the 2B/2C junction, allows intermediate proteins to perform specific functions, which is not possible as mature proteins (Gao et al., 2016). In one study, junctions cleaved by the $3C^{pro}$ have been compared from more than 100 FMDV strains (Carrillo et al., 2005). These junction sequences were, later on, divided into two groups according to their P1 residue (E or Q) (Curry et al., 2007), see Fig. 9, which gave an indication of the important amino acids for each junction group.

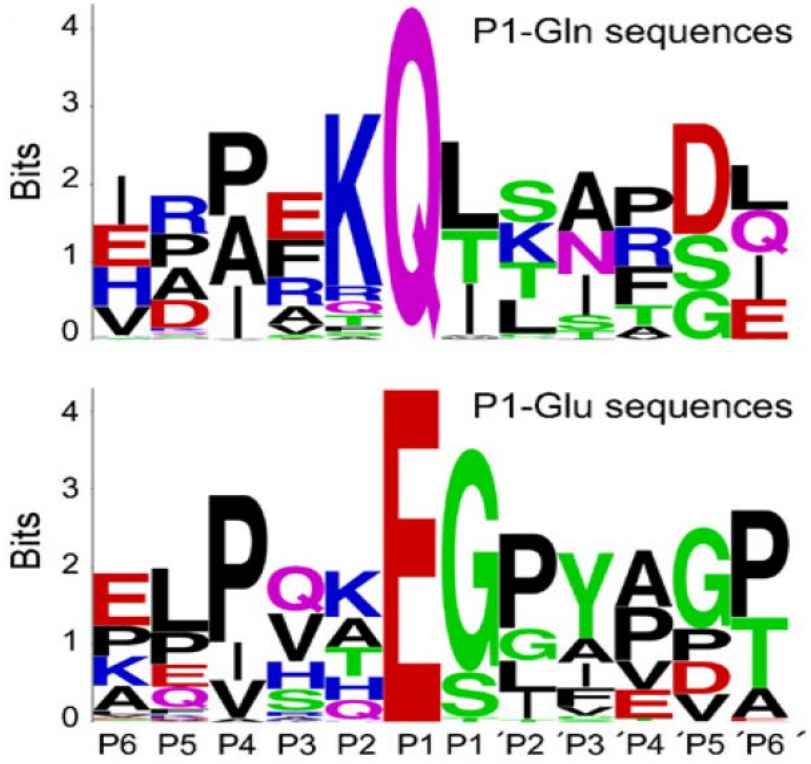

Figure 9 shows a logo plot of the amino acid sequences cleaved by the FMDV 3C protease. Sequences from over 100 FMDV strains (Carrillo et al., 2005) were aligned and split into two groups according to the nature of the P1 residue (i.e. the Q/x- and the E/x groups) (Curry et al., 2007).

The binding of a short peptide corresponding to the VP1/2A junction to the $3C^{pro}$, revealed that the alanine (A) positioned at residue P5 is largely solvent exposed. The sidechains of this residue point towards residue 143 methionine (M) of the $3C^{pro}$, but is not close enough to make contact. Substituting this P5 A to either arginine (R) or proline (P) only caused a two-fold reduction of $3C^{pro}$ activity, whereas substituting the P5 A to a leucine (L) did not have any major effect. The lack of contact most likely accounts for the finding, that this residue only had modest effect on the peptide cleavage activity (Zunszain et al., 2010).

In the Q/x group sites (e.g. at the VP1/2A junction), $3C^{pro}$ seem to have a preference for either a P, A or isoleucine (I) at the P4 position (Curry et al., 2007). The binding of a short peptide corresponding to the VP1/2A junction, which has a P at the P4 residue, to the $3C^{pro}$, revealed that this residue is

partly buried in the peptide binding grove, only exposing one C atom. This residue interact with sidechains from $3C^{pro}$ L142 (residue cysteine (C) 142 from the wt was substituted to L to make the $3C^{pro}$ more soluble), valine (V) 140 and tyrosine (Y) 190 (Zunszain et al., 2010). Interestingly, substituting the P4 P, to either a V, Y or L, completely prevented cleavage by the FMDV $3C^{pro}$ using a peptide cleavage assay. This was a bit surprising because these amino acids have sidechains of similar size and also because A and I are both found in the P4 position in other junctions belonging to the Q/x group. However, removing or introducing a P within a peptide/protein often results in a drastic change due to the very different structure of P compared to other amino acids. Furthermore, V is found at this position in several junctions belonging to the E/x group (Birtley et al., 2005; Zunszain et al., 2010).

A wide variety of amino acids (V, Q, E, histidine (H), phenylalanine (F), serine (S), R and A) are present as the P3 residue both within the Q/x and E/x groups (Curry et al., 2007). In common for all of these are that they most likely are able to make hydrophobic contacts with the side chain of $3C^{pro}$ M143 located within the β-ribbon (Zunszain et al., 2010). However, variation from a P3 A to either a Q, E or V (which is tolerated at this site in other FMDV junctions, including the Q/x group), within a short peptide corresponding to the VP1/2A junction, reduced the cleavage activity 5-10 fold. This might be due to the larger side chains of these amino acids, compared to the A, which might affect the positioning of the β-ribbon, thereby affecting interaction with other substrate residues (Zunszain et al., 2010). These findings indicate that correct cleavage is dependent on the amino acid sequence flanking the junction, and that one amino acid can have a huge impact on cleavage activity even though it is tolerated at other junctions belonging to the same group.

The grouping of the Q/x and E/x junctions revealed that junctions with a Q at the P1 position typically also had a lysine (K) at the P2 position (Curry et al., 2007). Using a short peptide corresponding to the VP1/2A junction revealed that the K at the P2 position made contact to the H46, L142 and M148 of the $3C^{pro}$. Moreover, the K also made salt bridges from the amine group to the side chains of aspartic acid (D) 144 and D146 within the $3C^{pro}$. The formation of one of the pockets within $3C^{pro}$, seems to be dependent on substrate binding, since L142, D144 and D146 within the $3C^{pro}$, adjust

their position upon binding to the substrate. Substitution of the P2 K to norleucine, which is similar to K but lacks the amine group prevented cleavage. Substitution of the P2 K to an R reduced cleavage by around 4-fold (Zunszain et al., 2010).

The P1 Q, of the VP1/2A junction forms three hydrogen bonds to the S1 pocket of the $3C^{pro}$ (Zunszain et al., 2010). Interestingly, the P1 Q, which is found in many other FMDV junctions, binds in approximately the same manner as the P1 E, thereby explaining the tolerance of FMDV $3C^{pro}$ for either amino acid at this specific site. Indeed, the Q in a short peptide corresponding to the VP1/2A junction can be substituted to E, which only reduced cleavage activity by two-fold (Birtley et al., 2005; Zunszain et al., 2010). Changing the P1 Q to either R or D completely prevented cleavage (Zunszain et al., 2010).

Large hydrophobic amino acids (i.e. L, I or threonine (T)) at the P1´ within the Q/x junction group (Curry et al., 2007) also seem to be of high importance for cleavage activity. Substituting the P1´ L to either glycine (G) or C, in the Q/x group, using a peptide cleavage assay, reduced cleavage activity of FMDV $3C^{pro}$ to around 10% and 50% respectively (Zunszain et al., 2010). Interestingly, the FMDV often has a G at the P1´ position when the P1 residue is E. Thus, also this amino acid seems to be affected by the overall sequence flanking the junction for correct positioning in regard to $3C^{pro}$ cleavage. The binding of the P1´ leucine in a short peptide corresponding to the VP1/2A junction binds in an unusual manner. Upon binding of the $3C^{pro}$ to the peptide, a pocket is formed where the P1´ leucine is incorporated. This pocket in $3C^{pro}$ is only present upon binding to the substrate (Zunszain et al., 2010).

There is a high variability of the amino acids at the P2´ positon within both the Q/x and the E/x groups, see Fig. 9 (Curry et al., 2007). The P2´ L in the short peptide corresponding to the VP1/2A junction binds at one end of the peptide-binding grove (Zunszain et al., 2010). The E/x group often has a P at the P2´ residue, but interestingly substituting the P2´ L to a P within the VP1/2A junction (Q/x group) within full length FMDV completely prevented cleavage of this junction (Gullberg et al.,

2014). However, it should be noted that a P is never present at this residue within the Q/x group, see Fig. 9.

Also the P3´ residue has a high sequence variation within both the Q/x and the E/x group, see Fig. 9. In the case of the short peptide corresponding to the VP1/2A junction, the P3´ L is almost completely exposed on the surface of the enzyme. However, it is positioned to form hydrogen bonds with residue E50 of the $3C^{pro}$ surface (Zunszain et al., 2010). However, several of the other amino acids found at this position would not be able to maintain the interaction with residue E50 of the $3C^{pro}$ (Zunszain et al., 2010), and thereby, it is unlikely that this interaction is of high importance for cleavage activity.

Also the P4´ residue has a high sequence variation within the two groups of junctions, see Fig. 9. In a short peptide corresponding to the VP1/2A junction the P4´ F is highly solvent exposed, with the exception of a small apolar contact with the upper surface of the C-terminus of one of the β-barrels. Moreover, substituting the P4´ F to R, P or A, which all have apolar features, only had a small effect on the cleavage activity (Zunszain et al., 2010).

The conformation of FMDV $3C^{pro}$ closely resembles the structure of chymotrypsin (Allaire et al., 1994), and indeed, it belongs to the family of chymotrypsin-like serine proteases. However, the S in the active site is replaced by a C, and thus has C163-H46-D84/E at the active site (Gosert et al., 1997; Birtley et al., 2005; Sweeney et al., 2007). The active site is located between two six-stranded β-barrels and binds to the polyprotein junction (Matthews et al., 1999). A two-strand β-ribbon structure folds over the peptide binding cleft, where it makes important interactions with the substrate, thereby contributing to substrate specificity (Matthews et al., 1999; Sweeney et al., 2007). The C142 within the $3C^{pro}$, which is located at the tip of the β-ribbon, seems to have a significant effect on the catalytic activity of the $3C^{pro}$.

The FMDV $3C^{pro}$ C142 maps closely to the position in the structure of the HRV2 3C residue L127. This suggests that these two amino acids in the different picornavirus genera play a very similar role. Indeed, both amino acids have a hydrophobic functional group, and it is suggested that this side chain is involved in positioning the substrate via interactions with the sidechains of the P2 and P4 residues (Sweeney et al., 2007). This hypothesis was further strengthened by the finding that substituting the P2 L to either T or R remarkably reduced cleavage, and substituting the P4 P to either V, L or I completely blocked the cleavage of these peptides (described as unpublished data in Sweeney et al. (2007)). Furthermore, substituting the FMDV 3C 142C to a S had no effect on substrate specificity in small peptide cleavage assay but caused a significant downregulation of $3C^{pro}$ activity (around 1% of wild type activity) (Sweeney et al., 2007). However, substitutions to other amino acids such as T, A or V, which are more apolar compared to the S had less effect on the proteolytic activity of the $3C^{pro}$. Interestingly, substituting this residue to an L, which is highly hydrophobic enhanced the catalytic activity of the $3C^{pro}$ compared to the wt (Sweeney et al., 2007). Later, studies have used the 3C C142S substitution in transient assays for cleavage of the P1-2A precursor, where the reduced activity of this mutant $3C^{pro}$ was verified (Polacek et al., 2013).

The peptide sequences flanking the junction are highly important for correct processing by the $3C^{pro}$, however the overall structure of the P1-2A precursor is also highly important for correct processing. Truncating the P1-2A precursor, by removing the 2A and 42 residues of the C-terminus of VP1 blocked the processing of both the VP0/VP3- and the VP3/VP1 junction, even though the sequence flanking the junctions were un-modified (Ryan et al., 1989). Similarly, truncating the P1-precursor of PV also blocked the processing of the mature capsid proteins by the PV $3CD^{pro}$ (Ypma-Wong & Semler, 1987). We recently showed that processing of the three junctions were mutually independent (Kristensen et al., 2018), see result section publication 2, indicating that the blocking of the cleavage at these two junctions, observed in the earlier studies, was likely due to an overall structure change in the precursor, rather than blocking of one junction thereby affecting the other junction. This observation will be further addressed in the result section in publication 3.

1.6.3. Assembly of the 5S protomers into the 12S pentamer

After the processing of the P1-2A precursor into VP0, VP3, VP1 and the short 2A peptide, the structural proteins (excluding the 2A peptide) remain together as a 5S protomer. Five of these protomers then assemble to form a 12S pentamer. Pentamers from different picornaviruses migrate with different rates through a sucrose gradient i.e. FMDV pentamers migrate at 12S while PV pentamers migrate at 14S. Myristoylation of the capsid precursor in many picornaviruses (with the exception of hepato- and parechoviruses) seems to stabilize the structure at the 5-fold axis symmetry of the virus particle. Interestingly, blocking myristoylation of the PV P1 precursor, by changing the G at VP4 residue 2 to an A prevents the formation of the PV pentamers (Ansardi et al., 1992). The assembly of correct FMDV 12S pentamers is also dependent on N-terminal myristoylation of the P1-2A precursor, as abnormal pentameric assembly (approximately 17S) occurred upon lack of myristoylation (Goodwin et al., 2009). In infected cells, incompletely myristoylated pentamers are believed to be excluded from virus particles.

The C-terminus of the capsid precursor of different genera within the picornavirus family differ regarding the presence, or absence, of the nonstructural protein 2A. In the enteroviruses, such as PV, the 2A protein is not included in the capsid precursor P1. In contrast, in other picornavirus genera, i.e. aphtho-, cardio- and hepatoviruses the 2A protein remains attached to the capsid precursor as P1-2A. The 2A protein plays an important role in hepatovirus capsid assembly. The HAV P1-2A precursor is cleaved by the HAV $3C^{pro}$ to generate VP0, VP3 and VP1-2A, which associate into pentamers. In HAV empty capsids and immature virus particles, the 2A is exposed on the surface of the particle, while in the mature HAV particle that contain the RNA, almost all 2A proteins have been removed by an unidentified cellular protease. Interestingly, deleting approximately 40% of the N-terminus 2A protein abolished HAV infectivity (Cohen et al., 2002). Transient expression of this HAV P1-2A mutant, revealed that the N-terminus of 2A was required for both efficient cleavage of the P1-2A precursor by $3C^{pro}$ and for assembling of the protomers into pentamers. These data indicate that the 2A protein plays an important role in relation to correct capsid precursor folding, to allow efficient processing by the $3C^{pro}$ (Cohen et al., 2002). In contrast to HAV, the FMDV P1 does not require the 2A protein for association of the protomers into pentamers (Goodwin et al., 2009). However, the formation of pentamers is not affected upon blocking of this junction (Goodwin et al.,

2009), and indeed, the pentamers containing the uncleaved VP1-2A junction can assemble to form infectious virus particles (Gullberg et al., 2013a).

1.6.4. Assembly of the 12S pentamers into 75S empty capsids

A prominent feature of the many picornavirus infections is the co-occurrence of several kinds of intermediate particle assemblies, e.g. protomers, pentamers and empty capsids. Structural studies, using x-ray crystallography, has only been reported for few picornavirus genera empty capsids, whereas many mature picornavirus structures have been determined. Empty capsids, contain 12 pentamers, like the virus particle, but no RNA genome. Empty capsids have been identified in cells infected by several picornavirus infections including entero- and aphthoviruses (Maizel Jr et al., 1967; Korant et al., 1975; Rowlands et al., 1975). The empty particles are formed from twelve pentamers, and are believed to assemble in a concentration dependent manner (Li et al., 2012). Interestingly, some FMDVs are more likely to form empty capsid than others i.e. especially the FMDV A22 Iraq tends to form many empty capsids (Abrams et al., 1995; Curry et al., 1997). It is generally believed that five protomers can self-assemble into a pentamer and that twelve of these pentamers can assemble into empty capsids or a virus particle. However, the mechanism governing the self-assembly leading to an empty capsid is poorly understood.

The myristoylation state also seems to be important for the FMDV empty capsid formation. Expression of the FMDV P1-2A (wt) precursor and the $3C^{pro}$ generated empty capsid particles. However, substituting the S to an A within the myristoylation signal sequence (G X X X S) blocked the formation of empty capsids even though the P1-2A precursor was efficiently processed by the $3C^{pro}$ (Abrams et al., 1995). However, based on this study, it is not possible to conclude, whether this interruption of the myristoylation signal blocked the formation of pentamers or the assembly of pentamers into empty capsids.

Using PV and bovine enterovirus (BEV), particles sedimenting at 45S have been reported, it is not clear whether these 45S particles are intermediates between the 14S pentamers and the 80S empty

particles (Su & Taylor, 1976; Rombaut et al., 1985). Although BEV is extremely cytopathogenic in cell cultures, the number of mature virus particles produced are relatively low. The study by Su & Taylor (1976) showed that the BEV infection resulted in the production of a high amount of 80S empty capsids, and a lesser amount of 160S mature virus particles, 130S provirons, 45S particles, 14S pentamers and 5S protomers. Interestingly, at high ionic strength the 45S particles were transformed into the 80S empty capsids, using pulse-chase experiments. In contrast, no precursor-product relationship was established from the 45S and 80S to the mature virus particles (Su & Taylor, 1976).

Several alternative hypotheses have been proposed for the presence of empty capsids. One hypothesis suggests that empty capsids are a precursor to the mature virus (Jacobson & Baltimore, 1968), into which the RNA can be inserted, as is the case for many bacteriophages (Black, 1989). Other studies have reported that the empty capsids can disassemble into pentamers, which led to the hypothesis that empty capsids are a storage form of pentamers, which are the direct precursors that assemble to form the virus particle (Nugent & Kirkegaard, 1995). One study has shown in a cell-free replication system, that only PV pentamers can interact with newly synthesized RNA to form mature virus particles (Verlinden et al., 2000). This suggest that empty capsids are just an excess of capsid proteins and thus a dead end product, that is formed when there is a temporary or continuing lack of newly produced viral RNA (Verlinden et al., 2000).

The true role of empty capsids within infected cells remains unknown. However, these empty capsids has proven useful for the formation of recombinant vaccines against FMDV (and other picornaviruses). For these vaccines, the capsid precursor, P1-2A, has been expressed together with the virus encoded protease, $3C^{pro}$ (Roosien et al., 1990; Lewis et al., 1991; Abrams et al., 1995; Gullberg et al., 2013b, Gullberg et al., 2016; Polacek et al., 2013; Porta et al., 2013). In addition, PV has been of interest with regard to the production of empty capsids for a vaccine. However, due to insufficient stability of the PV empty capsids, a possible vaccine using this strategy has only recently been achieved (Fox et al., 2017). This study took advantages of a known substitution in the type 3 Sabin vaccine strain that destabilizes capsid assembly intermediates, including the empty capsids,

without affecting stability of the mature PV (Macadam et al., 1991). Thus, the candidate residues for stabilizing the empty capsids were chosen based on observed secondary mutations in this strain, which increased the stability of assembly intermediates including empty capsids. Similarly, stabilizing mutations in type 1 and 2 strains were identified following introduction of this destabilizing mutation. This study was able to generate stable empty capsids for all three serotypes, which each generated high levels of protective antibodies in animal models (Fox et al., 2017).

1.6.5. RNA encapsidation - assembly of twelve pentamers into the proviron

Two different mechanisms for RNA encapsidation has been suggested. One is that pentamers assemble around a single RNA genome and form the proviron, and the other is that the RNA genome is inserted into an empty capsid (Jiang et al., 2014). One study that supports this first mechaninsm has shown that pentamers have RNA binding activity and that the binding of RNA to the pentamers alters their conformation. In addition, the same study showed that the empty capsids did not display any RNA binding activity (Nugent & Kirkegaard, 1995). These findings clearly supported the theory that the pentamers were the direct precursor for the proviron for RNA encapsidation. The theory was further strengthened when another study showed that both PV 5S protomer and 14S pentamers could be cross-linked with viral RNA associated with the PV replication complex (Pfister et al., 1995). Later on, a study showed that only PV pentamers interact with the newly synthesized RNA to form virus particles (Verlinden et al., 2000).

The exact mechanism of packaging of picornavirus RNA is still unclear, and especially the issue of which signals are necessary for RNA encapsidation remains unsolved. The picornavirus capsid, only encapsidates positive-sense RNA, linked to a VPg, thereby excluding all cellular RNAs (Nomotot et al., 1977; Grubman & Baxt, 2004). Moreover, only newly synthesized PV RNA genomes are encapsidated (Nugent et al., 1999), thereby also explaining the close association of capsid pentamers with the replication complex (Pfister et al., 1995). It is generally believed that there is one, or more, *cis*-acting packaging signal(s) present within the positive-sense RNA genome to enable encapsidation. For PV, the packaging signal does not appear to be present within the P1 coding area, since this region could be deleted (in defective interfering (DI) particles) and the RNA genome was

still packaged into PV capsids within co-infected cells (Kajigaya et al., 1985; Hagino-Yamagishi & Nomoto, 1989). In contrast, no DI particles have been detected in FMDV infected cells (Clarke & Spier, 1983). However, the complete P1 coding region from a number of picornaviruses, including FMDV can be replaced with a reporter gene, thus generating a replicon (McInerney et al., 2000). In this study, trans-encapsidation of this RNA lacking the FMDV P1 coding region, was also investigated, and found to be extremely inefficient (McInerney et al., 2000). Interestingly, the PV replicons (lacking the P1 coding area) can be encapsidated when capsid proteins are provided by transfecting the cells with a recombinant vaccinia virus that expresses the PV capsid protein P1 (Ansardi et al., 1994). Moreover, another study pointed out that a PV replicon (encoding firefly luciferase instead of the VP2-VP3-VP1 area) could be encapsidated by PV P1 from all subtypes (type 1, 2 and 3), but were not encapsidated when capsid proteins were provided from another picornavirus, i.e. BEV, coxsackievirus A21 or B3, or enterovirus 70 (Porter et al., 1998). These data, suggest that the packaging signal does not exist within the P1 coding area of PV RNA and that specific packaging signals are present for individual picornaviruses.

The first study to report a *cis*-acting encapsidation region within the picornavirus family, identified a stem-loop structure located in the 5´ end of the genome of a newly discovered picornavirus, Aichi virus. This stem-loop was shown to be highly important for encapsidation of the viral RNA (Sasaki & Taniguchi, 2003). PV is one of the most studied viruses within the picornavirus family but, as yet, no such RNA packaging signal has been identified within the PV genome. In addition, the $2C^{ATPase}$ (part of the replication complex) has been suggested to be implicated in the insertion of RNA into PV particles, via protein-protein interactions with the VP3 capsid protein (Liu et al., 2010). However, recently a study identified contacts between the RNA genome and the capsid of human parechovirus from the crystal structures, and these areas within the RNA genome have been confirmed as RNA packaging signals (Shakeel et al., 2017). Interestingly, a recent study has identified several places within the FMDV genome that might be important for RNA encapsidation (Logan et al., 2018). This study took advantage of the properties of the FMDV RNA-polymerase, which lacks proof-reading function and thereby introduces errors, resulting in a virus population with closely related RNA molecules. Cells infected with the FMDV were lysed to generate a sample containing both packaged and unpackaged genomes. From a portion of this sample, virus particles were

purified by ultracentrifugation through a sucrose gradient to obtain a sample of only packaged genomes. Deep sequencing was applied for both the total population of viral genomes (both packaged and un-packaged genomes) and for the purified virus particles, only containing the packaged genomes. Comparing these data, made it possible to identify several places in the RNA genome that might be important for RNA packaging. Three specific areas, within the L^{pro} and P1 coding sequence were chosen for further investigation. Interestingly, introducing silent mutations, which altered predicted stem loop structures within all three areas, significantly reduced the yield of FMDV. In contrast, no reduction was observed for the yield of empty capsids and protomers/pentamers, indicating that these areas of the genome are important specifically for RNA packaging (Logan et al., 2018).

1.6.6. The maturation cleavage of VP0 into VP4 and VP2

As with the empty capsids, the relevance of the proviron in relation to the virus assembly process is not completely elucidated. Early observations with PV had suggested that the proviron was an intermediate precursor of the mature virus (Fernandez-Tomas & Baltimore, 1973). However, these results has proven difficult to reproduce, and it is still not clear whether these particles are actual intermediates or are dead-end products in the assembly pathway.

The cleavage of VP0, also referred to as the maturation cleavage, to generate VP4 and VP2 is usually considered to occur during or after encapsidation of the viral RNA. However, the cleavage is not completely dependent on RNA encapsidation, since VP2 and VP4 are also observed in FMDV empty capsids (Curry et al., 1997; Gullberg et al., 2013b). However, a much higher level of cleaved VP0 (i.e. as VP2 and VP4) is found in the virus particles containing RNA. In PV particles, containing RNA, one or two copies of VP0 are thought to remain uncleaved and are present in the virus capsid as VP0 (Jacobson & Baltimore, 1968).

The outer surface of the protein shell in the empty capsids, provirons and the mature virus particles are very similar. The major differences are in the internal structure where many stabilizing

interactions that are present in the mature virus particle are missing in the empty capsids and provirons. Since the VP4/VP2 cleavage site is located on the internal side of the virus particle, thereby isolated from cellular and viral proteases, it is considered an autocatalytic event (Arnold et al., 1987).

The cleavage site in PV at the VP4/VP2 junction contains a motif of three amino acids, P, H and Q. In PV, the proline has been predicted to cause the amino acid chain to kink at this position, which allows water molecules to cause hydrolysis of the scissile band thereby separating the VP4 and VP2 proteins (Basavappa et al., 1994). In most FMDVs the VP4/VP2 junction has the sequence A-L-L-A/D-K-K-T (Carrillo et al., 2005), thus there is no proline at this junction, and it seems that processing of the FMDV VP2/VP4 junction occurs by a different mechanism than for the one suggested for PV. An earlier study suggested that a conserved serine at residue 10 within VP2 was involved in the cleavage of VP0 in several picornaviruses (Arnold et al., 1987). However, a couple of years later this theory was rejected, since substituting the serine to either a cysteine or alanine within PV did not affect VP0 cleavage (Harber et al., 1991). The RNA encapsidation has also been suggested to be necessary for cleavage of VP0 (Arnold et al., 1987). However, since FMDV empty capsids have been reported to contain some level of cleaved VP0 as VP2 (and VP4) (Curry et al., 1995, Curry et al., 1997; Gullberg et al., 2013b) whereas unassembled material predominatly had the intact VP0. Thus, it seems that the RNA encapsidation is not essential for this processing and perhaps it is the assembly process itself that is necessary to permit cleavage. So, the exact mechanism of cleavage at the VP4/VP2 junction remains unknown.

1.6.7. The FMDV particle

The structure of different picornaviruses has been solved by x-ray crystallography, e.g. PV (Hogle et al., 1985), HRV (Rossmann et al., 1985) and FMDV (Acharya et al., 1989). The structure is iscohedral and has 2-, 3- and 5-fold axes of symmetry (see Fig. 10). The VP2, VP3 and VP1 are located externally on the virus particle while VP4 is completely internal. The structures of VP2, VP3 and VP1 are very similar to one another and each of these proteins contain eight β-strands that are arranged to make up a β-barrel. The mature FMDV particles, containing an RNA genome and processed VP0, i.e. VP4

and VP2, are generally more stable than the empty capsids, which mostly contain unprocessed VP0 (Curry et al., 1995, Curry et al., 1997).

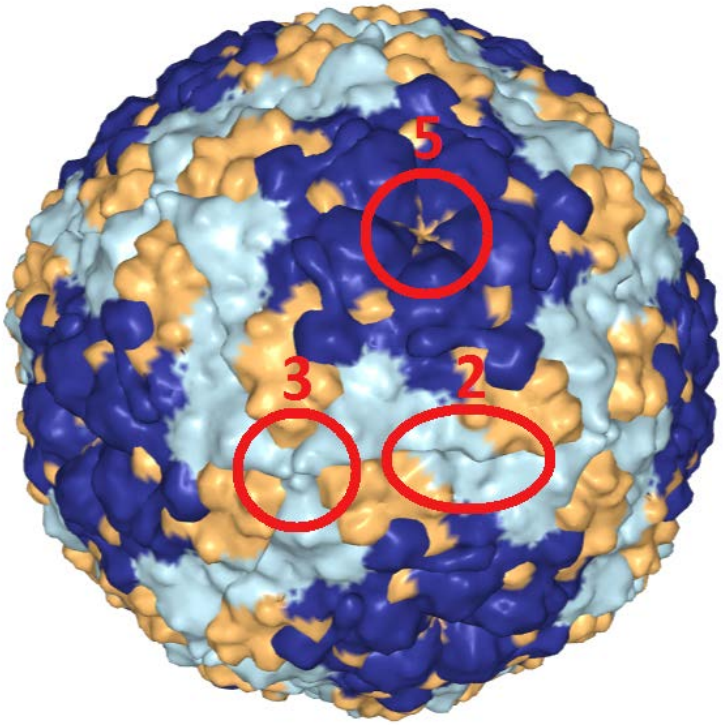

Figure 10 shows the structure of the FMDV A22 Iraq (PDB 4GH4) (Curry et al., 1996). The 2-, 3-, and 5-fold axes are marked with a red circle and indicated with the respective number.

The structure of the mature virus particles within the different picornavirus genera are very similar but clearly differences exist. The VP1 proteins (shown in dark blue) are clustered around the five-fold axes of symmetry, while VP2 (shown in light blue) and VP3 (shown in yellow) are clustered around the three-fold axes, see Fig. 10 (Hogle et al., 1985; Acharya et al., 1989). In PV, there is a sunken area, referred to as the "canyon", around the five-fold axes below VP1. The canyon is involved in receptor binding. In cardioviruses there is a series of smaller sunken areas, referred to as "pits", which also are involved in receptor attachment (reviewed by Tuthill et al., (2010)). The FMDV particle has a much smoother surface, and in contrast to several entero- and cardioviruses the FMDV has a flexible G-H loop, involved in receptor binding, sticking out from the surface of VP1 (Acharya et al., 1989; Logan et al., 1993). The structure of the entero-, cardio- and aphthoviruses are shown in Fig. 11. The FMDV does not have any major canyon or any pits as observed in the

entero- and cardioviruses. This might be because the structural proteins are substantially smaller in FMDV, and thus the protein shell is thinner. The FMDV VP1 protein comprises 211-213 residues (depending on serotype), whereas the VP1 of HRV14 and PV comprises 279 and 306 residues respectively.

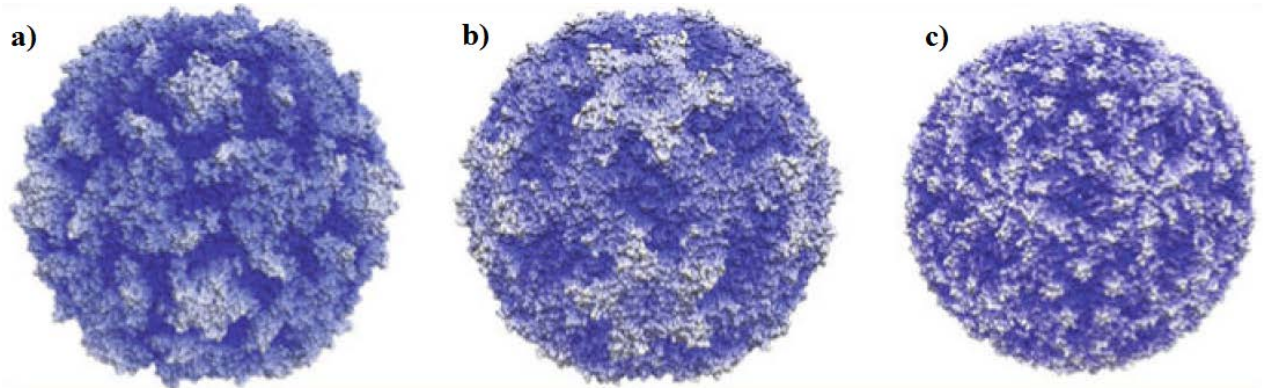

Figure 11 shows the structure of a) poliovirus (enterovirus), b) encephalomyocarditis virus (cardiovirus) and c) foot-and-mouth disease virus (aphthovirus). The dark blue represents the innermost surfaces and the white represents the outermost surfaces (Tuthill et al., 2010).

The pentamer interfaces of picornaviruses are stabilized by β-sheets between subunit junctions. A characteristic feature of FMDV is their extreme sensitivity towards low pH. When the pH is reduced to below 6.8 the FMDV is inactivated. The inactivation is caused by pentameric subunit dissociation, thereby releasing the RNA and VP4 (Brown & Cartwright, 1961; Burroughs et al., 1971). The pH sensitivity of FMDV is likely to be governed by the switch of the protonation state of a cluster of histidines at the pentameric boundaries (Vlijmen et al., 1998). The protonation, at low pH, of several histidine residues, but in particular H142 and H145 within VP3, is believed to disturb inter-pentamer interactions thereby causing capsid disassembly (Curry et al., 1995; Vlijmen et al., 1998; Fry et al., 2005). The location of these two histidine residues, in particular, at the interfaces of the pentameric subunits of the particle provides a possible explanation for the high acid sensitivity of the virus.

The knowledge of the structure of the virus has also had benefits in relation to the design of novel vaccines since modifications of selected residues at the pentamer boundaries has resulted in viruses

with higher thermostability (Mateo et al., 2008). Moreover, the knowledge of the structure has also been used to modify the virus by removing specific epitopes to create a marker vaccine (allowing discrimination between vaccinated and previously infected animals) (Fowler et al., 2011).

1.6.8. The involvement of cellular chaperones in the viral life cycle

Chaperones, including heat shock proteins (Hsps) exist in different cellular compartments, where they assist in protein folding, maturation, protein complex assembly and protein trafficking. The ability of cellular proteins to carry out specific functions is highly dependent on their correct folding. Furthermore, the correct folding is also necessary to prevent the proteins from degradation by the proteasome that removes misfolded proteins (reviewed by Geller et al. (2012)).

Proteins in the Hsp90 family are highly abundant within cells. There exist two mammalian cytoplasmic Hsp90 isoforms, one is the stress-induced Hsp90α, and the other one is the Hsp90β, which is constitutively expressed. In the ER, there is a Hsp90 homologue, called Grp94 and another homologue called TRAP1 is present within the mitochondria (reviewed by Geller et al. (2012)). Hsp90 is an ATPase, meaning that it accomplishes its role through a complex cycle regulated by the breakdown of ATP into ADP and a free phosphate ion as well as by interaction with numerous co-chaperones. The hydrolysis of ATP releases energy that is used to drive the folding of the target protein (Jhaveri et al., 2012). In the cytoplasm, the Hsp90 is involved in the maturation, folding and localization of a large set of proteins. In contrast to other chaperones, Hsp90 does not appear to interact with newly translated proteins (Geller et al., 2012). Instead, Hsp90 receives the target protein from other chaperone systems, where the protein has already been partially folded. For instance, protein kinases first interact with the Hsp90 co-chaperone Cdc37 (Pearl, 2005), and for steroid receptors, Hsp70 binds first and then another co-chaperone transfers the target protein to Hsp90 by interacting with both chaperone systems (Kimmins & MacRae, 2000; Geller et al., 2012). Besides being involved in the maturation and folding of various target proteins, Hsp90 and Hsp70 have also been shown to be important in relation to degradation of some proteins. Protein homeostasis depend on a balance between correct protein folding and protein degradation. The ability of chaperones to facilitate protein degradation is mediated by interactions with co-

chaperones such as the carboxyl terminus of Hsp70-interacting protein (CHIP). CHIP binds to both the Hsp70 and Hsp90 and is able to facilitate the targeting of proteins to the proteasome system (Dickey et al., 2008; Edkins, 2015). Thus, it seems that there is a fine line between correct protein folding and protein degradation that helps the cells to rapidly remove misfolded proteins. The protein substrates for Hsp90 are highly diverse. Hsp90 is required for many proteins and protein complexes. The protein targets include proteins involved in transcription, translation, mitochondrial function, membrane trafficking, signal transduction and cell division (Geller et al., 2012). Hsp90 is thought to be involved in the maturation of proteins that are already partially folded, and may also act to stabilize or remodel these proteins. For some protein complexes, Hsp90 appears to facilitate their assembly by stabilizing the unstable subunits and to be involved in the incorporation of the specific components into the protein complex. For other protein complexes, Hsp90 promotes change in the structure of the assembled complex. However, in both cases, Hsp90 does not appear to be part of the final assembled protein complex (Makhnevych & Houry, 2012).

Viral proteins, like cellular proteins need different chaperones to achieve their correct function and indeed a wide variety of both DNA and RNA viruses require chaperones to facilitate entry, genome replication, translation and assembly (Geller et al., 2012). Viruses have a very limited coding capacity, and thus they rely on different cellular factors to complete their replication cycles. Furthermore, due to the limited coding capacity of the viral genome, viral proteins often carry out several functions, which suggests that they might be structurally complex. The viruses often rapidly produce a large amount of these structurally complex proteins and thus it is likely that several different chaperones are involved in their folding (Geller et al., 2012). In addition, the viral precursor proteins are highly dependent on correct folding to enter a state that makes them accessible for processing and to avoid degradation by the proteasome. This has been proven to be essential for the P1 capsid precursor of PV, which is rapidly degraded upon inhibition of Hsp90 (Geller et al., 2007).

Using specific Hsp90 inhibitors has been shown to reduce the replication of diverse viruses *in vitro.* For example, Hsp90 appears to be important in the regulation of viral polymerase function in the

case of herpesvirus (Burch & Weller, 2005) and hepatitis B virus (Hu et al., 1997), whereas it seems to be required for capsid processing in different picornaviruses (Geller et al., 2007; Newman et al., 2017). The virus capsid is a complex structure and must be stable both within the host and outside it. Thus, the virus capsid must tolerate different environmental conditions but also be able to disassemble upon entry into cells to initiate new infections. Hsp90 is known to be involved in the folding of different picornavirus capsid precursors (Geller et al., 2007; Newman et al., 2017). In PV, the P1 capsid precursor has been found to interact with Hsp90 (possibly together with Hsp70), and likely in conjunction with its co-chaperone p23, and was found to be required for the processing of this precursor into the capsid subunits. Interestingly, neither of the other PV precursors, P2 and P3, seemed to interact with Hsp90 and in addition, the inhibition of Hsp90 did not prevent cleavage of the other viral protein precursors (i.e. P2 and P3). Thus, it is likely that Hsp90 is required for the PV capsid precursor to obtain the complex folding that enables recognition and cleavage by the viral protease (Geller et al., 2007). Furthermore, the interaction between Hsp90 and P1 is believed to protect the P1 capsid precursor from degradation by proteasomes (Geller et al., 2007). Similarly, it has recently been shown that Hsp90 is required for efficient growth of FMDV in cell cultures and for the P1-2A capsid precursor processing (Newman et al., 2017). This indicates that the FMDV capsid precursor is also highly dependent on this chaperone to obtain the correct conformation. An overview of the involvement of Hsp90 in the folding of the capsid precursor is shown in Fig. 12. Interestingly, the capsid precursor of HAV is not sensitive to the inhibition of Hsp90 (Aragonès et al., 2010), which suggest that HAVs might use other mechanisms for correct folding of its capsid precursor.

Among the many protein targets of Hsp90 are proteins involved in cell division including proteins related to tumorigenesis (Whitesell & Lindquist, 2005). As these cancer-related proteins are highly dependent on Hsp90, specific Hsp90 inhibitors have been suggested to act as cancer treatments. Several different pharmacological inhibitors of Hsp90 have been identified. These include Geldanamycin (GA) and the GA analogues 17-allyl-17-demethoxygeldanamycin (17-AAG) and 17-desmethoxy-17-N,N-dimethylaminoethylaminogeldanamycin (17-DMAG). These inhibitors function by competing with ATP for binding to the ATP-binding domain of Hsp90 (Jhaveri et al., 2012). These inhibitors are currently undergoing clinical evaluation for their use as an anticancer treatment and

results indicate that they have potential as cancer therapy against a wide variety of oncogene-related cancer types (Wang et al., 2016). Furthermore, the involvement of Hsp90 of various virus species has raised the possibility of using non-toxic doses of Hsp90 inhibitors as broad-spectrum antiviral agents against a variety of human and animal viruses.

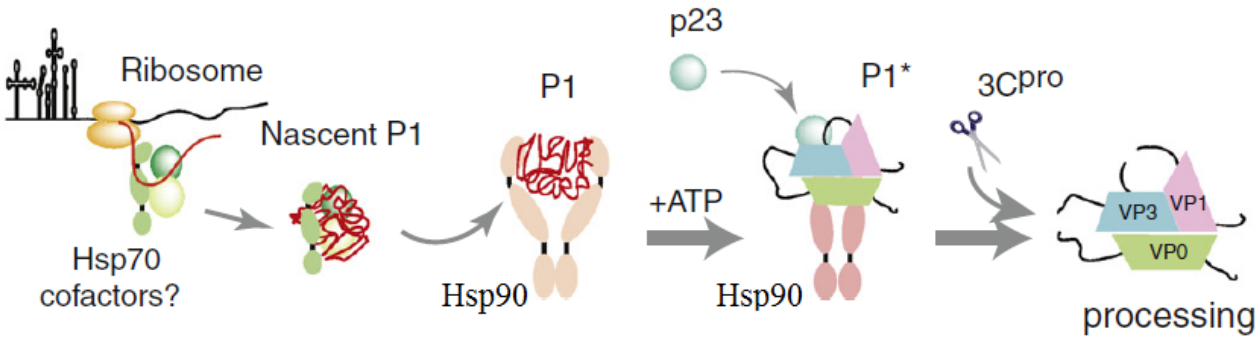

Figure 12 shows the possible involvement of Hsp90 and its co-chaperones in the folding of the picornavirus capsid precursor (in this example for the poliovirus capsid precursor). Hsp90 interacts with the P1 precursor, and is required for the precursor to achieve its correct conformation prior to its subsequent processing (Geller et al., 2012).

2. Thesis outline and aim

2. Thesis outline and aim

This Ph.D. study has focused on different factors required for FMDV capsid assembly and in particular for capsid precursor processing. The studies leading up to the three manuscripts were based on these three aims:

I. Analysis of role of the sequences flanking the VP1/2A junction in full-lengh FMDV A22 Iraq. The aim was to determine the effect of various amino acid substitutions at VP1 K210, for correct processing of this junction. The study was based on an earlier study, showing that the VP1 K210E substitution in FMDV O1 Manisa severely blocked processing of this junction (Gullberg et al., 2013a).

II. Analysis of the role of the sequences flanking the VP0/VP3- and the VP3/VP1 junctions. The aim of this study was to identify the effect of different amino acid substitutions adjacent to the two junctions separating the capsid proteins. Moreover, we wished to determine whether there was a strict order for processing of the junctions, i.e. the VP0/VP3-, VP3/VP1-, and VP1/2A junction.

III. Based on two earlier studies that showed that C-terminal truncation of the capsid precursor in both PV and FMDV, blocked processing at each of the junctions between the structural proteins (Ypma-Wong & Semler, 1987; Ryan et al., 1989), we hypothesized that there might be a region within the C-terminus of VP1, which is of high importance for correct capsid precursor processing. The aim of this study was to identify the region(s) that seemed to cause this block in protein processing.

In **manuscript 1** entitled "Determinants of the VP1/2A junction cleavage by the 3C protease in foot-and-mouth disease virus-infected cells" the effect of various substitutions at the VP1 K210 for correct processing of the VP1/2A junction was investigated. The VP1 K210 corresponds to the residue two aa upstream the junction (P2). Using reverse genetics, various substitutions were introduced at VP1 K210 in the cDNA encoding the full-length FMDV. These constructs were *in vitro*

transcribed and the RNA transcripts were introduced into baby hamster kidney (BHK) cells. After some few passages to obtain a high virus titter, the cleavage of the VP1/2A junction was investigated by western blot and immunofluorescence.

In **manuscript 2** with the title "Cleavages at the three junctions within the foot-and-mouth disease virus capsid precursor (P1–2A) by the 3C protease are mutually independent" the effect of various substitutions near the junctions between the capsid proteins, i.e. the VP0/VP3- and VP3/VP1 junctions were investigated. As it was likely that these substitutions would block cleavage of one of the junctions, which might be fatal for the virus, the effect of these changes was first tested using a transient expression assay to express the capsid precursor (P1-2A) in the absence and presence of $3C^{pro}$. Subsequently, the different substitutions were tested in the context of the full-length FMDV, however only one of the mutants could be rescued.

In **manuscript 3** entitled "Identification of a short, highly conserved, motif required for picornavirus capsid precursor processing at distal sites", we identified a region within the C-terminus of VP1 that was required for capsid precursor processing. In this study, we used mutagenic PCR to make different constructs encoding the P1-2A area with different modifications. First, we introduced Stop codons at different sites within the VP1 coding area, next we introduced small deletions in the area identified by the Stop codons. Lastly, we introduced single amino acid substitutions within the identified region. These modifications identified a short motif, which was highly conserved among many picornaviruses and had a huge impact on capsid precursor processing.

3. Manuscripts

3.1 Manuscript 1

Determinants of the VP1/2A junction cleavage by the 3C protease in foot-and-mouth disease virus-infected cells

Thea Kristensen[1], Preben Normann[1], Maria Gullberg[1], Ulrik Fahnøe[2], Charlotta Polacek[1], Thomas Bruun Rasmussen[1] and Graham J. Belsham[1]#

[1]National Veterinary Institute, Technical University of Denmark, Lindholm, Kalvehave 4771, Denmark

[2] Copenhagen Hepatitis C Program (CO-HEP), Department of Infectious Diseases and Clinical Research Centre, Hvidovre Hospital and Department of International Health, Immunology and Microbiology, Faculty of Health and Medical Sciences, University of Copenhagen, Denmark

Corresponding author: Graham J. Belsham, email: grbe@vet.dtu.dk, phone: +45 35 88 79 85

Published in Journal of General Virology

2016

Volume 98, pp 385-395

JOURNAL OF GENERAL VIROLOGY

RESEARCH ARTICLE

Kristensen *et al.*, *Journal of General Virology* 2017;98:385–395

DOI 10.1099/jgv.0.000664

MICROBIOLOGY SOCIETY

OPEN MICROBIOLOGY

Determinants of the VP1/2A junction cleavage by the 3C protease in foot-and-mouth disease virus-infected cells

Thea Kristensen, Preben Normann, Maria Gullberg, Ulrik Fahnøe,† Charlotta Polacek, Thomas Bruun Rasmussen and Graham J. Belsham*

Abstract

The foot-and-mouth disease virus (FMDV) capsid precursor, P1-2A, is cleaved by FMDV 3C protease to yield VP0, VP3, VP1 and 2A. Cleavage of the VP1/2A junction is the slowest. Serotype O FMDVs with uncleaved VP1-2A (having a K210E substitution in VP1; at position P2 in cleavage site) have been described previously and acquired a second site substitution (VP1 E83K) during virus rescue. Furthermore, introduction of the VP1 E83K substitution alone generated a second site change at the VP1/2A junction (2A L2P, position P2′ in cleavage site). These virus adaptations have now been analysed using next-generation sequencing to determine sub-consensus level changes in the virus; this revealed other variants within the E83K mutant virus population that changed residue VP1 K210. The construction of serotype A viruses with a blocked VP1/2A cleavage site (containing K210E) has now been achieved. A collection of alternative amino acid substitutions was made at this site, and the properties of the mutant viruses were determined. Only the presence of a positively charged residue at position P2 in the cleavage site permitted efficient cleavage of the VP1/2A junction, consistent with analyses of diverse FMDV genome sequences. Interestingly, in contrast to the serotype O virus results, no second site mutations occurred within the VP1 coding region of serotype A viruses with the blocked VP1/2A cleavage site. However, some of these viruses acquired changes in the 2C protein that is involved in enterovirus morphogenesis. These results have implications for the testing of potential antiviral agents targeting the FMDV 3C protease.

INTRODUCTION

Foot-and-mouth disease virus (FMDV) is the prototypic member of the genus *Aphthovirus* within the family *Picornaviridae* and seven different serotypes (O, A, C, SAT 1–3 and Asia-1) have been identified. All FMDVs have a positive-sense RNA genome (ca. 8400 nt) that includes a single large ORF (ca. 7000 nt) encoding a polyprotein [1]. The full-length polyprotein is never observed since during, and after, synthesis it is processed, mainly by virus-encoded proteases, to generate 15 distinct mature products plus multiple precursors. The FMDV polyprotein includes two *trans*-acting proteases; these are the Leader (L) protease and the 3C protease ($3C^{pro}$). The L protease is only responsible for one cleavage within the polyprotein that occurs at its own C-terminus (i.e. the L/P1-2A junction, [2, 3]). However, this protease also induces cleavage of the translation initiation factor eIF4G; this results in the inhibition of host cell, cap-dependent, protein synthesis (reviewed in [1]). The $3C^{pro}$ cleaves all the other junctions within the FMDV polyprotein except for the VP4/VP2 junction and the 2A/2B junction. Cleavage of VP0 to VP4 and VP2 occurs on encapsidation of the viral RNA and also within assembled empty capsid particles [4–6]. Separation of the 2A peptide from the 2B protein is dependent on the 2A coding sequence. However, this region only encodes 18 aa (without any protease motifs), but its presence results in a break in the polyprotein during its synthesis; this is described as 'ribosomal skipping' [7] or 'StopGo' [8].

The FMDV capsid protein precursor, P1-2A (Fig. 1), is processed by the $3C^{pro}$ to VP0, VP3, VP1 and 2A. The scission of the VP1-2A junction is the slowest of these cleavages within cell-free translation systems [9] and within mammalian cells [5, 6] since the uncleaved VP1-2A can still be detected when all other junctions are fully cleaved (e.g. when

Received 13 October 2016; Accepted 17 November 2016

Author affiliation: National Veterinary Institute, Technical University of Denmark, Lindholm, DK-4771 Kalvehave, Denmark.

***Correspondence:** Graham J. Belsham, grbe@vet.dtu.dk

Keywords: picornavirus; polyprotein processing; cleavage specificity; virus capsid assembly; proteolysis.

Abbreviations: BHK, baby hamster kidney; FMDV, foot-and-mouth disease virus; IF, immunofluorescence; NGS, next-generation sequencing; p.i., post-infection; Psg, passage; SNV, single nucleotide variant.

†Present address: Copenhagen Hepatitis C Program (CO-HEP), Department of Infectious Diseases and Clinical Research Centre, Hvidovre Hospital and Department of International Health, Immunology and Microbiology, Faculty of Health and Medical Sciences, University of Copenhagen, Denmark.

One supplementary table is available with the online Supplementary Material.

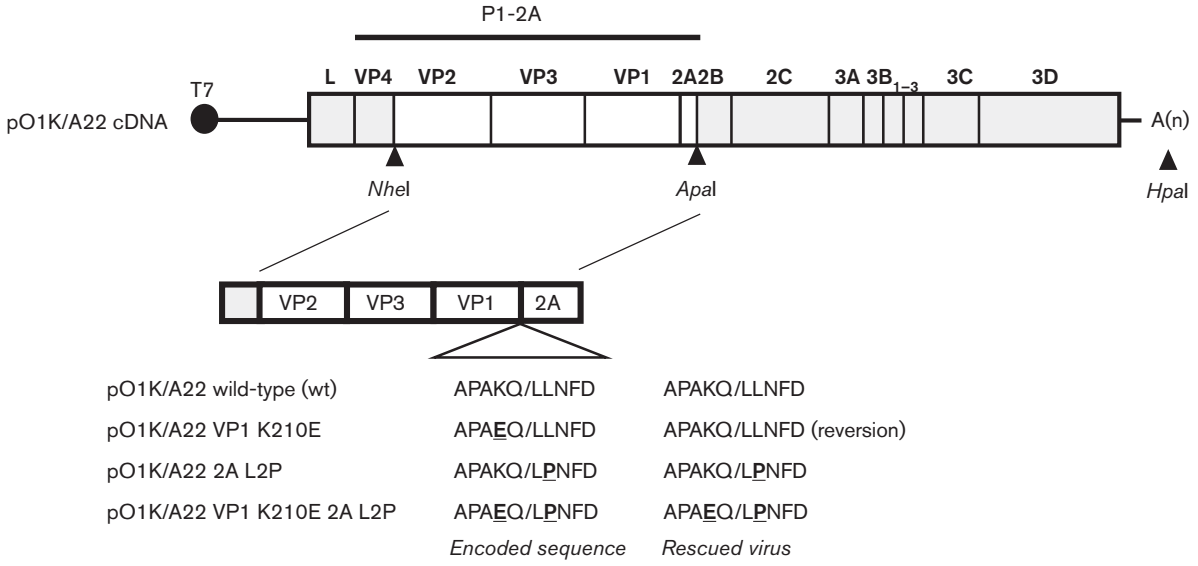

Fig. 1. Schematic structure of the plasmid containing the FMDV O1 Kaufbeuren (O1K)/A22 cDNA and derivatives. The *Nhe*I and *Apa*I restriction enzyme sites (as indicated) were used as described in Methods to introduce cDNA fragments encoding the serotype A FMDV capsid proteins VP2-VP3-VP1-2A (from A22 Iraq, white fill) into the plasmid pT7S3 [33], containing a full-length cDNA corresponding to the O1K B64 strain of FMDV (coding sequences marked in grey). The plasmid-encoded amino acid sequences at the VP1/2A junction are shown. The FMDV O1K/A22 wt, single mutants (VP1 K210E or 2A L2P) and double mutant (VP1 K210E and 2A L2P) were produced as described in Methods. The full-length plasmids were linearized using *Hpa*I prior to *in vitro* transcription and virus rescue. The locations of restriction sites used are marked: *Nhe*I, *Apa*I and *Hpa*I. Sequence changes in the capsid coding region of the rescued viruses are indicated.

P1-2A is expressed with a low level of $3C^{pro}$). However, in peptide cleavage assays, using short synthetic substrates, it has been found that the peptide corresponding to the VP1/2A cleavage site was the most rapidly processed [10].

The FMDV $3C^{pro}$ cleaves a variety of different junction sequences (the amino acid residues at the cleavage junctions are indicated as P4P3P2P1/P1′P2′P3′P4′). The cleavage sites recognized by the FMDV $3C^{pro}$ have either glutamine (Gln, Q) or glutamate (Glu, E) at the P1 position [11]. The consensus sequence (in single-letter code) for the VP1/2A junction in serotype O and A FMDVs is PxKQ/xLNF. The Q residue at the P1 position, together with the P4-Pro (P), P2-Lys (K) and P4′-Phe (F) residues, represent key determinants of $3C^{pro}$ specificity at this site [10–12]. Analysis of aligned FMDV $3C^{pro}$ cleavage sites from over 100 strains of the virus (including representatives of all serotypes) revealed that sites with P1-Q have a strong selectivity for P2-K, indicating that recognition of the P1 residue by $3C^{pro}$ is influenced by the P2 residue [11]. Recently, we have shown that changing the P2-K residue to E at the VP1/2A junction (i.e. K210E in VP1), in a serotype O virus, greatly inhibited cleavage at this junction and resulted in the formation of infectious virus particles containing the uncleaved VP1-2A [6]. The 'self-tagged' viruses containing this modification (K210E) also acquired, during the virus rescue procedure, a second amino acid substitution within VP1 (E83K). Interestingly, introduction of this E83K substitution alone into the virus generated a second site mutant (L2P, in the 2A sequence; this is position P2′ in the VP1/2A junction) that also blocked cleavage [13]. We have now expanded this analysis to identify the determinants of cleavage at the VP1/2A junction within the context of infectious serotype O and A FMDVs using a variety of different approaches. Within the serotype A FMDVs, no second site changes in VP1 were observed in viruses where the VP1/2A cleavage was inhibited, but some evidence for changes in 2C was obtained. For certain picornaviruses, within the enterovirus genus, interactions between the virus capsid proteins and the 2C nonstructural protein have been implicated in the process of virus morphogenesis [14–16].

RESULTS

Modification of the VP1/2A cleavage site in a serotype A FMDV

In order to determine whether the key elements of the results obtained with the serotype O FMDV sequences [13] also applied to serotype A FMDV, the effect of modifying the VP1/2A cleavage site within a serotype A FMDV was examined. The VP1/2A cleavage site sequence in the A22 strain of FMDV (AP**A**KQ/LLNFD) differs at just one out of the 10 residues flanking the junction from the serotype O (strain O1 Manisa, abbreviated throughout as O1M) sequence (AP**V**KQ/LLNFD) analysed previously [6, 13] (see Fig. 1). The K210E substitution (at the P2 position) was

introduced into a full-length FMDV cDNA, based on the backbone of a chimeric O1 Kaufbeuren (O1K) virus containing the coding sequence for the VP2-VP3-VP1-2A region of the A22 capsid protein precursor (Fig. 1). Virus was successfully rescued from this chimeric wt O1K/A22 plasmid and also from the O1K/A22 VP1 K210E mutant (this had changed the codon encoding VP1 residue 210 from AAA to GAA). However, when the capsid protein coding sequences within the rescued virus were determined, it was found that the K210E substitution in VP1 had reverted in the virus by passage 2 (Psg 2) to the wt sequence (this only requires a single nt change) (see Fig. 1).

Two further modifications were, therefore, introduced into the serotype A viruses: the 2A L2P modification was made in isolation (using 3 nt changes, TTG to CCA) and a double mutant containing both the K210E substitution (the single nt change) and the 2A L2P substitution. Viruses were rescued successfully from both of these mutant plasmids. Consensus sequencing indicated that the expected mutations were still present within these rescued viruses and that no other mutations were detected within the VP2-2A coding region (see Fig. 1).

Analysis of the FMDV capsid proteins within cells infected with the wt and mutant O1K/A22 viruses, as determined by immunoblotting using anti-VP2 and anti-2A antibodies, is shown in Fig. 2. As expected, the production of VP0 and VP2 was very similar in each of the infected cell extracts (Fig. 2a, lanes 2–7). However, the presence of the uncleaved VP1-2A was only observed with the mutant viruses, either containing the 2A L2P substitution alone (Fig. 2b, lanes 4 and 5) or with the double mutant (VP1 K210E and 2A L2P) (Fig. 2b, lanes 6 and 7).

These results were confirmed using immunofluorescence (IF) studies (Fig. 3). Consistent with the immunoblotting data, the presence of FMDV 2A (still attached to VP1) was detected in cells infected with the O1K/A22 2A L2P mutant virus (Fig. 3g) and with the double mutant (O1K/A22 VP1 K210E and 2A L2P) virus (Fig. 3h). In contrast, no signal for the 2A peptide was observed in cells infected with the wt O1K/A22 virus (Fig. 3f) or in uninfected cells (Fig. 3e). The presence of the FMDV capsid proteins could be detected in cells infected with each of the viruses (Fig. 3b–d) but not in uninfected cells (Fig. 3a). These results are consistent with those obtained using the serotype O FMDVs previously [13]. It seems that the free 2A peptide is not efficiently detected within cells using the IF approach; it is assumed that either it breaks down very quickly or the conditions of the IF assay are not suitable for detection of this short peptide.

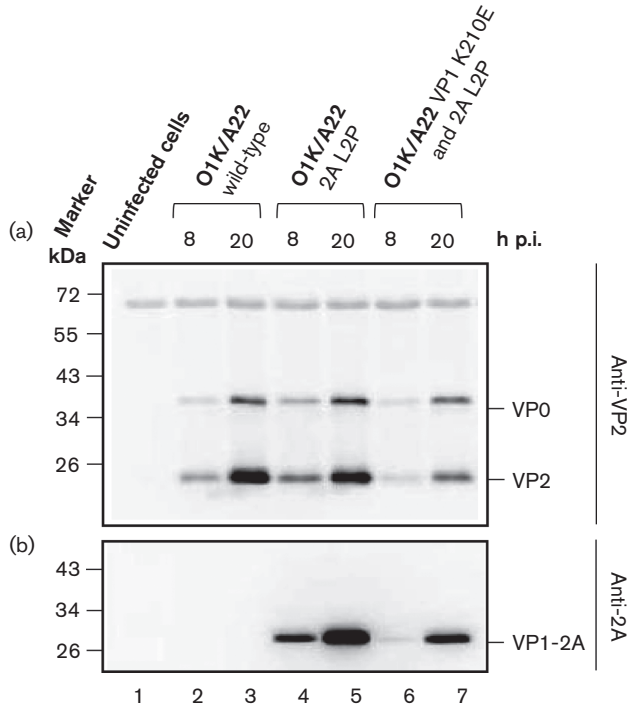

Fig. 2. Detection of FMDV capsid proteins in BHK cells infected with O1K/A22 wt and mutant viruses. Baby hamster kidney (BHK) cells were infected with O1K/A22 wt or mutant viruses (single mutant 2A L2P or double mutant VP1 K210E and 2A L2P) (m.o.i. of 0.1), and whole-cell lysates were prepared at the indicated times post-infection (p.i.). The presence of FMDV VP2 (and its precursor VP0) was detected by immunoblotting using anti-VP2 antibodies (a) and FMDV 2A (attached to VP1 as VP1-2A) was detected using anti-2A antibodies (b). Uninfected BHK cells were used as a negative control. Molecular mass markers (kDa) are indicated on the left.

Use of next-generation sequencing to determine sequence diversity within rescued FMDVs

As described previously [6, 13], consensus sequencing of the capsid coding region (P1-2A) of the serotype O FMDVs rescued from the K210E and E83K mutant forms of the O1K/O1M cDNAs identified the presence of additional amino acid substitutions in the rescued viruses. We wished to analyse these adaptations in more detail, in particular to examine the appearance of sub-consensus level changes throughout the near-complete genome sequence including the complete polyprotein coding region. To achieve this, RNA was extracted from the rescued O1K/O1M VP1 E83K and O1K/O1M VP1 K210E viruses (as described by Gullberg *et al.* [6, 13]) at Psg 2 and/or Psg 3. Two separate, but overlapping, cDNA fragments including the near-complete genome [ca. 8 kb, downstream of the poly(C) tract] were produced by reverse transcription (RT)-PCR, mixed and then sequenced using next-generation sequencing (NGS) at a coverage of about 5000 reads per nt (except near the extreme 5′- and 3′-termini).

This analysis showed that the rescued virus O1K/O1M VP1 E83K retained the expected substitution (encoding E83K) in 100 % of the progeny at Psg 2, but there was some heterogeneity in the sequence near the VP1/2A junction (see Table 1). As described earlier, the consensus sequencing indicated that a substitution (L2P) within the 2A sequence occurred within this rescued virus [13]. The analysis by NGS (see Table 1) demonstrated that at Psg 2, some 83 % of the reads

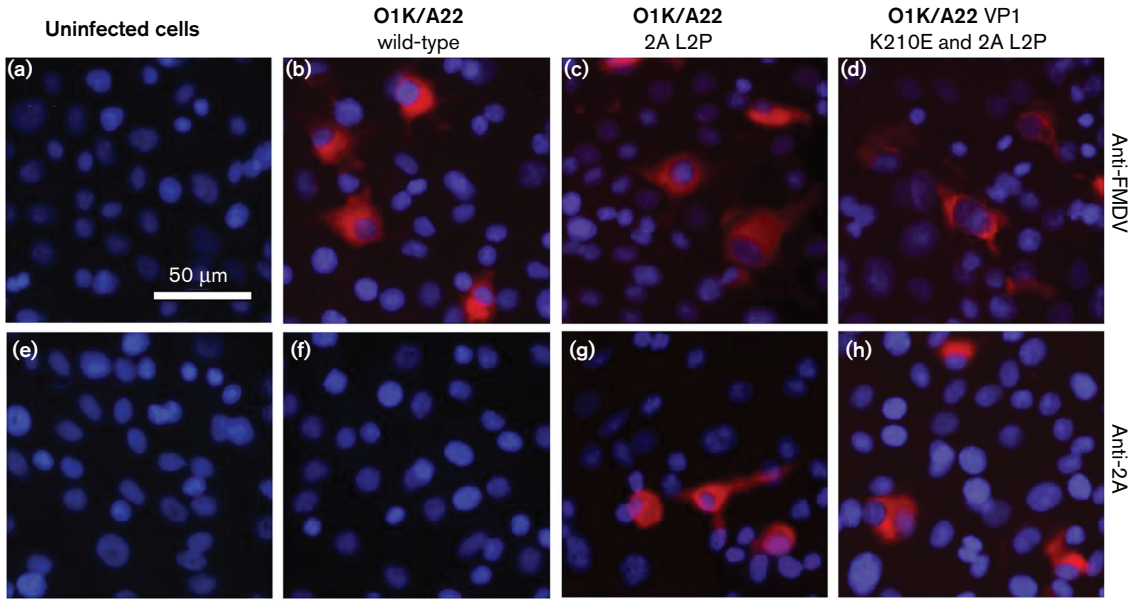

Fig. 3. IF staining of FMDV proteins within serotype A FMDV-infected cells. FMDV proteins within uninfected or FMDV-infected cells (using m.o.i. of 0.1) were detected (at 8 h p.i.) using an anti-FMDV A-Iraq polyclonal antibody (a–d) or an anti-2A antibody (e–h) and a secondary antibody labelled with Alexa Fluor 568 (red). Uninfected cells are shown in (a) and (e). Cells were infected with the viruses O1K/A22 (wt) (b and f), O1K/A22 2A L2P (c and g) or O1K/A22 VP1 K210E and 2A L2P (d and h) as indicated. The cellular nuclei were visualized with DAPI (blue). Bar, 50 µm.

corresponded to this L2P substitution in 2A, while two other variants were also present (albeit at relatively low levels, 4 and 9 %), which each encoded the K210N substitution in VP1 (c.f. the K210E change described previously in O1M, [13]). No other coding changes were present anywhere in the genome at an abundance of more than 3 %.

Consensus sequence analysis of the rescued O1K/O1M VP1 K210E virus has shown previously the generation of the E83K substitution [6]. Using NGS, it was found that the E83K substitution in VP1 was encoded in 78 % of the reads generated at Psg 2 and in 99 % of the reads at Psg 3 (Table 1), consistent with the earlier consensus sequencing

Table 1. Analysis of SNVs within rescued O1K/O1M viruses as determined by NGS

Nt position	Wt	Variant	O1K/O1M VP1 E83K (Psg 2) (%)*	O1K/O1M VP1 K210E (Psg 2) (%)*	O1K/O1M VP1 K210E (Psg 3) (%)*	SNV effect (whole polyprotein)	SNV effect (individual protein)
762	T	C	6	–	–	(in 5′ UTR)	–
948	T	G	–	1	3	(in 5′ UTR)	–
1811	T	C	6	–	–	–	–
1875	A	G	3	–	–	T253A	VP4 (T52A)
2102	C	T	3	–	–	–	–
2357	A	G	–	3	3	–	–
3537	G	A	100	78	99	E807K	VP1 (E83K)
3918	A	G	–	100	100	K934E	VP1 (K210E)
3920	A	C	4	–	–	K934N	VP1 (K210N)
3920	A	T	9	–	–	K934N	VP1 (K210N)
3928	T	C	83	–	–	L937P	2A (L2P)
5166	A	G	3	–	–	S1350G	2C (S243G)
7392	T	C	–	5	7	F2092L	3D (F228L)
7765	A	G	2	–	–	K2216R	3D (K353R)

SNV, single nucleotide variant.

*The percentage of each variant (≥1 %) is given to the nearest integer.

[6]. The K210E substitution was maintained in this rescued virus in 100 % of the reads at Psg 2 and Psg 3.

For the rescued serotype A viruses, consensus (Sanger) sequencing of the rescued O1K/A22 2A L2P virus demonstrated the maintenance of the introduced changes and did not reveal any additional modifications, resulting in amino acid substitutions within the P1-2A coding region. This was confirmed by NGS, but an A-to-G nucleotide change, resulting in a single amino acid substitution (T44 to A within the 2C protein), was found in 13 % of the reads from the rescued virus (Table 2). Within the O1K/A22 VP1 K210E and 2A L2P virus, only the expected changes in the P1-2A coding region were observed, but an additional change, resulting in the amino acid substitution A73V in the 2C protein, was detected in 100 % of the sequence reads (see Table 2). The plasmid pO1K/A22 K210E L2P from which this virus was rescued has been confirmed as having the expected sequence in the 2C coding region (100 % identity to O1K, data not shown), and thus, this sequence change had occurred during virus rescue. The significance of these changes in 2C is unknown; neither residue is completely conserved among FMDV strains [17]. The A73V change in 2C was not present in the rescued O1K/A22 wt or the O1K/A22 2AL2P, and there was no evidence for the T44A amino acid substitution in either the O1K/A22 wt or the O1K/A22 VP1 K210E and 2A L2P virus that was encoded in a minority of the O1K/A22 2A L2P virus reads.

Exploring potential sequence diversity at the VP1/2A cleavage site

The results described previously [6, 13] indicated that modification of the VP1/2A junction sequence from PxKQ/xLNF at the P2 position (from K to E) or the P2′ position (from L to P) was sufficient to strongly inhibit cleavage by $3C^{pro}$ at this protein junction, but these changes did not affect virus viability. Furthermore, the NGS data (Table 1) indicated that the K-to-N substitution at residue 210 of VP1 was also probably viable since some 13 % of the virus population acquired this change. To establish the range of amino acid substitutions that could be tolerated at this junction, mutagenesis of the codon for residue 210 within VP1 was undertaken within the context of the O1K/A22 full-length cDNA. The mutagenesis generated nine different codon sequences that encoded seven distinct amino

Table 2. Analysis of SNVs within rescued O1K/A22 viruses as determined by NGS

Nt position	Wt	Variant	O1K/A22 (wt) (Psg 2) (%)*	O1K/A22 2A L2P (Psg 3) (%)*	O1K/A22 VP1 K210E 2A L2P (Psg 3) (%)*	SNV effect (whole polyprotein)	SNV effect (individual protein)
932	A	C	–	2	–	(in 5′-UTR)	–
1060	T	G	2	–	–	(in 5′-UTR)	–
1124	T	A	–	7	–	N2K	L (N2K)
1341	C	T	–	–	4	P75S	L (P75S)
1400	G	T	–	–	2	–	–
1865	C	T	–	2	–	–	–
2175	T	C	–	2	–	F353L	VP2 (F67L)
2342	A	G	–	–	2	–	–
2684	C	T	–	3	–	–	–
3154	T	C	–	1	–	V679A	VP3 (V174A)
3824	G	C	2	–	–	–	–
3884	T	C	–	8	–	–	–
3921	A	G	–	–	100	K935E	VP1 (K210E)
3930	T	C	–	90	100	†	†
3931	T	C	–	98	100	L938P†	2A (L2P)†
3932	G	A	–	99	100	†	†
4572	A	G	–	13	–	T1152A	2C (T44A)
4660	C	T	–	–	100	A1181V	2C (A73V)
4821	A	C	–	1	–	I1235L	2C (I127L)
4843	G	T	–	1	–	R1242I	2C (R134I)
5080	C	T	–	5	–	T1321I	2C (T213I)
6924	C	T	–	11	–	–	–
7170	T	C	3	–	–	Y2018H	3D (Y155H)
7358	C	T	–	–	4	–	–

SNV, single nucleotide variant.

*The percentage of each variant (≥1 %) is given to the nearest integer.

†Change of the TTG to CCA codon was introduced by site-directed mutagenesis, and the three changes together result in the 2A (L2P) substitution.

acid substitutions (see Table 3). RNA transcripts were produced from the mutant cDNAs and electroporated into baby hamster kidney (BHK) cells, and infectious viruses were rescued in each case. From the virus harvests, RNA was extracted and the sequence of VP1-2A coding region was determined, and changes (if any) are shown in Table 3. Consistent with the studies described above, the O1K/A22 VP1 K210E mutant (with a single nt change, GAA) again reverted to the parental sequence; however, when 2 nt changes were introduced (GAG) to produce the K210E substitution, then viruses that retained these 2 nt changes were obtained. Thus, the VP1 substitutions K210Q, K210R, K210A, K210V, K210M, K210N and K210E (as the GAG double mutant) were all viable without reversion or other adaptation within VP1 (Table 3). Using consensus-level sequencing, no changes in the 2C coding region were detected in any of these rescued viruses either (data not shown).

The cleavage of the VP1/2A junction in cells infected with the rescued mutant viruses was assessed using the IF assay, as described above. The presence of the FMDV capsid proteins (using anti-FMDV antisera) and of the VP1-2A (using anti-2A antibodies) was determined in BHK cells infected with the different viruses. FMDV infection, but with no staining for VP1-2A, was observed in cells infected with the viruses containing the VP1 residue K210 (wt) and R210 (Fig. 4). In contrast, cells infected with the rescued viruses having the substitutions in VP1 K210Q, K210A, K210V, K210M, K210N and K210E (double mutant) each showed staining both for the FMDV capsid proteins and for 2A (using the anti-2A antisera), indicative of blocked VP1/2A cleavage (see Fig. 4, Table 3). No staining with either antiserum was observed in uninfected cells, as expected (Fig. 4).

To confirm these results, immunoblotting was performed using anti-2A antibodies to determine the presence of the uncleaved VP1-2A within infected cells. The results are shown in Fig. 5(a). Consistent with the IF results, no VP1-2A product was detected in uninfected cells or in wt (K210) or mutant K210R FMDV-infected cells. In contrast, the presence of VP1-2A was readily apparent within cells infected with mutant FMDVs having the K210Q, K210A, K210V, K210M, K210N and K210E substitutions. The presence of FMDV capsid proteins in the lysates from cells infected with each of the different FMDV variants was verified using anti-VP2 antibodies that recognize both VP0 and VP2 (Fig. 5b). These results support the IF data and indicate that the VP1/2A junction is only cleaved when residue 210 in VP1 is either K or R (these are both basic residues).

DISCUSSION

In our earlier studies, it was shown that the K210E substitution in VP1 within the FMDV O1M capsid inhibited cleavage of the VP1/2A junction and resulted in generation of a second site substitution (E83K in VP1) in the mutant virus [6]. Furthermore, introduction of the E83K substitution alone in VP1 resulted in the production of another second site change (with a substitution of L2P in 2A) that also blocked VP1/2A junction processing in cells infected with the rescued virus [13]. In contrast, this study has shown that when the K210E substitution (GAA mutant) was introduced into the VP1 of a serotype A virus (O1K/A22), the virus reverted to wt (AAA) very rapidly (single nt change). However, introduction of 2 nt changes (GAG codon) enabled the K210E substitution to be maintained. Consistent with the serotype O virus results [6, 13], this amino acid substitution alone was sufficient to block VP1/2A cleavage (see Figs 4 and 5). In addition, introduction of the 2A L2P change alone (employing 3 nt changes) or also with the K210E substitution resulted in the generation of viruses which maintained each of these changes. Furthermore, the presence of the uncleaved VP1-2A protein was observed within cells infected with these serotype A viruses (Figs 2 and 3). Thus, consistent with results using the O1K/O1M FMDV [6, 13], it is possible to obtain infectious

Table 3. Influence of residue K210 in VP1 on VP1/2A junction cleavage in FMDV-infected cells

Virus	VP1 210 codon	Viability	Rescued virus sequence	Rescued virus amino acid	Comment	VP1/2A cleavage*
pO1K/A22 K210	AAA	+	AAA	K	wt	+
pO1K/A22 K210Q	**C**AA‡	+	CAA	Q		–
pO1K/A22 K210R	A**G**A‡	+	AGA	R		+
pO1K/A22 K210A(v1)†	**GC**A‡	+	GCA	A		–
pO1K/A22 K210A(v2)†	**GCG**‡	+	GCG	A		–
pO1K/A22 K210V	**GTT**‡	+	GTT	V		–
pO1K/A22 K210M	A**TG**‡	+	ATG	M		–
pO1K/A22 K210N	AA**C**‡	+	AAC	N		–
pO1K/A22 K210E(v1)†	**G**AA‡	+	AAA	K	Reversion	+
pO1K/A22 K210E(v2)†	**GAG**‡	+	GAG	E		–

*VP1/2A cleavage was assessed from IF staining using anti-2A antibodies (as in Fig. 4) and by immunoblotting (Fig. 5a).

†v1 or v2 to distinguish different codons.

‡Nucleotide changes in this codon are indicated in bold font.

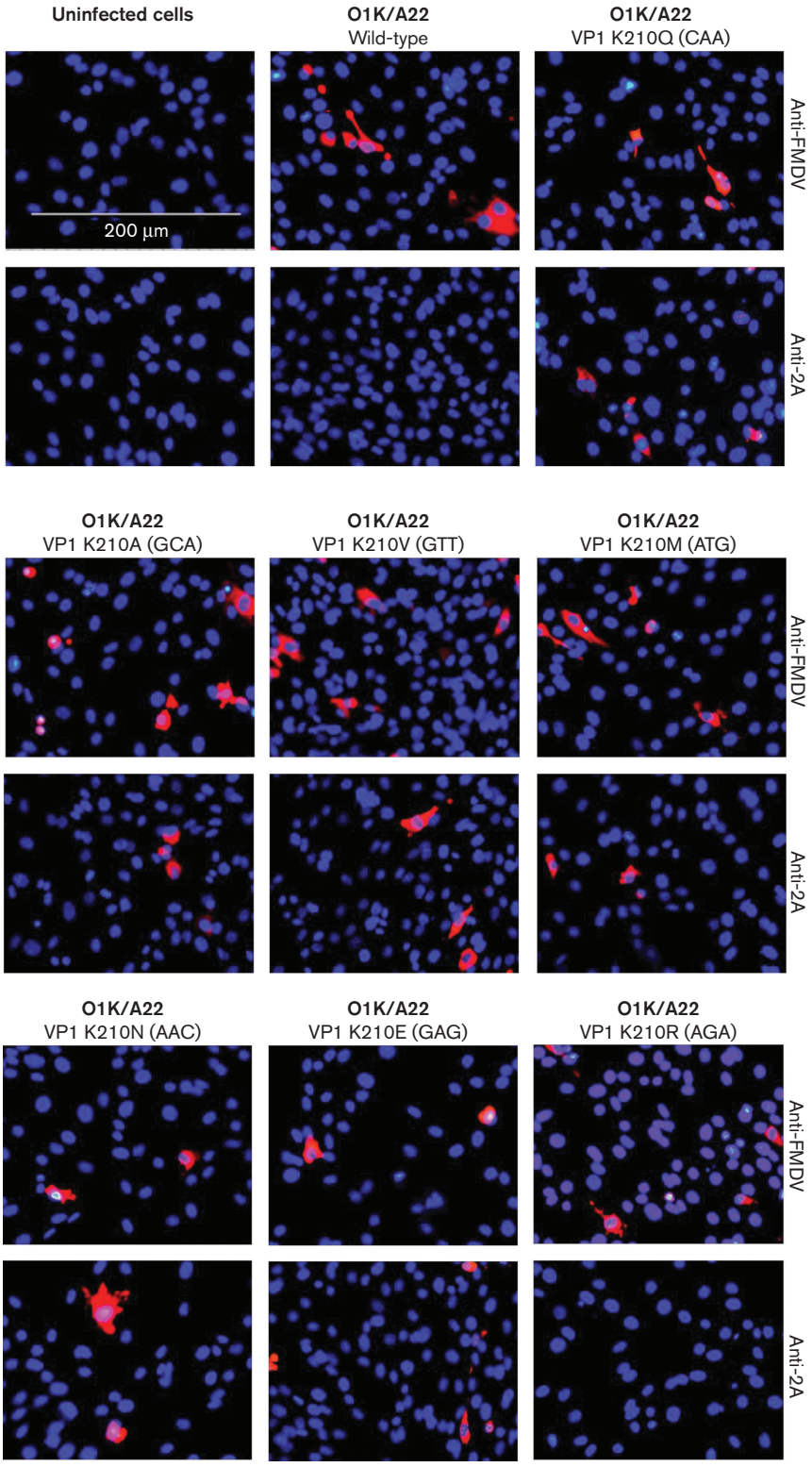

Fig. 4. Determination of VP1/2A cleavage by IF staining for FMDV proteins within cells. FMDV proteins within uninfected or FMDV-infected cells (using m.o.i. of 0.1) were detected (at 6 h p.i.) using an anti-FMDV A-Iraq polyclonal antibody or an anti-2A antibody (as indicated) and a secondary antibody labelled with Alexa Fluor 568 (red) as in Fig. 3. The codon for residue 210 within VP1 (in parentheses) and the resulting individual amino acid residue within the different rescued viruses are indicated. Uninfected cells were used as a negative control. The cellular nuclei were visualized with DAPI (blue). Bar, 200 µm.

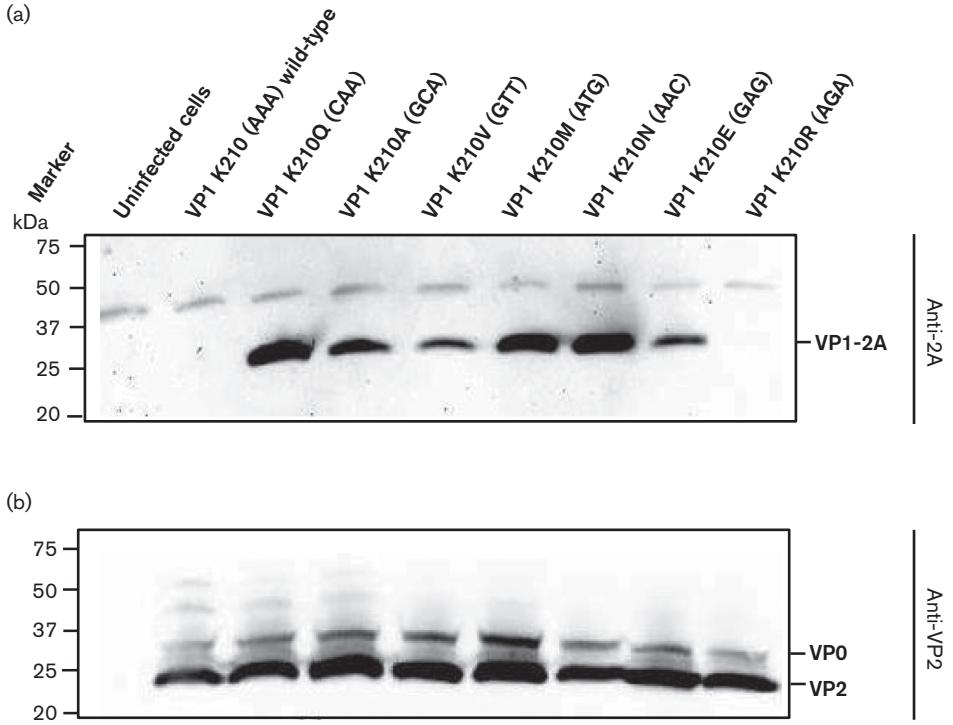

Fig. 5. Assessment of FMDV VP1/2A cleavage in FMDV-infected BHK cells by immunoblotting. Uninfected or FMDV-infected BHK cell lysates were analysed by SDS-PAGE and immunoblotting (as in Fig. 2). Where applicable, the cells were infected with the indicated viruses (at an m.o.i. of 0.1) and the presence of FMDV 2A (attached to VP1 as VP1-2A) was detected using anti-2A antibodies (a), while FMDV VP2 (and its precursor VP0) was detected by immunoblotting using anti-VP2 antibodies (b). Uninfected cells were used as a negative control. Molecular mass markers (kDa) are indicated on the left.

serotype A FMDVs, containing the uncleaved VP1-2A. However, in contrast to the results using the serotype O virus, there was no apparent selection for a substitution at residue E83 in VP1 (or elsewhere within the VP1) within the serotype A background. The basis for this difference is not known, but it is noteworthy that the serotype A capsid proteins assemble into FMDV empty capsids much more efficiently than the serotype O proteins [18, 19]. It is also apparent that some of the rescued serotype A viruses, with the VP1/2A junction rendered non-cleavable, acquired second site mutations within the non-structural protein 2C (see Table 2). In particular, the A73V variant within 2C was encoded by 100 % of the sequence reads at Psg 3 of the rescued O1K/A22 VP1-K210E and 2A-L2P virus. This suggests a strong selective pressure for this amino acid substitution. The significance of this is currently unknown, but there is some evidence for interactions between the capsid proteins and the 2C protein of enteroviruses (e.g. poliovirus) during virus morphogenesis [14–16].

Interestingly, it was also observed, using NGS, that during the rescue of the O1K/O1M VP1 E83K virus, a minority of the virus population encoded a K210N substitution in VP1 (c.f. the K210E substitution observed in a laboratory grown O1M virus, [6]). It should be noted that the majority of the serotype O VP1 E83K mutant virus RNA acquired the 2A L2P substitution during the virus rescue procedure (see Table 1). This encouraged analysis of the range of substitutions that can be accommodated at residue 210 in VP1; this is at position P2 relative to the VP1/2A cleavage site. Within the serotype A background, there appears to be significant selection pressure against the K210E substitution, since following independent transfections of a mutant RNA containing a single nt change (GAA) reversion to the wt (AAA) sequence occurred. However, when 2 nt changes were used (GAG) to make this amino acid substitution, then the K210E substitution was maintained. The single nt substitution to make the K210E substitution was also maintained in the O1K/A22 K210E and L2P double mutant; presumably the presence of the two substitutions that blocked VP1/2A cleavage overcame the selective pressure for reversion. In addition, a range of other amino acid substitutions was tolerated. Most of these substitutions (e.g. K210A, K210V, K210M and K210N) blocked cleavage of the VP1/2A junction; thus, the VP1-2A product was stable (see Figs 4 and 5). In contrast, the 2A peptide was released from the VP1 in the K210R mutant. Therefore, it appears that the presence of a positively charged residue (K or R) at residue 210 in VP1 is essential for VP1/2A cleavage, and a negative charge

(as in K210E) is less well tolerated by itself and was selected against. These results are consistent with the strong predominance of the K and R residues at this position in the 'logos plot' generated by Curry *et al.* [11] for $3C^{pro}$ cleavage sites, with Q at the P1 position, based on the known sequences of over 100 strains of FMDV.

Using peptide cleavage assays, the VP1/2A peptide was the most efficiently cleaved substrate for FMDV $3C^{pro}$ [10]. However, making the K210A substitution abrogated cleavage of this peptide, in accordance with the results presented here. Zunszain *et al.* [12] have described additional modifications to the peptide substrate, which corresponds to the VP1/2A junction. Changing the P2 residue in the cleavage site (corresponding to K210 in VP1) from K to R or to ornithine (also positively charged) had relatively modest effects on the cleavage rate. However, substitution to the neutral T residue abrogated cleavage as observed here, with the K210 changed to Q, A, V, M or N (see Table 3, Figs 4 and 5).

It has been proposed that the FMDV $3C^{pro}$ may be a good target for the development of an antiviral agent [20]. Furthermore, it was shown that compounds that resemble the peptide substrate can act as an efficient inhibitor of this protease. The presence of a positively charged residue at the P2 position generated the most effective inhibitors, while compounds containing neutral residues (e.g. G and Q) or a negatively charged residue (E) at this position were much less effective, consistent with the poor cleavage of the VP1/2A junction seen here in viruses containing equivalent substitutions.

It is important to note that viable FMDVs with the VP1/2A junction uncleaved can be obtained (as here, and as described previously for serotype O viruses [6, 13]). Thus, it may be wise to focus screens for such antiviral agents on other $3C^{pro}$ cleavage sites so that the block on polyprotein processing is most effective at inhibiting virus replication.

The results presented here demonstrate that the combination of reverse genetics and NGS provides powerful tools to direct and identify virus adaptation, thus permitting novel aspects of the virus biology to be identified.

METHODS

Plasmid construction

The structures of plasmids containing full-length FMDV cDNAs used in this study are indicated in Fig. 1. The chimeric pO1K/A22 plasmids (containing the A22 Iraq capsid coding sequences, as used in [19, 21]) in the FMDV O1K backbone were generated using the same procedures as used previously for the production of the pO1K/O1M VP1 K210E [6]. Briefly, the cDNAs corresponding to the A22 VP2-2A coding region were amplified from pGEM-3Z-A-P1-2A-mIRES-3C [5] and pGEM-3Z-A-P1-2A-mIRES-3C VP1K210E [6] with primers FMDVA_*Nhe*IVP4VP2_Fw and FMDVA_*Apa*I2A2B_Re (see Table S1, available in the online Supplementary Material) and used to generate the full-length cDNAs termed pO1K/A22 wt and pO1K/A22 VP1 K210E, respectively (Fig. 1). In order to produce pO1K/A22 2A L2P and the double mutant pO1K/A22 VP1 K210E and 2A L2P, intermediate plasmids (using pO1K/A22 wt and pO1K/A22 VP1K210E, as described above, as templates) were generated. This was achieved using the QuikChange site-directed mutagenesis method (with *Pfu*-Turbo DNA polymerase; Stratagene), according to the manufacturer's instructions, with primers containing the desired modifications (see Table S1, namely FMDVA_2AL2P_Fw together with FMDVA_2AL2P_Re or FMDVA_VP1-K210E_2AL2P_Re). The subsequent steps to produce the four pO1K/A22 variants were performed essentially as described for the serotype O plasmid pO1K/O1M VP1 E83K [13]. Plasmids were amplified in *Escherichia coli* Top10 cells (Invitrogen), purified (Midiprep kit; Thermo Scientific) and verified by sequencing of the capsid coding region (and for pO1K/A22 VP1 K210E the 2C coding region as well) with a BigDye Terminator v. 3.1 Cycle Sequencing kit and a 3500 Genetic Analyzer (Applied Biosystems).

Additional mutations, encoding changes at the VP1/2A junction, were introduced into the pO1K/A22 full-length FMDV cDNA (Fig. 1) by site-directed mutagenesis using a megaprimer (146 bp) that was prepared by PCR using primer O1PN20 and primer 13LPN21 (see Table S1) that had NNN at the position corresponding to the codon for the VP1 residue 210. This degenerate megaprimer was used, with the pO1K/A22 full-length cDNA template and *Pfu*-Turbo DNA polymerase (as above) to generate a collection of nine plasmids encoding a variety of different amino acids, with diverse properties, in place of VP1 residue K210; this is at position P2 relative to the VP1/2A cleavage site. The details of each modification made are indicated in Table 3.

Rescue of modified viruses from cDNA

Plasmids pO1K/A22 (wt), pO1K/A22 VP1 210E, pO1K/A22 2A L2P and pO1K/A22 VP1 K210E 2A L2P (as shown in Fig. 1) containing the full-length FMDV cDNA sequences were linearized by digestion with *Hpa*I, purified (using a QIAquick PCR purification kit; Qiagen) and transcribed *in vitro* using T7 RNA polymerase (Megascript kit; Ambion). The transcripts were analysed using agarose gel electrophoresis and then introduced into BHK cells by electroporation as described previously [22, 23]. At 2 days post-electroporation, the rescued viruses were harvested and amplified in one, or two, subsequent passages (Psg 2 and Psg 3) in BHK cells. After these passages, viral RNA was extracted (QIAamp RNA Blood Mini kit; Qiagen) and reverse transcribed using Ready-To-Go You-Prime First-Strand Beads (GE Healthcare Life Sciences), and the FMDV cDNA corresponding to the VP2-2A coding region was amplified in a PCR (Expand High-Fidelity PCR System; Roche). Control reactions, lacking reverse transcriptase, were used to show that the PCR products obtained were derived from the viral RNA and not from residual DNA template. The amplicons (~2000 bp) including the entire VP2-2A coding region were visualized in agarose gels, purified (GeneJET Gel Extraction kit, Thermo Scientific) and sequenced, on both

strands, as above. Sequences were analysed using Vector NTI software (Invitrogen).

For the library of VP1 K210 mutants, mutant viruses were rescued essentially as described above. The sequencing covered the VP1-2A coding region (from a PCR product of ca 700 bp) both before and after virus rescue. The sequence of the 2C coding region was also determined in selected cases. The rescued viruses were titrated (and were in most cases ca 10^6 to 10^7 $TCID_{50}$ ml^{-1}), and in some cases, a fourth passage in BHK cells was required to reach this titre.

The rescued serotype O viruses O1K/O1M VP1 E83K and O1K/O1M VP1 K210E viruses have been described previously [6, 13].

RT-PCR and NGS

For the purpose of NGS, extracted RNA (isolated as described above from virus harvests) was converted to cDNA using SuperScript III (Invitrogen) with a T_{27} reverse primer according to the manufacturer's protocol. Two cDNA amplicons were prepared by PCR using Phusion DNA polymerase (Thermo Fisher) with the primers 13-N PN 2+10-P PN 30 (Table S1) and separately 8-A PN 200 +13-N PN 3 (Table S1). These overlapping fragments (ca. 4 and 4.2 kb, respectively) correspond to most of the FMDV genome [downstream of the poly(C) tract, see Belsham [1]], including the complete polyprotein coding region (ca. 7 kb) but excluding the S-fragment at the 5′-terminus of the viral genome. The fragments were gel purified, mixed and then analysed by NGS essentially as described previously [24, 25]. The parental sequences of the FMDV chimeric O1K/O1M cDNA (as described by Gullberg *et al.* [6]) were assembled from the O1K sequence (accession no. X00871) and the coding sequence for the O1M capsid proteins (from accession no. AY593823) with known differences (see [6]), while the chimeric O1K/A22 sequence was generated using the O1K sequence and the A22 Iraq sequence ([17], accession no. AY593764.1). The derived sequences were used as the reference for mapping of sequence reads using SAMtools [26], VarScan 2 [27] and VCFtools [28], in succession, in order to generate consensus sequences from the mapped reads. Subsequently, consensus sequences were aligned using MAFFT in Geneious (Biomatters). Finally, a combination of SAMtools [26], Lo-Freq [29] and SnpEff [30] was used for downstream single nucleotide variant (SNV) analysis.

Virus infection of BHK cells

Virus titres were determined, as tissue culture infectious doses ($TCID_{50}$), by titration in BHK cells according to standard procedures [31].

Monolayers of BHK cells, grown in 35 mm wells, were inoculated with the rescued viruses at a m.o.i. of 0.1 $TCID_{50}$ /cell. At the indicated times post-infection (p.i.), cell lysates were prepared using 20 mM Tris/HCl (pH 8.0), 125 mM NaCl and 0.5 % NP-40, and clarified by centrifugation at 18 000 ***g*** for 10 min at 4 °C.

Immunoblot analysis

Immunoblotting was performed, using cell lysates, according to standard methods as described previously [21]. Briefly, aliquots of cell lysate were mixed with Laemmli sample buffer (with 25 mM DTT), and the proteins were separated by SDS-PAGE (12.5 or 4–15 % polyacrylamide) and transferred to PVDF membranes (Millipore). Specific proteins were detected with primary antibodies recognizing FMDV VP2 (monoclonal antibody 4B2, a gift from L. Yu, as described by Yu *et al.* [32]) and FMDV 2A (ABS31; Millipore). Bound proteins were visualized using appropriate HRP-conjugated secondary antibodies (Dako) and a chemiluminescence detection kit (ECL Prime, Amersham) with a Chemi-Doc XRS system (Bio-Rad).

IF assays

Monolayers of BHK cells, grown on glass coverslips in 35 mm well plates, were infected with the rescued O1K/A22 viruses (m.o.i. of 0.1). At 6–8 h p.i., the cells were fixed, stained and mounted as previously described [6] using rabbit anti-FMDV A-Iraq serum and anti-FMDV 2A (ABS31, as above) followed by a donkey Alexa Fluor 568-labelled anti-rabbit IgG (A10042, Life Technologies). The slides were mounted with Vectashield (Vector Laboratories) containing DAPI, and images were captured using an epifluorescence microscope.

Funding information
This work was supported by the Danish Council for Independent Research-Technology and Production Sciences (FTP grant 09-070549) to C. P. and G. J. B.

Acknowledgements
We wish to thank Li Yu (Chinese Academy of Agricultural Sciences, China) for the anti-VP2 antibody.

Conflicts of interest
The authors declare that there are no conlicts of interest.

References

1. Belsham GJ. Translation and replication of FMDV RNA. *Curr Top Microbiol Immunol* 2005;288:43–70.
2. Strebel K, Beck E. A second protease of foot-and-mouth disease virus. *J Virol* 1986;58:893–899.
3. Medina M, Domingo E, Brangwyn JK, Belsham GJ. The two species of the foot-and-mouth disease virus leader protein, expressed individually, exhibit the same activities. *Virology* 1993; 194:355–359.
4. Curry S, Abrams CC, Fry E, Crowther JC, Belsham GJ *et al.* Viral RNA modulates the acid sensitivity of foot-and-mouth disease virus capsids. *J Virol* 1995;69:430–438.
5. Gullberg M, Muszynski B, Organtini LJ, Ashley RE, Hafenstein SL *et al.* Assembly and characterization of foot-and-mouth disease virus empty capsid particles expressed within mammalian cells. *J Gen Virol* 2013;94:1769–1779.
6. Gullberg M, Polacek C, Bøtner A, Belsham GJ. Processing of the VP1/2A junction is not necessary for production of foot-and-mouth disease virus empty capsids and infectious viruses: characterization of 'self-tagged' particles. *J Virol* 2013;87:11591–11603.
7. Donnelly ML, Luke G, Mehrotra A, Li X, Hughes LE *et al.* Analysis of the aphthovirus 2A/2B polyprotein 'cleavage' mechanism

indicates not a proteolytic reaction, but a novel translational effect: a putative ribosomal 'skip'. *J Gen Virol* 2001;82:1013–1025.

8. **Atkins JF, Wills NM, Loughran G, Wu CY, Parsawar K *et al.*** A case for 'StopGo': reprogramming translation to augment codon meaning of GGN by promoting unconventional termination (Stop) after addition of glycine and then allowing continued translation (Go). *RNA* 2007;13:803–810.
9. **Ryan MD, Belsham GJ, King AM.** Specificity of enzyme-substrate interactions in foot-and-mouth disease virus polyprotein processing. *Virology* 1989;173:35–45.
10. **Birtley JR, Knox SR, Jaulent AM, Brick P, Leatherbarrow RJ *et al.*** Crystal structure of foot-and-mouth disease virus 3C protease. New insights into catalytic mechanism and cleavage specificity. *J Biol Chem* 2005;280:11520–11527.
11. **Curry S, Roqué-Rosell N, Zunszain PA, Leatherbarrow RJ.** Foot-and-mouth disease virus 3C protease: recent structural and functional insights into an antiviral target. *Int J Biochem Cell Biol* 2007; 39:1–6.
12. **Zunszain PA, Knox SR, Sweeney TR, Yang J, Roqué-Rosell N *et al.*** Insights into cleavage specificity from the crystal structure of foot-and-mouth disease virus 3C protease complexed with a peptide substrate. *J Mol Biol* 2010;395:375–389.
13. **Gullberg M, Polacek C, Belsham GJ.** Sequence adaptations affecting cleavage of the VP1/2A junction by the 3C protease in foot-and-mouth disease virus-infected cells. *J Gen Virol* 2014;95: 2402–2410.
14. **Liu Y, Wang C, Mueller S, Paul AV, Wimmer E *et al.*** Direct interaction between two viral proteins, the nonstructural protein 2C and the capsid protein VP3, is required for enterovirus morphogenesis. *PLoS Pathog* 2010;6:e1001066.
15. **Wang C, Jiang P, Sand C, Paul AV, Wimmer E.** Alanine scanning of poliovirus 2CATPase reveals new genetic evidence that capsid protein/2CATPase interactions are essential for morphogenesis. *J Virol* 2012;86:9964–9975.
16. **Wang C, Ma HC, Wimmer E, Jiang P, Paul AV.** A C-terminal, cysteine-rich site in poliovirus 2C(ATPase) is required for morphogenesis. *J Gen Virol* 2014;95:1255–1265.
17. **Carrillo C, Tulman ER, Delhon G, Lu Z, Carreno A *et al.*** Comparative genomics of foot-and-mouth disease virus. *J Virol* 2005;79: 6487–6504.
18. **Abrams CC, King AM, Belsham GJ.** Assembly of foot-and-mouth disease virus empty capsids synthesized by a vaccinia virus expression system. *J Gen Virol* 1995;76:3089–3098.
19. **Porta C, Xu X, Loureiro S, Paramasivam S, Ren J *et al.*** Efficient production of foot-and-mouth disease virus empty capsids in insect cells following down regulation of 3C protease activity. *J Virol Methods* 2013;187:406–412.
20. **Roqué Rosell NR, Mokhlesi L, Milton NE, Sweeney TR, Zunszain PA *et al.*** Design and synthesis of irreversible inhibitors of foot-and-mouth disease virus 3C protease. *Bioorg Med Chem Lett* 2014; 24:490–494.
21. **Polacek C, Gullberg M, Li J, Belsham GJ.** Low levels of foot-and-mouth disease virus 3C protease expression are required to achieve optimal capsid protein expression and processing in mammalian cells. *J Gen Virol* 2013;94:1249–1258.
22. **Nayak A, Goodfellow IG, Woolaway KE, Birtley J, Curry S *et al.*** Role of RNA structure and RNA binding activity of foot-and-mouth disease virus 3C protein in VPg uridylylation and virus replication. *J Virol* 2006;80:9865–9875.
23. **Bøtner A, Kakker NK, Barbezange C, Berryman S, Jackson T *et al.*** Capsid proteins from field strains of foot-and-mouth disease virus confer a pathogenic phenotype in cattle on an attenuated, cell-culture-adapted virus. *J Gen Virol* 2011;92:1141–1151.
24. **Fahnøe U, Pedersen AG, Risager PC, Nielsen J, Belsham GJ *et al.*** Rescue of the highly virulent classical swine fever virus strain 'Koslov' from cloned cDNA and first insights into genome variations relevant for virulence. *Virology* 2014;468–470:379–387.
25. **Hadsbjerg J, Friis MB, Fahnøe U, Nielsen J, Belsham GJ *et al.*** Sequence adaptations during growth of rescued classical swine fever viruses in cell culture and within infected pigs. *Vet Microbiol* 2016;192:123–134.
26. **Li H, Handsaker B, Wysoker A, Fennell T, Ruan J *et al.*** The sequence alignment/map format and SAMtools. *Bioinformatics* 2009;25:2078–2079.
27. **Koboldt DC, Zhang Q, Larson DE, Shen D, Mclellan MD *et al.*** VarScan 2: somatic mutation and copy number alteration discovery in cancer by exome sequencing. *Genome Res* 2012;22:568–576. http://varscan.sourceforge.net.
28. **Danecek P, Auton A, Abecasis G, Albers CA, Banks E *et al.*** The variant call format and VCFtools. *Bioinformatics* 2011;27:2156–2158.
29. **Wilm A, Aw PP, Bertrand D, Yeo GH, Ong SH *et al.*** LoFreq: a sequence-quality aware, ultra-sensitive variant caller for uncovering cell-population heterogeneity from high-throughput sequencing datasets. *Nucleic Acids Res* 2012;40:11189–11201.
30. **Cingolani P, Platts A, Wang LL, Coon M, Nguyen T *et al.*** A program for annotating and predicting the effects of single nucleotide polymorphisms, SnpEff: SNPs in the genome of *Drosophila melanogaster* strain w1118; iso-2; iso-3. *Fly (Austin)* 2012;6:80–92.
31. **Reed LJ, Muench H.** A simple method of estimating fifty percent endpoints. *Am J Hyg* 1938;27:493–497.
32. **Yu Y, Wang H, Zhao L, Zhang C, Jiang Z *et al.*** Fine mapping of a foot-and-mouth disease virus epitope recognized by serotype-independent monoclonal antibody 4B2. *J Microbiol* 2011;49:94–101.
33. **Ellard FM, Drew J, Blakemore WE, Stuart DI, King AM.** Evidence for the role of His-142 of protein 1C in the acid-induced disassembly of foot-and-mouth disease virus capsids. *J Gen Virol* 1999;80: 1911–1918.

Supplementary Table S1. Primers used for plasmid construction and cDNA synthesis

Primer name	Sequence (5´-3´)
FMDVA_*Nhe*IVP4VP2_Fw	CGCTCTGCTAGCCGATAAGAAGACCGAGGAGACCA
FMDVA_*Apa*I2A2B_Re	CTACTAGGGCCCGGGGTTGGACTCAACGTCTCCTG
FMDVA_2AL2P_Fw	CAACTT***CCA***AACTTCGATTTGCTCAAGTTGGCAGGAGAC
FMDVA_2AL2P_Re	GAAGTT***TGG***AAGTTGTTTTGCAGGTGCAATGATCTTCTG
FMDVA_VP1K210E_2AL2P_Re	GAAGTT***TGG***AAGTTGTT**C**TGCAGGTGCAATGATCTTCTG
13-N PN2	AAGTTTTACCGTCGTTCCCGACGTAAAAGGGAGGTAACCAC AAGCTTGAA
10-P PN 30	TCTGGACAGCACCTTTGTCG
8-A PN 200	GAGACGTTGAGTCCAACCC
13-N PN 3	CCGTAGGAGTGAAAATCCCGAAAGGGTTTTTCCCGCTTCCTT AATCCAAA
O1PN20	GACATGTCCTCCTGCATCTG
13LPN21	GCACCTGCA***NNN***CAACTTTTGAAC

[a] Underlined sequences represent restriction enzyme sites *NheI* and *ApaI*. Nucleotide changes producing amino acids substitutions are shown in boldface italics.

3.2 Manuscript 2

Cleavages at the three junctions within the foot-and-mouth disease virus capsid precursor (P1-2A) by the 3C protease are mutually independent

Thea Kristensen[1], Joseph Newman[2], Su Hua Guan[1], Tobias J. Tuthill[2] and Graham J. Belsham[1]#

[1]National Veterinary Institute, Technical University of Denmark, Lindholm, Kalvehave 4771, Denmark

[2]The Pirbright Institute, Ash Road, Pirbright, Surrey GU24 0NF, UK

Corresponding author: Graham J. Belsham, email: grbe@vet.dtu.dk, phone: +45 35 88 79 85

Published in Virology

2018

Volume 522, pp 260-270

Virology 522 (2018) 260–270

Contents lists available at ScienceDirect

Virology

journal homepage: www.elsevier.com/locate/virology

Cleavages at the three junctions within the foot-and-mouth disease virus capsid precursor (P1–2A) by the 3C protease are mutually independent

Thea Kristensen[a], Joseph Newman[b], Su Hua Guan[a], Tobias J. Tuthill[b], Graham J. Belsham[a,*]

[a] National Veterinary Institute, Technical University of Denmark, Lindholm, Kalvehave 4771, Denmark
[b] The Pirbright Institute, Ash Road, Pirbright, Surrey GU24 0NF, UK

ARTICLE INFO

Keywords:
Picornavirus
Polyprotein
Virus assembly
Protease cleavage site
Structural proteins

ABSTRACT

The foot-and-mouth disease virus capsid precursor, P1–2A, is cleaved by the 3C protease ($3C^{pro}$) to VP0, VP3, VP1 and 2A. The P1–2A precursor (wt or mutant) was expressed alone or with $3C^{pro}$ and processing of P1–2A was determined. The VP2 K217R and VP3 I2P substitutions (near the VP0/VP3 junction) strongly reduced the processing at this junction by $3C^{pro}$ while the substitution VP2 K217E blocked cleavage. At the VP3/VP1 junction, the substitutions VP3 Q2221P and VP1 T1P each severely inhibited processing at this site. Blocking cleavage at either junction did not prevent processing elsewhere in P1–2A. These modifications were also introduced into full-length FMDV RNA; only wt and the VP2 K217R mutant were viable. Uncleaved VP0-VP3 and the processed products were observed within cells infected with the mutant virus. The VP0-VP3 was not incorporated into empty capsids or virus particles. The three junctions within P1–2A are processed by $3C^{pro}$ independently.

1. Introduction

Foot-and-mouth disease (FMD) is a highly contagious disease of cloven-hoofed animals including cattle, pigs and sheep. The disease can cause enormous economic losses during an outbreak because of severe restrictions on international trade. FMD has been successfully eradicated from Europe but it is still endemic in large areas of Africa and Asia (Alexandersen et al., 2003). FMD sometimes causes epidemics in previously disease-free areas, as for instance the outbreak in the UK in 2001, which resulted in the loss of several million animals with total costs estimated at about £ 8 billion (Alexandersen et al., 2003).

FMD is caused by infection with foot-and-mouth disease virus (FMDV), which is a small, non-enveloped, RNA virus belonging to the genus *Aphthovirus* within the large family of picornaviruses. Each FMDV particle contains a single-stranded positive-sense RNA genome of around 8400 nucleotides (nt) surrounded by a protein shell (capsid), which is roughly spherical and about 25–30 nm in diameter. The capsid is composed of 60 copies of 4 different structural proteins, termed VP1, VP2, VP3 and VP4. There are seven different serotypes of FMDV, namely O, A, C, SAT1, SAT2, SAT3 and Asia-1. There is no cross-protection between these serotypes and there is significant nucleotide sequence diversity between them, especially in the capsid protein coding regions.

The FMDV genome contains a single, long open reading frame (ORF) of around 7000 nt. Translation initiation on the viral RNA to produce the encoded polyprotein is achieved by the internal ribosomal entry site (IRES), located within the 5′-untranslated region (UTR). The polyprotein is processed largely by virus-encoded proteases. Processing into the primary products, namely the Leader protease (L^{pro}), P1–2A, P2 and P3 occurs rapidly, during and after, synthesis. The L^{pro} is responsible for the cleavage at its own C-terminus, i.e. at the L/P1–2A junction, while the 2A peptide (only 18 amino acids long) is required for the “cleavage” at the 2A junction; this is a protease independent break in the polypeptide chain and is termed “ribosomal skipping” (Donnelly et al., 2001) or “StopGo” (Atkins et al., 2007). After this initial processing, all other cleavages are catalyzed by the 3C protease ($3C^{pro}$), except for the maturation of VP0 into VP2 and VP4. The P1–2A precursor is subsequently processed to VP0, VP3 and VP1 and the 2A peptide. The capsid proteins VP0, VP3 and VP1 remain associated with each other (in a protomer) and assemble into pentamers. Twelve of these pentamers can then assemble around a single RNA molecule to form a virus particle, but they are also able to assemble into empty capsid particles without any RNA (Abrams et al., 1995; Gullberg et al., 2013a). During the assembly of the pentamers into a virus particle, the VP0 is cleaved to generate VP2 and VP4 by a process that is currently not understood. The VP4 is entirely internal within the virus particle, whereas VP1, VP2 and VP3 are exposed on the capsid surface, contributing to the antigenic properties of the virus. Moreover, these

* Corresponding author.
E-mail address: grbe@vet.dtu.dk (G.J. Belsham).

https://doi.org/10.1016/j.virol.2018.07.010
Received 18 June 2018; Received in revised form 6 July 2018; Accepted 8 July 2018
Available online 26 July 2018

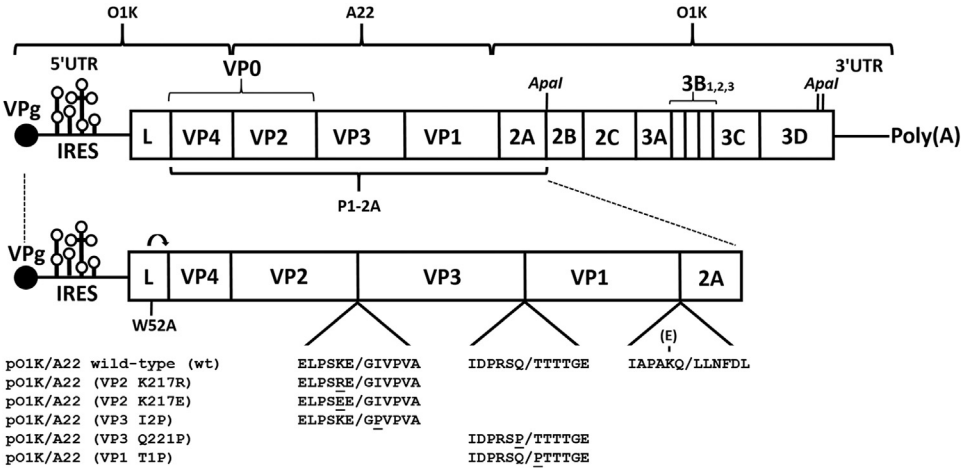

Fig. 1. Schematic representation of the FMDV genome and the plasmids used in the transient expression assays. The cDNA sequence encoding VP2-VP3-VP1–2A is derived from FMDV A22 Iraq. The viral cDNA backbone is derived from FMDV O1 Kaufbeuren (O1K), shown in the upper part of the figure. The *Apa*I sites were used to remove the coding sequence for the non-structural proteins. The Leader protease cleaves at its own C-terminus (as indicated by the arrow), and the $3C^{pro}$ is responsible for cleavage of the other junctions (except for VP4/VP2) within the expressed protein. In the lower part of the figure, the different amino acid substitutions encoded by the different plasmids are indicated.

proteins are responsible for interacting with cell surface receptors to promote virus entry into cells (Jackson et al., 2000). In FMDV empty capsid particles, cleavage of VP0 into VP2 and VP4 can also occur, however unprocessed VP0 is also present in the empty particles (Gullberg et al., 2013a; Curry et al., 1997).

Attempts to express the $3C^{pro}$ at the same level as the P1–2A precursor have been problematic. The $3C^{pro}$ is not only able to cleave different junctions in the FMDV polyprotein, but can also cleave a variety of cellular proteins that are important for normal cellular functions, e.g. the translation initiation factors eIF4A and eIF4G (Belsham et al., 2000), components of the cytoskeleton (Armer et al., 2008) and histone H3 (Falk et al., 1990). Due to this, $3C^{pro}$ is probably toxic to mammalian cells and high levels of the $3C^{pro}$ are known to inhibit protein expression (Polacek et al., 2013). During an FMDV infection, the P1–2A precursor and the $3C^{pro}$ will be expressed at about the same level. However, in the FMDV polyprotein, the $3C^{pro}$ has to cleave some ten different junctions while, in contrast, only three junctions (VP0/VP3, VP3/VP1 and VP1/2A are present in the P1–2A precursor. An earlier study, has shown that reducing the expression level of $3C^{pro}$ compared to that of P1–2A greatly increased the yield of the structural FMDV proteins (Polacek et al., 2013).

The $3C^{pro}$ from different picornaviruses cleave the protein junctions with different specificities, i.e. with different amino acids upstream and downstream of the cleavage site. The amino acid residues flanking the cleavage sites are designated as P4 P3 P2 P1 / P1′ P2′ P3′ P4′ respectively. In many picornaviruses (e.g. the enteroviruses, like poliovirus), the $3C^{pro}$ cleavage sites always contain a glutamine residue (Q) at the P1 position, however FMDV $3C^{pro}$ shows greater diversity in its recognition sequence and is able to process junctions containing either a glutamate (E) or a glutamine (Q) at the P1 position. The VP0/VP3 junction, in most FMDVs, belongs to the E/x (where x can be a variety of residues) group of sites (with the exception of most of the SAT serotypes, which have a Q). The amino acid sequence for this junction in A22 Iraq FMDV is PSKE/GIVP, whereas the consensus sequence for the VP0/VP3 junction for both serotype O and A FMDVs is PSKE/GIFP. However, comparison of the different FMDV junctions from different serotypes indicates that $3C^{pro}$ is able to process the E/x junction without being very constrained by the nature of the P2 residue, as it can be lysine (K), arginine (R), threonine (T), histidine (H) or glutamine (Q) (Curry et al., 2007). The P1′ residue seems to have a strong influence on the junction since it is generally a glycine (G) but sometimes serine (S). At residue P2′, the VP0/VP3 junction in A22 Iraq FMDV has an isoleucine (I) residue, interestingly in the E/x group of sites this residue is most often a proline (P), but can also be a G, leucine (L), valine (V) or I (as in the A22 Iraq strain) (Curry et al., 2007). However, for the VP0/VP3 junction it is commonly an isoleucine and only 10 out of 133 sequences have a valine (Carrillo et al., 2005). The VP3/VP1 junction generally belongs to the Q/x group of sites and thus usually has a Q at the P1 residue (Q/x) (with the exception of some serotype O viruses, which have an E at the P1 position). The amino acid sequence at the VP3/VP1 junction for the A22 Iraq FMDV sequence, as used here, is PRSQ/TTTT, and the consensus sequence for both serotype O and A FMDVs is xRxQ/TTxx.

We have earlier investigated the characteristics of the cleavage at the VP1/2A junction (Gullberg et al., 2013b; Gullberg et al., 2014), which belongs to the Q/x group of sites, and determined important properties of the amino acid residues at the P2 and P2′ positions at this junction (Gullberg et al., 2014; Kristensen et al., 2016). Surprisingly it was demonstrated that cleavage at the VP1/2A junction is not required for virus viability (Gullberg et al., 2013b; Kristensen et al., 2016). We have now expanded the analysis of FMDV capsid protein processing to investigate the junctions between VP0/VP3 and VP3/VP1 that belong to the E/x and Q/x groups respectively. These junction cleavages were investigated by expressing the P1–2A precursor alone or together with the $3C^{pro}$ in a transient expression assay and also using full-length FMDV RNA transcripts.

2. Results

2.1. Optimisation of the transient expression assay

The FMDV A22 Iraq P1–2A capsid precursor has been expressed, within BHK cells, both alone and in the presence of the FMDV $3C^{pro}$ using a transient expression system. The plasmid expressing the P1–2A product is a derivative of the full-length plasmids used for virus rescue and thus contains the IRES and the coding regions for the Leader protease (L^{pro}) as well as the P1–2A capsid precursor but has had the coding regions for the non-structural proteins (including $3C^{pro}$) removed, see Fig. 1. The L^{pro} can have an adverse effect on the level of product generated from the expression system (Polacek et al., 2013; Guan and Belsham, 2017). Therefore, a mutation which results in an amino acid substitution (W52A) within L^{pro} (Guan and Belsham, 2017) was introduced into the cDNA. The modified L^{pro} retains the L/P1 cleavage activity but does not efficiently induce cleavage of the translation initiation factor eIF4G; this factor is required for the initiation of cap-dependent protein synthesis. The presence of this modification greatly enhanced the expression of the P1–2A capsid precursor from such plasmids in the transient expression assay and, as expected, no loss of the intact eIF4G was detected within transfected cells (c.f. the constructs with the wt L^{pro}, see Supplementary material Fig. S1). Thus, for all the subsequent analyses in the transient expression system the W52A derivatives of the plasmids expressing the L-P1–2A region of the genome were employed. Furthermore, to get the highest levels of processed capsid protein expression, the amounts of the plasmids encoding the P1–2A precursor and the $3C^{pro}$ were optimized (see Methods).

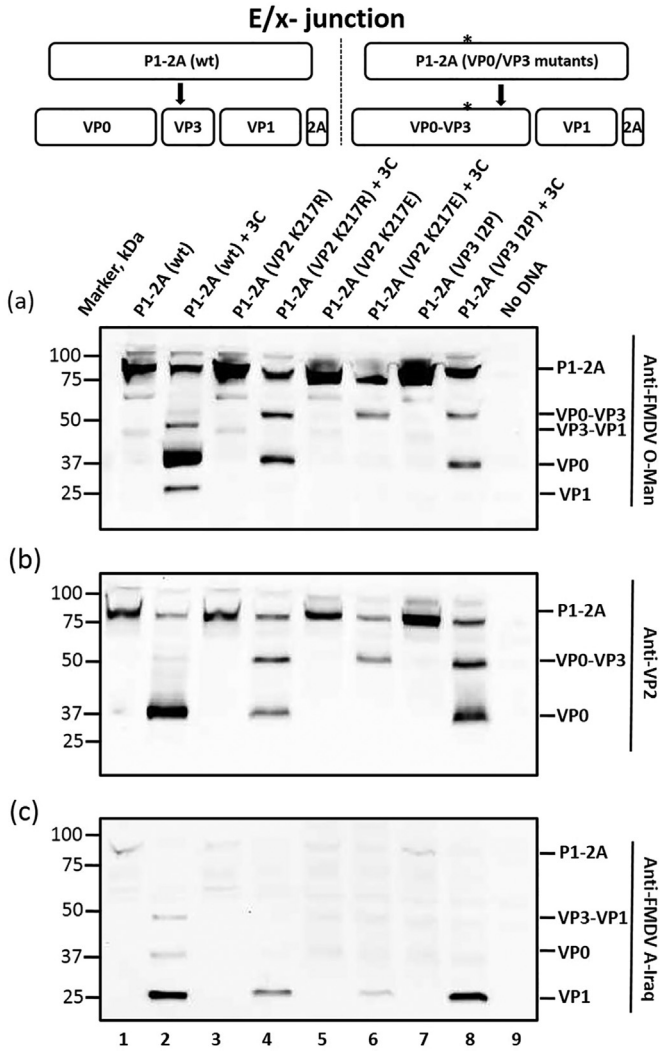

Fig. 2. Effect of substitutions at the VP0/VP3 junction on capsid precursor processing. BHK cells (infected with vTF7-3 (Fuerst et al., 1986) were transfected with plasmids that express the P1–2A (wt or mutant having a substitution at the VP0-VP3 junction) alone (odd numbered lanes) or with the plasmid pSKRH3C (Belsham et al., 2000) encoding the $3C^{pro}$ (even numbered lanes). A negative control (No DNA) was included (lane 9). Cell lysates were prepared and analysed by immunoblotting. Molecular mass markers (kDa) are indicated on the left. The structural proteins corresponding to the different bands are indicated on the right of the figure and were detected using the following: (a) guinea pig anti-FMDV O-Man antisera, (b) murine monoclonal anti-VP2 antibodies (4B2) and (c) guinea pig anti-FMDV A-Iraq antisera. Bound antibodies were visualized using the appropriate HRP-conjugated secondary antibodies (Dako) and a chemiluminescence detection kit (Pierce ® ECL Western Blotting Substrate, Thermo Fisher Scientific). The results are representative of at least 3 separate transfections that yielded similar results.

2.2. Processing of the P1–2A precursor at the VP0/VP3 junction

To investigate the effect of the P2 residue in the E/x junction (VP2/VP3) we introduced two different mutations individually into the cDNA that result in the VP2 K217R substitution and the VP2 K217E substitution, these were designed as fairly conservative (retaining the positive charge) or fairly drastic (positive to negative charge) changes, respectively. In addition, the VP3 I2P substitution was introduced to see whether this would have a similar effect on the E/x junction, as observed previously at the Q/x site (at the VP1/2A junction (Gullberg et al., 2014)). The different substitutions that were analysed are shown in Fig. 1.

Expression of the P1–2A coding region for the wt and the three different mutants (VP2 K217R, VP2 K217E and VP3 I2P), in the absence of $3C^{pro}$, led to the synthesis of products corresponding to the P1–2A precursor (approximately 85 kDa) (Fig. 2a, b and c, lanes 1, 3, 5 and 7), as expected. In the presence of $3C^{pro}$, the wt P1–2A was efficiently processed to generate VP0 (ca. 37 kDa) and VP1 (ca. 28 kDa) (note that the specific antibodies used do not detect VP3 (Gullberg et al., 2013a) but presumably this was also made) (Fig. 2a, b and c, lane 2). The processing of the VP3/VP1 junction in the wt P1–2A seems to happen a little more slowly than the processing of the VP0/VP3 junction, since the VP3-VP1 product (ca. 49 kDa) was readily detected but only very little of the VP0-VP3 product (ca. 58 kDa) was observed (Fig. 2a, lane 2).

When the VP0/VP3 junction was modified (as in the VP2 K217R, VP2 K217E and VP3 I2P mutants), products corresponding to the unprocessed VP0-VP3 were readily detected (see Fig. 2a and Fig. 2b, lanes 4, 6 and 8). Some cleavage of the modified junction still occurred with the VP2 K217R and VP3 I2P mutants since VP0 was also produced (Fig. 2a and b, lanes 4 and 8) but this was not the case with the VP2 K217E mutant (Fig. 2a and b, lane 6) suggesting a severe block on processing at this site as a result of this substitution. The production of VP1 (following cleavage of the unmodified VP3/VP1 junction) was detected from the wt precursor and also from each of the mutant precursors (Fig. 2c, lanes 2, 4, 6, 8). It is concluded that amino acid substitutions at the P2 and P2′ positions adversely affect the processing at the VP0/VP3 junction (an E/x site) but this change does not block processing at the VP3/VP1 junction.

2.3. Processing of P1–2A capsid precursor at the VP3/VP1 junction

Using similar analyses, the production and processing of the P1–2A precursor from the wt plasmid or one of the mutants encoding an amino acid substitution close to the VP3/VP1 junction, were analysed in transient expression assays by immunoblotting and the results are shown in Fig. 3.

The VP3/VP1 junction belongs to the Q/x group of sites, like the VP1/2A junction. To investigate the effect of changes near this junction we introduced substitutions at the P1 and the P1′ residues, namely VP3 Q221P and VP1 T1P, these were both expected to be highly deleterious to cleavage. The two different substitutions are indicated in Fig. 1.

As expected, expression of the plasmids encoding P1–2A (wt) and the mutants VP3 Q221P and VP1 T1P in the absence of $3C^{pro}$ led to the synthesis of products corresponding to the P1–2A precursor (Fig. 3a, lanes 1, 3 and 5). In the presence of $3C^{pro}$, the P1–2A wt was again efficiently processed to generate VP0 and VP1 (Fig. 3a, b and c, lane 2) as in Fig. 2. Processing of the VP3 Q221P and VP1 T1P P1–2A mutants also produced VP0 (Fig. 3a, b, lanes 4 and 6). However, in contrast to the P1–2A (wt) (lane 2), no VP1 was detected (Fig. 3c, lanes 4 and 6) but a major product corresponding to the uncleaved VP3-VP1 (ca. 49 kDa) was observed (Fig. 3c, lanes 4 and 6). This indicates that processing of the VP3/VP1 junction in the P1–2A precursor by $3C^{pro}$ was severely inhibited by these single amino acid substitutions. However, abrogating cleavage of this junction did not block processing of the VP0/VP3 junction within the P1–2A.

2.4. Processing of P1–2A capsid precursor at the VP1/2A junction

The VP1/2A junction also belongs to the Q/x group and was not modified in any of the mutants described above. However, the processing of the VP1/2A junction is known to be the slowest within the context of the P1–2A precursor (Gullberg et al., 2013a, 2013b; Ryan et al., 1989), and thus we investigated whether modifying the processing of one of the other junctions between the structural proteins affected the VP1/2A cleavage site.

Processing of the VP1/2A junction from the P1–2A precursor from the plasmids encoding the wt P1–2A or mutant P1–2As with single

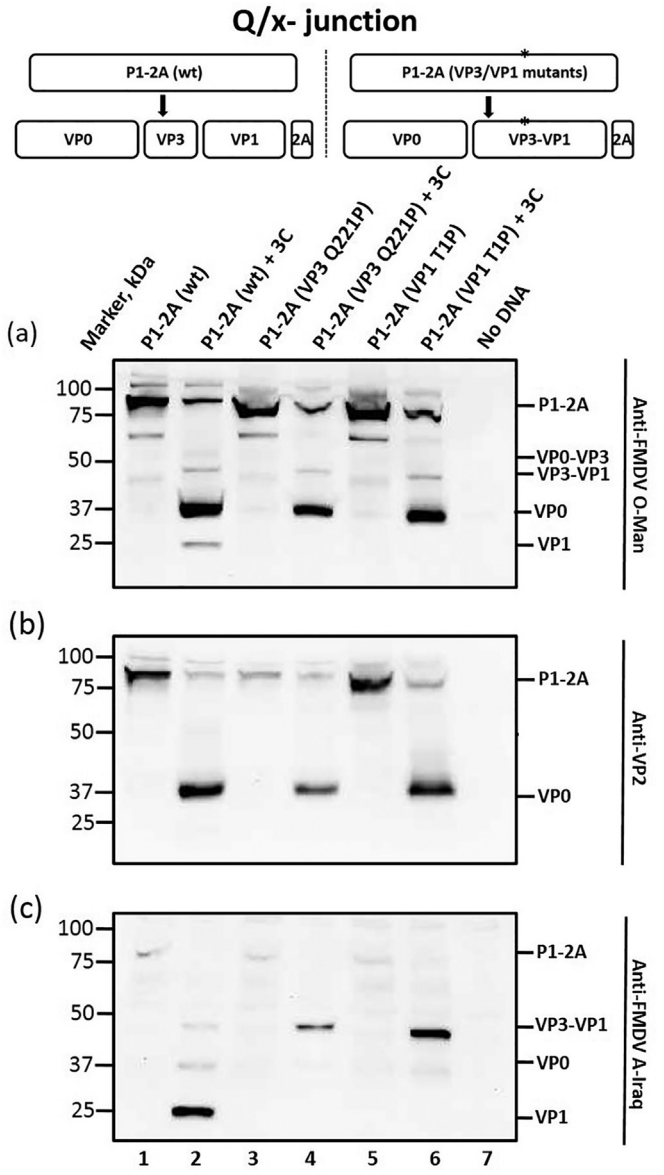

Fig. 3. Effect of substitutions at the VP3/VP1 junction on capsid precursor processing. The P1–2A precursor (wt or mutant having a substitution at the VP3-VP1 junction) was expressed alone or with $3C^{pro}$ in transient expression assays in BHK cells as in Fig. 2. Cell lysates were prepared and analysed by immunoblotting. The odd numbered lanes shows the P1–2A precursors expressed alone and the even numbered lanes shows the precursor co-expressed with the $3C^{pro}$. A negative control (No DNA) is included in lane 9. Molecular mass markers (kDa) are indicated on the left. The structural proteins corresponding to the different bands are indicated on the right of the figure and were detected using the following antibodies: (a) guinea pig anti-FMDV O-Man antisera, (b) murine anti-VP2 antibody and (c) guinea pig anti-FMDV A-Iraq antisera. Bound antibodies were visualized using the appropriate HRP-linked secondary antibodies (Dako) and a chemiluminescence detection kit (Pierce ® ECL Western Blotting Substrate, Thermo Fisher Scientific). The results are representative of 3 separate transfections that yielded similar results.

amino acid substitutions at either the VP0/VP3 or the VP3/VP1 junction, was determined in transient expression assays by immunoblotting using an anti-2A antibody and the results are shown in Fig. 4. A P1–2A mutant with the VP1 K210E substitution (Gullberg et al., 2013b; Kristensen et al., 2016), which inhibits cleavage at the VP1/2A junction, served as positive control (Fig. 4, lanes 8 and 9). Expression of the plasmids encoding the wt and mutant P1–2A products in the absence of $3C^{pro}$ led to the expected synthesis of the P1–2A precursor in each case

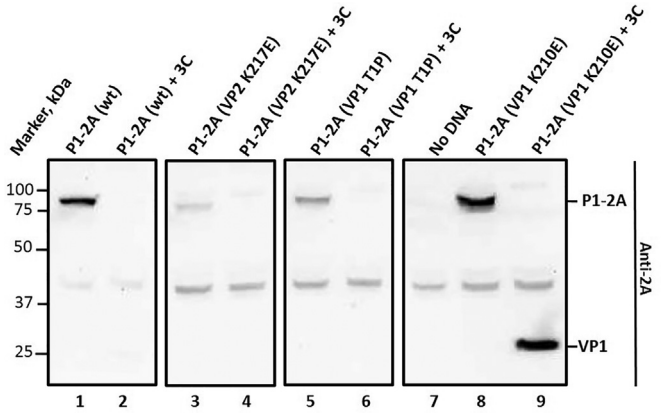

Fig. 4. Cleavage of the VP1/2A junction is unaffected by blocking cleavages elsewhere in P1–2A. BHK cells were transfected with the P1–2A (wt), P1–2A (VP2 K217E), P1–2A (VP1 T1P) and a positive control P1–2A (VP1 K210E) either alone or together with the plasmid encoding the $3C^{pro}$ as described for Fig. 2. Cell lysates were prepared and analysed by immunoblotting using a rabbit anti-2A antibody (ABS31 Merck Millipore). Bound antibodies were visualized using HRP–linked anti-rabbit secondary antibodies (Dako) and a chemiluminescence detection kit (Pierce ® ECL Western Blotting Substrate, Thermo Fisher Scientific). Molecular mass markers (kDa) are indicated on the left. The structural proteins containing 2A corresponding to the different bands are indicated on the right. A negative control (No DNA) (lane 7), and positive controls (where VP1–2A processing is blocked) (lanes 8 and 9) are shown. These analyses were performed following each of the transfections used to generate the results in Fig. 2 and Fig. 3 with very similar results.

(Fig. 4, lanes 1, 3, 5 and 8). When co-expressed with $3C^{pro}$, processing of the P1–2A occurred. The VP1 K210E mutant (positive control) yielded a clear product that is detected by the anti-2A antibody at around 28 kDa that is VP1–2A (Fig. 4, lane 9) as expected. In contrast, no VP1–2A could be detected from the wt or from the other mutants indicating that cleavage at the VP1/2A junction had occurred in each case (Fig. 4, lane 2, 4 and 6). Similarly, no product was detected in the negative control (No DNA, Fig. 4, lane 7). Taken together, these results indicate that blocking the cleavage at either the VP0/VP3 junction or the VP3/VP1 junction had no adverse effect on processing at the VP1/2A junction.

2.5. Substitutions at the VP0/VP3 or VP3/VP1 junctions in the full-length virus

The effect of modifying the VP0/VP3 and VP3/VP1 junctions on virus infectivity was also examined. The modifications resulting in the different amino acid substitutions were tested in conjunction with specific silent (synonymous) mutations (see Methods) within a full-length FMDV cDNA based on the backbone of a chimeric O1 Kaufbeuren (O1K) virus containing the coding region for the VP2-VP3-VP1–2A of the A22 Iraq strain of FMDV (as described previously, (Polacek et al., 2013; Kristensen et al., 2016; Porta et al., 2013)). The amino acid substitutions are indicated in Fig. 1. Full-length RNA transcripts were produced in vitro from the linearized plasmids and were introduced into BHK cells by electroporation. After 2 passages in cells, high titre virus stocks were obtained from the parental chimeric FMDV (wt) and from the FMDV (VP2 K217R) mutant. Three passages were performed for the other mutants, but none of them produced CPE and no virus could be rescued (Table 1). To determine whether the introduced mutations were retained in the FMDV (VP2 K217R) mutant, RNA was extracted from the virus harvests and following RT-PCRs, the region encoding the P1–2A precursor was sequenced at passage two, three and four. It was found that the rescued virus from the FMDV (VP2 K217R) mutant had retained both the encoded amino acid substitution and the silent mutation (tag). Moreover, no second site mutations were

Table 1
Rescued viruses.

Name	VP0/VP3 junction	VP3/VP1 junction	Rescued virus
pO1K/A22 wild-type (wt)	ELPSKE/GIVPVA	IDPRSQ/TTTTGE	+
pO1K/A22 (VP2 K217R)	ELPS**R**E/GIVPVA		+
pO1K/A22 (VP2 K217E)	ELPS**E**E/GIVPVA		–
pO1K/A22 (VP3 I2P)	ELPSKE/G**P**VPVA		–
pO1K/A22 (VP3 Q221P)		IDPRS**P**/TTTTGE	–
pO1K/A22 (VP1 T1P)		IDPRSQ/**P**TTTGE	–

observed within the sequence encoding the P1–2A precursor (data not shown).

2.6. Growth curve of the FMDV (wt) and FMDV (VP2 K217R)

The growth of the FMDV (wt) and the FMDV (VP2 K217R) mutant was determined by infecting BHK cells, using a MOI of 0.05 $TCID_{50}$/cell, and harvesting the cells at different time points post infection. From each time point, samples were titrated to determine the virus yield ($TCID_{50}$/ml). The results showed that there was no major difference between the growth rates of the two viruses (see Supplementary material Fig. S2).

2.7. Delayed processing of the VP0-VP3 junction within cells infected by the FMDV (VP2 K217R) mutant

The production of the viral capsid proteins within cells infected with the rescued viruses, FMDV (wt) and the FMDV (VP2 K217R mutant) was visualized from cell extracts by immunoblotting using antibodies directed against the different FMDV capsid proteins. BHK cells were infected with the FMDV (wt) and the FMDV (VP2 K217R), and cell lysates were prepared at different time points (as indicated in Fig. 5). The FMDV (wt) P1–2A precursor was efficiently processed to generate the structural proteins (VP0, VP2, VP1, see Fig. 5, lanes 3, 5 and 7) and, also presumably VP3 and VP4 (not detected by these antibodies). From the FMDV (VP2 K217R) P1–2A, each of the mature structural proteins was also detected, however the processing intermediate, VP0-VP3 (around 58 kDa) could also be detected at all time points (Fig. 5a and b, lanes 4, 6 and 8) indicating a significant delay in the processing of the modified VP0/VP3 junction (as observed in the transient expression assays, see Fig. 2a and b). This was particularly pronounced at the early stages of infection, when the level of the $3C^{pro}$ is relatively low.

2.8. The VP0-VP3 intermediate is not incorporated into either mature FMDV particles or empty capsids

To determine whether the uncleaved VP0-VP3 intermediate was incorporated into either empty capsids or virus particles, clarified lysates from cells infected with either FMDV (wt) or the FMDV (VP2 K217R) mutant were analysed by sucrose gradient ultra-centrifugation. The fractions were analysed by ELISA to determine the fractions containing either protomers/pentamers (fraction 2), empty capsids (fraction 9) or complete virus particles (fraction 20), see Fig. 6a. These three fractions were analysed by immunoblotting. Fraction 2 comprised unassembled material (Fig. 6b lanes 1 and 2) and included VP0 and also, for the mutant, VP0-VP3. Fraction 9 contained empty capsids and both VP0 and VP2 were present (Fig. 6b, lanes 3 and 4). Fraction 20 included intact virus particles; almost no VP0 was detected, but a high level of VP2 was observed (Fig. 6b, lanes 5 and 6). The VP0-VP3 intermediate could only be detected in fraction 2 for the FMDV (VP2 K217R) mutant, indicating that this intermediate was not incorporated into either the assembled empty capsids or the complete virus particles. Interestingly,

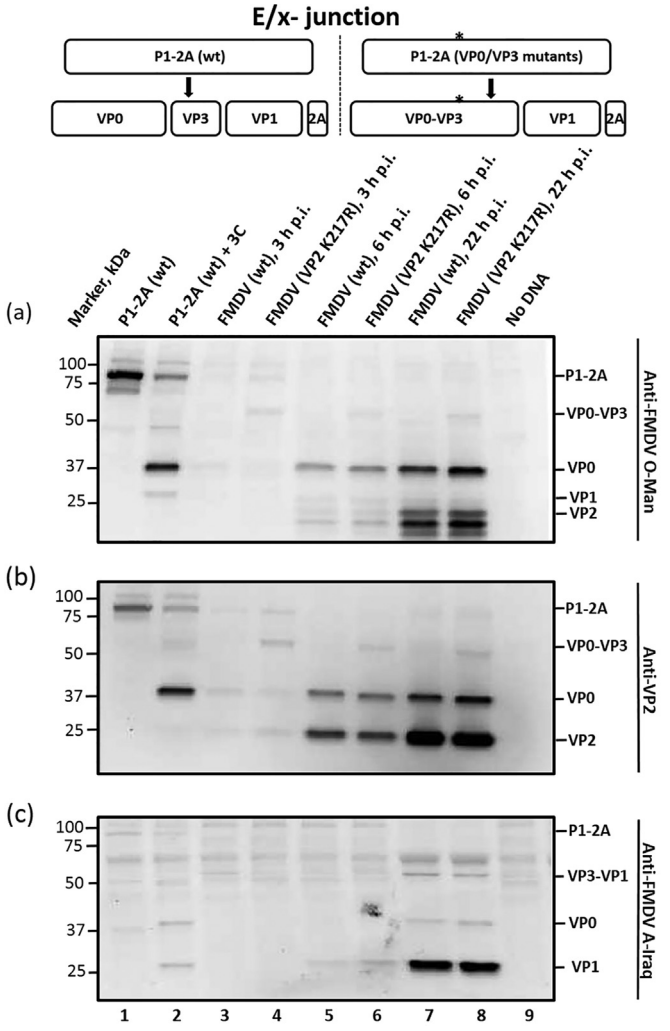

Fig. 5. Production of uncleaved VP0-VP3 within FMDV-infected cells. BHK cells were infected with FMDV (wt) and FMDV (VP2 K217R). Cell lysates were prepared at 3 h p.i. (lane 3 and 4), 6 h p.i. (lane 5 and 6) and 22 h p.i. (lane 7 and 8) and analysed by immunoblotting. Molecular mass makers (kDa) are indicated on the left. Cell extracts containing the wt P1–2A expressed alone and together with $3C^{pro}$ from a transient expression assay were included to act as markers for the structural proteins. Uninfected cells (negative control) were also included (lane 9). The structural proteins are indicated on the right of the figure. The antibodies used to detect the structural proteins were: (a) guinea pig anti-FMDV O-Man antisera, (b) murine anti-VP2 antibody and (c) guinea pig anti-FMDV A-Iraq antisera. Bound antibodies were visualized using appropriate HRP–linked secondary antibodies (Dako) and a chemiluminescence detection kit (Pierce ® ECL Western Blotting Substrate, Thermo Fisher Scientific). Similar results were obtained in 4 independent virus-infection experiments.

the intact P1–2A precursor could also be detected in fraction 2 for the FMDV (VP2 K217R) mutant, see Fig. 6b lane 2. The three different fractions were also analysed with the anti-FMDV O-Man antibody; this confirmed the presence of the unprocessed VP0-VP3 intermediate only being present in FMDV (VP2 K217R) fraction 2 (data not shown).

3. Discussion

The FMDV P1–2A precursor is processed by $3C^{pro}$ into VP0, VP3, VP1 and 2A The cleavage occurs either at Q/x or E/x junctions, and for both of these types of junction the nature of the residues flanking the junctions is of high importance for optimal cleavage. In the present study we have examined the consequences of either blocking or

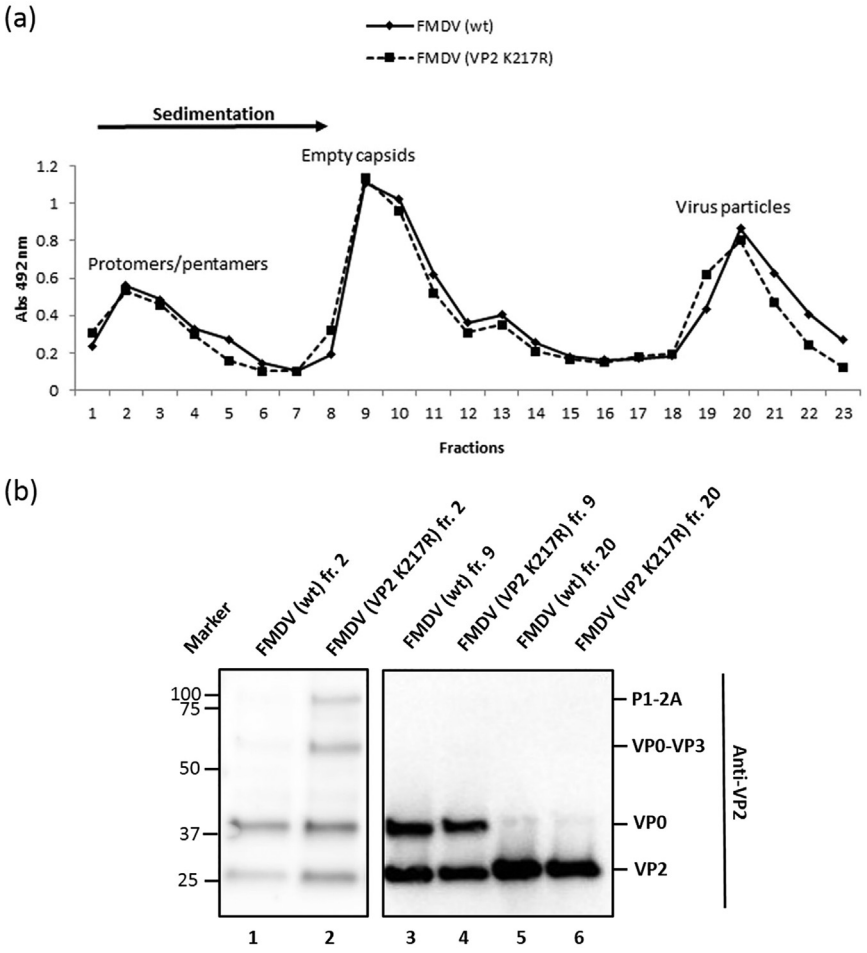

Fig. 6. Analysis of VP0-VP3 within assembled and unassembled virus components within FMDV-infected cells. (a) BHK cells were infected with FMDV wt (solid line) and FMDV VP2 K217R (dotted line), using an MOI of 1, and harvested at 18 h p.i. The clarified lysates were loaded on 15–30% sucrose gradients and separated into separate fractions following centrifugation. FMDV proteins in the different fractions were detected using a serotype specific antigen ELISA. The absorbances were plotted for each fraction. The background (mock infected BHK cells) OD was subtracted. The locations of protomers/pentamers, empty capsids and virus particles are indicated. Fraction 1 is the top of the gradient. (b) Proteins from fractions corresponding to the protomers/pentamers (fraction 2), the empty capsids (fraction 9) and the virus particles (fraction 20) were analysed by immunoblotting as in Figs. 2–4, using the monoclonal anti-VP2 antibody. Molecular mass makers (kDa) are indicated on the left and identification of the structural proteins are shown on the right. The results presented were generated from a single, optimized, experiment with the presence of the VP0-VP3 precursor being consistent with the analyses presented in Fig. 5.

delaying the processing of individual junctions within the FMDV P1–2A precursor by the $3C^{pro}$ by substituting specific amino acids flanking the junctions.

The structure of FMDV $3C^{pro}$ closely resembles the conformation of chymotrypsin (Allaire et al., 1994), and indeed, it belongs to the family of chymotrypsin-like serine proteases. The active site is responsible for the substrate binding and is located between two six-stranded β-barrels (Matthews et al., 1999). Normally, the serine proteases contain a catalytic triad composed of the amino acids Ser-His-Asp at the active site, but the FMDV $3C^{pro}$ has Cys-His-Asp/Glu at the active site (Sweeney et al., 2007; Gosert et al., 1997).

The active site of the enzyme typically recognizes the different side chains of the amino acids flanking the cleavage site. The side chains serve as features for binding and directing the peptide/polyprotein backbone into the correct orientation in the active site. Hydrogen bonds are formed between the substrate and the protease and these contacts are further strengthened by non-polar contacts between the peptide side chains and the protease. The S1 pocket of the FMDV $3C^{pro}$ is responsible for binding to the side chain of the P1 residue of the substrate (Birtley et al., 2005). The P1-E side chain binds in almost the same manner as the alternative P1-Q side chain, thus making the FMDV $3C^{pro}$ able to process junctions containing either of these amino acids at this position. The hydrogen bonds from the P1 residue to the side chains of His^{181} and Thr^{158} in the $3C^{pro}$ are important, as an earlier study showed that substitutions to other amino acids, within synthetic peptide substrates, that contained either uncharged (norleucine), longer (adipic acid) or shorter (aspartate) side chains, blocked the processing of these substrates (Zunszain et al., 2010).

3.1. Processing of the P1–2A precursor in the transient expression assay

At the VP0/VP3 junction (see Fig. 1), which has a glutamate (E) at the P1 position and a lysine (K) at the P2 position, we introduced different substitutions both upstream and downstream of the junction. Interestingly, the fairly conservative VP2 K217R substitution (each has a positively charged side chain) at residue 2 strongly affected the processing of this VP0/VP3 junction (E/x group). VP0 could be detected, but the elevated level of the processing intermediate VP0-VP3 indicated that the processing rate at the VP0/VP3 junction had been reduced. We previously reported that the VP1 K210R substitution at the VP1/2A junction (the P2 position in a Q/x group site) did not affect cleavage at this junction (Kristensen et al., 2016). However, it should be noted that the P2 position in the Q/x group is, in some FMDVs, an R whereas R is never present at the P2 position in the E/x sites (Curry et al., 2007).

Substituting the positively charged lysine (K) residue for the negatively charged glutamate (E) at the P2 residue in the VP0/VP3 junction (VP2 K217E) severely impeded the cleavage. This is consistent with earlier findings on the VP1/2A junction where the VP1 K210E substitution greatly reduced the processing of the VP1/2A junction (Gullberg et al., 2013b; Kristensen et al., 2016). These results revealed that the P2 residue is of high importance in the E/x group and that processing can be reduced to different degrees according to how conservative the substitution is.

The VP0/VP3 junction was also modified by changing one amino acid downstream of the cleavage site, at the P2′ position, in the VP3 I2P mutant. This substitution adversely affected the processing of the junction as seen with the VP2 K217R substitution. This is interesting as the introduction of a proline residue at P2′ may be expected to induce a more drastic change in structure compared to the arginine substitution

at the P2 position. It is clear that $3C^{pro}$ was able to process the modified junction since VP0 still could be detected (Fig. 2), but a product corresponding to VP0-VP3 was also detected at a similar level as with the K217R, indicating that the $3C^{pro}$ cleavage at this site was slowed. An earlier study has reported that a substitution from leucine to alanine at the P2′ residue in a synthetic peptide corresponding to a Q/x group site only caused a minor effect on the processing (Birtley et al., 2005). Interestingly, we have shown earlier that substituting the leucine for a proline at the P2′ residue in the VP1/2A junction in full length FMDV, completely blocked the processing of this junction (Gullberg et al., 2014). However proline is actually one of the most abundant amino acids at the P2′ position in the E/x group of sites within FMDVs, whereas it is never seen at the P2′ position in the Q/x group (Curry et al., 2007). This result indicates that even though changing an isoleucine to a proline is a fairly drastic change and the cleavage of this junction is clearly reduced, the $3C^{pro}$ has a broad tolerance for different amino acids at this position and a variety of residues are found in other FMDV junctions at this specific position in the E/x sites.

The VP3/VP1 junction has a glutamine (Q) at the P1 position. As mentioned above, $3C^{pro}$ is able to cleave junctions containing either a glutamate or a glutamine residue at the P1 position as the side chains of these amino acids are able to interact with the S1 pocket of the $3C^{pro}$. It was therefore not surprising that cleavage by $3C^{pro}$ was completely prevented when the P1 residue was changed to a proline (VP3 Q221P).

At the P1′ position, large hydrophobic side chains are required for optimal cleavage of the Q/x-group. The P1′ residue is very often either leucine, isoleucine or threonine (Curry et al., 2007). Leucine and isoleucine are very similar, but threonine seems to stand out from the group since it has an -OH side chain. An earlier study showed that substituting a leucine to a glycine at the P1′ position in a synthetic peptide representing the VP1/2A sequence caused a ten-fold reduction in cleavage rate. In contrast, substitutions to valine or cysteine, which both have non-polar side chains only reduced the cleavage rate by two-fold (Zunszain et al., 2010). In the VP3/VP1 junction a threonine is present at the P1′ position in all FMDVs (Carrillo et al., 2005). Threonine, does not have a large hydrophobic side chain, as leucine and isoleucine do, indicating that other properties of these amino acids must also affect the processing. Substituting the P1′ residue in the Q/x group (VP1 T1P) at the VP3/VP1 junction severely inhibited the processing of this junction. Introducing a proline is known to be very disruptive in the polypeptide chain and therefore was expected to have a negative effect. However, it is interesting that although for the Q/x group substitution to a proline at either P1′ in the VP3/VP1 junction (as shown here) or substitution to a proline at P2′ in the VP1/2A junction (Gullberg et al., 2014) almost completely blocked cleavage, in contrast changing the P2′ residue to a proline in the VP0/VP3 junction (E/x group) only caused a moderate reduction in processing by $3C^{pro}$.

For all of the mutants having a substitution near the VP0/VP3 junction, the production of VP1 from the modified P1–2A could be detected in the presence of $3C^{pro}$, and for all of the mutants having a substitution in the VP3/VP1 junction, VP0 could be detected following processing. Furthermore, the VP1/2A junction was also fully processed in all of these mutants. These results indicate that $3C^{pro}$ is able to process these 3 junctions independently and that processing of these junctions does not need to occur in a fixed order. However, it is noteworthy that in the wt protein, processing of the VP3/VP1 junction seems to occur more slowly than processing of the VP0/VP3 junction. This contrasts with earlier studies that indicated that initial processing of the P1–2A precursor happens at the VP3/VP1 junction, followed by processing of the VP0/VP3 junction with the final processing at the VP1/2 A junction (Bablanian and Grubman, 1993). For this earlier study, the rabbit reticulocyte lysate in vitro translation system was used to produce the P1–2A precursor. The use of this cell-free analysis versus the cell-based analysis used here might explain the differences observed. Blocking processing at either the VP0/VP3 or the VP3/VP1 junctions did not affect the processing of the VP1/2A junction, as shown in Fig. 4 (and indeed, we have shown earlier that blocking cleavage of the VP1/2A junction does not impede any of the other cleavages as viable virus can still be obtained with the 2A L2P mutant (Gullberg et al., 2014)).

3.2. Processing of the P1–2A precursor in infectious virus

Using the transient expression assay, we showed that the VP2 K217R and the VP3 I2P substitutions markedly reduced cleavage of the junction by the $3C^{pro}$, whereas the other substitutions tested essentially blocked the cleavage. Interestingly, the full-length FMDV RNA encoding the VP2 K217R substitution was the only one of the mutants that was able to form infectious virus particles and replicate. It is surprising that the mutant containing the VP3 I2P substitution did not replicate, since cleavage seemed to be reduced to about the same level as for the VP2 K217R substitution in the transient expression assay. Comparing the proteins expressed by the wt virus with the mutant virus containing the VP2 K217R substitution within infected cells clearly showed reduced processing of the VP0/VP3 junction, however this modification does not seem to affect the level of the mature structural proteins to a high degree, as similar amounts of the fully processed proteins were detected in cells infected with the wt and mutant virus containing the VP2 K217R substitution (Fig. 5). These results are consistent with our earlier findings for the Q/x group sites, showing that processing of the VP1/2A junction was not completely blocked by the substitution VP1 K210R (Kristensen et al., 2016).

Separation of protomers/pentamers, empty capsids and virus particles was achieved using sucrose gradient centrifugation (Fig. 6a). By immunoblotting, it was apparent that the VP0-VP3 intermediate was only present in unassembled material (Fig. 6b). This contrasts with the fact that FMDV is able to incorporate uncleaved VP1–2A into the virus particle (Gullberg et al., 2013b). However, based on the structure of the pentamer from an assembled A22 Iraq virus particle it is clear that the C-terminus of VP2 and the N-terminus of VP3 are located very far apart (Fig. 7) (Curry et al., 1996), (although adjacent in the uncleaved P1–2A) and this presumably explains why the assembled virus particles are not able to incorporate the VP0-VP3 intermediate. There was little difference in the growth rate of the FMDV (wt) and the FMDV (VP2 K217R) viruses (Fig. S2). High amounts of empty capsids are produced in both the wt and the mutant, thus suggesting that the structural proteins are produced in excess. Moreover, it seems that the majority of the VP0-VP3 intermediate gets cleaved, especially later in infection (Fig. 5). Both of these features may explain why a small amount of non-functional VP0-VP3 intermediate can be tolerated and not cause a selective disadvantage to the mutant FMDV.

Overall, the results presented here provide important information about the two different groups of junctions within the capsid precursor that are cleaved by the FMDV $3C^{pro}$. The results show that there is no strict order of cleavage of the structural proteins, as blocking of one junction did not prevent cleavage of the other junctions.

The $3C^{pro}$ is responsible for cleaving 10 out of the 13 cleavage sites in the polyprotein, thus making the enzyme an attractive drug target to interfere with the lifecycle of the virus (Curry et al., 2007). Moreover, $3C^{pro}$ is functionally conserved among different serotypes of FMDV, which provides a possibility of targeting multiple serotypes instead of just one serotype, as is the case with current vaccines.

4. Methods

4.1. Plasmid construction

The plasmid pO1K/A22 contains a full-length cDNA corresponding to a chimeric FMDV genome as previously described (Polacek et al., 2013; Kristensen et al., 2016). It includes the capsid coding sequence from FMDV A22 Iraq and the rest of the genome from FMDV O1K. Variants of this plasmid encoding amino acid substitutions at either the

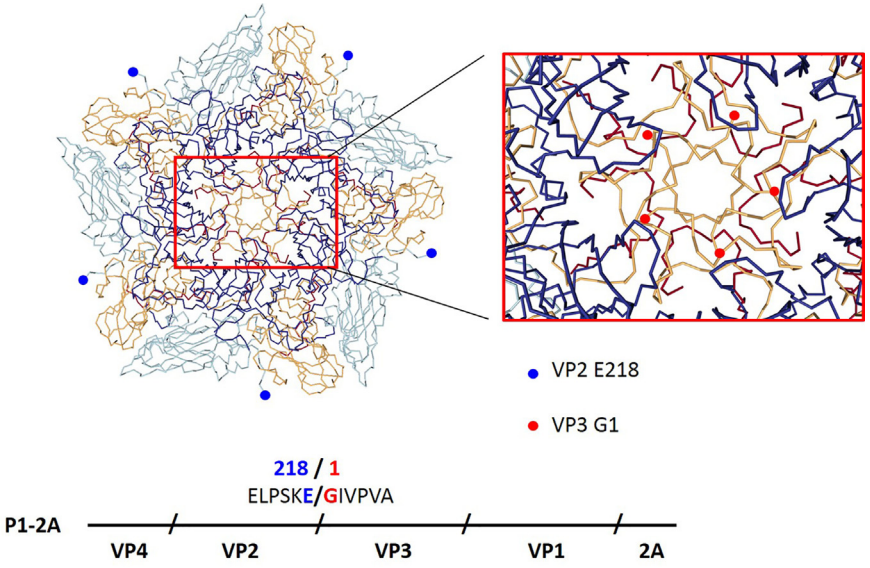

Fig. 7. Separation of the C-terminus of VP2 and the N-terminus of VP3 during capsid assembly. The structure of the FMDV A22 Iraq capsid pentamer (PDB 4GH4) (Curry et al., 1996) was visualized using pdb-viewer. An enlargement of the 5-fold axis of the pentamer is shown in the red box where the N-termini of the VP3s are marked with red symbols. The C-termini of the VP2s are marked with blue circles. The cleavage site in the uncleaved P1–2A precursor is also indicated.

Table 2
Primers used for site-directed mutagenesis.

Primers for megaprimers	Changes	Name
Plasmids for the Transient expression assay, introducing Leader (W52A) substitution		
SG31_Fw: CCACGACAACTGC**GC**GTTGAACGCC	Leader (W52A) TGG- > GCG	P1–2A (wt)
14TPN6_Rev: CAAACAGGTGCTTCTTGAAAAATCTTTC		
Plasmids for the Transient expression assay, introducing substitutions in the VP2/VP3 and VP3/VP1 junctions, note that all constructs contains the Leader (W52A) substitution		
14TPN5_Fw: GAGTGTGGGAGTCACGTACG	VP2 K217R (AAA- > CGT)	P1–2A (VP2 K217R)
1PTK18_Rev: GACCGGAACAATCCCCTC**ACG**CGAGGGGAG	VP3 V3V (GTA- > GTT)	
13LPN48_Fw: CCCCTCG**GA**G**G**AGGGGATTGTACCG	VP2 K217E (AAA- > GAG)	P1–2A (VP2 K217E)
13LPN50_Rev: GCACGCCTCAGCCACATCCAAC		
13LPN49_Fw: CCCCTCGAAGGAGGGG**CC**TGTACCG	VP3 I2P (ATT- > CCT)	P1–2A (VP3 I2P)
13LPN50_Rev: GCACGCCTCAGCCACATCCAAC		
13LPN22_Fw: GCTCAC**C**CACCACTACCACCGGG	VP3 Q221P (CAA- > CCC)	P1–2A (VP3 Q221P)
13LPN30_Rev: GAGGTCAATGACATGTGTGG		
13LPN23_Fw: GCTCACAA**C**CCACTACCACCGGG	VP1 T1P (ACC- > CCC)	P1–2A (VP1 T1P)
13LPN30_Rev: GAGGTCAATGACATGTGTGG		
Plasmids for production of full-length FMDV RNAs		
14TPN5_Fw: GAGTGTGGGAGTCACGTACG	VP2 K217R (AAA- > CGT)	pO1K/A22 (VP2 K217R)
1PTK18_Rev: GACCGGAACAATCCCCTC**ACG**CGAGGGGAG	VP3 V3V (GTA- > GTT)	
14TPN5_Fw: GAGTGTGGGAGTCACGTACG	VP2 K217E (AAA- > GAG)	pO1K/A22 (VP2 K217E)
1PTK22_Rev: AGCGACCGGTACGATCCCCTC**CT**CCGAGGG	VP3 I2I (ATT- > ATC)	
14TPN5_Fw: GAGTGTGGGAGTCACGTACG	VP3 I2P (ATT- > CCT)	pO1K/A22 (VP3 I2P)
1PTK20_Rev: GTACA**GG**CCCCTCCTTCGAGGGGAGCTCAC	VP2 K217K (AAA- > AAG)	
14TPN7_Fw: GACAAATCAAGGTTTATGCCAACATTGC	VP3 Q221P (CAA- > CCC)	pO1K/A22 (VP3 Q221P)
1PTK24_Rev: CGGTGGTAGTAGT**GG**GTGAGCGGGGGTCAA	VP1 T1T (ACC- > ACT)	
14TPN7_Fw: GACAAATCAAGGTTTATGCCAACATTGC	VP1 T1P (ACC- > CCC)	pO1K/A22 (VP1 T1P)
1PTK26_Rev: CCGGTGGTAGTGG**GC**TGTGAGCGGGGGTCA	VP3 Q221Q (CAA- > CAG)	

Bold = Nucleotide changes generating amino acid changes. Underlined = silent mutations.

VP0/VP3 or VP3/VP1 cleavage sites were produced using site-directed mutagenesis (Chen et al., 2000). Phusion® High-Fidelity DNA Polymerase (Thermo Fisher Scientific) was used in all of the PCR amplifications according to the manufacturer's instructions unless otherwise noted. Briefly, fragments were amplified in PCRs, using the pO1K/A22 plasmid as template, together with primers specifying the desired mutations, see Table 2. The PCR products (580 bp for the VP0/VP3 junction and 160 bp for the VP3/VP1 junction) were gel purified using the GeneJET Gel purification kit (Thermo Fisher Scientific) and used as megaprimers for a second round of PCR, again using the wt pO1K/A22 as template to make full length plasmids of approximately 11,000 bp. After the PCR and subsequent *Dpn*I digestion of the template DNA, the products were purified using the GeneJET PCR purification kit (Thermo Fisher Scientific) and transformed into chemically competent *Escherichia coli* (*E. coli*) cells. Plasmids were amplified from individual colonies, purified using the GeneJet Plasmid Miniprep Kit (Thermo Fisher Scientific) and sequenced by Sanger Sequencing using the BigDye Terminator v.3.1 Cycle Sequencing kit and a 3500 Genetic Analyzer (Applied Biosystems).

To prepare constructs (lacking the $3C^{pro}$ coding region) suitable for the transient expression assays, plasmids were digested with *Apa*I to remove most of the cDNA encoding the non-structural proteins downstream of the 2 A peptide (Fig. 1). The digested plasmids were analysed using agarose gel electrophoresis and the largest fragments purified using the GeneJET Gel Extraction Kit (Thermo Fisher Scientific). The fragments were self-ligated using Ready To Go T4 DNA ligase (Amersham Biosciences) and transformed into *E. coli*. From the resulting colonies, plasmids were purified using a Plasmid Midi Kit (Qiagen) and sequenced to confirm the absence of the FMDV sequence downstream of the 2 A. These constructs contained the cDNA region encoding the wt

Leader (L) protease, which adversely affects the expression level of the P1–2A precursor in the transient expression assay (see Supplementary material Fig. S1). The W52A mutant form of the L^{pro} retains the L/P1 cleavage activity but is unable to induce cleavage of the translation initiation factor eIF4G (Guan and Belsham, 2017). This modification was introduced into each of the constructs by site-directed mutagenesis, as described above, see Table 2 for primers. The PCR products were *Dpn*I digested, transformed into *E. coli*, purified using a Plasmid Midi Kit (Qiagen) and sequenced to confirm the presence of expected mutations and the absence of other changes in the P1–2A region. All of these constructs contained the Leader (W52A) substitution and lacked the coding region for the non-structural proteins. These constructs were called: P1–2A (wt), P1–2A (VP2 K217R), P1–2A (VP2 K217E), P1–2A (VP3 I2P), P1–2A (VP3 Q221P) and P1–2A (VP1 T1P).

The five mutant plasmids (derived from pO1K/A22) containing the chimeric full-length FMDV coding sequence with different substitutions (VP2 K217R, VP2 K217E, VP3 I2P, VP3 Q221P or VP1 T1P) were further modified to introduce different silent mutations near the modified junctions enabling tracking of each mutant in case of potential sequence reversions. The silent changes introduced and primers used to make them are listed in Table 2. Briefly, forward and reverse primers were used in PCRs with each of the five plasmids to create megaprimers (580 bp for the VP0/VP3 junction and 160 bp for the VP3/VP1 junction), which were subsequently used in a long PCR with the same template to introduce the silent mutations. The PCR products were *Dpn*I digested, transformed into *E. coli* and the presence of the desired silent mutation in each plasmid was verified by sequencing. These constructs were termed: pO1K/A22 (VP2 K217R), pO1K/A22 (VP2 K217E), pO1K/A22 (VP3 I2P), pO1K/A22 (VP3 Q221P) and pO1K/A22 (VP1 T1P). See Fig. 1 for an overview of the different substitutions (note that the silent mutations are not shown in Fig. 1, but can be seen in Table 2).

4.2. Transient expression assays

For the transient expression assays, baby hamster kidney (BHK) cells were seeded into 35-mm wells approximately 24 h before starting the assay. The BHK cells (around 90% confluent) were infected with a recombinant vaccinia virus, termed vTF7-3 (Fuerst et al., 1986), that expresses the T7 RNA polymerase. After one hour, this virus was removed and the infected cells were transfected with the indicated plasmid DNA using FuGENE 6 (Promega) essentially as described previously (Belsham et al., 2008). For the co-transfections, 1 μg of the plasmid containing the FMDV P1–2A coding region and 10 ng of the plasmid (pSKRH3C) (Belsham et al., 2000) encoding the FMDV $3C^{pro}$ were mixed prior to transfection. The cells were incubated in 5% CO_2 at 37 °C overnight. The cells were lysed with 500 μL Buffer C (20 mM Tris-HCl (pH 8.0), 125 mM NaCl and 0.5% NP-40) and the cell extracts were clarified by centrifugation at 18,000 ×*g* for 10 min at 4 °C.

4.3. Immunoblot analysis of samples from transient expression assay

Immunoblotting was performed using cell lysates mixed with either 2 × Laemmli sample buffer (Bio-Rad) or red loading buffer Pack (New England BioLabs) (containing 25 mM DTT). The proteins were separated by SDS-PAGE (4–20%, 12% or a 7.5% Bis-Tris gels (Bio-Rad)) and transferred to either PVDF membranes (Milipore) or nitrocellulose membranes (Bio-Rad). PBS containing bovine serum albumin (BSA) (5%), (for the anti-VP2 antibody and the anti-FMDV O-Man antibody) or skimmed milk powder (5%) (for the anti-2A antibody, the anti-eIF4G antibody and the anti-FMDV A-Iraq antibody) and Tween (0.1%) was used as blocking buffer and dilution buffer for the primary and secondary antibodies. The proteins were detected using guinea pig anti-FMDV O-Manisa antisera (1:1000), or anti-VP2 antibodies (1:2000) (mouse monoclonal antibody 4B2 (Yu et al., 2011), kindly provided by L. Yu, Harbin, P. R. China), guinea pig anti-FMDV A-Iraq antisera (1:1000), FMDV anti-2A-peptide antibody (1:1000) (Rabbit, ABS31 Merck Millipore) or anti-eIF4G antibody (1:1000) (Goat, SC-9602 Santa Cruz Biotechnology) as primary antibodies. The bound proteins were visualized using appropriate HRP-conjugated secondary antibodies (Dako) and a chemiluminescence detection kit (Pierce ® ECL Western Blotting Substrate, Thermo Fisher Scientific). Images were captured using either a Chem-Doc XRS system (Bio-Rad) or a G:BOX Chemi XX6 (Syngene).

4.4. Rescue of infectious virus from modified FMDV cDNA

The plasmids, containing the full-length wt or mutant FMDV cDNAs, i.e. pO1K/A22 (VP2 K217R), pO1K/A22 (VP2 K217E), pO1K/A22 (VP3 I2P), pO1K/A22 (VP3 Q221P) and pO1K/A22 (VP1 T1P) were linearized by digestion with *Hpa*I and purified using the GeneJET PCR purification kit (Thermo Fisher Scientific). The linearized plasmids were transcribed in vitro using the MEGAscript® T7 Transcription Kit (Thermo Fisher Scientific). An aliquot (1 μL) of each RNA sample was visualized following agarose gel electrophoresis to check yield and integrity and the rest (19 μL) was introduced into BHK cells by electroporation as described previously (Nayak et al., 2006).

The cells were transferred to Falcon flasks and Eagle's medium containing 5% calf serum was added. The cells were incubated overnight at 37 °C. The rescued viruses were amplified using three passages in BHK cells. Cytopathic effect (CPE) was only detected with the FMDV (wt) and the mutant virus containing the VP2 K217R substitution, termed FMDV (VP2 K217R). After each passage, viral RNA, from the wt and the mutant virus was isolated using the RNeasy Mini Kit (Qiagen) and reverse transcribed using Ready-To-Go You-Prime First-Strand Beads (GE Healthcare Life Sciences) together with random primers. The cDNA corresponding to the P1–2A region was amplified as four overlapping fragments of around 1000 bp by AmpliTaq Gold DNA Polymerase (Thermo Fisher Scientific), visualized on agarose gels and purified using the GeneJET PCR purification kit (Thermo Fisher Scientific) (primers listed in Table S1, see Supplementary material). For each RNA, a negative control, lacking the reverse transcriptase, was included in the RT-PCRs to verify that the PCR products were obtained from viral RNA and not from residual plasmid template. The PCR products were sequenced (primers are listed in Table S1, see Supplementary material) using the BigDye Terminator v.3.1 Cycle Sequencing kit and a 3500 Genetic Analyzer (Applied Biosystems). Sequences were analysed using Geneious 9.0.2 (Biomatters).

4.5. Titration of FMDV (wt) and FMDV (VP2 K217R)

After the three passages in BHK cells, both the rescued FMDV (wt) and the FMDV (VP2 K217R) stocks were titrated. Briefly, 50 μL BHK suspension (400,000 cells/ml in Eagles medium with 20% fetal bovine serum (FBS)) were loaded in each well of a 96-well plate and 50 μL Eagles medium was added. Lastly, 50 μL of virus dilutions from 10^{-2} to 10^{-9} were added to the wells. Each dilution was tested in quintuplicate together with two negative controls. The plates were incubated at 37 °C in 5% CO_2 and read each day for three days after infection, and the titres ($TCID_{50}$ /ml) were calculated.

4.6. Immunoblot analysis of FMDV-infected cells

Monolayers of BHK cells, grown in 35 mm wells (approximately 200,000 cells per well), were infected with either the FMDV (wt) or the FMDV (VP2 K217R) at a MOI of 1 $TCID_{50}$/cell. Cells were lysed using Buffer C (as described above) at 3, 6 and 22 h post-infection. The samples were analysed by immunoblotting as described above.

4.7. Growth curve of FMDV (wt) and FMDV (VP2 K217R)

BHK cells were infected with the FMDV (wt) and the FMDV (VP2 K217R) using a MOI = 0.05. Samples were harvested at 0, 2, 5, 10, 15,

24 and 30 h p.i. and then titrated as described above.

4.8. Sucrose gradient analysis

BHK cells (1 well in a 6-well plate) were infected with O1K/A22 FMDV (wt) or O1K/A22 FMDV (VP2 K217R) (MOI of 1 $TCID_{50}$ per cell). At 18 h p.i., the medium was removed and the cells were lysed with 250 µL buffer C containing protease inhibitor (cOmplete Mini, EDTA-free protease inhibitor (Roche)). Samples were clarified by centrifugation for 18,000 g for 10 min and 200 µL of the supernatant was loaded directly onto each 15–30% sucrose gradient. For making the gradients, sucrose was dissolved in PBS and the 15% sucrose solution was added to the tube. The 30% sucrose solution was applied afterwards in the bottom by putting a needle through the 15% sucrose solution. Lastly the gradients were finished using a gradient maker (Gradient Master 108 (BIOCOMP)). The samples were centrifuged at 245,000 ×*g* in a SW 55 Ti rotor (Beckman Coulter) for 1 h at 10 °C. Fractions of 240 µL were collected from the top of the gradient by using a Piston Gradient Fractionator™ (BIOCOMP) and analysed by antigen ELISA (see below) and immunoblotting (as above).

4.9. ELISA

An antigen detection enzyme-linked immunosorbent assay (ELISA) against FMDV serotype A, was performed as described previously (Gullberg et al., 2013b; Roeder et al., 1987). Briefly plates were coated with FMDV A22 Iraq rabbit antisera overnight, the plate was washed and blocked with dilution buffer (2% BSA diluted in PBS buffer with 1% Tween) and the gradient fractions were added. Detection of the bound FMDV proteins was achieved using polyclonal guinea pig anti-FMDV A22 Iraq sera plus rabbit anti-guinea pig Ig conjugated to horseradish peroxidase (Dako). A dissolved SIGMAFAST™ OPD tablet (Sigma-Aldrich) was added, and after seeing colour develop, Stop-solution (1 mM H_2SO_4) was added. The plates were read in a SpectraMax® i3 plate reader (Molecular Devices).

Acknowledgements

This study was funded by internal resources from the National Veterinary Institute within the Technical University of Denmark. We also acknowledge the Danish Council for Independent Research/Natural Sciences for supporting this study (grant number 1323-00117B to G. J. B.). Furthermore, we are grateful to EPIZONE, who supported an external research stay by T.K. at The Pirbright Institute in the U.K. We wish to thank Li Yu (The Chinese Academy of Agricultural Sciences, China) for the anti-VP2 antibody. We also thank Preben Normann and Jani Christensen for their excellent technical assistance. The authors declare that there is no conflict of interest associated with this study.

Appendix A. Supporting information

Supplementary data associated with this article can be found in the online version at doi:10.1016/j.virol.2018.07.010.

References

Abrams, C.C., King, A.M.Q., Belsham, G.J., 1995. Assembly of foot-and-mouth disease virus empty capsids synthesized by a vaccinia virus expression system. J. Gen. Virol. 76, 3089–3098.
Alexandersen, S., Zhang, Z., Donaldson, A.I., Garland, A.J.M., 2003. The pathogenesis and diagnosis of foot-and-mouth disease. J. Comp. Pathol. 129, 1–36.
Allaire, M., Chernaia, M.M., Malcolm, B.A., James, M.N.G., 1994. Picornaviral 3C cysteine proteinases have a fold similar to chymotrypsin-like serine proteinases. Nature 369, 72–76.
Armer, H., Moffat, K., Wileman, T., Belsham, G.J., Jackson, T., Duprex, W.P., Ryan, M., Monaghan, P., 2008. Foot-and-mouth disease virus, but not bovine enterovirus, targets the host cell cytoskeleton via the nonstructural protein 3C pro. J. Virol. 82, 10556–10566.
Atkins, J.F., Wills, N.M., Loughran, G., Wu, C., Parsawar, K., Ryan, M.D., Wang, C., Nelson, C.C., 2007. A case for "'StopGo'": reprogramming translation to augment codon meaning of GGN by promoting unconventional termination (Stop) after addition of glycine and then allowing continued translation (Go). RNA 13, 803–810.
Bablanian, G.M., Grubman, M.J., 1993. Characterization of the foot-and-mouth disease virus 3C protease expressed in Escherichia coli. Virology 197, 320–327.
Belsham, G.J., McInerney, G.M., Ross-Smith, N., 2000. Foot-and-mouth disease virus 3C protease induces cleavage of translation initiation factors eIF4A and eIF4G within infected cells. J. Virol. 74, 272–280.
Belsham, G.J., Nielsen, I., Normann, P., Royall, E., Roberts, L.O., 2008. Monocistronic mRNAs containing defective hepatitis C virus-like picornavirus internal ribosome entry site elements in their 5′ untranslated regions are efficiently translated in cells by a cap-dependent mechanism. RNA 14, 1671–1680.
Birtley, J.R., Knox, S.R., Jaulent, M., Brick, P., Leatherbarrow, R.J., Curry, S., 2005. Crystal structure of foot-and-mouth disease virus 3C protease. J. Biol. Chem. 280, 11520–11527.
Carrillo, C., Tulman, E.R., Delhon, G., Lu, Z., Carreno, A., Vagnozzi, A., Kutish, G.F., Rock, D.L., 2005. Comparative genomics of foot-and-mouth disease virus. J. Virol. 79, 6487–6504.
Chen, G.J., Qiu, N., Karrer, C., Caspers, P., Page, M.G., 2000. Restriction site-free insertion of PCR products directionally into vectors. Biotechniques 28 (498–500), 504–505.
Curry, S., Fry, E., Blakemore, W., Abu-Ghazaleh, R., Jackson, T., King, A., Lea, S., Newman, J., Rowlands, D., Stuart, D., 1996. Perturbations in the surface structure of A22 Iraq foot-and-mouth disease virus accompanying coupled changes in host cell specificity and antigenicity. Structure 4, 135–145.
Curry, S., Fry, E., Blakemore, W., Abu-Ghazaleh, R., Jackson, T., King, A., Lea, S., Newman, J., Stuart, D., 1997. Dissecting the roles of VP0 cleavage and RNA packaging in picornavirus capsid stabilization: the structure of empty capsids of foot-and-mouth disease virus. J. Virol. 71, 9743–9752.
Curry, S., Zunszain, P.A., Leatherbarrow, R.J., 2007. Foot-and-mouth disease virus 3C protease: recent structural and functional insights into an antiviral target. Int. J. Biochem. Cell Biol. 39, 1–6.
Donnelly, M.L.L., Luke, G., Mehrotra, A., Li, X., Hughes, L.E., Gani, D., Ryan, M.D., 2001. Analysis of the aphthovirus 2A / 2B polyprotein " cleavage" mechanism indicates not a proteolytic reaction, but a novel translational effect: a putative ribosomal "skip.". J. Gen. Virol. 82, 1013–1025.
Falk, M.M., Grigera, P.R., Bergmann, I.E., Zibert, A., Multhaup, G., Beck, E., 1990. Foot-and-mouth disease virus protease 3C induces specific proteolytic cleavage of host cell histone H3. J. Virol. 64, 748–756.
Fuerst, T.R., Niles, E.G., Studier, F.W., Moss, B., 1986. Eukaryotic transient-expression system based on recombinant vaccinia virus that synthesizes bacteriophage T7 RNA polymerase. Proc. Nati Acad. Sci. USA 83, 8122–8126.
Gosert, R., Dollenmaier, G., Weitz, M., 1997. Identification of active-site residues in protease 3C of hepatitis A virus by site-directed mutagenesis. J. Virol. 71, 3062–3068.
Guan, S.H., Belsham, G.J., 2017. Separation of foot-and-mouth disease virus leader protein activities; identification of mutants that retain efficient self- processing activity but poorly induce eIF4G cleavage. J. Gen. Virol. 98, 671–680.
Gullberg, M., Muszynski, B., Organtini, L.J., Ashley, R.E., Hafenstein, S.L., Belsham, G.J., Polacek, C., 2013a. Assembly and characterization of foot-and-mouth disease virus empty capsid particles expressed within mammalian cells. J. Gen. Virol. 94, 1769–1779.
Gullberg, M., Polacek, C., Bøtner, A., Belsham, G.J., 2013b. Processing of the VP1 / 2A junction is not necessary for production of foot-and-mouth disease virus empty capsids and infectious viruses: characterization of "self-tagged" particles. J. Virol. 87, 11591–11603.
Gullberg, M., Polacek, C., Belsham, G.J., 2014. Sequence adaptations affecting cleavage of the VP1 / 2A junction by the 3C protease in foot-and-mouth disease virus-infected cells. J. Gen. Virol. 95, 2402–2410.
Jackson, T., Sheppard, D., Denyer, M., Blakemore, W., King, A.M.Q., 2000. The epithelial integrin αvβ6 is a receptor for foot-and-mouth disease virus. J. Virol. 74, 4949–4956.
Kristensen, T., Normann, P., Gullberg, M., Fahnøe, U., Polacek, C., Rasmussen, T.B., Belsham, G.J., 2016. Determinants of the VP1 / 2A junction cleavage by the 3C protease in foot-and-mouth disease virus-infected cells. J. Gen. Virol. 98, 385–395.
Matthews, D.A., Dragovich, P.S., Webber, S.E., Fuhrman, S.A., Patick, A.K., Zalman, L.S., Hendrickson, T.F., Love, R.A., Prins, T.J., Marakovits, J.T., Zhou, R., Tikhe, J., Ford, C.E., Meador, J.W., Ferre, R.A., Brown, E.L., Binford, S.L., Brothers, M.A., Delisle, D.M., Wordland, S.T., 1999. Structure-assisted design of mechanism-based irreversible inhibitors of human rhinovirus 3C protease with potent antiviral activity against multiple rhinovirus serotypes. Proc. Natl. Acad. Sci. USA 96, 11000–11007.
Nayak, A., Goodfellow, I.G., Woolaway, K.E., Birtley, J., Curry, S., Belsham, G.J., 2006. Role of RNA structure and RNA binding activity of foot-and-mouth disease virus 3C protein in VPg uridylylation and virus replication. J. Virol. 80, 9865–9875.
Polacek, C., Gullberg, M., Li, J., Belsham, G.J., 2013. Low levels of foot-and-mouth disease virus 3C protease expression are required to achieve optimal capsid protein expression and processing in mammalian cells. J. Gen. Virol. 94, 1249–1258.
Porta, C., Xu, X., Loureiro, S., Paramasivam, S., Ren, J., Al-khalil, T., Burman, A., Jackson, T., Belsham, G.J., Curry, S., Lomonossoff, G.P., Parida, S., Paton, D., Li, Y., Wilsden, G., Ferris, N., Owens, R., Kotecha, A., Fry, E., Stuart, D.I., Charleston, B., Jones, I.M., 2013. Efficient production of foot-and-mouth disease virus empty capsids in insect cells following down regulation of 3C protease activity. J. Virol. Methods 187, 406–412.
Roeder, P.L., Le Blanc, Smith, P.M., 1987. Detection and typing of foot-and-mouth disease virus by enzyme-linked immunosorbent assay: a sensitive, rapid and reliable technique for primary diagnosis. Res. Vet. Sci. 43, 225–232.
Ryan, M.D., Belsham, G.J., King, A.M.Q., 1989. Specificity of enzyme-substrate

interactions in foot-and-mouth disease virus polyprotein processing. Virology 173, 35–45.
Sweeney, T.R., Birtley, J.R., Leatherbarrow, R.J., Curry, S., 2007. Structural and mutagenic analysis of foot-and-mouth disease virus 3C protease reveals the role of the β-ribbon in proteolysis. J. Virol. 81, 115–124.
Yu, Y., Wang, H., Zhao, L., Zhang, C., Jiang, Z., Yu, L., 2011. Fine mapping of a foot-and-mouth disease virus epitope recognized by serotype-independent monoclonal antibody 4B2. J. Microbiol 49, 94–101.
Zunszain, P.A., Knox, S.R., Sweeney, T.R., Yang, J., Belsham, G.J., Leatherbarrow, R.J., Curry, S., 2010. Insights into cleavage specificity from the crystal structure of foot-and-mouth disease virus 3C protease complexed with a peptide substrate. J. Mol. Biol. 395, 157–389.

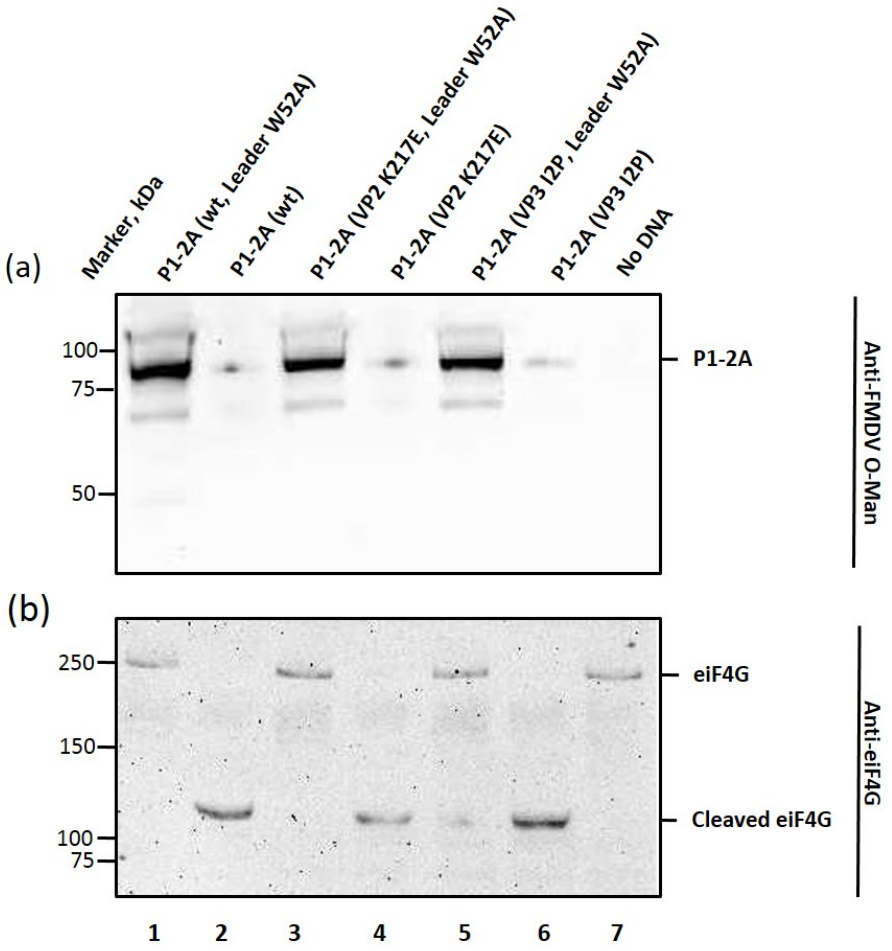

Figure S1

Influence of wt and mutant Leader proteases on the expression level of the P1-2A within transient expression assays. Two versions of three different plasmids expressing either the mutant (W52A) Leader protease (lanes 1, 3 and 5) or the wt Leader (lanes 2, 4, and 6) were transfected into cells infected with vTF7-3 (29). Cell extracts were prepared after 20h and analysed by immunoblotting with an anti-FMDV O-Man antibody (a). The status of the cellular translation factor eIF4G was determined in these extracts using anti-eIF4G antibodies (b).

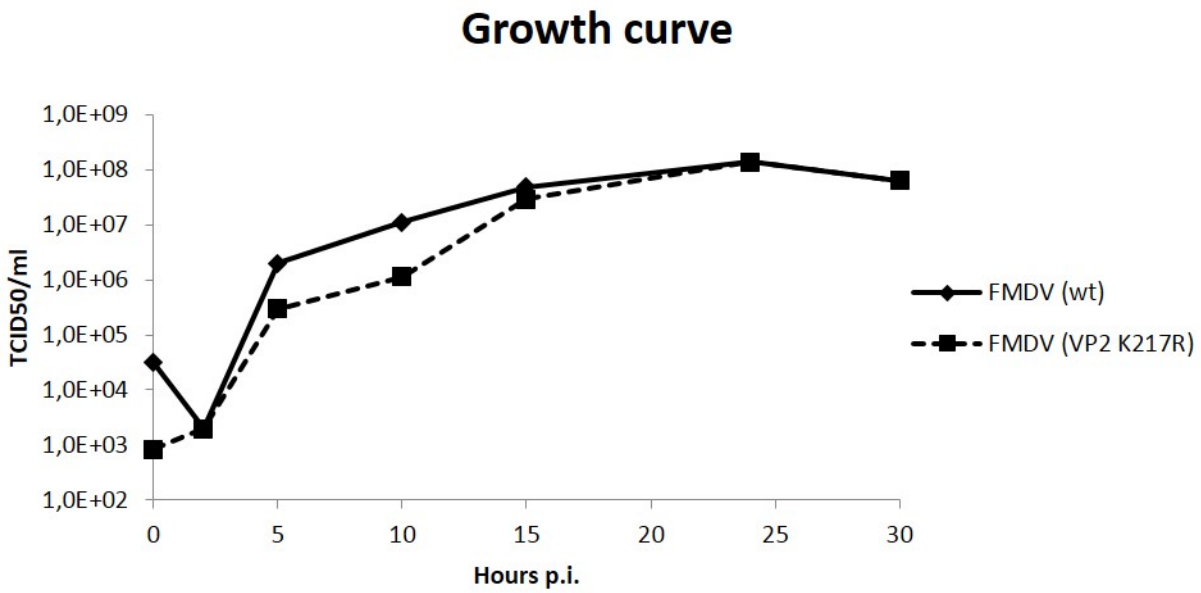

Figure S2

Growth curve of FMDV (wt) and FMDV (VP2 K217R) mutant in BHK cells. The wt and mutant viruses were used to infect BHK cells at a MOI of 0.05 $TCID_{50}$/cell, and harvested by freezing at the indicated time points post infection. The samples from the different time point were titrated and the virus yield (as $TCID_{50}$/ml) was calculated and plotted against time.

Table S1: Primers for generating PCR products from cDNA and their sequencing

Primers for PCR product	Primers for sequencing the PCR product
11FPN40_Fw: ACCTCYRAHGGGTGGTACGC 14TPN8_Rev: CGTCCGAACAAGCGACCGGTA	14TPN5_Fw: GAGTGTGGGAGTCACGTACG 14TPN6_Rev: CAAACAGGTGCTTCTTGAAAATCTTTC
14TPN5_Fw: GAGTGTGGGAGTCACGTACG 14TPN10_Rev: CTGCCACATCAGACGCAGTGT	14TPN7_Fw: GACAAATCAAGGTTTATGCCAACATTGC 14TPN8_Rev: CGTCCGAACAAGCGACCGGTA
14TPN7_Fw: GACAAATCAAGGTTTATGCCAACATTGC 14TPN12_Rev: GGAGCGCGAGCCTCGTAAAT	14TPN9_Fw: ATCCATGCTGAGTGGGACACAG 14TPN10_Rev: CTGCCACATCAGACGCAGTGT
14TPN9_Fw: ATCCATGCTGAGTGGGACACAG 14TPN14_Rev: GTCGAGACCGGTTCTGATGGC	14TPN11_F: AACCTAACCTGGGTACCCAATGG 14TPN12_Rev: GGAGCGCGAGCCTCGTAAAT

Y = C or T; R = A or G; H = A or C or G.

3.3 Manuscript 3

Identification of a short, highly conserved, motif required for picornavirus capsid precursor processing at distal sites

Short title:

Conserved motif required for picornavirus capsid precursor processing

Thea Kristensen[1] and Graham J. Belsham[1]#

[1]DTU National Veterinary Institute, Technical University of Denmark, Lindholm, Kalvehave 4771, Denmark

Corresponding author: Graham J. Belsham, email: grbe@vet.dtu.dk, phone: +45 35 88 79 85

Manuscript submitted

Abstract

Many picornaviruses cause important diseases in humans and other animals including poliovirus, rhinoviruses (causing the common cold) and foot-and-mouth disease virus (FMDV). These small, non-enveloped viruses consist of a positive-stranded RNA genome (ca. 7-9 kb) enclosed within a protein shell composed of 60 copies of three or four different capsid proteins. For the aphthoviruses (e.g. FMDV) and cardioviruses, the capsid precursor, P1-2A, is cleaved by the 3C protease ($3C^{pro}$) to generate the capsid proteins, VP0, VP3 and VP1 plus 2A. For enteroviruses, e.g. poliovirus, the capsid precursor is P1 alone, which is cleaved by the 3CD protease ($3CD^{pro}$) to generate just VP0, VP3 and VP1. The sequences required for correct processing of the FMDV capsid protein precursor in mammalian cells were analyzed. Truncation of the P1-2A precursor from its C-terminus showed that loss of the 2A peptide (18 residues long) and 27 residues from the C-terminus of VP1 (211 residues long) resulted in a precursor that cannot be processed by $3C^{pro}$ although it still contained two unmodified internal cleavage sites (VP0/VP3 and VP3/VP1 junctions). Furthermore, introduction of small deletions within P1-2A identified residues 185-190 within VP1 as being required for $3C^{pro}$-mediated processing and for optimal accumulation of the precursor. Within this C-terminal region of VP1, five of these residues (YCPRP), are very highly conserved in all FMDVs and are also conserved amongst other picornaviruses. Mutant FMDV P1-2A precursors with single amino acid substitutions within this motif were highly resistant to cleavage at internal junctions. Furthermore, these results can explain earlier observations that loss of the C-terminus (including the conserved motif) from the poliovirus capsid precursor conferred resistance to processing. Thus, this motif seems essential for maintaining the correct structure of picornavirus capsid precursors prior to processing and subsequent capsid assembly; it may represent a site that interacts with cellular chaperones.

Author Summary

The picornavirus family includes clinically important human and animal pathogens, for example: poliovirus, rhinovirus (causing the common cold) and foot-and-mouth disease virus (FMDV) that infects cloven-hoofed animals. Picornaviruses contain a positive-sense RNA genome surrounded by a protein shell, also called a capsid. The capsid proteins are made from a precursor and correct processing and assembly of these capsid proteins is necessary in the virus life cycle to create new infectious virus particles. In this study, we have identified a short motif (just 5 amino acids long)

within the capsid precursor, which is highly conserved among picornaviruses. Deletion of this motif inhibited processing of the junctions between the mature structural proteins within this precursor, with one junction being more than 400 amino acids away from this region. This motif also seems to be required for the optimal accumulation of the capsid precursor in cells. We hypothesize that the motif may be involved in binding to a cellular protein, such as a chaperone, to stabilize the capsid precursor and promote its correct folding to allow it to be processed by the viral protease prior to capsid assembly.

Introduction

Picornaviruses comprise a large family of non-enveloped RNA viruses that includes important human and animal pathogens. Examples include poliovirus (PV) (genus: *Enterovirus*), hepatitis A virus (*Hepatovirus*), encephalomyocarditis virus (*Cardiovirus*) and foot-and-mouth disease virus (FMDV) *(Aphthovirus).*

In picornavirus particles, the RNA genome (ca. 7,100-8,900 nt) is surrounded by a protein shell (capsid) consisting of the four structural proteins VP1, VP2, VP3 and VP4 [1], with the exception of parechoviruses and kobuviruses in which the VP0 (the precursor of VP2 and VP4) remains uncleaved (reviewed by [2]). The capsid is composed of 60 copies of each of these structural proteins; VP1, VP2 and VP3 are exposed on the surface of the particle while VP4 is entirely internal [3–5].

Translation of the positive-sense RNA genome is dependent on the internal ribosomal entry site (IRES) within the 5**′** untranslated region (UTR) that directs cap-independent translation initiation [6]. During and after translation of the single open reading frame, processing of the newly synthesized polyprotein occurs (reviewed in [2]). Usually three or four primary products are formed, namely the Leader (in many picornaviruses), the capsid precursor P1 or P1-2A (depending on the genus) and the precursors of the non-structural proteins, namely P2 and P3. Many of these viruses, e.g. members of the *Cardiovirus*, *Hepatovirus* and *Aphthovirus* genera, have a Leader protein at the N-terminus of the polyprotein, i.e. upstream of the capsid precursor. In the *Aphthoviruses*, the Leader protein is a protease (L^{pro}), which cleaves itself from the N-terminus of the P1-2A precursor, see Fig. 1. Cleavage of the junction between the structural and non-structural proteins, at either the VP1/2A

or the 2A/2B junction, is usually mediated by the 2A protein, but the function of the 2A protein varies between the genera [7], see Fig. 1. In the cardio- and aphthoviruses cleavage at the 2A/2B junction (at the C-terminus of 2A) is protease independent and happens during translation by a process termed “ribosomal skipping” [8] or “StopGo” [9]. In this case, the 2A protein remains attached to the precursor of the structural proteins (as P1-2A) until it is removed by the 3C protease ($3C^{pro}$). In the enteroviruses, the cleavage at the VP1/2A junction (i.e. at the N-terminus of 2A), to release P1, is mediated by the 2A protein that is a chymotrypsin-like protease [10,11].

The P2-P3 junction and the other protein junctions within these precursors are cleaved by $3C^{pro}$ to produce the mature non-structural proteins. However, the P1 capsid precursor of enteroviruses requires the 3CD protease ($3CD^{pro}$) for its processing [12,13] whereas for the cardio- and aphthoviruses the $3C^{pro}$ is sufficient to cleave the P1-2A precursor into three structural proteins (VP0, VP3 and VP1) plus 2A [1,14], see Fig. 1. During capsid assembly, VP0 is cleaved (in most picornaviruses) to generate VP2 and VP4 by a process that is currently not understood.

There are seven different serotypes of FMDV: O, A, C, SAT 1, SAT 2, SAT 3 and Asia 1. There is a high level of sequence variation between the surface exposed structural proteins of these different serotypes. The internal VP4 protein is the most conserved of the capsid proteins with 81% of the residues being invariant [15]. In contrast, only 26% of the VP1 protein residues are invariant and furthermore it ranges in size (209-213 aa) between serotypes [16]. VP1 is the most surface exposed capsid protein [3] and has been one of the most studied FMDV proteins due to its antigenic importance and role in virus attachment [17].

One of the antigenic sites in VP1 is located on the G-H loop (including residues 141-160), which contains an arginine-glycine-aspartate (RGD) motif that is involved in the attachment of the virus to cellular integrin receptors [18,19]. Surprisingly, previous work has demonstrated that a cell-culture adapted FMDV, lacking part of this G-H loop (aa 142-154), is still able to replicate and grow normally in cell culture through the use of heparan sulfate proteoglycans (HSPG) as receptor [20].

Viruses have only a very limited coding capacity within their genomes and thus they rely on cellular factors and pathways to complete their life cycle. Several studies have suggested that cellular chaperones, including various different heat shock proteins (Hsps), are required to facilitate virus entry, genome replication, protein expression and protein assembly for a variety of viruses, including picornaviruses. Viral proteins, like cellular proteins, are dependent on such chaperones for their correct folding and assembly [21–24]. Studies on the role of Hsp90, using specific inhibitors, have shown that these agents reduce the replication of diverse viruses *in vitro.* The Hsp90 appears to be involved in the regulation of viral polymerase function in the case of herpesvirus [25] and hepatitis B virus [21], whereas this chaperone seems to be required for capsid processing and assembly in different picornaviruses [23,26]. Hsp90 and Hsp70 have been reported to interact with the PV capsid precursor, P1 [23,27]. The interaction between PV P1 and Hsp90 (possibly together with Hsp70), and likely in conjunction with its co-chaperone p23, is believed to protect the P1 from degradation by proteasomes (which remove misfolded proteins) and is also involved in the folding of P1 allowing it to be correctly processed by the $3CD^{pro}$ [23].

Recently, we have shown that impeding the processing of one of the cleavage sites within the FMDV P1-2A, at either the VP0-VP3 or the VP3-VP1 junctions, did not block processing of the other cleavage sites, indicating that processing of these junctions is mutually independent [28]. However, in an earlier study, it was shown that truncation of VP1 (removing the C-terminal 42 amino acids of VP1) completely blocked processing of the residual capsid precursor at both the VP0-VP3 and the VP3-VP1 junctions by $3C^{pro}$ in a cell-free system [29]. Similarly, truncating the PV P1 precursor, by removing 50 aa from the C-terminus of VP1 (302 residues in length), blocked cleavage of the 2 junctions within the P1 precursor *in vitro* [30]. The basis for these effects has not been explained. However, taken together, these results suggest that the C-terminus of VP1 is important in relation to the processing of the entire capsid precursor of picornaviruses.

In this study, we have now identified a short region within the C-terminus of VP1 that is critical for the processing of the FMDV capsid precursor. This region contains a stretch of five amino acids that are very highly conserved amongst all FMDVs. Furthermore, this region is also strongly conserved

between most other picornaviruses, including PV, suggesting a shared role for this motif for capsid processing and assembly within the picornavirus family.

Results

Truncation of the capsid precursor prevents its processing by $3C^{pro}$ in cells

Previous studies have shown that truncation of the FMDV P1-2A, by removal of the 2A peptide and the C-terminal 42 residues of VP1, completely abrogated processing by $3C^{pro}$ *in vitro* [29] even though the cleavage sites between VP0 and VP3 and between VP3 and VP1 were unmodified. To confirm these observations, within cells, stop codons were introduced at different positions within the P1-2A coding sequence. Transient expression assays were used to express the FMDV A22 Iraq P1-2A capsid precursor and its derivatives, within BHK cells, both in the absence and presence of the FMDV $3C^{pro}$. The plasmids encoding both the P1-2A (wt) and the P1 alone (truncated at the first amino acid of the 2A peptide) served as positive controls. Both of these controls yielded the expected products corresponding to the P1-2A precursor and the P1 precursor (approximately 85 kDa), respectively in the absence of $3C^{pro}$ (Fig. 2, lanes 1 and 3). When these plasmids were co-transfected with a plasmid that expresses the $3C^{pro}$, both of these products were efficiently processed as indicated by the production of VP0 (approximately 37 kDa) (Fig. 2, lanes 2 and 4) and VP1 (approximately 28 kDa, data not shown), note that the antibodies do not recognize VP3 [31], but presumably this was also made. Thus, the absence of the 2A peptide did not affect processing of the capsid precursor by $3C^{pro}$ (as observed previously [14,26]).

Plasmids encoding mutant precursors, truncated to residue 205 in VP1 and 199 in VP1 (VP1 being 211 aa in length in FMDV A22 Iraq (wt)), generated products of approximately 85 kDa in the absence of $3C^{pro}$ (Fig. 2, lanes 5 and 7), and these were efficiently processed in the presence of $3C^{pro}$ (Fig. 2, lanes 6 and 8). The four additional mutants, P1 (VP1 Y185Stop), P1 (VP1 L158Stop), P1 (VP1 A107Stop) and P1 (VP1 L53Stop) all yielded products corresponding to their expected size in the absence of $3C^{pro}$ (Fig. 2, lanes 9, 11, 13 and 15), however it is noteworthy that these truncated products accumulated to a lower level in the cell lysates. Strikingly, no processing of these truncated

precursors was detected for any of these four mutants in the presence of $3C^{pro}$ (Fig. 2, lanes 10, 12, 14 and 16) although each of these products contained the unmodified VP0/VP3 and VP3/VP1 junctions. As expected, no products were detected in the negative control (no DNA) (Fig. 2, lane 17).

Mapping of the determinants of $3C^{pro}$ mediated processing of the capsid-precursor

In order to map the determinants of capsid processing more precisely, plasmids were constructed to express mutant forms of the P1-2A precursor with fairly small internal deletions within the C-terminal portion of VP1. To serve as positive controls, both the P1-2A (wt) and a mutant form with a deletion within VP1, designated P1-2A (VP1 Δ142-154), were included. The latter deletion is tolerated by the infectious virus [20] and thus it was expected that $3C^{pro}$ should be able to fully process all of the junctions in this deletion mutant. As expected, expression of both the P1-2A (wt) and the P1-2A (VP1 Δ142-154) led to the synthesis of products corresponding to the P1-2A precursor (approximately 85 kDa) (Fig. 3, lanes 1 and 13). Furthermore, both the P1-2A (wt) and the P1-2A (VP1 Δ142-154) products were efficiently processed in the presence of $3C^{pro}$ (Fig. 3, lanes 2 and 14). Notice that the VP1 product derived from the P1-2A (VP1 Δ142- 154) mutant migrated faster than the VP1 produced from the P1-2A (wt) due to the internal deletion.

Five different short deletions were introduced into the region of VP1 spanning residues 185-199 (the region found to be critical by the truncation analysis), namely P1-2A (VP1 Δ185-199), P1-2A (VP1 Δ185-189), P1-2A (VP1 Δ188-192), P1-2A (VP1 Δ191-195) and P1-2A (VP1 Δ194-199). Each of these constructs generated products that were very similar in size as the wt P1-2A in the absence of $3C^{pro}$ (Fig. 3, lanes 3, 5, 7, 9 and 11). However, in the presence of $3C^{pro}$ the mutant having the largest deletion, P1-2A (VP1 Δ185-199) could not be processed (Fig. 3, lane 4). The same product, corresponding to the P1-2A precursor, was observed both in the absence and presence of $3C^{pro}$. Similarly, the mutants P1-2A (VP1 Δ185-189) and P1-2A (VP1 Δ188-192) were also not processed in the presence of $3C^{pro}$ (Fig. 3, lanes 6 and 8). It is again noteworthy that the mutant P1-2A products that could not be processed accumulated to a lower level in the cell lysates than the P1-2A precursors that could be processed (c.f. lanes 3, 5, 7 and 1, 9, 11, 13). In contrast, co-expression of $3C^{pro}$ with the P1-2A (VP1 Δ191-195) and P1-2A (VP1 Δ194-199) led to production of VP0 indicating

that processing of these mutant precursors had occurred (Fig. 3, lanes 10 and 12). However, it is noteworthy that no product corresponding to VP1 was detected, when P1-2A (VP1 Δ191-195) was co-expressed with $3C^{pro}$ (Fig. 4a, lane 4). Furthermore, unexpectedly, when the P1-2A (VP1 Δ194-199) was co-expressed with $3C^{pro}$ a major product corresponding to the intermediate VP3-VP1 (approximately 49 kDa) was detected (Fig 4a, lane 6). Only a weak signal corresponding to the mature VP1 was detected indicating severe inhibition of processing at the VP3/VP1 junction in this mutant (Fig 4a, lane 6), n.b. this cleavage site is located over 190 residues away in the linear sequence. No products were detected in the negative control lane. (Fig. 4a, lane 9).

Due to inefficient detection of VP1 from some of the mutant precursors, an extra modification that blocks processing of the VP1/2A junction (2A L2P) [32] was introduced into the plasmids that express P1-2A (VP1 Δ191-195), P1-2A (VP1 Δ194-199) and the positive controls; P1-2A (wt) and P1-2A (VP1 Δ142-154). The additional modification (2A L2P) ensured that the 2A peptide remained fused to the VP1 (as VP1-2A). Each of these constructs generated products corresponding to the P1-2A precursor in the absence of $3C^{pro}$ (Fig. 4b, lanes 1, 3, 5 and 7). The 2A L2P substitution increased the sensitivity of VP1 detection when using the anti-FMDV A-Iraq antibody. This showed that the P1-2A (wt + 2A L2P) and the P1-2A (VP1 Δ142-154 + 2A L2P, positive control) precursors were fully processed to yield VP0 and VP1-2A in the presence of $3C^{pro}$ as expected (Fig. 4b, lanes 2 and 8). It also verified that cleavage at the VP3-VP1 junction in the P1-2A (VP1 Δ194-199 +2A L2P) occurred at a slower rate compared to wt, since the VP3-VP1-2A intermediate was far more abundant for the P1-2A (VP1 Δ194-199 + 2A L2P) than for the P1-2A (wt +2A L2P) in the presence of $3C^{pro}$ (compare lanes 6 and 2 in Fig. 4b). It should be noted that some mature VP1-2A could be detected from the P1-2A (VP1 Δ194-199 + 2A L2P) and thus cleavage of the VP3/VP1 junction was not completely blocked (Fig. 4b, lane 6). Furthermore, the P1-2A (VP1 Δ191-195 + 2A L2P) could be processed to generate VP0 and VP1-2A (Fig. 4b, lane 4). However, the VP3-VP1 intermediate produced from the P1-2A (VP1 Δ191-195 +2A L2P) mutant was also more abundant than the intermediate seen with the P1-2A (wt + 2A L2P) indicating that this mutant also had a slower processing at the VP3/VP1 junction (Fig. 4b, lane 4).

The cleavage of the unmodified VP1/2A junction in the P1-2A precursors with different internal deletions, was investigated using an anti-2A antibody. As expected, both the P1-2A (wt) and the positive control P1-2A (VP1 Δ142-154) generated products of approximately 85 kDa corresponding to the P1-2A precursor in the absence of $3C^{pro}$ (see supplementary material Fig. S1, lanes 1 and 13). In the presence of $3C^{pro}$, no products were detected by the anti-2A antibodies from either the P1-2A (wt) or the positive control P1-2A (VP1 Δ142-154) indicating that the VP1/2A junction had been processed (Fig. S1, lanes 2 and 14); note the 2A peptide itself is only 18 residues long and is not detected by immunoblotting. The two mutants, P1-2A (VP1 Δ191-195) and P1-2A (VP1 Δ194-199) that showed slower processing of the VP3-VP1 junction also generated products corresponding to the P1-2A precursor in the absence of $3C^{pro}$ (Fig. S1, lanes 9 and 11). However, in the presence of $3C^{pro}$, no products were detected by the anti-2A antibodies (Fig. S1, lanes 10 and 12), indicating that these two deletions in VP1 did not affect processing of the VP1/2A junction. Surprisingly, the non-processable precursors, i.e. P1-2A (VP1 Δ185-199), P1-2A (VP1 Δ185-189) and P1-2A (VP1 Δ188-192), could not be detected using the anti-2A antibody, either in the absence or presence of $3C^{pro}$, and thus we cannot conclude whether cleavage of this junction was affected by the deletions (Fig. S1, lanes 3-8). No products were detected in the negative control (No DNA, Fig. S1, lane 15).

Identification of critical residues in the P1-2A-precursor for $3C^{pro}$ processing

Alanine-scanning mutagenesis was employed to identify individual residues within the C-terminal region of VP1 (between residues 185 and 199 of VP1) that are required for $3C^{pro}$ processing of the P1-2A precursor. The wt and mutant precursors were expressed alone and also in the presence of the FMDV $3C^{pro}$ as above. As expected, the P1-2A (wt) and all 15 of the single amino acid substitution mutants each generated products corresponding to the P1-2A precursor in the absence of $3C^{pro}$ (see Figs. 5, 6 and 7, odd numbered lanes). The wt and some 13 different mutant P1-2A precursors, excluding the mutants P1-2A (VP1 Y185A) and P1-2A (VP1 R188A), were processed by $3C^{pro}$ to yield VP0 and VP1 (Fig. 5, 6 and 7 even numbered lanes). In contrast, the P1-2A (VP1 Y185A) and P1-2A (VP1 R188A) mutants were highly resistant to cleavage by the $3C^{pro}$ (Fig. 5, lanes 4 and 10). Furthermore, it was again apparent that the accumulation of these mutant P1-2A products in the cell lysates was lower than for the wt precursor and for the other mutants that could be processed

(Fig. 5, lanes 3 and 9). Thus, the single amino acid substitutions VP1 Y185A and VP1 R188A were individually able to severely inhibit processing at both the VP0/VP3 and the VP3/VP1 junctions within the P1-2A precursor and had a deleterious effect on the level of the unprocessed product generated within cells.

Surprisingly, none of the single alanine substitutions in the VP1 194-199 region had any effect on the processing of the junctions within the P1-2A precursor (Fig. 7, lanes 4, 6, 8, 10, 12 and 14). None of these produced the severe block on cleavage of the VP3-VP1 junction that was detected with the P1-2A (VP1 Δ194-199) mutant (Fig 4, lane 6). However, interestingly the P1-2A (VP1 V193A) was processed more slowly at the VP3-VP1 junction compared to the P1-2A (wt) and the other alanine mutants (Fig. 6, lane 12).

The cleavage of the VP1/2A junction of the P1-2A precursors with different alanine substitutions, was also investigated using the anti-2A antibody. As expected, the P1-2A (wt) generated a product of approximately 85 kDa corresponding to the P1-2A precursor in the absence of $3C^{pro}$ (see supplementary material Fig. S2, lane 1). However, in the presence of $3C^{pro}$, no product (containing 2A) was observed from the P1-2A (wt) showing that VP1/2A junction had been processed (Fig. S2, lane 2). The two mutants, P1-2A (VP1 C186A) and P1-2A (VP1 P187A) that were correctly processed at the VP0/VP3 and the VP3/VP1 junction also generated products corresponding to the P1-2A precursor in the absence of $3C^{pro}$ (Fig. S2, lanes 5 and 7). However, as with the wt protein, in the presence of $3C^{pro}$ no products including 2A could be detected, indicating that these two substitutions individually did not prevent processing at the VP1/2A junction. Neither of these mutant precursors, with single amino acid substitutions, which were highly resistant to cleavage at the VP0/VP3 and the VP3/VP1 junctions, i.e. P1-2A (VP1 Y185A) and P1-2A (VP1 R188A), could be detected by the anti-2A antibody, either in the absence or presence of $3C^{pro}$. Thus, we cannot conclude whether this junction was affected by these substitutions (Fig. S2, lanes 3, 4, 9 and 10). These results are consistent with the inability to detect the mutant capsid precursors P1-2A (VP1 Δ185-199), P1-2A (VP1 Δ185-189) and P1-2A (VP1 Δ188-192), with the anti-2A antibody, as shown in Fig. S1 (see above).

Discussion

The FMDV $3C^{pro}$ is able to cleave a variety of different junction sequences in the virus polyprotein [33]. We have shown previously that blocking cleavage of one junction in the FMDV P1-2A did not affect processing of the other junctions [28]. In the current studies, it has been shown that modifications that modify or delete a short motif in the C-terminus of VP1, can prevent processing of the FMDV capsid precursor P1-2A at each of the usual cleavage sites, which are far separated, in the linear sequence, from the site of the modifications. The VP0/VP3 cleavage site is more than 400 amino acids away from the modified motif in the linear sequence while the VP3/VP1 junction is almost 200 amino acids away. It seems very likely that this reflects a major change in protein conformation for these mutant proteins. Viral proteins, like cellular proteins, are dependent on cellular chaperones for correct folding, assembly and function [24]. The viral capsid precursor must fold to a conformation that is soluble and recognizable by the viral protease to be processed. After the cleavage of the precursor, the mature capsid proteins assemble around the viral genome to form the protein shell, which contains 60 copies of each of the subunits. These structures must be stable both within, but also outside, the host cells to permit virus spread. Moreover, the virus particle must also be able to disassemble upon entry into cells to deliver the viral genome to initiate a new infection. Thus, the core structure of the capsid proteins (as distinct from the antigenic loops) is probably tightly constrained.

Within the picornavirus family, the general structure of the capsid proteins are very similar [2]. Several chaperones are known to facilitate folding of picornavirus capsid proteins [23,26]. The mature picornavirus capsid proteins are generated by cleavage of the P1, P1-2A or L-P1-2A precursors. Both Hsp90 and p23, a co-chaperone of Hsp90, have been reported to be required for processing of the PV P1 precursor into the mature structural proteins [23]. However, interestingly, hepatitis A virus (HAV) is not sensitive to the inhibition of Hsp90 function [34]. This indicates that HAVs might employ other strategies for correct folding of the capsid precursor. However, it is noteworthy that HAV also has several unique characteristics that distinguish it from most other

members of the picornavirus family, e.g. slow growth rate, lack of capsid protein myristoylation and use of only a single viral protease ($3C^{pro}$) for polyprotein processing [35–38].

An earlier study showed that Hsp90 mediates PV P1 folding in cells. Inhibition of this chaperone lead to misfolding of P1, which resulted in the targeting of the PV P1 for degradation by the cellular quality-control system (proteasome pathway), and thus the level of the PV P1 was strongly reduced [23]. These observations are consistent with the results presented here on the FMDV P1-2A. All of the FMDV P1-2A precursors that cannot be processed by $3C^{pro}$ accumulated to a lower level than the P1-2A (wt). This was apparent for the truncated precursors (VP1 Y185Stop, VP1 L158Stop, VP1 A107Stop, VP1 L53Stop), precursors with small internal deletions (VP1 Δ185-199, VP1 Δ185-189, VP1 Δ182-192) and two precursors with single amino acid substitutions (VP1 Y185A and VP1 R188A). Thus, it may be that the mutant precursors, which cannot be processed, are misfolded and therefore targeted for degradation, hence the reduced level of these products within cells.

Interestingly, Geller et al., [23] showed that inhibition of the Hsp90 chaperone in a cell-free system (rabbit reticulocyte lysate), where the proteasomal degradation system is inhibited by free hemin, did not reduce the yield of P1 [23]. However, even in the absence of proteasomal degradation, the Hsp90 was still required for P1 to fold into a processing-competent conformation, since the PV P1 precursor, in the absence of Hsp90, adopted a misfolded conformation that could not be recognized by the $3CD^{pro}$ and thus could not be processed into the mature capsid proteins [23].

As indicated above, a critical region that is required for the correct processing of the FMDV capsid precursor has now been identified. This motif (YCPRP) is very highly conserved among FMDVs. Indeed, the YCPR sequence was found to be completely conserved in over 100 FMDV strains, with representatives from all 7 serotypes [15]); only variation to YCPRA has been observed (Fig. 8). However, previously, no function for this conserved sequence had been identified. The YCPRP motif is also highly conserved among other picornaviruses as well, e.g. it exists as FCPRP in cardioviruses and WCPRP in enteroviruses, see Fig. 9. Indeed, both Y to F and Y to W are very conservative amino acid substitutions, since all three amino acids have similar properties with non-polar, aromatic side

chains. This high conservation likely reflects its importance for correct folding of the capsid precursor. The high resistance to cleavage of the junctions between the structural proteins following substitution of residues VP1 Y185 and VP1 R188 individually indicates that correct cleavage may be dependent on the interaction with several amino acids in this region and thus the whole motif seems to be of high importance for correct folding and subsequent processing of the capsid precursor.

An earlier study has showed that removing 50 residues from the C-terminus of the PV VP1 prevented cleavage of the two junctions, VP0/VP3 and VP3/VP1, within the capsid precursor *in vitro* [30]. Significantly, these 50 amino acids include the highly conserved motif (WCPRP) identified here, and thus indicates the importance of this motif, not only for FMDV, but also more widely within the picornavirus family. Similarly, as indicated above, removal of 42 residues (including the YCPRP) from the C-terminus of the FMDV VP1 protein completely prevented cleavage of the capsid precursor by the $3C^{pro}$ in a cell-free system [29]. Recently, we have shown that blocking cleavage of one of the junctions within the FMDV P1-2A precursor did not block the cleavage of the other junction within the capsid precursor [28]. Thus, the severe inhibition of cleavage of both junctions likely reflects a changed overall structure of the capsid precursor, thereby preventing cleavage of both junctions.

It is interesting to note that in HAV, the equivalent region of VP1 has the sequence YFPRA, perhaps the two substitutions together account for the lack of sensitivity of HAV assembly to Hsp90 inhibitors [34]. It can be proposed that the conserved motif serves as a binding site for an important chaperone, e.g. Hsp90 (or its partners), that are necessary for correct protein folding. A co-chaperone of Hsp90, called p23, also seems to be involved in the correct folding of the PV P1. It has been reported that treatment with geldanamycin (GA) did not affect the PV P1-Hsp90 interaction, but abolished the P1-p23 interaction and thereby affected P1 maturation [23], thus indicating different possibilities for chaperone interaction at this specific site.

Picornaviruses are able to adapt very rapidly since they have an RNA dependent RNA polymerase with a high error rate and no error correction mechanism. However, Geller et al., [23] showed that

PV was unable to adapt to an Hsp90-independent P1 folding pathway during several passages in cells in culture or in PV-infected mice when the function of Hsp90 was inhibited by the presence of GA. Thus it seems that for the virus to adapt to a folding pathway without the involvement of Hsp90 requires extensive change [23].

It is interesting that the deletion VP1 Δ194-199 strongly inhibited cleavage at the VP3-VP1 junction, without affecting the cleavage of the VP0-VP3 junction (Fig. 4, lane 6). Surprisingly, the alanine scanning substitutions through this specific region did not identify any individual residue that affected cleavage of any of the junctions (Fig. 7, lanes 4, 6, 8, 10, 12 and 14). However, interestingly the P1-2A (VP1 V193A) mutant, modified at a residue adjacent to the deletion, also displayed a slower processing rate of this VP0/VP3 junction compared to the wt and the other alanine mutants (Fig. 6, lane 12). However, this VP1 V193A mutant does not seem to affect the processing of the VP3-VP1 junction to the same extent as the VP1 Δ194-199 mutant. In addition, the VP1 Δ191-195 mutant also showed a lower processing of this VP3/VP1 junction (Fig. 4b, lane 4) as judged by the elevated level of the VP3-VP1 product. These results indicate that the cleavage of the VP3-VP1 junction, may be dependent on the interaction with several amino acids and that residues within the VP1 aa 193-199 region are important for optimal processing of the VP3-VP1 junction, more than 190 aa away from the site.

We have noted previously that the K210E change in VP1 that severely limited processing at the VP1/2A junction also enhanced the yield of VP3-VP1-2A [14]. These studies also identified a genetic link between the processing of the VP1/2A junction and the substitution E83K in VP1. Furthermore, Escarmis et al., [39] showed that the substitution M54I within the VP1 of serotype C FMDV resulted in less efficient processing at the VP3/VP1 junction. Thus, there are multiple, complex, interactions, some of which operate “at a distance”, that govern picornavirus capsid protein processing and assembly.

Methods

Plasmid construction

The plasmid pO1K/A22 contains a T7 promoter upstream of a full-length FMDV cDNA with the A22 Iraq capsid coding sequence within an FMDV O1K backbone as previously described [28,40,41]. To investigate the effect of different modifications within the P1-2A, the FMDV cDNA was digested with *Apa*I and then religated to remove most of the sequence encoding the non-structural proteins (including the $3C^{pro}$) downstream of the 2A-peptide, as described previously [28]. These constructs contained a modified form (W52A substitution) of the L^{pro} to overcome the negative effect of the L protease on protein expression in cells. The modified L^{pro} with the W52A substitution retains the L/P1 cleavage activity but is defective at inducing cleavage of the translation initiation factor eIF4G [42]; the primer sequences used to make this modification are listed in Table 1. This parental plasmid is referred to throughout as P1-2A (wt) and all modifications were made in this background.

P1-2A plasmids specifying different truncations

Variants of the plasmid, with in-frame stop codons introduced to truncate the capsid precursor at different sites either at the start of the 2A sequence or within the VP1 coding sequence, were generated using site-directed mutagenesis [43]. Briefly, fragments were amplified in PCRs using Phusion High-Fidelity DNA Polymerase (Thermo Fisher Scientific), according to the manufacturer's instructions, to create mega-primers, using the P1-2A (wt) plasmid as template and reverse primers specifying the introduction of STOP codons, together with the forward primer; 14TPN9_F, see Table 1. The PCR products (between 350 and 900 bp in length depending on where the modification was made) were gel purified using the GeneJET Gel purification kit (Thermo Fisher Scientific). These PCR products were used as megaprimers for a second round of PCR (500 ng megaprimer, and 100 ng template), using the P1-2A (wt) as template to produce the modified plasmids. After the PCR and subsequent *Dpn*I digestion of the template plasmid, the products were transformed into chemically competent *Escherichia coli* (*E*. *coli*) cells. Plasmids were amplified from individual colonies, purified using the GeneJet Plasmid Miniprep Kit (Thermo Fisher Scientific) and screened by Sanger Sequencing using the BigDye Terminator v.3.1 Cycle Sequencing kit and a 3500 Genetic Analyzer (Applied Biosystems). Plasmids encoding the desired modifications were amplified and purified using the QIAGEN Plasmid Midi Kit (Qiagen). All of these constructs encoded P1 that was truncated

at different sites by introducing two STOP codons. The plasmids (listed in Table 1) were labelled to denote the location of the Stop codons as follows; P1-2A (2A L1Stop), P1-2A (VP1 I205Stop), P1-2A (VP1 D199Stop), P1-2A (VP1 Y185Stop), P1-2A (VP1 L158Stop), P1-2A (VP1 A107Stop) and P1-2A (VP1 L53Stop); for primer sequences, see Table 1.

Plasmids encoding P1-2A with internal deletions within the VP1 coding region

Variants of the P1-2A plasmid that express mutant proteins with various different deletions in the C-terminal region of VP1 between residues VP1 185 and VP1 199 were created using site-directed mutagenesis, essentially as described above; for primer sequences see Table 1. The plasmids were labelled as follows: P1-2A (VP1 Δ185-199), P1-2A (VP1 Δ185-189), P1-2A (VP1 Δ188-192), P1-2A (VP1 Δ191-195) and P1-2A (VP1 Δ194-199). Furthermore, an additional positive control was included in which 13 amino acids within VP1 were deleted, this construct was called P1-2A (VP1 Δ142-154). An earlier study had shown that FMDV with this deletion is able to replicate [20,44].

Alanine scanning mutagenesis of P1-2A

Alanine substitutions were introduced at the codons for each residue individually between VP1 185 and VP1 199, with the exception of VP1 A192, where the original alanine codon was substituted by one encoding a serine. The mutations were produced using site-directed mutagenesis, as described above; the primer sequences are listed in Table 1. These modifications resulted in 15 different plasmids: P1-2A (VP1 Y185A), P1-2A (VP1 C186A), P1-2A (VP1 P187A), P1-2A (VP1 R188A), P1-2A (VP1 P189A), P1-2A (VP1 L190A), P1-2A (VP1 L191A), P1-2A (VP1 A192S), P1-2A (VP1 V193A), P1-2A (VP1 E194A), P1-2A (VP1 V195A), P1-2A (VP1 S196A), P1-2A (VP1 S197A), P1-2A (VP1 Q198A) and P1-2A (VP1 D199A).

Transient expression assays

Baby hamster kidney (BHK) cells (originally obtained from the ATCC (CCL-10)) were grown in 35-mm wells to about 90% confluence, when they were infected with the recombinant vaccinia virus, termed vTF7-3 [45] that expresses the T7 RNA polymerase. All the various P1-2A plasmids and the 3C plasmid (pSKRH3C [46]) express the FMDV cDNA under the control of a T7 promotor. After one hour incubation at 37°C, the vaccinia virus was removed and the cells were transfected with the specified plasmid DNA using FuGENE 6 (Promega), as described previously [47]. To obtain the

highest levels of processed capsid protein expression, 1000 ng of the P1-2A plasmid alone or with 10 ng of the $3C^{pro}$ plasmid were used for each transfection of cells [28]. The cells were incubated in a CO_2 incubator, at 37°C overnight and then, after removal of the medium, lysed with 500 µl Buffer C (20mM Tris-HCl (pH 8.0), 125 mM NaCl and 0.5% NP-40); the cell extracts were clarified by centrifugation at 18,000 x g for 10 min at 4°C.

Immunoblot analysis

Immunoblotting was performed using clarified cell lysates mixed with 2 x Laemmli sample buffer (Bio-Rad) (containing 25 mM DTT). The proteins were separated by SDS-PAGE using a 12 % Bis-Tris gels (Bio-Rad) and transferred to PVDF membranes (Milipore), by wet blotting, at 200 mA for 1.5 hours. PBS containing bovine serum albumin (BSA) (5%) and Tween20 (0.1%) was used as blocking buffer (1 hour at room temperature (RT)) and dilution buffer for the guinea pig anti-FMDV O-Manisa (Man) antisera (prepared "in house", as used previously [28]) (overnight at 4 °C) and their corresponding secondary antibodies (2 hours at RT). PBS containing skimmed milk powder (5%) and Tween20 (0.1%) was used as blocking buffer (1 hour at RT) and dilution buffer for the primary guinea pig anti-FMDV A-Iraq antisera (prepared "in house", as used previously [28]) and the anti-2A-peptide antibody (overnight at 4 °C) and their corresponding secondary antibody (2 hours at RT). The proteins were detected using the following primary antibodies: guinea pig anti-FMDV O-Man antisera (1:1000), guinea pig anti-FMDV A-Iraq antisera (1:500) or FMDV anti-2A-peptide antibody (1:1000) (Rabbit, ABS31 Merck Millipore). Appropriate HRP-conjugated secondary antibodies (Dako) and a chemiluminescence detection kit (Pierce ® ECL Western Blotting Substrate, Thermo Fisher Scientific) were used to detect the proteins bound by the primary antibodies. Images were captured using a Chem-Doc XRS system (Bio-Rad).

Acknowledgements

We wish to thank Preben Normann for excellent technical assistance.

References

1. Belsham GJ. Translation and replication of FMDV RNA. Curr Top Microbiol Immunol. 2005;288: 43–70.

2. Jiang P, Liu Y, Ma H-C, Paul A V., Wimmer E. Picornavirus morphogenesis. Microbiol Mol Biol Rev. 2014;78: 418–437.

3. Acharya R, Fry E, Stuart D, Fox G, Rowlands D, Brown F. The three-dimensional structure of foot-and-mouth disease virus at 2.9 Å resolution. Nature. 1989;337: 709–716.

4. Rossmann MG, Arnold E, Erickson JW, Frankenberger EA, Griffith JP, Hecht H-J, et al. Structure of a human common cold virus and fuctional relationship to other picornaviruses. Nature. 1985;318: 556–557.

5. Hogle JM, Chow M, Filman DJ. Three-dimensional structure of poliovirus at 2.9 Å resolution. Science. 1985;229: 1358–1365.

6. Martinez-Salas E, Belsham GJ. Genome organization, translation and replication of foot-and-mouth disease virus RNA. In: “Foot-and-mouth disease virus: current research and emerging trends.” Caister Academic Press; 2017. pp. 13–42.

7. Luke GA, Felipe P De, Lukashev A, Kallioinen SE, Bruno EA, Ryan MD. Occurrence, function and evolutionary origins of “2A-like” sequences in virus genomes. J Gen Virol. 2008;89: 1036–1042.

8. Donnelly MLL, Luke G, Mehrotra A, Li X, Hughes LE, Gani D, et al. Analysis of the aphthovirus 2A/2B polyprotein “cleavage” mechanism indicates not a proteolytic reaction, but a novel translational effect: a putative ribosomal “skip.” J Gen Virol. 2001;82: 1013–1025.

9. Atkins JF, Wills NM, Loughran G, Wu C-Y, Parsawar K, Ryan MD, et al. A case for “StopGo”: reprogramming translation to augment codon meaning of GGN by promoting unconventional termination (Stop) after addition of glycine and then allowing continued translation (Go). RNA. 2007;13: 803–810.

10. Sommergruber W, Zorn M, Blaas D, Fessl F, Volkmann P, Maurer-Fogy I, et al. Polypeptide 2A of human rhinovirus type 2: identification as a protease and characterization by mutational analysis. Virology. 1989;169: 68–77.

11. Toyoda H, Nicklin MJH, Murray MG, Anderson CW, Dunn JJ, Studier FW, et al. A second virus-encoded proteinase involved in proteolytic processing of poliovirus polyprotein. Cell. 1986;45: 761–770.

12. Ypma-Wong MF, Dewalt PG, Johnson VH, Lamb JG, Semler BL. Protein 3CD is the major proteinase responsible for cleavage of the P1 capsid precursor. Virology. 1988;166: 265–270.

13. Jore J, De Geus B, Jackson R, Pouwels P, Enger-Valk B. Poliovirus protein 3CD is the active protease for processing of the precursor protein P1 in vitro. J Gen Virol. 1988;69: 1627–1636.

14. Gullberg M, Polacek C, Bøtner A, Belsham GJ. Processing of the VP1/2A junction is not necessary for production of foot-and-mouth disease virus empty capsids and infectious viruses: characterization of " self-tagged " particles. J Virol. 2013;87: 11591–11603.

15. Carrillo C, Tulman ER, Delhon G, Lu Z, Carreno A, Vagnozzi A, et al. Comparative genomics of foot-and-mouth disease virus. J Virol. 2005;79: 6487–6504.

16. Feng Q, Chen X, Ma O, Liu Y, Ding M, Collins RA, et al. Serotype and VP1 gene sequence of a foot-and-mouth disease virus from Hong Kong (2002). Biochem Biophys Res Commun. 2003;302: 715–721.

17. Jackson T, King AMQ, Stuart I, Fry E. Structure and receptor binding. Virus Res. 2003;91: 33–46.

18. Fox G, Parry NR, Barnett P V., McGinn B, Rowlands DJ, Brown F. The cell attachment site on foot-and-mouth disease virus includes the amino acid sequence RGD (arginine-glycine-aspartic acid). J Gen Virol. 1989;70: 625–637.

19. Jackson T, Sharma A, Ghazaleh RA, Blakemore WE, Ellard FM, Simmons DL, et al. Arginine-glycine-aspartic acid-specific binding by foot-and-mouth disease viruses to the purified integrin αvβ3 in vitro. J Virol. 1997;71: 8357–8361.

20. Fowler VL, Knowles NJ, Paton DJ, Barnett P V. Marker vaccine potential of a foot-and-mouth

disease virus with a partial VP1 G-H loop deletion. Vaccine. 2010;28: 3428–3434.

21. Hu J, O.Toft D, Seeger C. Hepadnavirus assembly and reverse transcription require a multi-component chaperone complex which is incorporated into nucleocapsids. EMBO J. 1997;16: 59–68.

22. Braakman I, van Anken E. Folding of viral envelope glycoproteins in the endoplasmic reticulum. Traffic. 2000;1: 533–539.

23. Geller R, Vignuzzi M, Andino R, Frydman J. Evolutionary constraints on chaperone-mediated folding provide an antiviral approach refractory to development of drug resistance. Genes Dev. 2007;21: 195–205.

24. Geller R, Taguwa S, Frydman J. Broad action of Hsp90 as a host chaperone required for viral replication. Biochim Biophys Acta. 2012;1823: 698–706.

25. Burch AD, Weller SK. Herpes simplex virus type 1 DNA polymerase requires the mammalian chaperone Hsp90 for proper localization to the nucleus. J Virol. 2005;79: 10740–10749.

26. Newman J, Asfor AS, Berryman S, Jackson T, Curry S, Tuthill TJ. The cellular chaperone heat shock protein 90 is required for foot-and-mouth disease virus capsid precursor processing and assembly of capsid pentamers. J Virol. 2017;92: 1–14.

27. Macejak DG, Sarnow P. Association of heat shock protein 70 with enterovirus capsid precursor P1 in infected human cells. J Virol. 1992;66: 1520–1527.

28. Kristensen T, Newman J, Guan SH, Tuthill TJ, Belsham GJ. Cleavages at the three junctions within the foot-and-mouth disease virus capsid precursor (P1-2A) by the 3C protease are mutually independent. Virology. 2018; DOI: 10.1016 (in press).

29. Ryan MD, Belsham GJ, King AMQ. Specificity of enzyme-substrate interactions in foot-and-mouth disease virus polyprotein processing. Virology. 1989;173: 35–45.

30. Ypma-Wong MF, Semler BL. Processing determinants required for in vitro cleavage of the poliovirus P1 precursor to capsid proteins. J Virol. 1987;61: 3181–3189.

31. Gullberg M, Muszynski B, Organtini LJ, Ashley RE, Hafenstein SL, Belsham GJ, et al. Assembly

and characterization of foot-and-mouth disease virus empty capsid particles expressed within mammalian cells. J Gen Virol. 2013;94: 1769–1779.

32. Gullberg M, Polacek C, Belsham GJ. Sequence adaptations affecting cleavage of the VP1/2A junction by the 3C protease in foot-and-mouth disease virus-infected cells. J Gen Virol. 2014;95: 2402–2410.

33. Curry S, Zunszain PA, Leatherbarrow RJ. Foot-and-mouth disease virus 3C protease: recent structural and functional insights into an antiviral target. Int J Biochem Cell Biol. 2007;39: 1–6.

34. Aragonès L, Guix S, Ribes E, Bosch A, Pintó RM. Fine-tuning translation kinetics selection as the driving force of codon usage bias in the hepatitis A virus capsid. PLOS Pathog. 2010;6: 1–12.

35. Bishop NE, Anderson DA. Uncoating kinetics of hepatitis A virus virions and provirions. J Virol. 2000;74: 3423–3426.

36. Tesar M, Jia X-Y, Summers DF, Ehrenfeld E. Analysis of a potential myristoylation site in hepatitis A virus capsid protein VP4. Virology. 1993;194: 616–626.

37. Spall VE, Shanks M, Lomonossoff GP. Polyprotein processing as a strategy for gene expression in RNA viruses. Semin Virol. 1997;8: 15–23.

38. Kumar V, Das S, Jameel S. The biology and pathogenesis of hepatitis viruses. Curr Sci. 2010;98: 312–325.

39. Escarmís C, Perales C, Domingo E. Biological effect of Muller's ratchet: distant capsid site can affect picornavirus protein processing. J Virol. 2009;83: 6748–6756.

40. Kristensen T, Normann P, Gullberg M, Fahnøe U, Polacek C, Rasmussen TB, et al. Determinants of the VP1/2A junction cleavage by the 3C protease in foot-and-mouth disease virus-infected cells. J Gen Virol. 2016;98: 385–395.

41. Polacek C, Gullberg M, Li J, Belsham GJ. Low levels of foot-and-mouth disease virus 3C protease expression are required to achieve optimal capsid protein expression and processing in mammalian cells. J Gen Virol. 2013;94: 1249–1258.

42. Guan SH, Belsham GJ. Separation of foot-and-mouth disease virus leader protein activities; identification of mutants that retain efficient self- processing activity but poorly induce eIF4G cleavage. J Gen Virol. 2017;98: 671–680.

43. Chen GJ, Qiu N, Karrer C, Caspers P, Page MG. Restriction site-free insertion of PCR products directionally into vectors. Biotechniques. 2000;28: 498–500, 504–505.

44. Fowler V, Bashiruddin JB, Belsham GJ, Stenfeldt C, Bøtner A, Knowles NJ, et al. Characteristics of a foot-and-mouth disease virus with a partial VP1 G-H loop deletion in experimentally infected cattle. Vet Microbiol. 2014;169: 58–66.

45. Fuerst TR, Niles EG, Studier FW, Moss B. Eukaryotic transient-expression system based on recombinant vaccinia virus that synthesizes bacteriophage T7 RNA polymerase. Proc Natl Acad Sci USA. 1986;83: 8122–8126.

46. Belsham GJ, McInerney GM, Ross-Smith N. Foot-and-mouth disease virus 3C protease induces cleavage of translation initiation factors eIF4A and eIF4G within infected cells. J Virol. 2000;74: 272–280.

47. Belsham GJ, Nielsen I, Normann P, Royall E, Roberts LO. Monocistronic mRNAs containing defective hepatitis C virus-like picornavirus internal ribosome entry site elements in their 5' untranslated regions are efficiently translated in cells by a cap-dependent mechanism. RNA. 2008;14: 1671–1680.

Tables

Table 1: Primers used for site-directed mutagenesis

Primers for Megaprimers	Changes	Name
Plasmids for the Transient expression assay, introducing Leader (W52A) substitution		
SG31_Fw: CCACGACAACTGCgcGTTGAACGCC 14TPN6_Rev: CAAACAGGTGCTTCTTGAAAAATCTTTC	Leader (W52A) TGG->GCG	P1-2A (wt)
Plasmids for the Transient expression assay, introducing Stop codons (truncations) in VP1, note that all constructs contains the Leader (W52A) substitution		
14TPN9_Fw: ATCCATGCTGAGTGGGACACAG 1PTK41_R: GAGCAAATCGAAGTTttattaTTGTTTTGC	2A L1StopStop (CTTTTG-> TAATAA)	P1-2A (2A L1Stop)
14TPN9_Fw: ATCCATGCTGAGTGGGACACAG 1PTK40_R: AAGTTGTTTTGCAGGttattaGATCTTCTG	VP1 I205StopStop (ATTGCA -> TAATAA)	P1-2A (VP1 I205Stop)
14TPN9_Fw: ATCCATGCTGAGTGGGACACAG 1PTK39_R: ATCTTCTGTTTGTGttattaTTGAGACGAC	VP1 D199StopStop (GACAGA -> TAATAA)	P1-2A (VP1 D199Stop)
14TPN9_Fw: ATCCATGCTGAGTGGGACACAG 1PTK38_R: CAACAGTGGTCTGGGttattaGAGTTCGGC	VP1 Y185StopStop (TACTGC -> TAATAA)	P1-2A (VP1 Y185Stop)
14TPN9_Fw: ATCCATGCTGAGTGGGACACAG 1PTK37_R: AAGTTGAAAGAAGCttattaCTGAGCGGCG	VP1 L158StopStop (CTTCCT -> TAATAA)	P1-2A (VP1 L158Stop)
14TPN9_Fw: ATCCATGCTGAGTGGGACACAG 1PTK36_R: AATGGTGCCTTGAGttattaGGTGGGGTTG	VP1 A107StopStop (GCCTAC -> TAATAA)	P1-2A (VP1 A107Stop)
14TPN9_Fw: ATCCATGCTGAGTGGGACACAG 1PTK35_R: TGTTGGTGGGTTTGttattaGTCAATGACA	VP1 L53StopStop (CTCATG -> TAATAA)	P1-2A (VP1 L53Stop)
Plasmids for the Transient expression assay, introducing small deletions in the VP1 C-terminus between VP1 185 and VP1 199 , note that all constructs contains the Leader (W52A) substitution		
14TPN9_Fw: ATCCATGCTGAGTGGGACACAG 1PTK42_R: TGATCTTCTGTTTGTGTC**TG**AGTTCGGCACGC		**P1-2A (VP1 Δ185-199)**
14TPN9_Fw: ATCCATGCTGAGTGGGACACAG 1PTK43_R: ACACCTCCACTGCCAACA**GG**AGTTCGGCACGCT		**P1-2A (VP1 Δ185-189)**
14TPN9_Fw: ATCCATGCTGAGTGGGACACAG 1PTK44_R: TTGAGACGACACCTCCA**CG**GGGCAGTAGAGT		**P1-2A (VP1 Δ188-192)**
14TPN9_Fw: ATCCATGCTGAGTGGGACACAG 1PTK45_R: TTGTGTCTGTCTTGAGACG**AC**AGTGGTCTGG		**P1-2A (VP1 Δ191-195)**
14TPN9_Fw: ATCCATGCTGAGTGGGACACAG 1PTK46_R: ATGATCTTCTGTTTGTGTC**TC**TCCACTGCCAA		**P1-2A (VP1 Δ194-199)**
14TPN9_Fw: ATCCATGCTGAGTGGGACACAG 1PTK47_R: AGCAGGAAGCTGAGCGG**CC**GTACCACCTGCGGA		**P1-2A (VP1 Δ142-154)** **Positive control**

Small letters = Nucleotide changes. Bold = Deletion between the two bold nucleotides.

Table 2: Primers used for site-directed mutagenesis (alanine substitutions)

Primers for Megaprimers	Changes	Name
Plasmids for the Transient expression assay, introducing alanine substitutions in the VP1 C-terminus between VP1 185 and VP1 199 (with the exception of VP1 192 where an alanine was substituted to a serine, note that all constructs contains the Leader (W52A) substitution		
14TPN9_Fw: ATCCATGCTGAGTGGGACACAG 1PTK48_R: CAGTGGTCTGGGGCAagcGAGTTCGGCA	VP1 Y185A (TAC-> AGC)	P1-2A (VP1 Y185A)
14TPN9_Fw: ATCCATGCTGAGTGGGACACAG 1PTK49_R: CCAACAGTGGTCTGGGagcGTAGAGTTC	VP1 C186A (TGC-> AGC)	P1-2A (VP1 C186A)
14TPN9_Fw: ATCCATGCTGAGTGGGACACAG 1PTK50_R: ACTGCCAACAGTGGTCTagcGCAGTAGA	VP1 P187A (CCC-> AGC)	P1-2A (VP1 P187A)
14TPN9_Fw: ATCCATGCTGAGTGGGACACAG 1PTK51_R: CCACTGCCAACAGTGGagcGGGGCAGTA	VP1 R188A (AGA-> AGC)	P1-2A (VP1 R188A)
14TPN9_Fw: ATCCATGCTGAGTGGGACACAG 1PTK52_R: CCTCCACTGCCAACAGagcTCTGGGGCA	VP1 P189A (CCA-> AGC)	P1-2A (VP1 P189A)
14TPN9_Fw: ATCCATGCTGAGTGGGACACAG 1PTK53_R: ACACCTCCACTGCCAAagcTGGTCTGGG	VP1 L190A (CTG-> AGC)	P1-2A (VP1 L190A)
14TPN9_Fw: ATCCATGCTGAGTGGGACACAG 1PTK54_R: CGACACCTCCACTGCagcCAGTGGTCTG	VP1 L191A (TGG-> AGC)	P1-2A (VP1 L191A)
14TPN9_Fw: ATCCATGCTGAGTGGGACACAG 1PTK55_R: TGAGACGACACCTCCACagaCAACAGTG	VP1 A192S (GCA-> TCT)	P1-2A (VP1 A192S)
14TPN9_Fw: ATCCATGCTGAGTGGGACACAG 1PTK56_R: CTTGAGACGACACCTCagcTGCCAACAG	VP1 V193A (GTG-> AGC)	P1-2A (VP1 V193A)
14TPN9_Fw: ATCCATGCTGAGTGGGACACAG 1PTK57_R: GTCTTGAGACGACACagcCACTGCCAAC	VP1 E194A (GAG-> AGC)	P1-2A (VP1 E194A)
14TPN9_Fw: ATCCATGCTGAGTGGGACACAG 1PTK58_R: TGTCTGTCTTGAGACGAagcCTCCACTG	VP1 V195A (GTG-> AGC)	P1-2A (VP1 V195A)
14TPN9_Fw: ATCCATGCTGAGTGGGACACAG 1PTK59_R: TTTGTGTCTGTCTTGAGAagcCACCTCC	VP1 S196A (TCG-> AGC)	P1-2A (VP1 S196A)
14TPN9_Fw: ATCCATGCTGAGTGGGACACAG 1PTK60_R: CTGTTTGTGTCTGTCTTGagcCGACACC	VP1 S197A (TCT-> AGC)	P1-2A (VP1 S197A)
14TPN9_Fw: ATCCATGCTGAGTGGGACACAG 1PTK61_R: TCTGTTTGTGTCTGTCagcAGACGACAC	VP1 Q198A (CAA-> AGC)	P1-2A (VP1 Q198A)
14TPN9_Fw: ATCCATGCTGAGTGGGACACAG 1PTK62_R: TCTGTTTGTGTCTagcTTGAGACGACAC	VP1 D199A (GAC-> AGC)	P1-2A (VP1 D199A)

Small letters = Nucleotide changes.

Figures

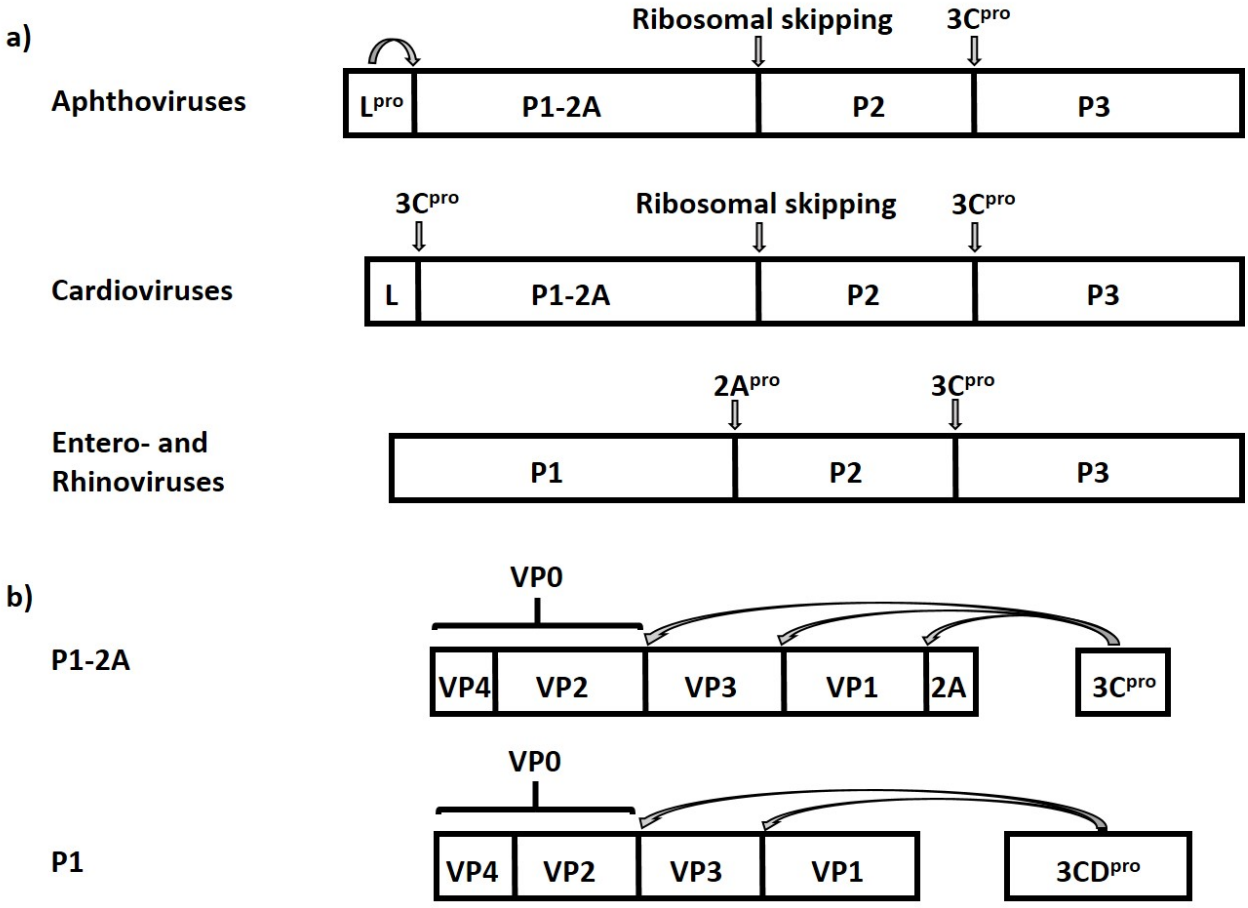

Figure 1

Schematic representation of the polyprotein processing in three different genera of picornaviruses. a) The RNA genome of viruses in the genus *Aphthovirus*, in which FMDV is the prototypic member, encodes a polyprotein that is processed into four primary products namely the Leader protease (L^{pro}), P1-2A, P2 and P3 during, and after, synthesis. The "cleavage" at the 2A/2B junction occurs during synthesis by a mechanism known as "ribosomal skipping" [8] or "StopGo" [9]. The L^{pro} mediated cleavage occurs at its own C-terminus, i.e. at the L/P1-2A junction while the $3C^{pro}$ is responsible for cleavage of the P2/P3 junction. The *Cardiovirus* polyprotein is also processed into the primary products, Leader, P1-2A, P2 and P3 but the Leader protein is removed from the capsid precursor by the $3C^{pro}$. The *Entero-* and *Rhinoviruses*, do not have a Leader protein and the polyprotein is thus processed into only three primary products, namely P1, P2 and P3. In the *Entero-*

and *Rhinoviruses* the 2A protein is a protease that cleaves the P1/P2 junction. The $3C^{pro}$ is responsible for cleavage of the P2/P3 junction.

b) The $3C^{pro}$ is sufficient for processing of the capsid precursor, P1-2A, in *Aphthoviruses* and *Cardioviruses*. The precursor is processed to generate VP0, VP3 and VP1, and a short 2A peptide. In *Entero*- and *Rhinoviruses* the $3CD^{pro}$ is responsible for processing the capsid precursor P1 to VP0, VP3 and VP1.

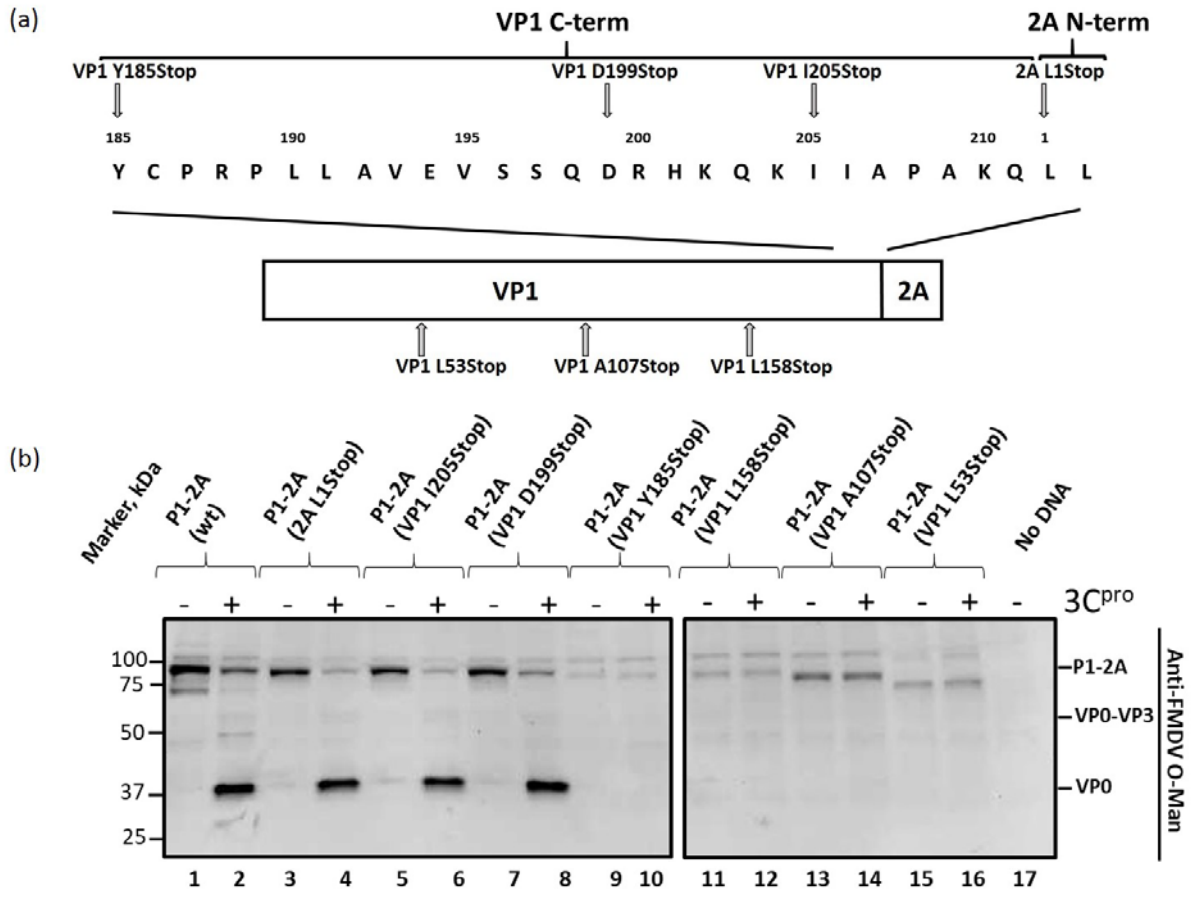

Figure 2

Truncations in the C-terminus of FMDV VP1 affect capsid precursor processing.

a) Constructs encoding the FMDV P1-2A (wt) were modified to introduce truncations at different sites in the VP1 coding sequence. The 2A L1Stop truncation served as a second positive control for processing.

b) Cell lysates from BHK cells (infected with vTF7-3 [45]) transfected with plasmids that express the FMDV P1-2A (wt or truncated at the VP1) alone (odd numbered lanes) or with the plasmid pSKRH3C [46] encoding the FMDV $3C^{pro}$ (even numbered lanes) were analyzed by immunoblotting. Molecular mass markers (kDa) are indicated on the left. A negative control (No DNA) was included (lane 17). The different structural proteins are indicated on the right of the figure and were detected using guinea pig anti-FMDV O-Man antisera. Bound antibodies were visualized using the anti-guinea pig HRP-conjugated secondary antibodies and a chemiluminescence detection kit.

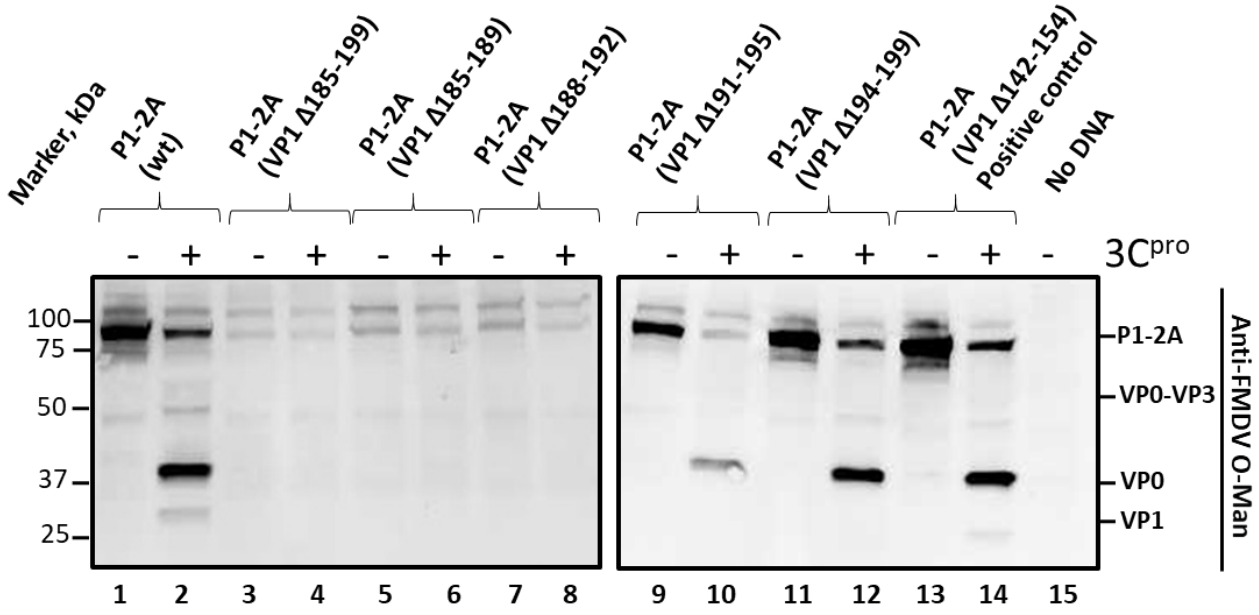

Figure 3

A short region near the C-terminus of FMDV VP1 is required for capsid precursor processing

Cell lysates were prepared from BHK cells (infected with vTF7-3 [45]) following transfection with plasmids that express the FMDV P1-2A wt or with small deletions as indicated either alone (odd numbered lanes) or with the plasmid pSKRH3C [46] encoding the $3C^{pro}$ (even numbered lanes). The samples were analyzed by immunoblotting. A positive control with a deletion known to be tolerated in infectious FMDV [20] was included, P1-2A (VP1 Δ142-154), lanes 13 and 14. Molecular mass markers (kDa) are indicated on the left. A negative control (No DNA) was used in lane 15. The structural proteins corresponding to the different bands are indicated on the right of the figure and were detected using guinea pig anti-FMDV O-Man antisera. Bound antibodies were visualized using the anti-guinea pig HRP-conjugated secondary antibodies and a chemiluminescence detection kit.

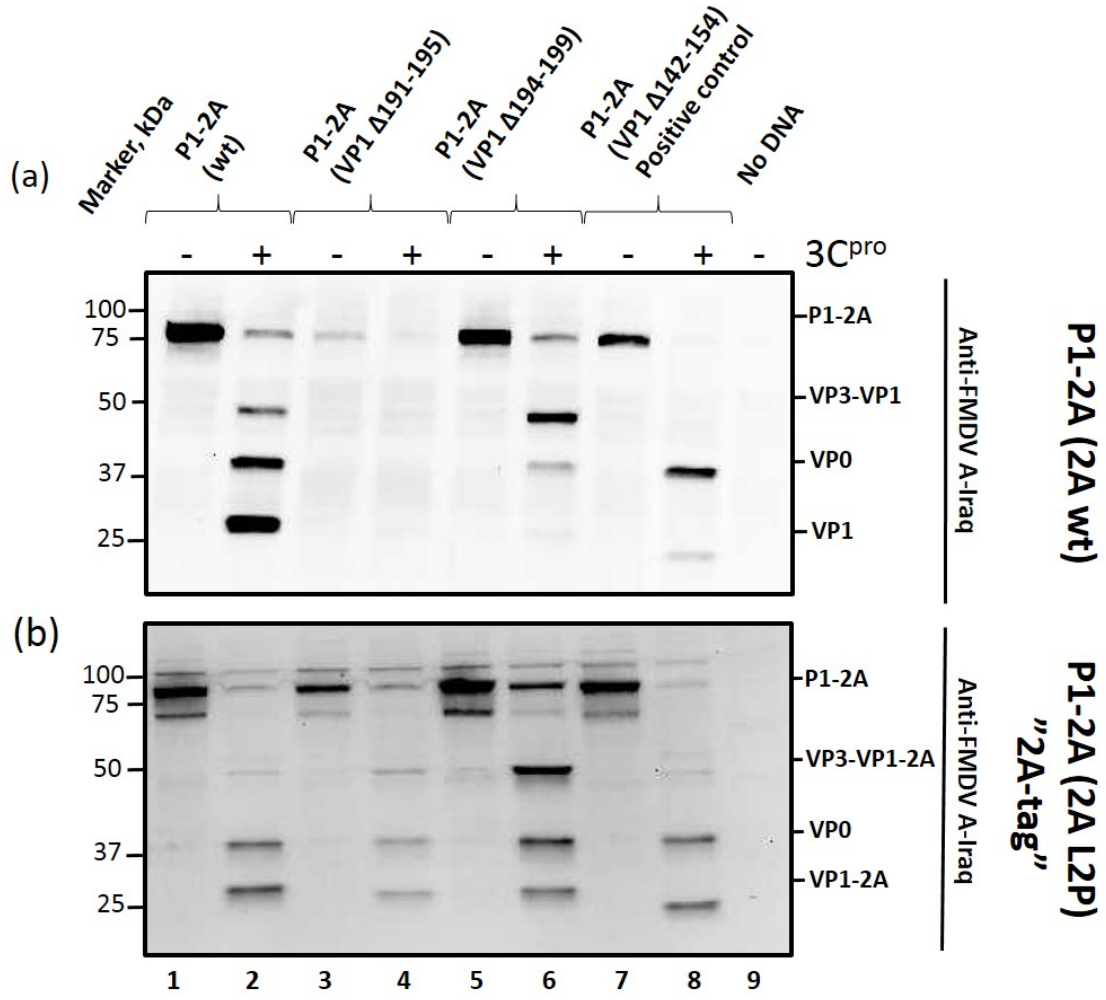

Figure 4

A region near the C-terminus of FMDV VP1 required for processing of the VP3/VP1 junction. a) The P1-2A precursor (wt or with small deletions as indicated) was expressed alone or with $3C^{pro}$ in transient expression assays in BHK cells as for Fig. 3. Cell lysates were prepared and analyzed by immunoblotting. The structural proteins corresponding to the different bands are indicated and were detected using guinea pig anti-FMDV A-Iraq antisera. Bound antibodies were visualized using the anti-guinea pig HRP-conjugated secondary antibodies and chemiluminescence detection. The odd numbered lanes show the P1-2A precursors expressed alone and the even numbered lanes show the precursor co-expressed with $3C^{pro}$. Molecular mass markers (kDa) are indicated on the left. A negative control (No DNA) is included in lane 9. A positive control with a deletion known to be tolerated in replicating FMDV [20] was included, P1-2A (VP1 Δ142-154), lanes 7 and 8.

b) The 2A L2P substitution was introduced into the plasmids encoding P1-2A (wt), P1-2A (VP1 Δ191-195), P1-2A (VP1 Δ194-199) and the positive control P1-2A (VP1 Δ142-154). This 2A L2P substitution blocks cleavage of the VP1/2A junction and increased the sensitivity of detection of VP1. The negative control (No DNA) is indicated.

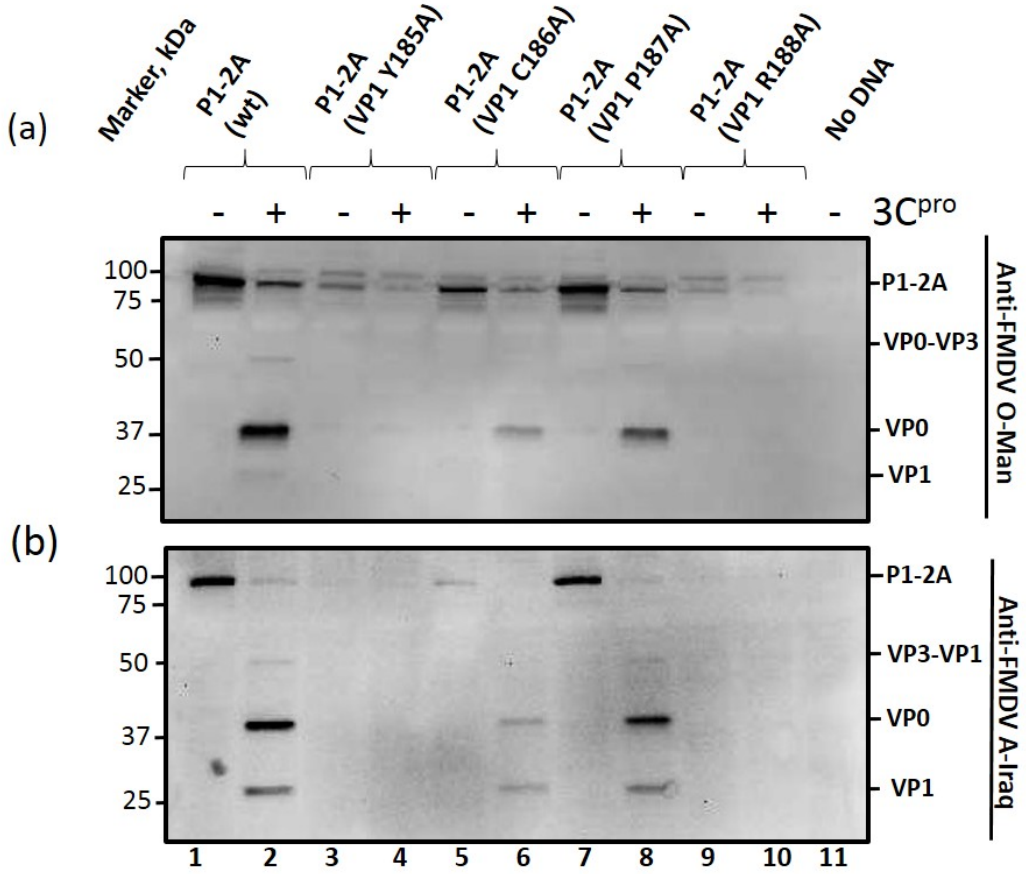

Figure 5

Identification of amino acids between residues VP1 185 and 188 required for capsid precursor processing

The P1-2A precursors (wt or having alanine substitutions between VP1 185 and VP1 188) were expressed alone or in the presence of $3C^{pro}$ and analyzed by immunoblotting (as above). The structural proteins corresponding to the different products are indicated on the right of the figure and were detected using guinea pig anti-FMDV O-Man antisera (a) or guinea pig anti-FMDV A-Iraq antisera (b). Bound antibodies were visualized using the anti-guinea pig HRP-conjugated secondary antibodies and a chemiluminescence detection kit. Molecular mass markers (kDa) are indicated on the left. A negative control (No DNA) is included in lane 11.

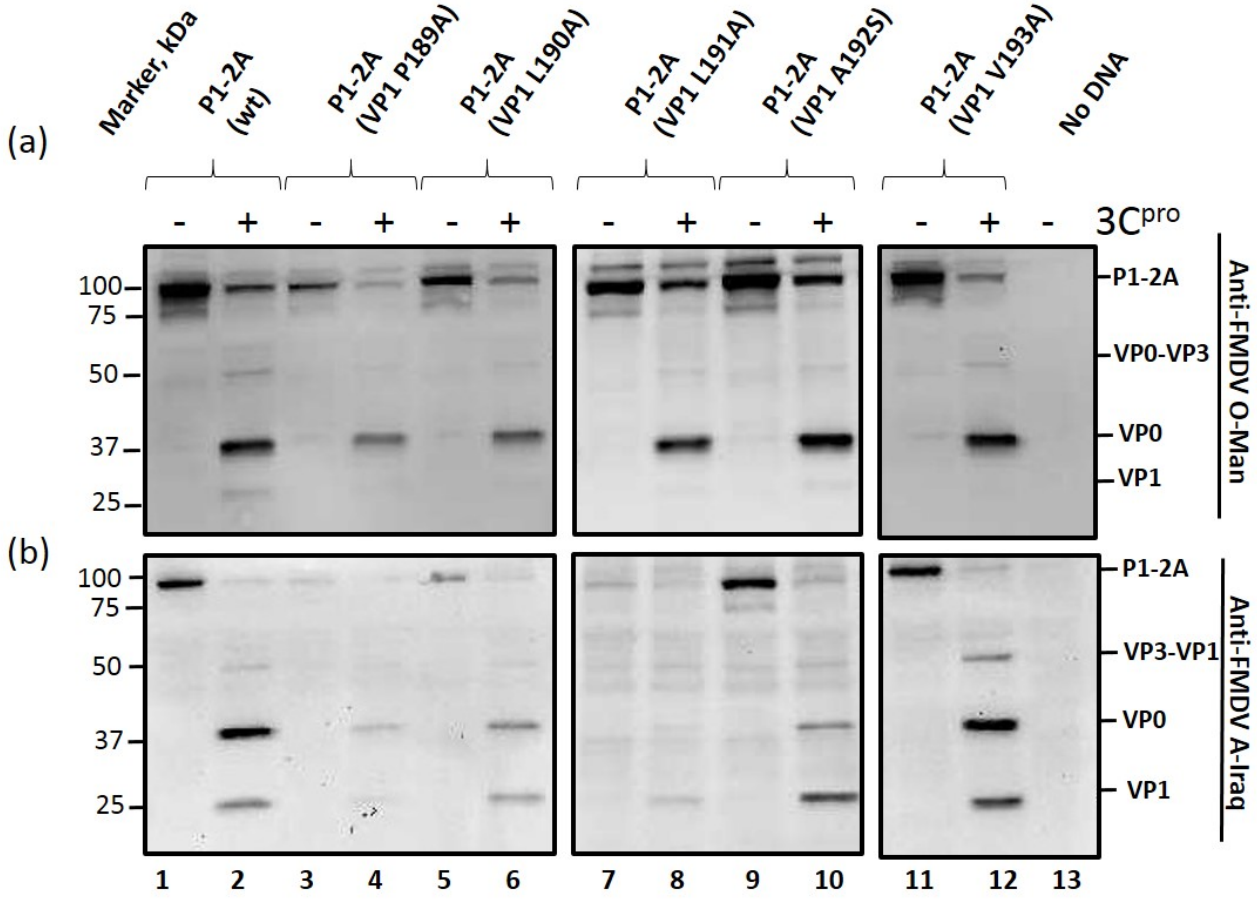

Figure 6

Identification of residues between VP1 189 and 193 required for processing at the VP3/VP1 junction. The P1-2A precursors (wt or with alanine substitutions between VP1 189 and VP1 193, with the exception of VP1 192 where an alanine were substituted to a serine, as indicated) were expressed alone or in the presence of $3C^{pro}$ and analyzed by immunoblotting. The capsid proteins are indicated on the right of the figure. Proteins were detected using guinea pig anti-FMDV O-Man antisera (a) or with guinea pig anti-FMDV A-Iraq antisera (b). Bound antibodies were visualized using the anti-guinea pig HRP-conjugated secondary antibodies and a chemiluminescence detection kit. Molecular mass markers (kDa) are indicated on the left. A negative control (No DNA) is included in lane 13.

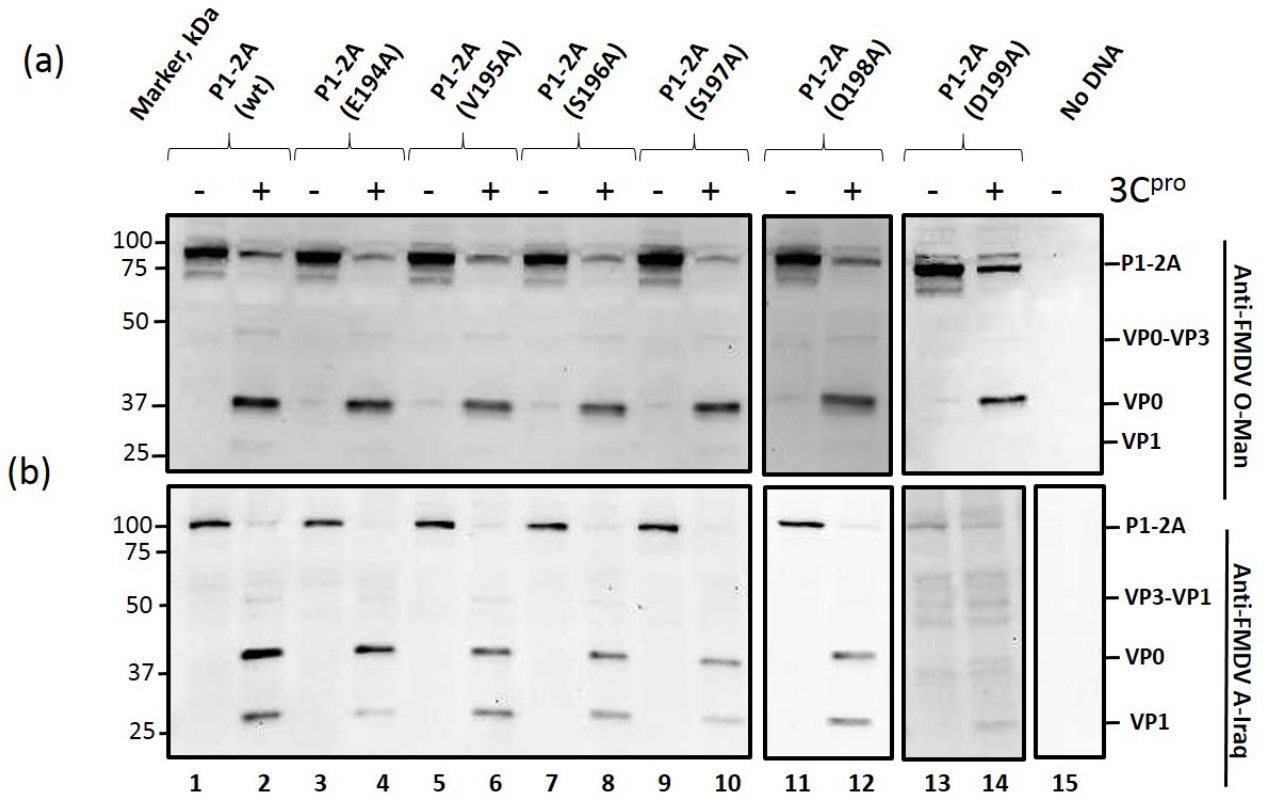

Figure 7

Multiple residues within the VP1 194-199 region are important for processing of the VP3/VP1 junction.

The P1-2A precursors (wt or with alanine substitutions between VP1 194 and VP1 199, as indicated) were expressed alone or in the presence of $3C^{pro}$ and analyzed by immunoblotting. The different capsid proteins are indicated on the right of the figure. Proteins were detected using guinea pig anti-FMDV O-Man antisera (a) or guinea pig anti-FMDV A-Iraq antisera (b). Bound antibodies were visualized using the anti-guinea pig HRP-conjugated secondary antibodies and a chemiluminescence detection kit. Molecular mass markers (kDa) are indicated on the left. A negative control (No DNA) is included in lane 15.

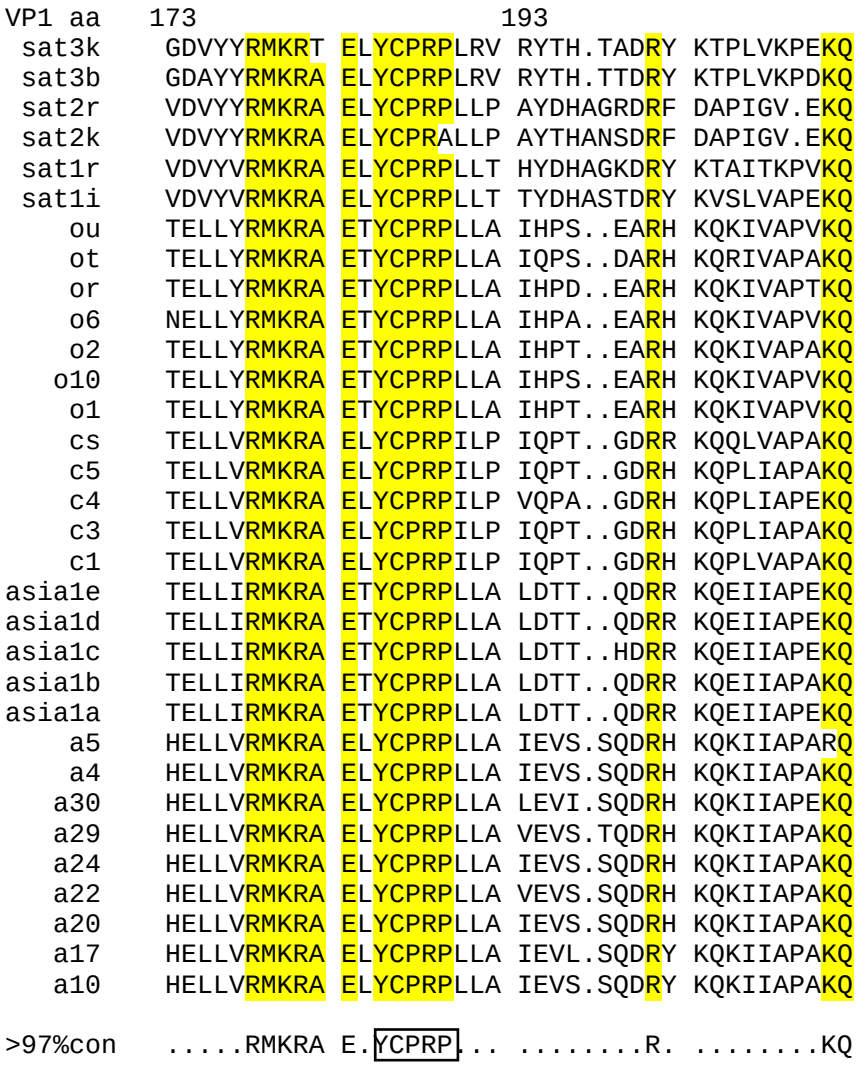

Figure 8

Alignment of the VP1 C-terminus from different FMDV serotypes

Amino acid alignment of the VP1 C-terminus of different strains of FMDV, including examples of all seven serotypes. The yellow color represents amino acids that are more that 97% conserved among the different strains. The conserved motif YCPRP (VP1 185-189) is marked with a box in the consensus sequence. The alignment was prepared from sequences published previously [15].

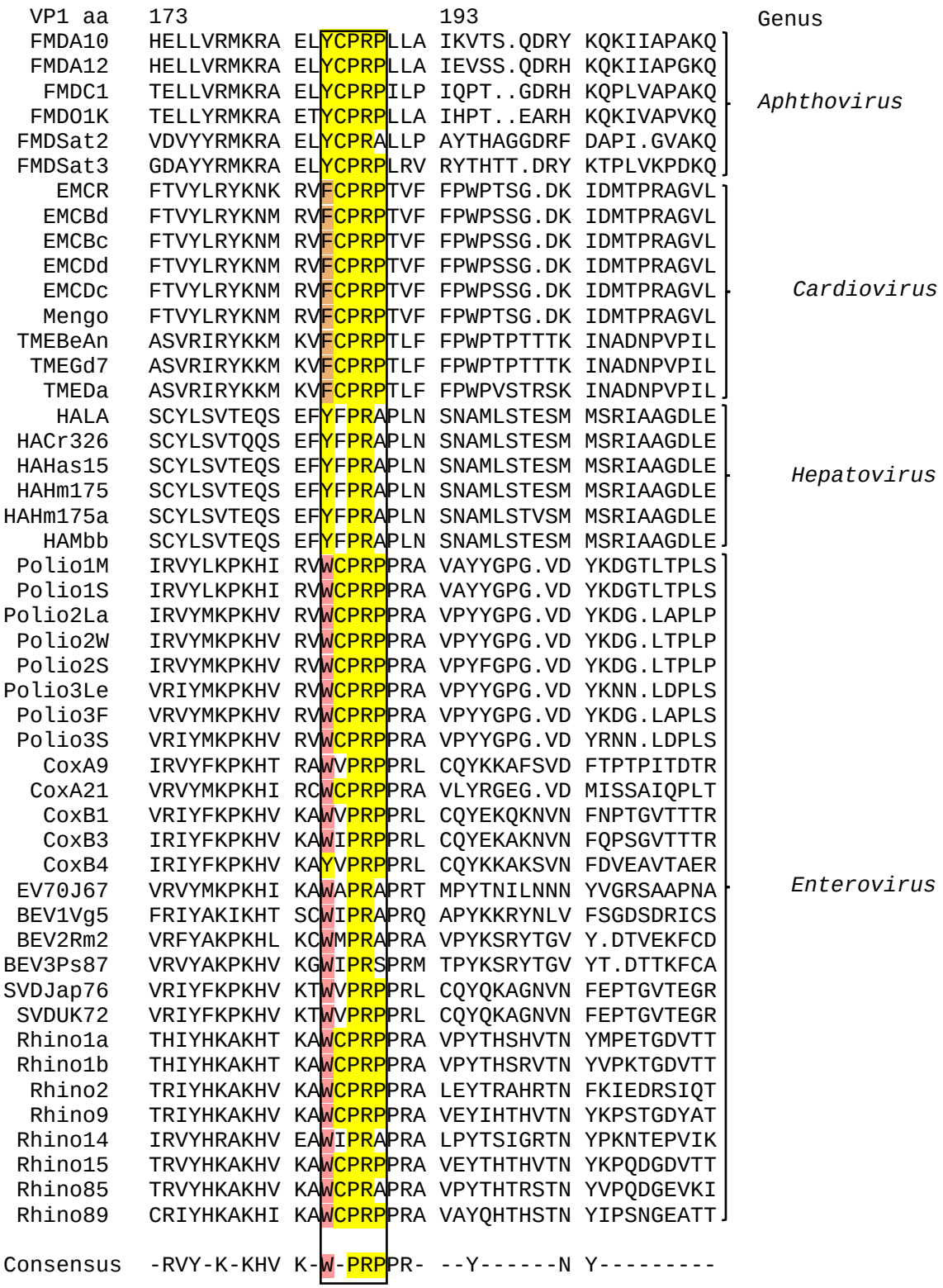
VP1 aa 173 193 Genus
FMDA10 HELLVRMKRA ELYCPRPLLA IKVTS.QDRY KQKIIAPAKQ
FMDA12 HELLVRMKRA ELYCPRPLLA IEVSS.QDRH KQKIIAPGKQ
FMDC1 TELLVRMKRA ELYCPRPILP IQPT..GDRH KQPLVAPAKQ
FMDO1K TELLYRMKRA ETYCPRPLLA IHPT..EARH KQKIVAPVKQ
FMDSat2 VDVYYRMKRA ELYCPRALLP AYTHAGGDRF DAPI.GVAKQ
FMDSat3 GDAYYRMKRA ELYCPRPLRV RYTHTT.DRY KTPLVKPDKQ
Aphthovirus
EMCR FTVYLRYKNK RVFCPRPTVF FPWPTSG.DK IDMTPRAGVL
EMCBd FTVYLRYKNM RVFCPRPTVF FPWPSSG.DK IDMTPRAGVL
EMCBc FTVYLRYKNM RVFCPRPTVF FPWPSSG.DK IDMTPRAGVL
EMCDd FTVYLRYKNM RVFCPRPTVF FPWPSSG.DK IDMTPRAGVL
EMCDc FTVYLRYKNM RVFCPRPTVF FPWPSSG.DK IDMTPRAGVL
Mengo FTVYLRYKNM RVFCPRPTVF FPWPTSG.DK IDMTPRAGVL
TMEBeAn ASVRIRYKKM KVFCPRPTLF FPWPTPTTTK INADNPVPIL
TMEGd7 ASVRIRYKKM KVFCPRPTLF FPWPTPTTTK INADNPVPIL
TMEDa ASVRIRYKKM KVFCPRPTLF FPWPVSTRSK INADNPVPIL
Cardiovirus
HALA SCYLSVTEQS EFYFPRAPLN SNAMLSTESM MSRIAAGDLE
HACr326 SCYLSVTQQS EFYFPRAPLN SNAMLSTESM MSRIAAGDLE
HAHas15 SCYLSVTEQS EFYFPRAPLN SNAMLSTESM MSRIAAGDLE
HAHm175 SCYLSVTEQS EFYFPRAPLN SNAMLSTESM MSRIAAGDLE
HAHm175a SCYLSVTEQS EFYFPRAPLN SNAMLSTVSM MSRIAAGDLE
HAMbb SCYLSVTEQS EFYFPRAPLN SNAMLSTESM MSRIAAGDLE
Hepatovirus
Polio1M IRVYLKPKHI RVWCPRPPRA VAYYGPG.VD YKDGTLTPLS
Polio1S IRVYLKPKHI RVWCPRPPRA VAYYGPG.VD YKDGTLTPLS
Polio2La IRVYMKPKHV RVWCPRPPRA VPYYGPG.VD YKDG.LAPLP
Polio2W IRVYMKPKHV RVWCPRPPRA VPYYGPG.VD YKDG.LTPLP
Polio2S IRVYMKPKHV RVWCPRPPRA VPYFGPG.VD YKDG.LTPLP
Polio3Le VRIYMKPKHV RVWCPRPPRA VPYYGPG.VD YKNN.LDPLS
Polio3F VRVYMKPKHV RVWCPRPPRA VPYYGPG.VD YKDG.LAPLS
Polio3S VRIYMKPKHV RVWCPRPPRA VPYYGPG.VD YRNN.LDPLS
CoxA9 IRVYFKPKHT RAWVPRPPRL CQYKKAFSVD FTPTPITDTR
CoxA21 VRVYMKPKHI RCWCPRPPRA VLYRGEG.VD MISSAIQPLT
CoxB1 VRIYFKPKHV KAWVPRPPRL CQYEKQKNVN FNPTGVTTTR
CoxB3 IRIYFKPKHV KAWIPRPPRL CQYEKAKNVN FQPSGVTTTR
CoxB4 IRIYFKPKHV KAYVPRPPRL CQYKKAKSVN FDVEAVTAER
EV70J67 VRVYMKPKHI KAWAPRAPRT MPYTNILNNN YVGRSAAPNA
BEV1Vg5 FRIYAKIKHT SCWIPRAPRQ APYKKRYNLV FSGDSDRICS
BEV2Rm2 VRFYAKPKHL KCWMPRAPRA VPYKSRYTGV Y.DTVEKFCD
BEV3Ps87 VRVYAKPKHV KGWIPRSPRM TPYKSRYTGV YT.DTTKFCA
SVDJap76 VRIYFKPKHV KTWVPRPPRL CQYQKAGNVN FEPTGVTEGR
SVDUK72 VRIYFKPKHV KTWVPRPPRL CQYQKAGNVN FEPTGVTEGR
Rhino1a THIYHKAKHT KAWCPRPPRA VPYTHSHVTN YMPETGDVTT
Rhino1b THIYHKAKHT KAWCPRPPRA VPYTHSRVTN YVPKTGDVTT
Rhino2 TRIYHKAKHV KAWCPRPPRA LEYTRAHRTN FKIEDRSIQT
Rhino9 TRIYHKAKHV KAWCPRPPRA VEYIHTHVTN YKPSTGDYAT
Rhino14 IRVYHRAKHV EAWIPRAPRA LPYTSIGRTN YPKNTEPVIK
Rhino15 TRVYHKAKHV KAWCPRPPRA VEYTHTHVTN YKPQDGDVTT
Rhino85 TRVYHKAKHV KAWCPRAPRA VPYTHTRSTN YVPQDGEVKI
Rhino89 CRIYHKAKHI KAWCPRPPRA VAYQHTHSTN YIPSNGEATT
Enterovirus
Consensus -RVY-K-KHV K-W-PRPPR- --Y------N Y---------

Figure 9

Alignment of different picornaviruses at the VP1 C-terminus

Amino acid alignment of the VP1 C-terminus of diverse picornaviruses. The black box indicates the highly conserved motif (VP1 185-189 in FMDV) that is important for correct processing of the capsid precursor. The sequences are numbered according to the FMDV residues. The yellow color represents amino acids that are identical with the YCPRP motif found in FMDV. Conservative substitutions are indicated with a similar color i.e. yellow for Y, orange for F and pink for W. The C residue at VP1 186 (according to FMDV VP1 numbers) is conserved in 31 out of 48 aligned picornaviruses (marked with yellow). The P and R at VP1 187 and 188 are 100% conserved amongst all of the aligned picornaviruses (marked with yellow). The P at VP1 189 (according to FMDV VP1 numbers) is conserved in 35 out of 48 of the aligned picornaviruses, differences from the P are seen in all of the *hepatoviruses* and a few of the *enteroviruses*. The alignment was taken from Ann Palmenberg's laboratory website (http://www.virology.wisc.edu/acp/Aligns/aligns/picorna.p1) and highlighted manually.

Abbreviations: FMDV = Foot-and-mouth disease virus, EMC = Encephalomyocarditis virus, TME = Theiler's murine encephalomyelitis virus, HA = Hepatitis A virus, Cox = Coxsackievirus, EV = Enterovirus, BEV = Bovine enterovirus, SVD = Swine vesicular disease virus.

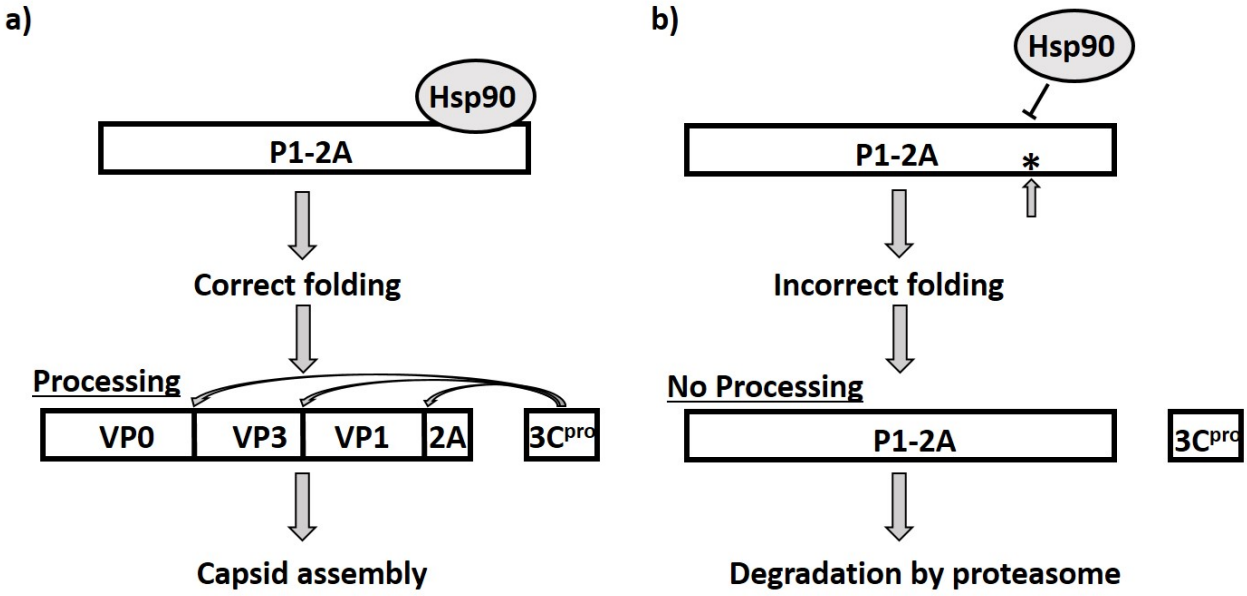

Figure 10

Model: Potential role of chaperone binding to a conserved motif for correct capsid precursor folding

a) Hsp90 (or other chaperones and co-chaperones) is believed to bind to the P1-2A precursor (or P1 for enteroviruses) to facilitate folding into a state where the $3C^{pro}$ (or $3CD^{pro}$) is able to process the precursor to the mature structural capsid proteins prior to particle assembly.

b) It is hypothesized that the conserved motif, YCPRP, in the C-terminus of VP1 is required for the binding of a chaperone (or co-chaperone). In the absence of this interaction, the precursor will be incorrectly folded and hence $3C^{pro}$ (or $3CD^{pro}$) will not recognize the cleavage sites; the misfolded, intact, precursor will be degraded by the proteasome.

Supplementary figures

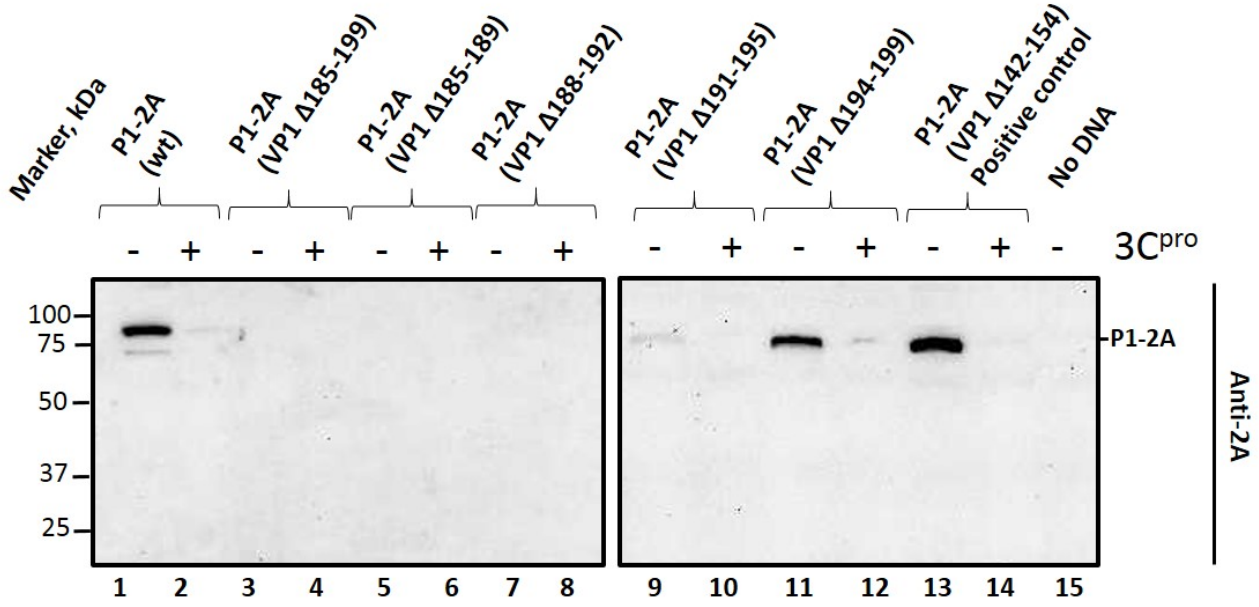

Figure S1

Effect of small deletions on processing of P1-2A at the FMDV VP1/2A junction. The P1-2A precursor (wt or with small deletions as indicated) was expressed alone or with $3C^{pro}$ in transient expression assays in BHK cells as for Fig. 3. Cell lysates were prepared and analyzed by immunoblotting using rabbit anti-2A antibodies. Bound antibodies were visualized using the anti-rabbit HRP-conjugated secondary antibodies and chemiluminescence detection. The odd numbered lanes show the P1-2A precursors expressed alone and the even numbered lanes show the precursor co-expressed with $3C^{pro}$. Molecular mass markers (kDa) are indicated on the left. A negative control (No DNA) is included in lane 15. A positive control with a deletion known to be tolerated in replicating FMDV [20] was included, P1-2A (VP1 Δ142-154), lanes 13 and 14. Note, the free 2A peptide (18 residues long) is too small to detect in this system.

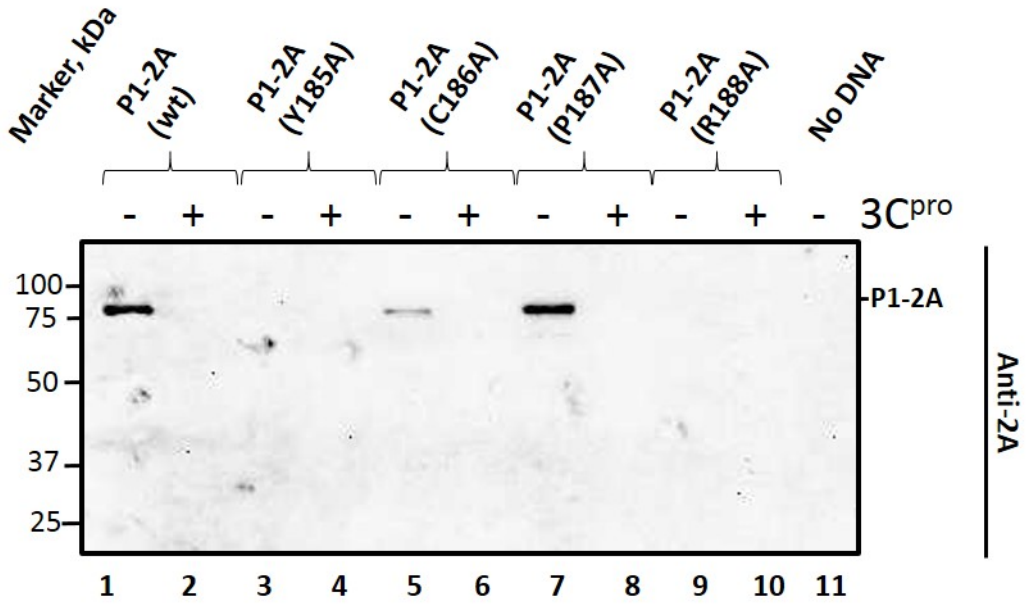

Figure S2.

Analysis of processing at the FMDV VP1/2A junction in P1-2A precursors modified at individual residues between VP1 185 and 188

The P1-2A precursors (wt or having alanine substitutions between VP1 185 and VP1 188) were expressed alone or in the presence of $3C^{pro}$ and analyzed by immunoblotting. The P1-2A was detected using rabbit anti-2A antibodies and visualized using rabbit HRP-conjugated secondary antibodies and a chemiluminescence detection kit. Molecular mass markers (kDa) are indicated on the left. A negative control (No DNA) is included in lane 11. Note, the free 2A peptide (18 residues long) is too small to detect in this system.

4. Conclusion and perspectives

4. Conclusion and perspectives

FMDV remains an important global threat to animal production and the related economy. FMD is still endemic in many countries worldwide, and the distribution of the disease roughly reflects lack of economic development. The disease has been eradicated from the more developed countries, but outbreaks in such countries sometimes still occur and then cause huge economic losses. Despite substantial information about the virus, FMD remains a major threat to the livestock industries. Vaccination alone is unlikely to control the disease and strict control of animal movement is also required. In less developed countries there are often deficiencies in submitting samples to reference laboratories, which makes early detection and response difficult (Jamal & Belsham, 2013). Alternative, strategies to control the disease may also be required to achieve eradication globally.

The structural proteins, VP0, VP3 and VP1 are generated by processing of the capsid precursor P1-2A. Correct processing of these junctions is crucial for the virus to create new infectious virus particles and thus this is very important in the virus lifecycle. This makes the processing of the capsid precursor an attractive target for antiviral drugs to interfere or block the virus lifecycle. To increase the knowledge about processing of the capsid precursor, this Ph.D. study has been focused on the features of the P1-2A precursor that affect it's processing.

In the first manuscript, we have modified the amino acid sequences at the VP1/2A junction. Interestingly, it was recently shown that this junction could be blocked by introducing a substitution VP1 K210E (at the P2 residue in the VP1/2A junction), without interfering with the virus lifecycle (Gullberg et al., 2013a). This finding, made it possible to introduce different substitutions near this junction in full-length FMDV to investigate the effect of these substitutions without blocking virus infectivity, even though the processing of this junction could be modified. In contrast, it was expected that blocking cleavage of one of the junctions between the structural proteins i.e. the VP0/VP3- or the VP3/VP1 junction would prevent the formation of new virus particles, and thus made these junctions harder to study in full length FMDVs.

The grouping of cleavage sites according to the Q/x or E/x junctions revealed that sites belonging to the Q/x group typically also had a K at the P2 position (Curry et al., 2007). The FMDV A22 Iraq VP1/2A junction has a Q at the P1 position and indeed has a K at the P2 position. In manuscript 1 we substituted the P2 lysine in the VP1/2A junction with different amino acids (Q, A, V, M, N, E and R) (note that the E was already known to block processing of this junction in FMDV O1 Manisa (Gullberg et al., 2013a)) by modifying the full-length FMDV cDNA. Interestingly, only the P2 K (wt) junction and the mutant with the substitution to an R could be processed by the $3C^{pro}$, indicating that $3C^{pro}$ has a strong preference for a positively charged amino acid at this specific site, see manuscript 1.

As mentioned, the junctions belonging to the Q/x group typically have a K at the P2 position. Results from manuscript 1, showed that the VP1/2A junction could be processed only when having the wt lysine or a substitution to an arginine at the P2 indicating that, the $3C^{pro}$ preferred a positively charged amino acid. In contrast, the $3C^{pro}$ can process the E/x group of sites without being very constrained about the P2 residue, as there are an almost equal number of E/x junctions having either a K, A, T, H or Q at the P2 position. However, an arginine is never observed at the P2 residue in the E/x junctions. The VP0/VP3 junction of the FMDV A22 Iraq belongs to the E/x group and has a lysine on the P2 residue (VP2 K217). However, introducing an R at this residue in a transient expression system expressing the P1-2A precursor together with $3C^{pro}$, strongly reduced the cleavage efficiency, indicating that the R is not optimal at this site. However, some VP0 was detected upon the VP2 K217R substitution indicating that the $3C^{pro}$ could still process this junction but at a slower rate. In contrast, introducing the VP2 K217E, which is never observed at this position in any of the FMDV junctions (Carrillo et al., 2005; Curry et al., 2007), completely prevented cleavage of the VP0/VP3 junction by the $3C^{pro}$ in the transient expression assay, see manuscript 2 (Kristensen et al., 2018). This finding is consistent with earlier findings on the VP1/2A junction where the VP1 K210E (P2 residue) severely blocked processing of this junction (Gullberg et al., 2013a; Kristensen et al., 2016).

A substitution encoding VP3 I2P downstream of the VP0/VP3 junction was introduced at the P2´ residue. Substitutions with a proline are usually considered as very drastic substitutions, because

the P residue induces a kink in the amino acid chain, and thus can influence the structure. However, a P at the P2´residue within the E/x junction is actually the most abundant amino acid at this specific site, and thus it was believed that $3C^{pro}$ might be able to partially process this junction. The expression of the P1-2A (VP3 I2P) in the transient expression assay revealed that processing of the VP0/VP3 junction can occur, but at a slower rate compared to the P1-2A (wt), and equal amounts of the VP0-VP3 intermediate and processed VP0 were detected, see Fig.2 in Manuscript 2. Interestingly, even though the P1-2A (VP2 K217R) and the P1-2A (VP3 I2P) were expressed and cleaved, in the transient expression assay, at approximately the same rate by the $3C^{pro}$, the full length FMDV (VP3 I2P) did not generate any infectious virus, whereas the FMDV (VP2 K217R) did.

The P1 Q, at the VP1/2A junction in a small peptide assay forms three hydrogen bonds to the S1 pocket of the $3C^{pro}$ (Zunszain et al., 2010). Interestingly, the P1 E binds in approximately the same manner, thereby explaining the broader tolerance of FMDV $3C^{pro}$ for either E or Q at the P1 residue compared to the $3C^{pro}$ from other picornaviruses. It was earlier shown that the Q in a short peptide corresponding to the VP1/2A junction could be substituted to an E, which only reduced cleavage activity by two-fold (Birtley et al., 2005; Zunszain et al., 2010). In contrast, changing the P1 Q to either asparagine (N) or aspartate (D) completely prevented cleavage. In manuscript 2, the FMDV A22 Iraq VP3/VP1 junction, which belongs to the Q/x group, was modified just upstream or downstream of the cleavage site, i.e. at P1 and P1´ in two different constructs. Since the FMDV $3C^{pro}$ has only been reported to be able to cleave junctions containing either an E or Q, it was expected that the VP3 Q221P substituting would completely prevent cleavage. The transient expression of this mutant revealed that cleavage of this junction had been severely blocked, since no VP1 could be detected but only the VP3-VP1 intermediate.

Large hydrophobic amino acids (i.e. L, I or T) are required at the P1´ within the Q/x junction group (Curry et al., 2007). Substituting the P1´ L to either G or C, in the Q/x group, as assessed using a peptide cleavage assay, reduced cleavage activity of FMDV $3C^{pro}$ to around 10% and 50% respectively (Zunszain et al., 2010). Interestingly the binding of the P1´ L within this short peptide creates a pocket within the $3C^{pro}$, where the L is incorporated (Zunszain et al., 2010). Thus, this

residue seems to be in close interaction with the $3C^{pro}$. The P1´residue within the Q/x group is most often an L, T or I (Curry et al., 2007), however S, V, A and M are also found at this specific site (Carrillo et al., 2005). In manuscript 2, a proline was introduced at the P1´ residue, P1-2A (VP1 T1P), which completely prevented cleavage by the $3C^{pro}$.

In manuscript 1 (Kristensen et al., 2016), we showed that the VP1/2A junction could be fully processed by the $3C^{pro}$ following the VP1 K210R substitution in full length FMDV, and thus it was a bit surprising that cleavage of the VP0/VP3 junction within the P1-2A (VP2 K217R) mutant was clearly reduced, see manuscript 2 (Kristensen et al., 2018). However, the FMDV (VP2 K217R) was the only full-length FMDV mutant, with modifications at the cleavage sites (at the VP0/VP3 and VP3/VP1 junctions) in the capsid precursor that could be rescued. Interestingly, cleavage of the VP0/VP3 junction in the full length FMDV (VP2 K217R) in the later state of infection did not seem to be impeded to the same degree as the in the transient expression of P1-2A (VP2 K217R), compare Fig. 2 and 5, manuscript 2. However, at the early state of infection (3 h p.i.) there is approximately similar amount of the VP0-VP3 intermediate and VP0. This probably reflects that the $3C^{pro}$ is cleaving this mutant junction at a slower rate. However, at later stages in the FMDV infection there will be much more $3C^{pro}$ present, and thus more enzyme to cleave the mutant VP0-VP3 intermediate.

Based on sucrose gradient analysis, separating un-assembled material, empty capsids and virus particles it was clear that the VP0-VP3 intermediate was neither incorporated into empty capsids nor into the virus particles but was only present in un-assembled material. However, based on the known structure from a pentamer within the FMDV A22 Iraq capsid (Curry et al., 1996), it was clear that the VP2 C-terminus and the VP3 N-terminus are located very far from each other in the virus structure, see manuscript 2, Fig. 7. It is very likely that this is the reason why the intermediate was not incorporated into neither the empty capsids nor the virus particles.

Overall, manuscript 1 and 2 provided important information about the junctions separating the capsid proteins. The VP0/VP3 junction belongs to the E/x group whereas the VP3/VP1- and the

VP1/2A junction belongs to the Q/x group, for the FMDV A22 Iraq. For this strain, the virus has a K on the P2 residue, both within the VP0/VP3- and the VP1/2A junction. Substituting this K to an E severely impeded cleavage of both junctions. However, substituting the K to an R, which is considered a fairly conservative substitution since both amino acids have positively charged sidechains, had different effect on the two junctions. Based on the logo plot separating the two junction groups (Fig. 9), it was clear that the Q/x group (VP1/2A) has a high preference for a K at this site. Nevertheless, an R at this site allowed the junction to be fully processed, whereas for instance a Q or an A blocked processing of the junction. Interestingly, all of these three amino acids are all present at the P2 residue in different junctions belonging to the Q/x group (Carrillo et al., 2005; Curry et al., 2007). This clearly indicates, that the $3C^{pro}$ is very constrained about the specific amino acid sequences flanking the different junctions. Furthermore, it tells us that one amino acid which is tolerated in one junction might not be tolerated in another junction, even though the junctions belongs to the same group. Moreover, an arginine is never observed at the P2 position in the E/x group. However, introducing this amino acid at the VP0/VP3 junction caused a reduced rate of cleavage at this specific site but it appeared that $3C^{pro}$ was still able to recognize the junction since the processed VP0 was readily detected. Furthermore, the substitution could be tolerated in full-length FMDV.

Before conducting the studies described in manuscripts 1 and 2, we were aware that the FMDV $3C^{pro}$ was a very complex enzyme, recognizing various amino acids within different junctions all over the FMDV polyprotein. However, based on the results presented in manuscripts 1 and 2, we could conclude that some amino acids, which are present at a specific site within one of the junction groups, might not be tolerated at the same site in another junction within the same group. Moreover, we concluded in manuscript 2, that blocking processing of one junction i.e. the VP0/VP3 or the VP3/VP1 did not prevent processing of the other junction or the VP1/2A junction. Thus, it seems that there is no strict order of processing within the P1-2A capsid precursor. Furthermore, in manuscript 2, we were able to rescue a FMDV displaying reduced cleavage of the VP0/VP3 junction. Interestingly, this mutant FMDV was not significantly affected in the growth rate by this reduced cleavage. The FMDV A22 Iraq tends to form many empty capsids during an infection (Curry et al.,

1997), which suggests that an excess of capsids is produced. This might also explain, why this FMDV (VP2 K217R) is not affected in its growth rate and why adaptions did not occur.

As described in manuscripts 1 and 2, the sequences flanking the junction are highly important for correct processing by the $3C^{pro}$. However, the correct folding of the P1-2A precursor is also highly important for the processing. An earlier study showed that truncating the P1-2A precursor, by removing the 2A and 42 residues of the C-terminus of VP1, blocked the processing of both the VP0/VP3- and the VP3/VP1 junctions (Ryan et al., 1989) in a cell-free translation system . Similarly, truncating the PV P1-precursor, by removing 50 aa from the C-terminus of VP1 also blocked the processing of the capsid precursor by the PV $3CD^{pro}$ (Ypma-Wong & Semler, 1987). Manuscript 2 revealed that processing of the three junctions in the FMDV capsid precursor were mutually independent (Kristensen et al., 2018), indicating that the blocking of the cleavage observed in these earlier studies was likely due to an overall structure change in the capsid precursor, rather than blocking of one junction thereby affecting the other junction.

Based on these two studies on different picornaviruses, Stop-codons was introduced at different sites within the VP1-coding region in a construct containing the coding sequence for FMDV A22 Iraq P1-2A. These constructs, with truncations at different sites, were expressed in a transient expression assay in the presence and absence of $3C^{pro}$. Interestingly, this identified a region within the VP1 185-199 that was important for processing. The truncation to VP1 199 resulted in processed capsid proteins in the presence of $3C^{pro}$, just like the wt. In contrast, the truncation to VP1 185 resulted in a non-processed capsid precursor in the presence of $3C^{pro}$. Moreover, this non-processable P1-2A (VP1 185Stop) mutant accumulated to a lower level in the cells lysates compared to the wt and the other processable mutants. After identifying this region (VP1 185-199), smaller deletions were introduced into this region, which clearly indicated that the sequence VP1 185-190 was required for capsid precursor processing. In addition, the mutants having small deletions within this region also accumulated to a lower level than wt. Further analysis of this critical region was carried out by introducing single amino acid substitutions. This identified two residues of high importance within the area, namely VP1 Y185 and R188. Substituting these aa to an A, individually, severely impeded

cleavage of precursor by the $3C^{pro}$. In addition, these non-processable single-aa-substitution precursors also accumulated to a lower level compared to the wt and the mutants that could be processed by the $3C^{pro}$.

Based on the experiments in manuscript 3, it was found that this YCPRP motif was required for processing of the FMDV capsid precursor. Interestingly this motif is located more than 400 aa away from the VP0/VP3 junction and almost 200 aa away from the VP3/VP1 junction. An alignment revealed that the YCPRP motif was highly conserved among FMDVs from all 7 serotypes. Indeed, this motif was conserved among more than 100 FMDV strains (Carrillo et al., 2005)); only one strain had a variation to YCPRA, see manuscript 3, Fig. 8). The YCPRP motif was also found to be highly conserved amongst other picornaviruses. In cardioviruses, it exists as FCPRP and in enteroviruses it is present as WCPRP, see manuscript 3, Fig. 9. The high conservation of this motif likely reflects its importance for correct folding and subsequent processing of the capsid precursor. This conserved motif also provided an explanation about the earlier findings with FMDV and PV where capsid precursor processing was prevented upon truncation of the capsid precursor (Ypma-Wong & Semler, 1987; Ryan et al., 1989). Indeed, this motif was removed upon the truncation used in both of these studies and thus the results are fully consistent.

It is likely that this conserved motif is involved in the binding of different cellular factors, such as chaperones, required for correct capsid precursor folding. Hsp90 seems to be required for capsid precursor processing and assembly in different picornaviruses (Geller et al., 2007; Newman et al., 2017). Both Hsp90 and Hsp70 have been found to interact with the PV capsid precursor (Macejak & Sarnow, 1992; Geller et al., 2007). The interaction between PV P1 and Hsp90 is believed to be required for correct folding and for protecting the PV capsid precursor from degradation by proteasomes (Geller et al., 2007). In the study by Geller et al., (2007), it was shown that the PV capsid precursor accumulated to a lower level in the cell lysate following inhibition of Hsp90, due to degradation by the proteasome. All of the mutants identified in manuscript 3, that were highly resistant to processing by the $3C^{pro}$ and displayed decreased accumulation therefore mirrors the known effects of blocking interaction between the capsid precursor and Hsp90 (Geller et al., 2007;

Newman et al., 2017). Thus, it seems likely that the conserved motif acts as an interaction site with a chaperone (or its co-chaperone), perhaps the Hsp90.

Further investigation of the motif identified in manuscript 3, would be of high relevance in relation to the lifecycle of many different picornaviruses. The identification of the conserved motif and the effect upon changing this, was "only" carried out expressing the FMDV P1-2A precursor together with the $3C^{pro}$ in a transient expression assay. However, very recently we have introduced some of these modifications into full-length FMDVs (Kristensen & Belsham, unpublished data). We have not been able to rescue virus from the FMDV (VP1 Y185A) mutant (consistent with the failure to produce processed capsid proteins) but surprisingly we got virus back from the FMDV (VP1 R188A) mutant. Sequencing of the rescued mutant virus has revealed that adaptions had occurred resulting in aa substitutions within both the VP2 and VP3 proteins, one of them being in close contact with the conserved motif in the mature virus particle. Hopefully, we will be able to determine the relevance of these aa substitutions in the near future. Furthermore, it would also be very relevant to identify proteins that interact with this motif. It is likely that the Hsp90 is involved, either directly or indirectly through interaction with a co-chaperone. However, it is also possible that this newly identified motif interacts with another protein, which has not previously been associated with the picornavirus family. Earlier results indicate that inhibitors of hsp90 can function as an effective antiviral agent (Geller et al., 2007; Newman et al., 2017). However, identification of the interacting cellular factors with the conserved motif, might identify other important proteins which might have advantages as a target for new antiviral compounds.

5. References

Abrams C.C., King A.M.Q., Belsham G.J. 1995. Assembly of foot-and-mouth disease virus empty capsids synthesized by a vaccinia virus expression system. J Gen Virol. 76, 3089–98.

Acharya R., Fry E., Stuart D., Fox G., Rowlands D., Brown F. 1989. The three-dimensional structure of foot-and-mouth disease virus at 2.9 Å resolution. Nature. 337, 709–16.

Agirre A., Barco A., Carrasco L., Nieva J.L. 2002. Viroporin-mediated membrane permeabilization - pore formation by nonstructural poliovirus 2B protein. J Biol Chem. 277, 40434–41.

Alexandersen S., Zhang Z., Donaldson A.I. 2002. Aspects of the persistence of foot-and-mouth disease virus in animals — the carrier problem. Microbes Infect. 4, 1099–110.

Alexandersen S., Zhang Z., Donaldson A.I., Garland A.J.M. 2003. The pathogenesis and diagnosis of foot-and-mouth disease. J Comp Pathol. 129, 1–36.

Alexandersen S., Mowat N. 2005. Foot-and-mouth disease: host range and pathogenesis. Curr Top Microbiol Immunol. 288, 9–42.

Allaire M., Chernaia M.M., Malcolm B.A., James M.N.G. 1994. Picornaviral 3C cysteine proteinases have a fold similar to chymotrypsin-like serine proteinases. Nature. 369, 72–6.

Ansardi D.C., Porter D.C., Morrow C.D. 1992. Myristylation of poliovirus capsid precursor P1 is required for assembly of subviral particles. J Virol. 66, 4556–63.

Ansardi D.C., Moldoveanu Z., Porter D.C., Walker D.E., Conry R.M., Lobuglio A.F., Mcpherson S., Morrow C.D. 1994. Characterization of poliovirus replicons encoding carcinoembryomc antigen. Cancer Res. 54, 6359–64.

Aragonès L., Guix S., Ribes E., Bosch A., Pintó R.M. 2010. Fine-tuning translation kinetics selection as the driving force of codon usage bias in the hepatitis A virus capsid. PLOS Pathog. 6, e1000797.

Arias A., Perales C., Escarmís C., Domingo E. 2010. Deletion mutants of VPg reveal new cytopathology determinants in a picornavirus. PLOS One. 5, e10735.

Arnold E., Luo M., Vriend G., Rossmann M.G., Palmenbergt A.C., Parkst G.D., Nicklint M.J.H., Wimmert E. 1987. Implications of the picornavirus capsid structure for polyprotein processing. Proc Natl Acad Sci USA. 84, 21–5.

Arzt J., Belsham G.J., Lohse L., Bøtner A., Stenfeldt C. 2018. Transmission of foot-and-mouth disease from persistently infected carrier cattle to naive cattle via transfer of oropharyngeal fluid. mSpehere. 3, 1–12.

Atkins J.F., Wills N.M., Loughran G., Wu C.-Y., Parsawar K., Ryan M.D., Wang C., Nelson C.C. 2007. A case for “StopGo”: reprogramming translation to augment codon meaning of GGN by promoting unconventional termination (Stop) after addition of glycine and then allowing continued translation (Go). RNA. 13, 803–10.

Basavappa R., Syed R., Flore O., Icenogle J.P., Filman D.J., Hogle J.M. 1994. Role and mechanism of the maturation cleavage of VPO in poliovirus assembly: structure of the empty capsid assembly intermediate at 2.9 Å resolution. Protein Sci. 3, 1651–69.

Baxt B., Becker Y. 1990. The Effect of peptides containing the arginine-glycine-aspartic acid sequence on the adsorption of foot-and-mouth disease virus to tissue culture cells. Virus Genes. 4, 73–83.

Belsham G.J., Bostock C.J. 1988. Studies on the infectivity of foot-and-mouth disease virus RNA using microinjection. J Gen Virol. 69, 265–74.

Belsham G.J., Abrams C.C., King A.M.Q., Roosien J., Vlak J.M. 1991. Myristoylation of foot-and-mouth disease virus capsid protein precursors is independent of other viral proteins and occurs in both mammalian and insect cells. J Gen Virol. 72, 747–51.

Belsham G.J. 1992. Dual initiation sites of protein synthesis on foot-and-mouth disease virus RNA are selected following internal entry and scanning of ribosomes in vivo. EMBO J. 11, 1105–10.

Belsham G.J., McInerney G.M., Ross-Smith N. 2000. Foot-and-mouth disease virus 3C protease induces cleavage of translation initiation factors eIF4A and eIF4G within infected cells. J Virol. 74, 272–80.

Belsham G.J. 2005. Translation and replication of FMDV RNA. Curr Top Microbiol Immunol. 288, 43–70.

Belsham G.J. 2013. Influence of the Leader protein coding region of foot-and-mouth disease virus on virus replication. J Gen Virol. 94, 1486–95.

Birtley J.R., Knox S.R., Jaulent M., Brick P., Leatherbarrow R.J., Curry S. 2005. Crystal structure of foot-and-mouth disease virus 3C protease. J Biol Chem. 280, 11520–7.

Black L.W. 1989. DNA packaging in dsDNA bacteriophages. Annu Rev Microbiol. 43, 267–92.

Bøtner A., Kakker N.K., Barbezange C., Berryman S., Jackson T., Belsham G.J. 2011. Capsid proteins from

field strains of foot-and-mouth disease virus confer a pathogenic phenotype in cattle on an attenuated, cell-culture-adapted virus. J Gen Virol. 92, 1141–51.

Brown C.C., Piccone M.E., Mason P.W., McKenna T.S., Grubman M.J. 1996. Pathogenesis of wild-type and leaderless foot-and-mouth disease virus in cattle. J Virol. 70, 5638–41.

Brown F., Cartwright B. 1961. Dissociation of foot-and-mouth disease virus into its nucleic acid and protein components. Nature. 192, 1163–4.

Burch A.D., Weller S.K. 2005. Herpes simplex virus type 1 DNA polymerase requires the mammalian chaperone Hsp90 for proper localization to the nucleus. J Virol. 79, 10740–9.

Burroughs J.N., Rowlands D.J., Sangar D. V, Talbot P., Brown F. 1971. Further evidence for multiple proteins in the foot-and-mouth disease virus particle. J Gen Virol. 13, 73–84.

Carrillo C., Tulman E.R., Delhon G., Lu Z., Carreno A., Vagnozzi A., Kutish G.F., Rock D.L. 2005. Comparative genomics of foot-and-mouth disease virus. J Virol. 79, 6487–504.

Carrillo E.C., Giacheiti C., Campos R.H. 1984. Effect of lysosomotropic agents on the foot-and-mouth disease virus replication. Virology. 135, 542–5.

Chase A.J., Daijogo S., Semler B.L. 2014. Inhibition of poliovirus-induced cleavage of cellular protein PCBP2 reduces the levels of viral RNA replication. J Virol. 88, 3192–201.

Chinsangaram J., Piccone M.E., Grubman M.J. 1999. Ability of foot-and-mouth disease virus to form plaques in cell culture is associated with suppression of alpha/beta interferon. J Virol. 73, 9891–8.

Clarke B.E., Brown A.L., Currey K.M., Newton S.E., Rowlands D.J., Carroll A.R. 1987. Potential secondary and tertiary structure in the genomic RNA of foot and mouth disease virus. Nucleic Acids Res. 15, 7067–79.

Clarke J.B., Spier R.E. 1983. An investigation into causes of a cloned line of BHK cells to a strain of foot-and-mouth disease virus. Vet Microbiol. 8, 259–70.

Cohen L., Bénichou D., Martin A. 2002. Analysis of deletion mutants indicates that the 2A polypeptide of hepatitis A virus participates in virion morphogenesis. J Virol. 76, 7495–505.

Curry S., Abrams C.C., Fry E., Crowther J.C., Belsham G.J., Stuart D.I., King A.M.Q. 1995. Viral RNA modulates the acid sensitivity of foot-and-mouth disease virus capsids. J Virol. 69, 430–8.

Curry S., Fry E., Blakemore W., Abu-Ghazaleh R., Jackson T., King A., Lea S., Newman J., Rowlands D., Stuart D. 1996. Perturbations in the surface structure of A22 Iraq foot-and-mouth disease virus

accompanying coupled changes in host cell specificity and antigenicity. Structure. 4, 135–45.

Curry S., Fry E., Blakemore W., Abu-Ghazaleh R., Jackson T., King A., Lea S., Newman J., Stuart D. 1997. Dissecting the roles of VP0 cleavage and RNA packaging in picornavirus capsid stabilization: the structure of empty capsids of foot-and-mouth disease virus. J Virol. 71, 9743–52.

Curry S., Zunszain P.A., Leatherbarrow R.J. 2007. Foot-and-mouth disease virus 3C protease: recent structural and functional insights into an antiviral target. Int J Biochem Cell Biol. 39, 1–6.

Devaney M.A., Vakharia V.N., Lloyd R.E., Ehrenfeld E., Grubman M.J. 1988. Leader protein of foot-and-mouth disease virus is required for cleavage of the p220 component of the cap-binding protein complex. J Virol. 62, 4407–9.

Dickey C.A., Koren J., Zhang Y., Xu Y., Jinwal U.K., Birnbaum M.J., Monks B., Sun M., Cheng J.Q., Patterson C., Bailey R.M., Dunmore J., Soresh S., Leon C., Morgan D., Petrucelli L. 2008. Akt and CHIP coregulate tau degradation through coordinated interactions. PNAS. 105, 3622–7.

Doedens J.R., Kirkegaard K. 1995. Inhibition of cellular protein secretion by poliovirus proteins 2B and 3A. EMBO J. 14, 894–907.

Domingo E., Sheldon J., Perales C. 2012. Viral quasispecies evolution. Microbiol Mol Biol Rev. 76, 159–216.

Donnelly M.L.L., Luke G., Mehrotra A., Li X., Hughes L.E., Gani D., Ryan M.D. 2001. Analysis of the aphthovirus 2A/2B polyprotein 'cleavage' mechanism indicates not a proteolytic reaction, but a novel translational effect: a putative ribosomal 'skip.' J Gen Virol. 82, 1013–25.

Doronina V.A., de Felipe P., Wu C., Sharma P., Sachs M.S., Ryan M.D., Brown J.D. 2008a. Dissection of a co-translational nascent chain separation event. Biochem Soc Trans. 36, 712–6.

Doronina V.A., Wu C., de Felipe P., Sachs M.S., Ryan M.D., Brown J.D. 2008b. Site-specific release of nascent chains from ribosomes at a sense codon. Mol Cell Biol. 28, 4227–39.

Drew J., Belsham G.J. 1994. trans complementation by RNA of defective foot-and-mouth disease virus internal ribosome entry site elements. J Virol. 68, 697–703.

Edkins A.L. 2015. CHIP: a co-chaperone for degradation by the proteasome. Subcell Biochem. 78, 1–24.

Escarmís C., Toja M., Medina M., Domingo E. 1992. Modifications of the 5' untranslated region of foot-and-mouth disease virus after prolonged persistence in cell culture. Virus Res. 26, 113–25.

Escarmís C., Dopazo J., Dhvila M., Palma E.L., Domingo E. 1995. Large deletions in the 5'-untranslated

region of foot-and-mouth disease virus of serotype C. Virus Res. 35, 155–67.

Fernandez-Tomas C.B., Baltimore D. 1973. Morphogenesis of poliovirus II. Demonstration of a new intermediate, the proviron. J Virol. 12, 1122–30.

Fowler V., Bashiruddin J.B., Belsham G.J., Stenfeldt C., Bøtner A., Knowles N.J., Bankowski B., Parida S., Barnett P. 2014. Characteristics of a foot-and-mouth disease virus with a partial VP1 G-H loop deletion in experimentally infected cattle. Vet Microbiol. 169, 58–66.

Fowler V.L., Knowles N.J., Paton D.J., Barnett P. V. 2010. Marker vaccine potential of a foot-and-mouth disease virus with a partial VP1 G-H loop deletion. Vaccine. 28, 3428–34.

Fowler V.L., Bashiruddin J.B., Maree F.F., Mutowembwa P., Bankowski B., Gibson D., Cox S., Knowles N., Barnett P. V. 2011. Foot-and-mouth disease marker vaccine: cattle protection with a partial VP1 G–H loop deleted virus antigen. Vaccine. 29, 8405–11.

Fox G., Parry N.R., Barnett P. V., McGinn B., Rowlands D.J., Brown F. 1989. The cell attachment site on foot-and-mouth disease virus includes the amino acid sequence RGD (arginine-glycine-aspartic acid). J Gen Virol. 70, 625–37.

Fox H., Knowlson S., Minor P.D., Macadam A.J. 2017. Genetically thermo-stabilised, immunogenic poliovirus empty capsids; a strategy for non- replicating vaccines. PLOS Pathog. 13, e1006117.

Fry E.E., Stuart D.I., Rowlands D.J. 2005. The stucture of foot-and-mouth disease virus. In: Foot-and-mouth disease virus. Springer; 2005. p. 71–101.

Gao Y., Sun S.-Q., Guo H.-C. 2016. Biological function of foot-and-mouth disease virus non-structural proteins and non-coding elements. Virol J. 13, 1–17.

Geller R., Vignuzzi M., Andino R., Frydman J. 2007. Evolutionary constraints on chaperone-mediated folding provide an antiviral approach refractory to development of drug resistance. Genes Dev. 21, 195–205.

Geller R., Taguwa S., Frydman J. 2012. Broad action of Hsp90 as a host chaperone required for viral replication. Biochim Biophys Acta. 1823, 698–706.

Gerber K., Wimmer E., Paul A. V. 2001. Biochemical and genetic studies of the initiation of human rhinovirus 2 RNA replication: identification of a cis-replicating element in the coding sequence of 2A pro. J Virol. 75, 10979–90.

Gerrish P.J., García-Lerma J.G. 2003. Mutation rate and the efficacy of antimicrobial drug treatment. Lancet

Infect Dis. 3, 28–32.

Goodfellow I., Chaudhry Y., Richardson A., Meredith J., Almond J.W., Barclay W., Evans D.J. 2000. Identification of a cis-acting replication element within the poliovirus coding region. J Virol. 74, 4590–600.

Goodwin S., Tuthill T.J., Arias A., Killington R.A., Rowlands D.J. 2009. Foot-and-mouth disease virus assembly: processing of recombinant capsid precursor by exogenous protease induces self-assembly of pentamers in vitro in a myristoylation-dependent manner. J Virol. 83, 11275–82.

Gosert R., Dollenmaier G., Weitz M. 1997. Identification of active-site residues in protease 3C of hepatitis A virus by site-directed mutagenesis. J Virol. 71, 3062–8.

Gradi A., Foeger N., Strong R., Yuri V., Sonenberg N., Skern T., Graham J., Svitkin Y. V, Belsham G.J. 2004. Cleavage of eukaryotic translation initiation factor 4GII within foot-and-mouth disease virus-infected cells: identification of the L-protease cleavage site in vitro. J Virol. 78, 3271–8.

Grubman M.J., Baxt B. 2004. Foot-and-mouth disease. Clin Microbiol Rev. 17, 465–93.

Gullberg M., Polacek C., Bøtner A., Belsham G.J. 2013a. Processing of the VP1/2A junction is not necessary for production of foot-and-mouth disease virus empty capsids and infectious viruses: characterization of " self-tagged " particles. J Virol. 87, 11591–603.

Gullberg M., Muszynski B., Organtini L.J., Ashley R.E., Hafenstein S.L., Belsham G.J., Polacek C. 2013b. Assembly and characterization of foot-and-mouth disease virus empty capsid particles expressed within mammalian cells. J Gen Virol. 94, 1769–79.

Gullberg M., Polacek C., Belsham G.J. 2014. Sequence adaptations affecting cleavage of the VP1/2A junction by the 3C protease in foot-and-mouth disease virus-infected cells. J Gen Virol. 95, 2402–10.

Gullberg M., Lohse L., Anette B., Mcinerney G.M., Burman A., Jackson T., Polacek C., Belsham G.J. 2016. A prime-boost vaccination strategy in cattle to prevent foot-and-mouth disease using a "single-cycle" alphavirus vector and empty capsid particles. PLOS One. 11, e0157435.

Hagino-Yamagishi K., Nomoto A. 1989. In vitro construction of poliovirus defective interfering particles. J Virol. 63, 5386–92.

Harber J.J., Bradley J., Anderson C.W., Wimmer E. 1991. Catalysis of poliovirus VP0 maturation cleavage is not mediated by serine 10 of VP2. J Virol. 65, 326–34.

Herod M.R., Gold S., Lasecka-Dykes L., Wright C., Ward J.C., McLean T.C., Forrest S., Jackson T., Tuthill T.J., Rowlands D.J., Stonehouse N.J. 2017. Genetic economy in picornaviruses: foot-and-mouth disease virus replication exploits alternative precursor cleavage pathways. PLOS Pathog. 13, e1006666.

Hogle J.M., Chow M., Filman D.J. 1985. Three-dimensional structure of poliovirus at 2.9 Å resolution. Science. 229, 1358–65.

Hu J., O.Toft D., Seeger C. 1997. Hepadnavirus assembly and reverse transcription require a multi-component chaperone complex which is incorporated into nucleocapsids. EMBO J. 16, 59–68.

Jackson T., Ellard F.M., Ghazaleh R.A.B.U., Brookes S.M., Blakemore W.E., Corteyn A.H., Stuart D.I., Newman J.W.I., King A.M.Q. 1996. Efficient infection of cells in culture by type O foot-and-mouth disease virus requires binding to cell surface heparan sulfate. J Virol. 70, 5282–7.

Jackson T., Sheppard D., Denyer M., Blakemore W., King A.M.Q. 2000. The epithelial integrin αvβ6 is a receptor for foot-and-mouth disease virus. J Virol. 74, 4949–56.

Jacobson M.F., Baltimore D. 1968. Morphogenesis of poliovirus I. Association of the viral RNA with coat protein. J Mol Biol. 33, 369–78.

Jamal S.M., Belsham G.J. 2013. Foot-and-mouth disease: past, present and future. Vet Res. 44, 1–14.

Jamal S.M., Belsham G.J. 2018. Molecular epidemiology, evolution and phylogeny of foot-and-mouth disease virus. Infect Genet Evol. 59, 84–98.

Jhaveri K., Taldone T., Modi S., Chiosis G. 2012. Advances in the clinical development of heat shock protein 90 (Hsp90) inhibitors in cancers. Biochim Biophys Acta. 1823, 742–55.

Jiang P., Liu Y., Ma H.-C., Paul A. V., Wimmer E. 2014. Picornavirus morphogenesis. Microbiol Mol Biol Rev. 78, 418–37.

Jore J., De Geus B., Jackson R., Pouwels P., Enger-Valk B. 1988. Poliovirus protein 3CD is the active protease for processing of the precursor protein P1 in vitro. J Gen Virol. 69, 1627–36.

Kajigaya S., Arakawa H., Kuge S., Koi T., Imura N., Nomoto A. 1985. Isolation and characterization of defective-interfering particles of poliovirus sabin 1 strain. Virology. 142, 307–16.

Kimmins S., MacRae T.H. 2000. Maturation of steroid receptors: an example of functional cooperation among molecular chaperones and their associated proteins. Cell Stress Chaperones. 5, 76–86.

King A.M.Q., Adams M.J., Carstens E.B., Lefkowitz E.J. (Eds.). 2011. Picornaviridae. In: Virus taxonomy:

ninth report of the international committee on taxonomy of viruses. Elsevier; 2011. p. 855–80.

Kingsbury N. 2008. DHS lacks evidence to conclude that foot-and- mouth disease research can be done safely on the U.S. mainland. *United States Goverment Accountability Office*. https://www.gao.gov/products/GAO-08-821T.

Kjær J., Belsham G.J. 2018a. Modifications to the foot-and-mouth disease virus 2A peptide; influence on polyprotein processing and virus replication. J Virol. 92, e02218-17.

Kjær J., Belsham G.J. 2018b. Selection of functional 2A sequences within foot-and-mouth disease virus; requirements for the NPGP motif with a distinct codon bias. RNA. 24, 12–7.

Kloc A., Segundo F.D., Schafer E.A., Rai D.K., Kenney M., Santos T.D.L., Rieder E. 2017. Foot-and-mouth disease virus 5' -terminal S fragment is required for replication and modulation of the innate immune response in host cells. Virology. 512 August, 132–43.

Knipe T., Rieder E., Baxt B., Ward G., Mason P.W. 1997. Characterization of synthetic foot-and-mouth disease virus provirions separates acid-mediated disassembly from infectivity. J Virol. 71, 2851–6.

Knowles N.J., Davies P.R., Henry T., Donnell V.O., Pacheco J.M., Mason P.W. 2001. Emergence in Asia of foot-and-mouth disease viruses with altered host range: characterization of alterations in the 3A protein. J Virol. 75, 1551–6.

Korant B.D., Lonberg-Holm K., Yin F.H., Noble-Harvey J. 1975. Fractionation of biologically active and inactive populations of human rhinovirus type 2. Virology. 63, 384–94.

Kristensen T., Normann P., Gullberg M., Fahnøe U., Polacek C., Rasmussen T.B., Belsham G.J. 2016. Determinants of the VP1/2A junction cleavage by the 3C protease in foot-and-mouth disease virus-infected cells. J Gen Virol. 98, 385–95.

Kristensen T., Newman J., Guan S.H., Tuthill T.J., Belsham G.J. 2018. Cleavages at the three junctions within the foot-and-mouth disease virus capsid precursor (P1-2A) by the 3C protease are mutually independent. Virology. 522, 260–70.

Lauring A.S., Andino R. 2010. Quasispecies theory and the behavior of RNA viruses. PLOS Pathog. 6, e1001005.

Lawrence P., Rieder E. 2009. Identification of RNA helicase A as a new host factor in the replication cycle of foot-and-mouth disease virus. J Virol. 83, 11356–66.

Leippert M., Beck E., Weiland F., Pfaff E. 1997. Point mutations within the βG-βH loop of foot-and-mouth disease virus O1K affect virus attachment to target cells. J Virol. 71, 1046–51.

Lewis S.A., Morgan D.O., Grubman M.J. 1991. Expression, processing, and assembly of foot-and-mouth disease virus capsid structures in heterologous systems: induction of a neutralizing antibody response in guinea pigs. J Virol. 65, 6572–80.

Li C., Wang J.C., Taylor M.W., Zlotnick A. 2012. In vitro assembly of an empty picornavirus capsid follows a dodecahedral path. J Virol. 86, 13062–9.

Liu Y., Wang C., Mueller S., Paul A. V, Wimmer E., Jiang P. 2010. Direct interaction between two viral proteins, the nonstructural protein 2C ATPase and the capsid protein VP3, is required for enterovirus morphogenesis. PLOS Pathog. 6, e1001066.

Logan D., Abu-Ghazaleh R., Blakemore W., Curry S., Jackson T., King A., Lea S., Lewis R., Newman J., Parry N., Rowlands D., Stuart D., Fry E. 1993. Structure of a major immunogenic site on foot-and-mouth disease virus. Nature. 362, 566–8.

Logan G., Newman J., Wright C.F., Lasecka-dykes L., Haydon D.T., Cottam E.M., Tuthill T.J. 2018. Deep sequencing of foot-and-mouth disease virus reveals RNA sequences involved in genome packaging. J Virol. 92, e01159-17.

Lovert P.-E., Escriou N., Ruelle J., Michiels T. 1999. A coding RNA sequence acts as a replication signal in cardioviruses. Proc Natl Acad Sci USA. 96, 11560–5.

Luke G.A., Felipe P. De, Lukashev A., Kallioinen S.E., Bruno E.A., Ryan M.D. 2008. Occurrence, function and evolutionary origins of '2A-like' sequences in virus genomes. J Gen Virol. 89, 1036–42.

Macadam A.J., Ferguson G., Arnold C., Minor P.D. 1991. An assembly defect as a result of an attenuating mutation in the capsid proteins of the poliovirus type 3 vaccine strain. J Virol. 65, 5225–31.

Macejak D.G., Sarnow P. 1992. Association of heat shock protein 70 with enterovirus capsid precursor P1 in infected human cells. J Virol. 66, 1520–7.

MacLachlan N.J., Dubovi E.J. (Eds.). 2017. Picornaviridae. In: Fenner's Veterinary Virology. 2017. p. 478–95.

Maizel Jr J. V, Phillips B.A., Summers D.F. 1967. Composition of artificially produced and naturally occurring empty capsids of poliovirus type 1. Virology. 32, 692–9.

Makhnevych T., Houry W.A. 2012. The role of Hsp90 in protein complex assembly. Biochim Biophys Acta.

1823, 674–82.

Marc D., Masson G., Girard M., Werf S. Van Der. 1990. Lack of myristoylation of poliovirus capsid polypeptide VPO prevents the formation of virions or results in the assembly of noninfectious virus particles. J Virol. 64, 4099–107.

Martinez-Salas E., Belsham G.J. 2017. Genome organization, translation and replication of foot-and-mouth disease virus RNA. In: Foot-and-mouth disease virus: current research and emerging trends. Caister Academic Press; 2017. p. 13–42.

Mason P.W., Bezborodova S. V, Henry T.M. 2002. Identification and characterization of a cis-acting replication element (cre) adjacent to the internal ribosome entry site of foot-and-mouth disease virus. J Virol. 76, 9686–94.

Mateo R., Luna E., Rincón V., Mateu M.G. 2008. Engineering viable foot-and-mouth disease viruses with increased thermostability as a step in the development of improved vaccines. J Virol. 82, 12232–40.

Matthews D.A., Dragovich P.S., Webber S.E., Fuhrman S.A., Patick A.K., Zalman L.S., Hendrickson T.F., Love R.A., Prins T.J., Marakovits J.T., Zhou R., Tikhe J., Ford C.E., Meador J.W., Ferre R.A., Brown E.L., Binford S.L., Brothers M.A., Delisle D.M., Wordland S.T. 1999. Structure-assisted design of mechanism-based irreversible inhibitors of human rhinovirus 3C protease with potent antiviral activity against multiple rhinovirus serotypes. Proc Natl Acad Sci USA. 96, 11000–7.

McInerney G.M., King A.M.Q., Ross-smith N., Belsham G.J. 2000. Replication-competent foot-and-mouth disease virus RNAs lacking capsid coding sequences. J Gen Virol. 81, 1699–702.

McKenna T.S.C., Lubroth J., Rieder E., Baxt B., Mason P.W. 1995. Receptor binding site-deleted foot-and-mouth disease (FMD) virus protects cattle from FMD. J Virol. 69, 5787–90.

Mcknight K.L., Lemon S.M. 1998. The rhinovirus type 14 genome contains an internally located RNA structure that is required for viral replication. RNA. 14, 1569–84.

Medina M., Domingo E., Brangwyn J.K., Belsham G.J. 1993. The two species of the foot-and-mouth disease virus leader protein, expressed individually, exhibit the same activities. Virology. 194, 3355–9.

Moffat K., Howell G., Knox C., Belsham G.J., Monaghan P., Ryan M.D., Wileman T. 2005. Effects of foot-and-mouth disease virus nonstructural proteins on the structure and function of the early secretory pathway: 2BC but not 3A blocks endoplasmic reticulum-to-golgi transport. J Virol. 79, 4382–95.

Monaghan P., Cook H., Jackson T., Ryan M., Wileman T. 2004. The ultrastructure of the developing

replication site in foot-and-mouth disease virus-infected BHK-38 cells. J Gen Virol. 85, 933–46.

Nayak A., Goodfellow I.G., Belsham G.J. 2005. Factors required for the uridylylation of the foot-and-mouth disease virus 3B1, 3B2, and 3B3 peptides by the RNA-dependent RNA polymerase (3D pol) in vitro. J Virol. 79, 7698–706.

Nayak A., Goodfellow I.G., Woolaway K.E., Birtley J., Curry S., Belsham G.J. 2006. Role of RNA structure and RNA binding activity of foot-and-mouth disease virus 3C protein in VPg uridylylation and virus replication. J Virol. 80, 9865–75.

Newman J., Asfor A.S., Berryman S., Jackson T., Curry S., Tuthill T.J. 2017. The cellular chaperone heat shock protein 90 is required for foot-and-mouth disease virus capsid precursor processing and assembly of capsid pentamers. J Virol. 92, 1–14.

Nfon C., Lung O., Embury-Hyatt C., Alexandersen S. 2017. Clinical signs and pathology of foot-and-mouth disease. In: Foot-and-mouth disease virus - current research and emerging trends. 2017. p. 171–8.

Nomotot A., Kitamura N., Golini F., Wimmerf E. 1977. The 5’-terminal structures of poliovirion RNA and poliovirus mRNA differ only in the genome-linked protein VPg. Proc Natl Acad Sci USA. 74, 5345–9.

Nugent C.I., Kirkegaard K. 1995. RNA binding properties of poliovirus subviral particles. J Virol. 69, 13–22.

Nugent C.I., Johnson K.L., Sarnow P., Kirkegaard K. 1999. Functional coupling between replication and packaging of poliovirus replicon RNA. J Virol. 73, 427–35.

Pacheco J.M., Henry T.M., Donnell V.K.O., Gregory J.B., Mason P.W. 2003. Role of nonstructural proteins 3A and 3B in host range and pathogenicity of foot-and-mouth disease virus. J Virol. 77, 13017–27.

Palmenberg A.C., Parks G.D., Hall D.J., Ingraham R.H., Seng T.W., Pallal P. V. 1992. Proteolytic processing of the cardioviral cleavage in clone-derived P2 region: primary 2A/2B precursors. Virology. 190, 754–62.

Paul A. V, Schultzt A., Pincus S.E., Oroszlant S., Wimmer E. 1987. Capsid protein VP4 of poliovirus is N-myristoylated. Proc Natl Acad Sci USA. 84, 7827–31.

Paul A. V, Rieder E., Kim D.W., Jacques H.V.B., Wimmer E. 2000. Identification of an RNA hairpin in poliovirus RNA that serves as the primary template in the in vitro uridylylation of VPg. J Virol. 74, 10359–70.

Pearl L.H. 2005. Hsp90 and Cdc37 – a chaperone cancer conspiracy. Curr Opin Genet Dev. 15, 55–61.

Pfister T., Egger D., Bienz K. 1995. Poliovirus subviral particles associated with progeny RNA in the

replication complex. J Gen Virol. 76, 63–71.

Pierschbacher M.D., Ruoslahti E. 1984. Variants of the cell recognition site of fibronectin that retain attachment-promoting activity. Proc Natl Acad Sci USA. 81, 5985–8.

Polacek C., Gullberg M., Li J., Belsham G.J. 2013. Low levels of foot-and-mouth disease virus 3C protease expression are required to achieve optimal capsid protein expression and processing in mammalian cells. J Gen Virol. 94, 1249–58.

Porta C., Xu X., Loureiro S., Paramasivam S., Ren J., Al-khalil T., Burman A., Jackson T., Belsham G.J., Curry S., Lomonossoff G.P., Parida S., Paton D., Li Y., Wilsden G., Ferris N., Owens R., Kotecha A., Fry E., Stuart D.I., Charleston B., Jones I.M. 2013. Efficient production of foot-and-mouth disease virus empty capsids in insect cells following down regulation of 3C protease activity. J Virol Methods. 187, 406–12.

Porter D.C., Ansardi D.C., Wang J., McPherson S., Moldoveanu Z., Morrow C.D. 1998. Demonstration of the specificity of poliovirus encapsidation using a novel replicon which encodes enzymatically active firefly luciferase. Virology. 243, 1–11.

Rieder E., Bunch T., Brown F., Mason P.W. 1993. Genetically engineered foot-and-mouth disease viruses with poly(C) tracts of two nucleotides are virulent in mice. J Virol. 67, 5139–45.

Rombaut B., Vrijsen R., Delgadillo R., Berghe D. Vanden, Boeyé A. 1985. Characterization and assembly of poliovirus-related 45 S particles. Virology. 146, 111–9.

Roosien J., Belsham G.J., Ryan M.D., King A.M.Q., Vlak J.M. 1990. Synthesis of foot-and-mouth disease virus capsid proteins in insect cells using baculovirus expression vectors. J Gen Virol. 71, 1703–11.

Rossmann M.G., Arnold E., Erickson J.W., Frankenberger E.A., Griffith J.P., Hecht H.-J., Johnson J.E., Kamer G., Luo M., Mosser A.G., Rueckert R.R., Sherry B., Vriend G. 1985. Structure of a human common cold virus and fuctional relationship to other picornaviruses. Nature. 318, 556–7.

Rowlands D.J., Sangar D. V, Brown F. 1975. A comparative chemical and serological study of the full and empty particles of foot-and mouth disease virus. J Gen Virol. 26, 227–38.

Rowlands D.J. 2017. Introduction: foot-and-mouth disease - much progress but still a lot to learn. In: Foot-and-mouth disease virus - current research and emerging trends. Caister Academic Press; 2017. p. 1–12.

Ryan M.D., Belsham G.J., King A.M.Q. 1989. Specificity of enzyme-substrate interactions in foot-and-mouth disease virus polyprotein processing. Virology. 173, 35–45.

Sa-carvalho D., Rieder E., Baxt B., Rodarte R., Tanuri A., Mason P.W. 1997. Tissue culture adaptation of foot-and-mouth disease virus selects viruses that bind to heparin and are attenuated in cattle. J Virol. 71, 5115–23.

Sáiz M., Gómez S., Martínez-Salas E., Sobrino F. 2001. Deletion or substitution of the aphthovirus 3' NCR abrogates infectivity and virus replication. J Gen Virol. 82, 93–101.

Sasaki J., Taniguchi K. 2003. The 5´-end sequence of the genome of aichi virus, a picornavirus, contains an element critical for viral RNA encapsidation. J Virol. 77, 3542–8.

Saunders K., King A.M.Q. 1982. Guanidine-resistant mutants of aphthovirus induce the synthesis of an altered nonstructural polypeptide, P34. J Virol. 42, 389–94.

Serrano P., Pulido M.R., Sáiz M., Martínez-Salas E. 2006. The 3' end of the foot-and-mouth disease virus genome establishes two distinct long-range RNA–RNA interactions with the 5' end region. J Gen Virol. 87, 3013–22.

Shakeel S., Dykeman E.C., White S.J., Ora A., Cockburn J.J.B., Butcher S.J., Stockley P.G., Twarock R. 2017. Genomic RNA folding mediates assembly of human parechovirus. Nat Commun. 8, 1–11.

Sommergruber W., Zorn M., Blaas D., Fessl F., Volkmann P., Maurer-Fogy I., Pallai P., Merluzzi V., Matteo M., Skern T., Kuechler E. 1989. Polypeptide 2A of human rhinovirus type 2: identification as a protease and characterization by mutational analysis. Virology. 169, 68–77.

Su R.T., Taylor M.W. 1976. Morphogenesis of picornaviruses: characterization and assembly of bovine enterovirus subviral particles. J Gen Virol. 30, 317–28.

Sutmoller P., Olascoaga R.C. 2002. Unapparent foot and mouth disease infection (sub-clinical infections and carriers): implications for control. RevSciTech. 21, 519–29.

Sweeney T.R., Birtley J.R., Leatherbarrow R.J., Curry S. 2007. Structural and mutagenic analysis of foot-and-mouth disease virus 3C protease reveals the role of the β-ribbon in proteolysis. J Virol. 81, 115–24.

Tiley L., King A.M.Q., Belsham G.J. 2003. The foot-and-mouth disease virus cis-acting replication element (cre) can be complemented in trans within infected cells. J Virol. 77, 2243–6.

Towler D.A., Gordon J.I. 1988. The biology and enzymology of eukaryotic protein acylation. Ann Rev Biochem. 57, 69–99.

Toyoda H., Nicklin M.J.H., Murray M.G., Anderson C.W., Dunn J.J., Studier F.W., Wimmer E. 1986. A second

virus-encoded proteinase involved in proteolytic processing of poliovirus polyprotein. Cell. 45, 761–70.

Tuthill T.J., Groppelli E., Hogle J.M., Rowlands D.J. 2010. Picornaviruses. Curr Top Microbiol Immunol. 343, 43–89.

Verlinden Y., Cuconati A., Wimmer E., Rombaut B. 2000. Cell-free synthesis of poliovirus: 14S subunits are the key intermediates in the encapsidation of poliovirus RNA. J Gen Virol. 81, 2751–4.

Vilhelmsen C. 2017. Lyset slukkes for Lindholm. https://sn.dk/Vordingborg/Lyset-slukkes-for-Lindholm/artikel/666773.

Vlijmen H.W.T. Van, Curry S., Schaefer M., Karplus M. 1998. Titration calculations of foot-and-mouth disease virus capsids and their stabilities as a function of pH. J Mol Biol. 275, 295–308.

Walsh J., Yeibio L. 2010. DHS report on risks of proposed Kansas biocontainment lab is incomplete, says national research council. *News from the National Academies*. http://www8.nationalacademies.org/onpinews/newsitem.aspx?RecordID=13031.

Wang H.E., Lu M., Yao M., Zhu W.E.I. 2016. Effects of treatment with an Hsp90 inhibitor in tumors based on 15 phase II clinical trials. Mol Clin Oncol. 5, 326–34.

Whitesell L., Lindquist S.L. 2005. Hsp90 and the chaperoning of cancer. Nat Rev Cancer. 5, 761–72.

Ypma-Wong M.F., Semler B.L. 1987. Processing determinants required for in vitro cleavage of the poliovirus P1 precursor to capsid proteins. J Virol. 61, 3181–9.

Ypma-Wong M.F., Dewalt P.G., Johnson V.H., Lamb J.G., Semler B.L. 1988. Protein 3CD is the major proteinase responsible for cleavage of the P1 capsid precursor. Virology. 166, 265–70.

Zunszain P.A., Knox S.R., Sweeney T.R., Yang J., Belsham G.J., Leatherbarrow R.J., Curry S. 2010. Insights into cleavage specificity from the crystal structure of foot-and-mouth disease virus 3C protease complexed with a peptide substrate. J Mol Biol. 395, 157–389.